



Vadose Zone Nitrate-N Study: Final Report

*Hastings Wellhead Protection Area: City of Hastings, NE
April 30, 2020*

By: Daniel Snow, Ph.D., Arindam Malakar, Ph.D., Jahangeer, Ph.D., Craig Adams, M.S. & Chittaranjan Ray, Ph.D., University of Nebraska-Lincoln Water Sciences Laboratory



Contents

Contents.....	i
List of Figures	iii
List of Tables	iv
List of Abbreviations	v
Executive Summary.....	1
Introduction	3
Overview of Previous Work	3
Statement of Current Objectives & Tasks.....	4
Objectives	4
Tasks.....	4
Study Area.....	5
Topography	6
Land Use.....	6
Geology	7
Hydrogeology.....	10
Drilling and Retrieval of Core Samples.....	14
Nitrate, Ammonia and Pesticides	16
Laboratory Methods	16
Nitrate-N and Ammonia-N Concentrations in the Vadose Zone	17
Pesticide Results	26
Nitrate and Water Isotopes, Chloride and Groundwater Ages.....	27
Methods.....	28
Nitrate Isotope in the Vadose Zone	29
Porewater Isotope Composition.....	30
Vadose Zone Chloride Composition.....	33
Groundwater Gases, Chemistry and Model Age Measurements	34
Nitrate Loading and Travel Time Estimates	38
Methods.....	39
Site Description.....	39
Model Overview.....	40
Calibration and Validation Procedures of RZWQM2 and HYDRUS 1D.....	44

Vadose Zone Travel Time Model Estimates.....	48
Saturated Hydraulic Conductivity and Soil Water Retention Curve	48
Calibration and validation of models.....	49
Estimated Travel Time of Nitrate-N in Vadose Zone	57
Conclusions	59
Arsenic and Uranium in the Hastings WHPA Vadose Zone.....	64
Materials and Methods.....	66
Soil digestion and quantification of As and U	66
DOC extraction method and analysis.....	67
X-Ray Fluorescence	67
Statistical Treatment of Results	67
Results and discussion	67
Vadose Zone Arsenic.....	70
Vadose Zone Uranium	70
Detailed As and U profiles Compared to Nitrate	71
Elemental Composition of Vadose Zone Related to U and As.....	72
Relationship of Irrigation to Vadose Zone As and U.....	75
Comparison to Groundwater As and U.....	79
Conclusions	79
Summary & Conclusions	83
References	85
Appendix A: Nitrate, Ammonia and Pesticides.....	A
Appendix B: Nitrate and Water Isotopes, Chloride and Groundwater Ages	A
Appendix C: Travel Time Estimates for Nitrate.....	C

List of Figures

Figure 1: Natural Resource District and wellhead protection area (WHPA) surrounding Hastings, NE	5
Figure 2: Land use type in the Hastings' WHPA and its surroundings	6
Figure 3: Map of the study site with locations of coring locations used to develop two cross-sections that display the geology of the WHPA	7
Figure 4: Lithologic cross-section of A – A'	8
Figure 5: Lithologic cross-section of B – B'	9
Figure 6: Unsaturated thickness in the Hastings' WHPA and its surroundings	11
Figure 7: Changes in groundwater nitrate-N concentrations over a 25-year period in the Hastings' WHPA compared to vadose zone sampling sites using data from the Nebraska Agrichemical Clearinghouse database.....	12
Figure 8: CME drill and Geoprobe vadose zone core locations	14
Figure 9: Nitrate-N in the vadose zone beneath gravity irrigated site HC-12-W.....	17
Figure 10: Pore water nitrate-N at dryland corn site HC-2.	18
Figure 11: Average nitrate-N of gravity irrigated sites in 2011 that have since converted to pivot irrigation. Asterisks indicate a statistical significance (p-value ≤ 0.05) between the two groups at a particular depth.	19
Figure 12: Profile characteristics beneath urban lawn site HC-6.....	21
Figure 13: Nitrate-N in the vadose zone of barnyard site HC-7.....	22
Figure 14: Average nitrate-N and ammonium-N of three different land use groups collected in 2016. Asterisks indicate a statistical significance (p-value ≤ 0.05) between different groups at a particular depth.....	24
Figure 15: Average pore water nitrate-N and moisture content of three different land use groups collected in 2016.....	25
Figure 16. Expected variation of $\delta^{15}\text{N-NO}_3$ and $\delta^{18}\text{O-NO}_3$ from a variety of sources, along with the predicted trends due to denitrification (Kendall et al 2008).	27
Figure 17. Variation of the nitrogen isotope composition of vadose zone versus depth for the Hastings WHPA vadose zone samples. Light blue shaded region indicates expected range for $\delta^{15}\text{N}$ of nitrogen from commercial fertilizer while the light green region represents the range for organic sources such as animal manure or septic systems. Numbers correspond to core ID.....	29
Figure 18. Plot of nitrogen versus oxygen isotope composition for nitrate in vadose zone core samples compared to expected ranges for nitrate (e.g. - KNO_3) fertilizer, nitrification of commercial ammonia and organic nitrogen sources.	30
Figure 19. Weekly δD and $\delta^{18}\text{O}$ of water in precipitation between 1989 and 1994 from samples collected near North Platte, Nebraska together with the monthly averages for each isotope (Harvey and Welker, 2000).....	31
Figure 20. Dual isotope plot of δD and $\delta^{18}\text{O}$ of extracted pore water samples from cores HC3A and HC14.	32
Figure 22. Vertical profiles of pore water chloride in Hastings cores HC3A and HC14 E.	34
Figure 23. Compartments where RZWQM2 and HYDRUS 1D were used to estimate nitrate transport....	39
Figure 24. Main component of RZWQM2 model having daily loop and hourly time loop process. The all component are interlinked to each other in air soil water plant continuum (Ahuja et al., 2000).	41

Figure 25. The SWRC for soil core HC1E generated after curve fitting by RETC. The black line represents fitted data and black circle shows observed values of the water content.	49
Figure 26. The calibration and validation with observed and predicted soil water content in the upper 180 cm profile at the selected sites	51
Figure 27. The calibration and validation with observed and predicted pore water nitrate-N concentrations in the upper 180 cm profile at the selected sites	53
Figure 28. calibration and validation with observed and predicted soil moisture content from root zone to deep water table at the selected sites.	55
Figure 29. Calibration and validation with observed and predicted soil water nitrate-N concentrations from root zone to deep water table.	56
Figure 30. Pore water nitrate-N concentrations simulated using the coupled RZWQ2 and HYDRUS 1D model. Nitrate-N peak reach up to 1600 cm (52 ft) over a 20 year simulation.....	58
Figure 31: (a) Shows map of Hastings wellhead protection area (WHPA) where different locations were cored and arrows represent As and U values greater than equal to or less than the average concentrations observed in the present study, (b) shows a coring sites which have higher As and U than the average value of the study area.	69
Figure 32: Shows mean concentration of arsenic and uranium for different irrigation type where there was increase or decrease of nitrate content in the unsaturated zone compared to 2011 Hastings study. The error bar represents standard error of mean.	71
Figure 33: Shows arsenic, uranium, gravimetric water content, nitrate, ammonia, pore water nitrate, lithology and dissolved organic carbon (DOC) profile of site HC-3A against depth.	72
Figure 34: Arsenic, uranium, gravimetric water content, nitrate, ammonia, pore water nitrate and dissolved organic carbon (DOC) profile of site HC-14E against depth.....	73
Figure 35: Shows scatter plot of (a) U vs Fe, (b) As vs Fe, (c) U vs Clay, (d) As vs Clay, and (e) Fe vs Clay .	77
Figure 36: Conceptual hypothesis about U mobilization and ammonia formation in the unsaturated zone	78

List of Tables

Table 1: Annual rainfall precipitation for Hastings, NE over the last eight years	13
Table 2: CME drill and Geoprobe vadose zone cores and land use	14
Table 3: Summary statistics of detected Pesticide	26
Table 4. Results of groundwater chemistry for monitoring wells	35
Table 5. Dissolved gas concentrations, helium isotopes and tritium activity in four groundwater samples collected from the Hastings WHPA. Xenon and argon could not be measured because of a trap malfunction. Air-equilibrated water values at 25° are provided for comparison.	36
Table 6. List of all the scenarios for which coupled model was utilized to estimate nitrate transport	39
Table 7. The description of site land use and soil samples from 32 sites at Hasting, NE.	40
Table 8. Key parameters required for HYDRUS 1D model	44
Table 9. Summary of model components and input parameters needed.....	45
Table 10. Physical properties of soil horizon information from the laboratory.	47
Table 11. Laboratory measured soil properties and saturated hydraulic conductivity of the soil cores. ...	48
Table 12. Estimated pedotransfer function for the soil cores at different depth.	49

Table 13: US-EPA Regional Screening Level (RSL) Resident Soil to GW Table (TR=1E-06, HQ=1) April 2019 (USEPA, 2019) 65

Table 14: Shows mass% of major elements in soil cores against depth and clay%.* 74

List of Abbreviations

<u>Abbreviation</u>	<u>Description</u>
ANOVA	Analysis of Variance
AOI	Area of Interest
ASTM	American Society for Testing
BMP	Better Management Practices
CME	Central Mine Equipment
CPNRD	Central Platte Natural Resource District
DOC	Dissolved Organic Carbon
GIS	Geographic Information System
GWMA	Ground Water Management Area
K_d	Soil-partitioning Coefficient
K_{sat}	Saturated Hydraulic Conductivity
LIDAR	Light Detection and Ranging
MCL	Maximum Contamination Limit
N	Nitrogen
NRD	Natural Resource District
SOP	Standard Operating Procedure
SSURGO	USDA Web Soil Survey Soil Spatial Dataset
UNL	University of Nebraska-Lincoln
USDA	United States Department of Agriculture
USCS	Unified Soil Classification System
WHPA	Well Head Protection Area
WSL	UNL Water Sciences Laboratory

Executive Summary

Increasing groundwater nitrate-N concentrations have been impacting the quality of water delivered by Hastings, Nebraska public supply wells for the past decade or more. A significant and transient reservoir of nitrate-N and other contaminants exists in the deep vadose zone situated above and upgradient of these wells. A total of 32 cores were collected in 2016 from urban and agricultural sites and compared with a baseline study conducted in 2011. Detailed lithological characterization and measurement of hydraulic properties permitted development of a coupled nitrogen leaching model for the area. Nitrate-N accumulations in the vadose zone beneath corn and soybean fields ranged from 230 to 1,400 lbs-N/acre. Some agricultural sites showed increases in nitrate-N storage over the five-year sampling span, while others showed a reduction. The average mass of nitrate-N stored in the vadose zone beneath irrigated cropland changed from 400 ± 140 to 520 ± 280 lbs-N/acre between 2011 and 2016, an increase of roughly 30%. The largest difference in vadose zone nitrate-N was beneath a gravity irrigated cropland. A field converted from gravity to sprinkler irrigation showed an average 170 lbs-N/acre reduction in vadose zone nitrate-N. Vadose zone nitrate was lowest beneath the dryland crop. Average vadose zone nitrate declined beneath the urban sites from 480 ± 440 to 270 ± 200 lbs-N/Acre between 2011 and 2016. Average vadose zone nitrate beneath barns and parks increased from 260 ± 120 to 560 ± 130 lbs-N/acre. Average pore water nitrate-N concentrations were highest beneath gravity irrigated cropland and lowest beneath residential areas. More effective management of nitrate leaching must include better management of both fertilizer and water use.

Ammonia-N, generally considered immobile, showed statistically significant trends with highest concentrations beneath sprinkler irrigated fields and lowest concentrations beneath residential areas. On average, between half and two-thirds of total vadose zone nitrogen was in the form of ammonia-N. Trace levels of atrazine were detected in about 20% of core samples and most detections while most occurred in samples collected near the root zone a few were at significant depth. Nitrate isotope analysis of the vadose zone indicates most nitrogen derived from nitrification of manure and commercial nitrogen fertilizer sources. Elevated $^{15}\text{N-NO}_3$ generally occurs beneath areas with a high density of livestock feeding operations and is consistent with a manure or septic origin, and there is evidence that this source is also impacted local groundwater. Hydrogen and oxygen isotope composition of porewater in two cores are consistent with a seasonally variable component of irrigation water and precipitation. Five groundwater samples were collected from monitoring wells in the WHPA an used to characterize incoming groundwater chemical composition and recharge ages. Estimated age of recharge, or the elapsed time after intercepting the water table, for three of the samples range from 16.5 to almost 45 years.

A coupled nitrate loading and leaching model was used to estimate production and leaching loss of nitrate based on fertilizer and water application rates and timing. The USDA Root Zone Water Quality Model (RZWQ2) accounts for plant activity and soil nitrification while the HYDRUS 1D one dimensional transport model estimated movement of water and nitrate through the deep vadose zone. Using saturated hydraulic conductivity and other measurements from selected core samples, water movement and nitrate leaching was simulated under gravity-irrigated, pivot irrigated, dryland, and urban/barnyard land uses. Both RZWQ2 and HDYRUS 1D models were calibrated using measured soil moisture and nitrate-N concentrations from each of the four locations and then used to product nitrate-N leaching rates and travel times beneath each land use. Simulation results support the observation that pivot

irrigation results in reduce nitrate leaching beneath the crop root zone, though unsurprisingly any form of irrigation increases water content and nitrate loading to the vadose zone. Nitrate leaching is lower under a corn-soybean rotation scenario if the full nitrogen legume credit is used to offset fertilizer application rates. Simulated nitrate transport under gravity irrigated corn is ~2.6ft/year, compared to 1.9 ft/year under pivot irrigated corn and 1.3 ft/year beneath the residential and barnyard land uses. Crop rotation does not affect transport rates. Transport rates beneath dryland crops is between 1.2 and 1.7 ft/year. Assuming these are conservative transport rates which do not account for more rapid preferential flow, travel times between the root zone and the water table are likely on the order of 20-30 years.

Finally, a detailed analysis of the relationship of arsenic and uranium to nitrate in the unsaturated zone revealed some interesting trends that could help explain increasing groundwater uranium concentrations in the area. Acid leachable uranium and arsenic in core samples averaged $0.32 \pm 0.38 \mu\text{g/g}$ and $3.66 \pm 1.06 \mu\text{g/g}$ respectively, and slightly higher arsenic concentrations occurred beneath non-irrigated land uses. Overall, As showed a very strong relationship with iron and clay content of the vadose zone sediments, while the distribution of U was not as strongly influenced by iron. Larger differences in U concentrations were observed and were strongly related to surface irrigation, nitrate leaching and land use. As and U concentrations in the unsaturated zone are both likely affected by recharge, nitrate leaching and potentially from recurrent microbial activity driven by changing moisture content and readily available water-soluble organic carbon. The data suggests that nitrate loading in the vadose zone can mobilize U resulting in leaching to local groundwater. The iron-rich vadose zone coupled with water-soluble carbon may serve as a reactive subsurface for microbial redox processes controlling both forms of iron and mobilization of both As and U followed by subsequent leaching to the water table. Future in-depth analysis of iron chemistry, in addition to continued monitoring of nitrate transformation and movement, is suggested to provide more information about specific biogeochemical processes controlling As and U mobilization in the unsaturated zone. Ongoing changes in cropping practices focused on more efficient use of fertilizer and water will likely have a significant impact on contaminant loading to the vadose zone, and over time will improve the quality of groundwater in this area. It is recommended that regular (~5-7 years) monitoring of the deep vadose zone be conducted to better demonstrate predicted responses to changes at the surface.

Introduction

The City of Hastings has been facing increasing nitrate and uranium concentrations in groundwater supplying their municipal wells. City wells pump from multiple locations into a distribution system. No central treatment or storage facility exists or is possible without a complete redesign of the utility. Groundwater in several wells, and in areas up-gradient from these wellheads, are approaching or exceeding the regulatory drinking water standard for nitrate (10 mg/L NO₃-N). In addition to nitrate contamination, the City is also experiencing issues with uranium exceeding the maximum contaminant level of 30 µg/L in several wells. Selenium and pH level also appear to be increasing, and traces of atrazine also occur in the groundwater. In order to better understand how to manage these problems, the City hired the Nebraska Water Sciences Laboratory (WSL) to collect soil cores in the capture zones of selected public supply wells, estimate the amount of nitrate and other agrichemicals stored in the vadose zone, and better predict the time for the stored nitrate mass to reach the water table based on the current physical and chemical characteristics of the sediments. This will enable the City to anticipate eventual water quality impacts to their public water supply.

Overview of Previous Work

In an effort to assist the City of Hastings in managing the nitrate contamination issue, the University of Nebraska conducted an initial assessment in 2010 of nitrate and atrazine residues present in the vadose zone (Spalding and Toavs, 2011). A total of 36 continuous soil cores were taken in the well-head protection area (WHPA). These sites were chosen by the City based on several factors including land use, cropping history, relative location within the WHPA, and access to sampling site. These 36 cores represented nitrate in sediment from the crop rooting zone and were extracted within the top 60 feet of the vadose zone. Because the depth to ground water was in excess of 60 feet, making the soil profile incomplete, the total mass of nitrate and pesticides available for leaching in the vadose zone could not be estimated.

Core samples collected in the 2010 study were tested for nitrate, ammonia and atrazine residues. Stable isotope analysis in grab samples of groundwater nitrate suggested that most of the nitrogen was derived primarily from commercial fertilizer. Ground water nitrate sampled at a borehole (HC-11) showed a decline from 8.56 mg/L at a depth of 115 ft to 3.41 mg/L at 145 ft, suggesting that denitrification may be occurring with depth in the aquifer at this location. Lower concentration of nitrate in the deeper groundwater sample potentially indicates older groundwater, though age dating was not conducted in this study (Spalding and Toavs, 2011). To improve estimates of projected increases in nitrate concentrations at public supply wells, it is important to know the extent and rate of movement of nitrate in the unsaturated zone and understand any potential for nitrate attenuation during transport.

Statement of Current Objectives & Tasks

Objectives

The following are the goals fulfilled by this research project:

- I. To improve estimates of the current masses of nitrate and pesticide in the vadose zone from the same locations as previously sampled;
- II. To estimate travel time from land surface to ground water for various scenarios; and
- III. To estimate the potential for denitrification in the vadose zone and associated groundwater.

Tasks

In order to achieve these objectives, the following tasks were undertaken:

A. Drilling and retrieval of core samples

The sites selected earlier by the City of Hastings were revisited by the Nebraska Conservation and Survey Division. Wherever possible, core depths were extended to intersect and sample the water table.

B. Describe and analyze core samples for nitrate, ammonia and pesticides

C. Extract and measure nitrate and water isotopes, chloride, and analyze groundwater samples for age estimation

D. Conduct detailed analysis of vadose zone arsenic and uranium to evaluate occurrence and leaching potential

E. Model travel time to provide estimates for nitrate loading and leaching

An unsaturated flow and transport model (HYDRUS-1D by Simunek et al., 1993) was coupled to the Root-Zone Water Quality Model (RZWQ2) to simulate leaching of nitrate.

Study Area

Capture zones for municipal wells northwest of Hastings, NE in Adams County were previously delineated (Hastings Utilities, 1997). The wellhead protection area shown in Figure 1 includes portions of the Little Blue and Big Upper Blue NRDs and is just south of Central Platte NRD.

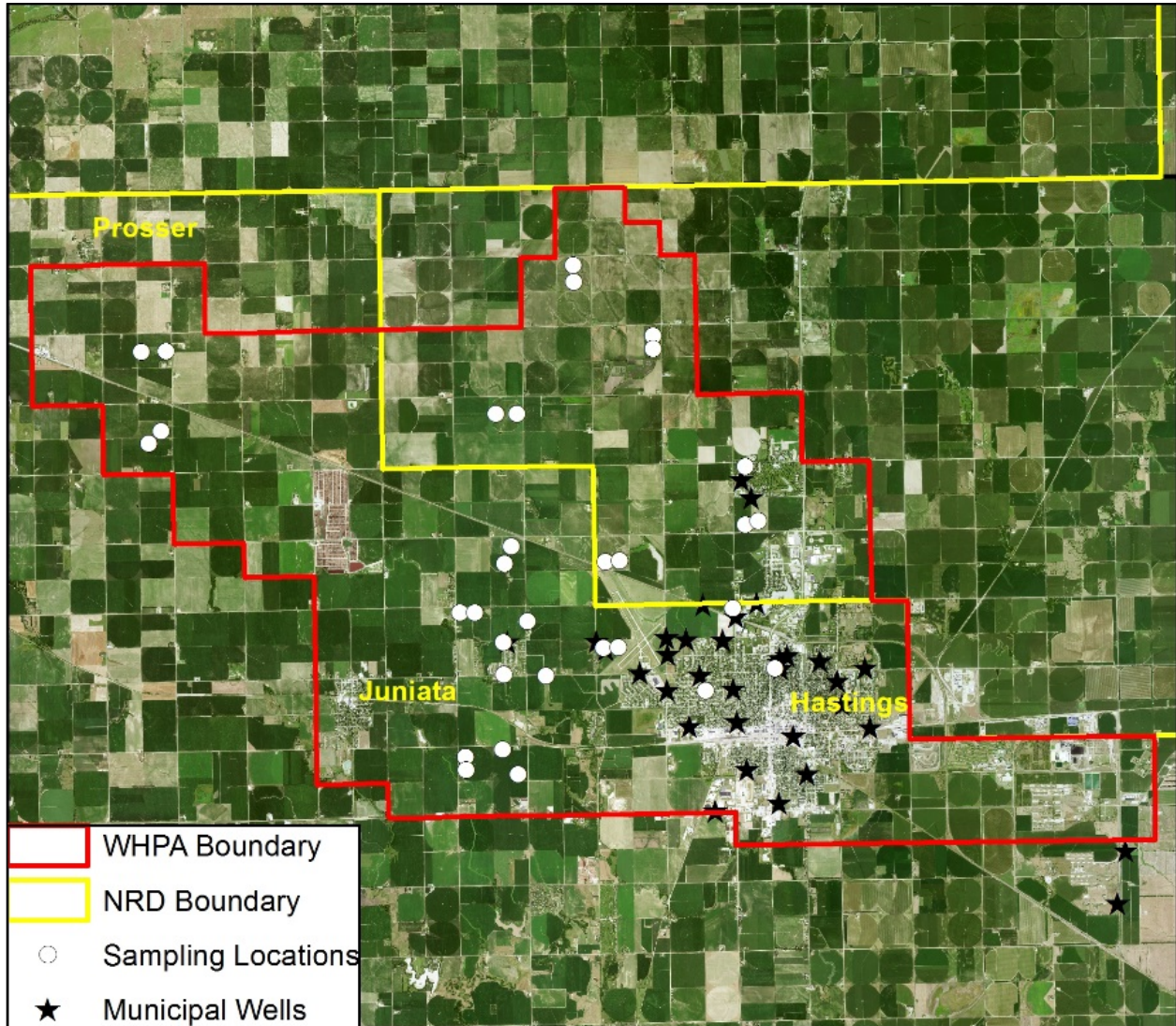


Figure 1: Natural Resource District and wellhead protection area (WHPA) surrounding Hastings, NE

Locations for vadose zone core collection and municipal supply wells within the WHPA can be seen in **Figure 1**. This map along with all other ArcGIS maps are displayed using a Lambert Conformal Conic projection. The coordinate system used is NAD_1983_StatePlane_Nebraska_FIPS_2600_Feet. Characterization of soil characteristics, land use, and low-lying land can help municipalities detect areas that are vulnerable to nitrate-N and other contaminant leaching. Hastings, NE has designated a WHPA, which contains the city's municipal supply wells.

Topography

The topography in the area of study is a mix of flat valleys running parallel to the Platte River and neighboring plains consisting of glacial, wind, and alluvial deposited sediments. Elevation data shows the lowest-lying areas in the southeastern portion of the map. The land surfaces gently slope south to southeast, except in the areas where streams sharply dissect the uplands (Hastings Utilities, 1997). Examining elevation gradients at a site-by-site scale can indicate areas where ponding may occur, activating preferential pathways and expediting fluid transport rates.

Land Use

To simplify land uses depicted in **Figure 2**, the data was reclassified to reduce the number of categories. All dryland crops and irrigated crops were grouped together. These included alfalfa, corn, soybeans, grains, sorghum, and sunflower. Other agricultural land was combined with summer fallow. The primary land use is cropland consisting of irrigated hybrid corn with some soybean rotation. Land use in the area consists of 61% irrigated agriculture, totaling 283 mi². Dryland makes up only 16%, totaling 73 mi². Corn makes up 56% of the irrigated and dryland agriculture in Figure 3, with soybeans being the next most widely-planted crop.

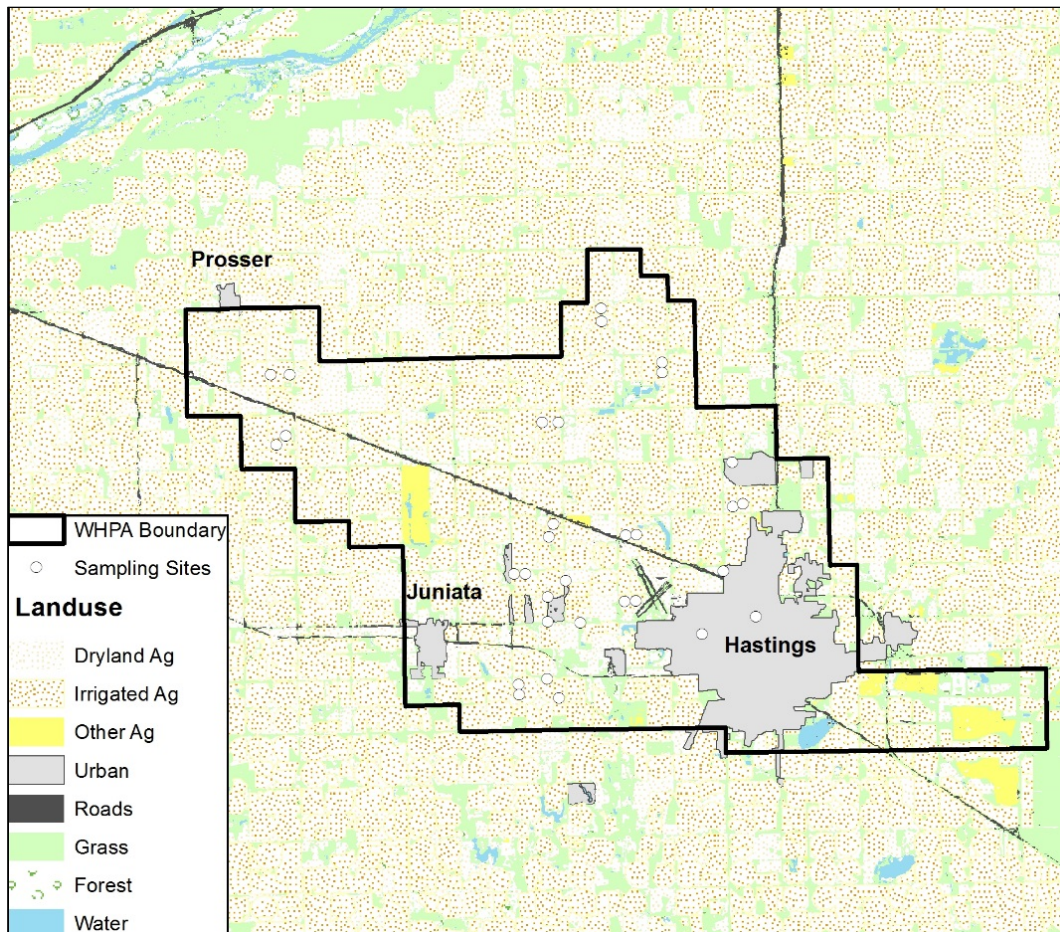


Figure 2: Land use type in the Hastings' WHPA and its surroundings

Geology

Soil classifications at the different sampling locations were collected using the USDA web soil survey (USDA, 2014).

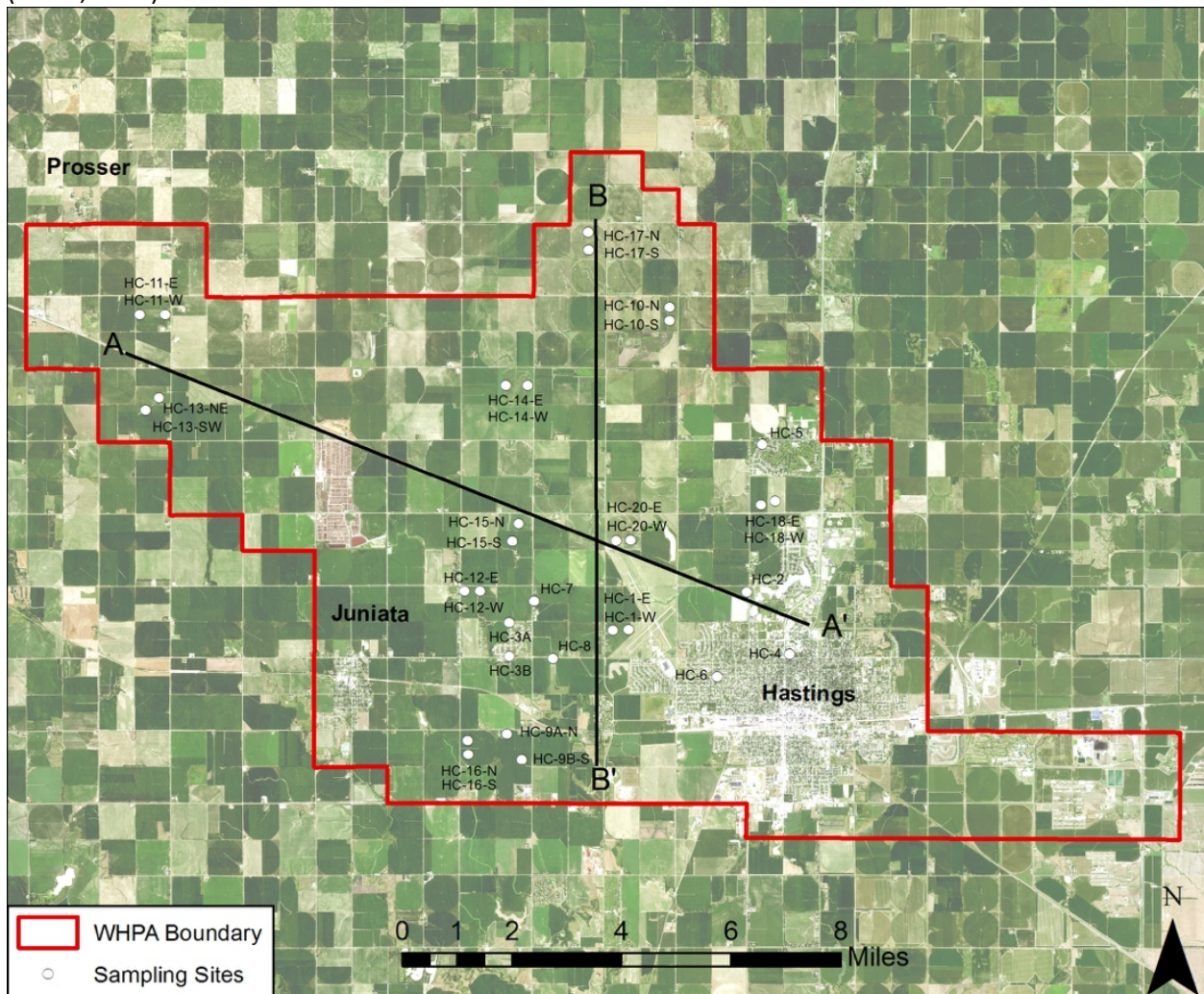


Figure 3: Map of the study site with locations of coring locations used to develop two cross-sections that display the geology of the WHPA

In **Figure 3**, two additional cross-sections were generated from 16 coring locations within the WHPA. All lithologic descriptions used to generate the cross-sections were taken during core breakdown in the Water Sciences Laboratory. The A – A' cross-section generated in Figure 4 was drawn from northwest to southeast. It is ~10 miles in length, has an elevation gradient of ~100 ft, and generally follows the groundwater flow of the underlying aquifer. A number of sand lenses can be observed throughout the cross-section, but primarily in the southeastern end at sites HC-2, HC-4, and HC-20-W. The sand lenses in this area are present 70 and 90 ft below the surface. The shallowest portion of the groundwater intersects a sand layer roughly 100 ft below the surface. To the northwest, the groundwater intersects with layers of silts and clays, with alternating sand and clay layers overlying this area. The B – B' cross-section generated in Figure 5 was drawn north to south, just west of the Hastings city limit. The elevation of the ten-mile long cross section generally averages ~1,970 ft. Sand lenses can be observed

primarily in the southern end at sites HC-1-W, HC-7, HC-8, HC-15-N, and HC-20-W. Like Figure 4, these lenses are present 70 and 90 ft below the surface. This region, along with the far northern section containing HC-17, has an additional sand lens present at 30 ft below the surface. The shallowest portion of the groundwater intersects a sand layer 100 ft below the surface, extending the length of the cross-section. Throughout the unsaturated zone, alternating clay and silt layers are present and average roughly 10 ft in thickness. Numerous deposits of alluvial clay and eolian silt and sand were too thin to be represented in **Figure 4** and **Figure 5**.

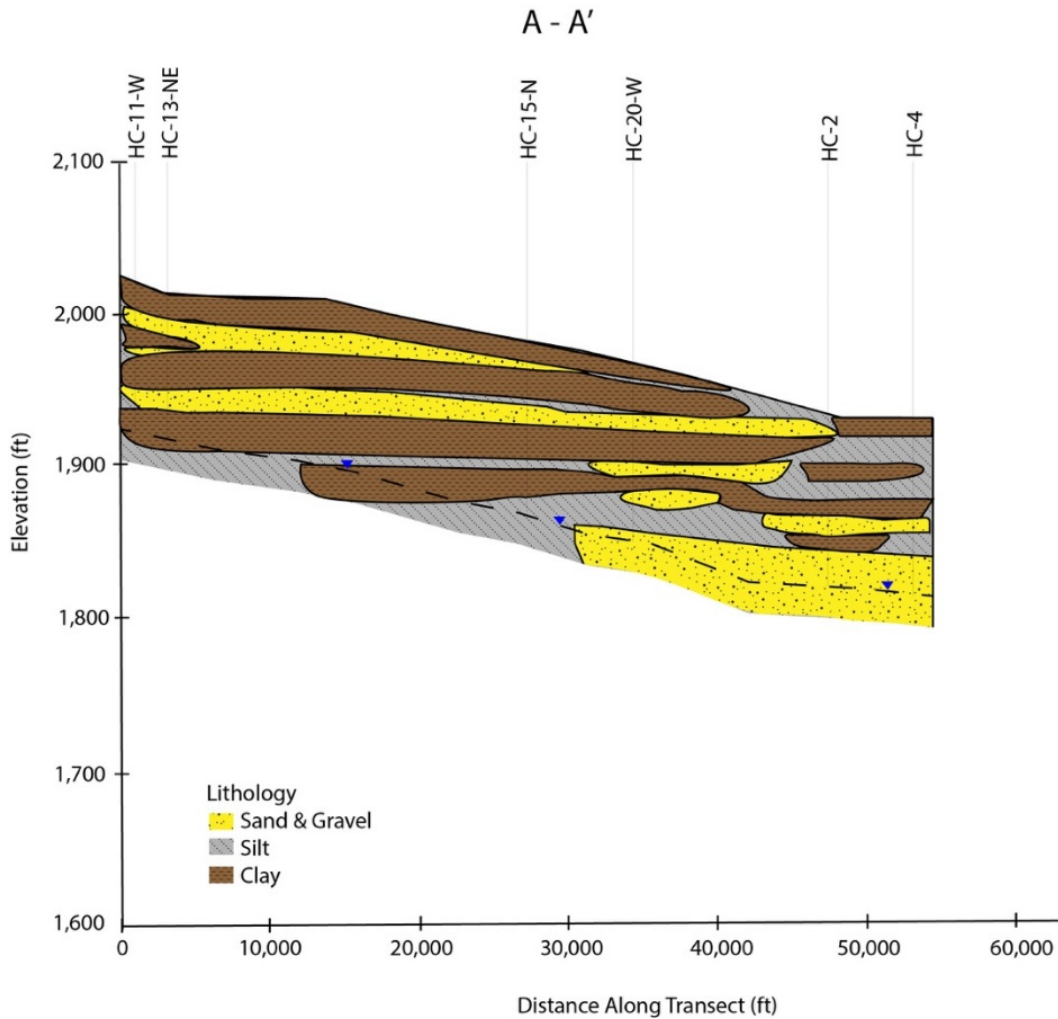


Figure 4: Lithologic cross-section of A – A'

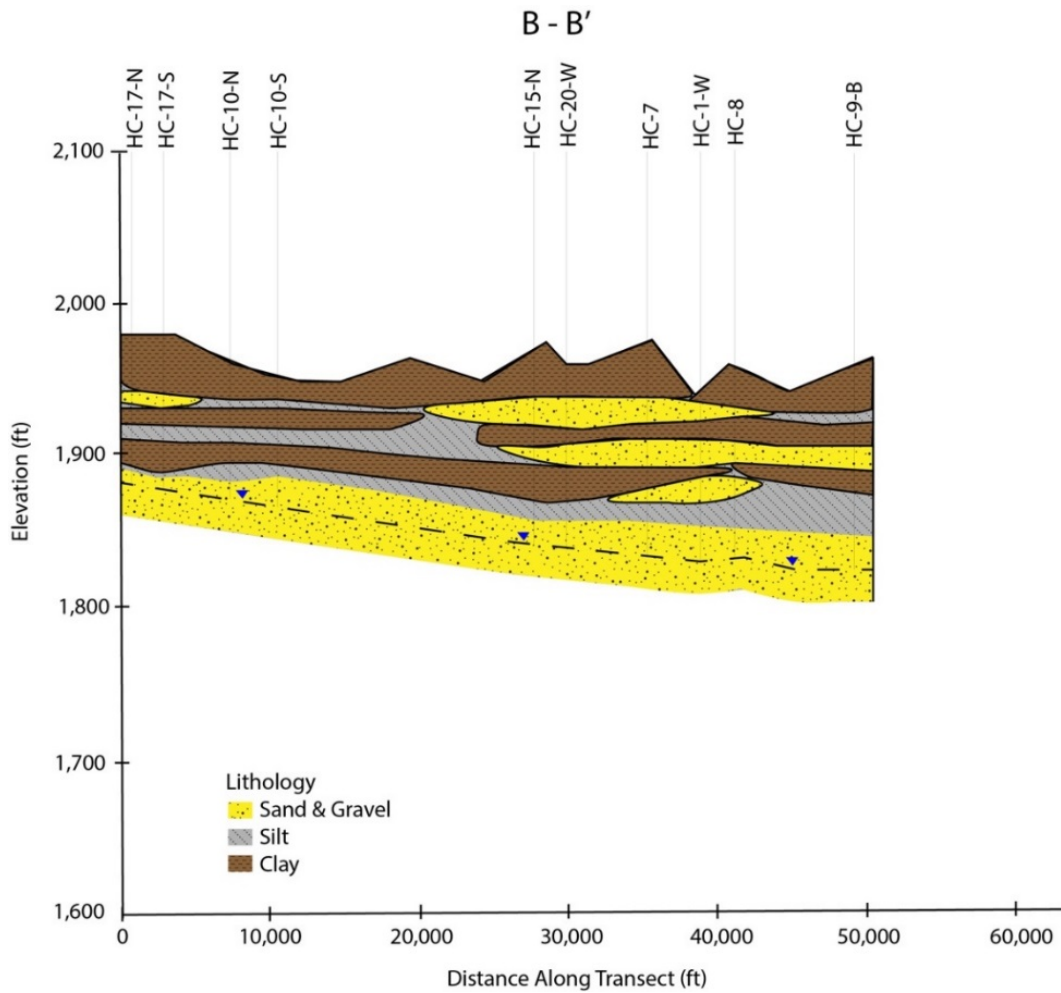


Figure 5: Lithologic cross-section of B – B’

Sediment type and soil organic matter content for Adams and Hall County were made available by the USDA Soil Survey (Soil Survey Staff, 2017). Areas with higher amounts of soil organic matter could increase potential for denitrification at the surface. Ammonium can sorb to organic matter, preventing its downward movement.

Hydrogeology

The city of Hastings, NE municipal wells pump directly from the Ogallala and High Plains Aquifer system. Beneath the WHPA, the thickness of the unconsolidated aquifer is roughly 100 ft. Below the aquifer lies the Ogallala bedrock formation, containing unconsolidated deposits of Pleistocene-age and semi-consolidated deposits of Tertiary-age sand, silt, and clay (Little Blue NRD, 2011). This formation covers one-fifth of Adams County (Keech & Dreeszen, 1968). Originally, these sediments most likely covered the entire area, but erosion from streams removed a large portion of deposits in Central Nebraska. The bedrock primarily contains lenticular deposits of sandstone, shale, chalk, and limestone (Hastings Utilities, 1997). No major faults exist in the study area that would impact the hydrogeology.

Groundwater travels into Adams County from adjoining areas to the North, West, and South (Keech & Dreeszen, 1968). Groundwater movement is augmented by precipitation, irrigation water, and well-withdrawals. Water pumped from the aquifer would otherwise move toward the Little Blue River valley and be discharged through evapotranspiration, seepage into the Little Blue River, or movement east as sub-surface outflow. The amount of groundwater being pumped from the aquifer reflects heavily on changes in irrigation rates due to seasonal differences in climate. A 1968 study sampled wells in Adams County for dissolved solids (Keech & Dreeszen, 1968). Dissolved solids ranged from 100 – 300 ppm, water in sandy soils had much lower concentrations than in areas with fine-textured soils. The groundwater composition was characterized as calcium bicarbonate type, some with increased hardness due to calcium and magnesium.

Unsaturated thickness maps were created using water table contours from a 2012 Cooperative Hydrology Study (COHYST) dataset and a two-meter LIDAR digital elevation model from the Department of Natural Resources **Figure 6**. It should be noted that groundwater levels fluctuate over time, so current unsaturated thickness may vary from that depicted in the figure. The unsaturated soil thickness in the alluvial valleys of the Platte River and the Little Blue River can be less than 10-ft thick with shallow groundwater generally occurring near stream channels. Thicker unsaturated zones can lengthen fluid transport rates, making the groundwater less vulnerable to certain contaminants. A previously drilled well three miles west of Juniata had an unsaturated zone as deep as 150 feet (Keech & Dreeszen, 1968). Of the 32 sites cored, residential sampling sites HC-3A and HC-7 have the deepest unsaturated zones, at 130 ft. Pivot irrigated sites HC-10-N and HC-10-S have a thickness of only ~80 ft.

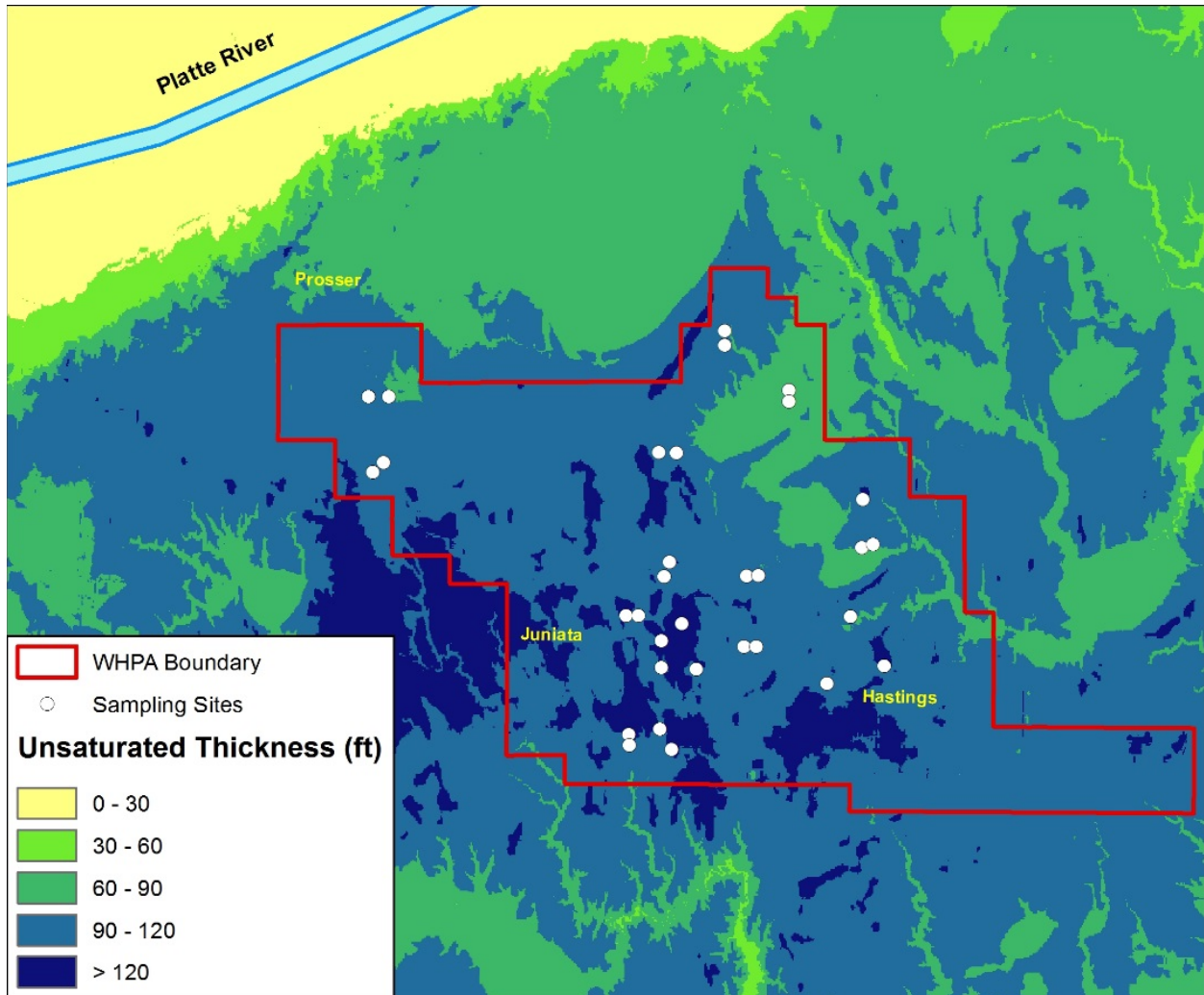


Figure 6: Unsaturated thickness in the Hastings' WHPA and its surroundings

The average rate of horizontal groundwater flow in Adams County ranges from 0.5 – 1 ft/day (Keech & Dreeszen, 1968). Water levels of some monitoring wells within the city of Hastings, NE fluctuate greatly due to large pumping from the Hastings Utilities wellfield (Hastings Utilities, 1997).

Spatial changes in groundwater nitrate-N concentrations from this area were evaluated using data from the Nebraska Agrichemical Clearinghouse database and used to examine spatial changes in groundwater nitrate-N over the last 25 years (**Figure 7**). In the 1990 to 2000 period, concentrations exceeding the MCL are visible under a portion of the Platte River Valley, with larger areas present north of Juniata and southeast of the Hastings. In the 2011 to 2015 period, the contaminated region along the Platte River Valley appears to have spread, consuming the town of Prosser. Groundwater within the WHPA starts to show high nitrate-N, with concentrations over the MCL present within the city limits of Hastings and its municipal supply wells. Groundwater nitrate-N concentrations increased in 68% of the total area between 1990 and 2015.

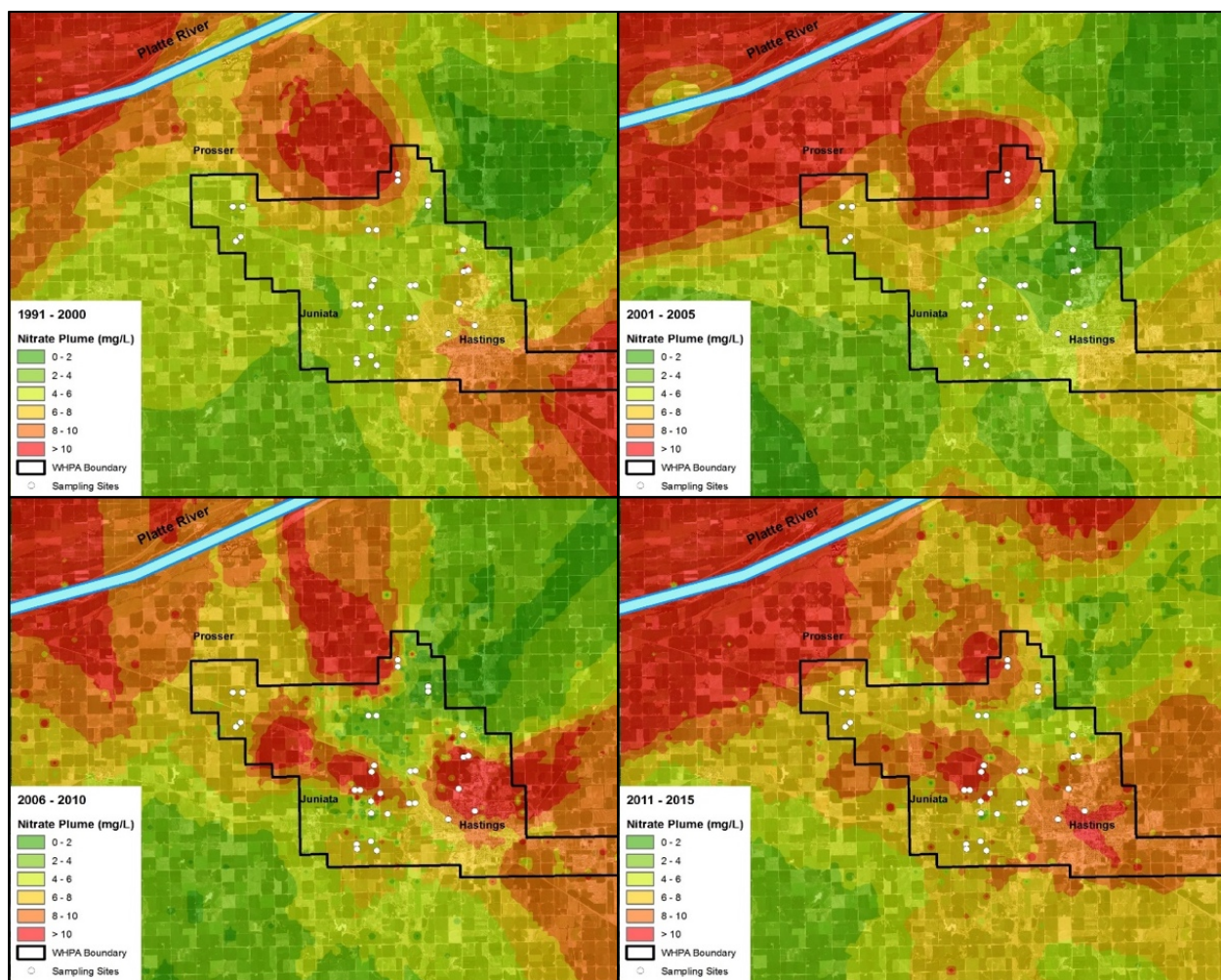


Figure 7: Changes in groundwater nitrate-N concentrations over a 25-year period in the Hastings' WHPA compared to vadose zone sampling sites using data from the Nebraska Agrichemical Clearinghouse database

Precipitation changes can affect nitrate-N accumulation and transport rates in the vadose zone. Average annual precipitation within the study area from 1941 to 1970 was found to be 25 inches (Hastings Utilities, 1997). During early 2012 through summer 2013, much of western and central Nebraska experienced drought. Precipitation totals in Hastings presented in **Table 1** reflect the last eight years, with only 20 inches of rain in 2012. The average for this time period was 26 inches.

A 1997 study conducted a 50-year groundwater travel assessment in the area of study (Hastings Utilities, 1997). Based on the model, it was estimated to take ~50 - 75 years for groundwater to travel from the Platte River to the municipal wells in Hastings. Using a modeling approach, source of groundwater within the WHPA was estimated to be 50% from the Platte River, 25% from irrigation recharge, and 25% from participation recharge.

Table 1: Annual rainfall precipitation for Hastings, NE over the last eight years

<i>Year</i>	<i>Rainfall (in.)</i>
2010	26.79
2011	27.12
2012	20.49
2013	25.25
2014	29.20
2015	29.89
2016	20.66
2017	30.28

Drilling and Retrieval of Core Samples

Data collected in this study builds on a 2010 UNL study funded by the Nebraska Environmental Trust and Nebraska Department of Environmental Quality to assist Hastings Utilities with management planning for safe source water (R. Spalding & Toavs, 2011). Continued sampling of this municipality will allow for a better correlation of nitrate-N concentration profiles and estimates of transport rates.

The current investigation used locations previously sampled to evaluate changes in stored nitrate-N over time and, wherever possible, penetrated the entire vadose zone to better estimate accumulated nitrate-N. Sampling sites were selected based on accessibility on previous locations and are shown in **Figure 8** and described in **Table 2**.

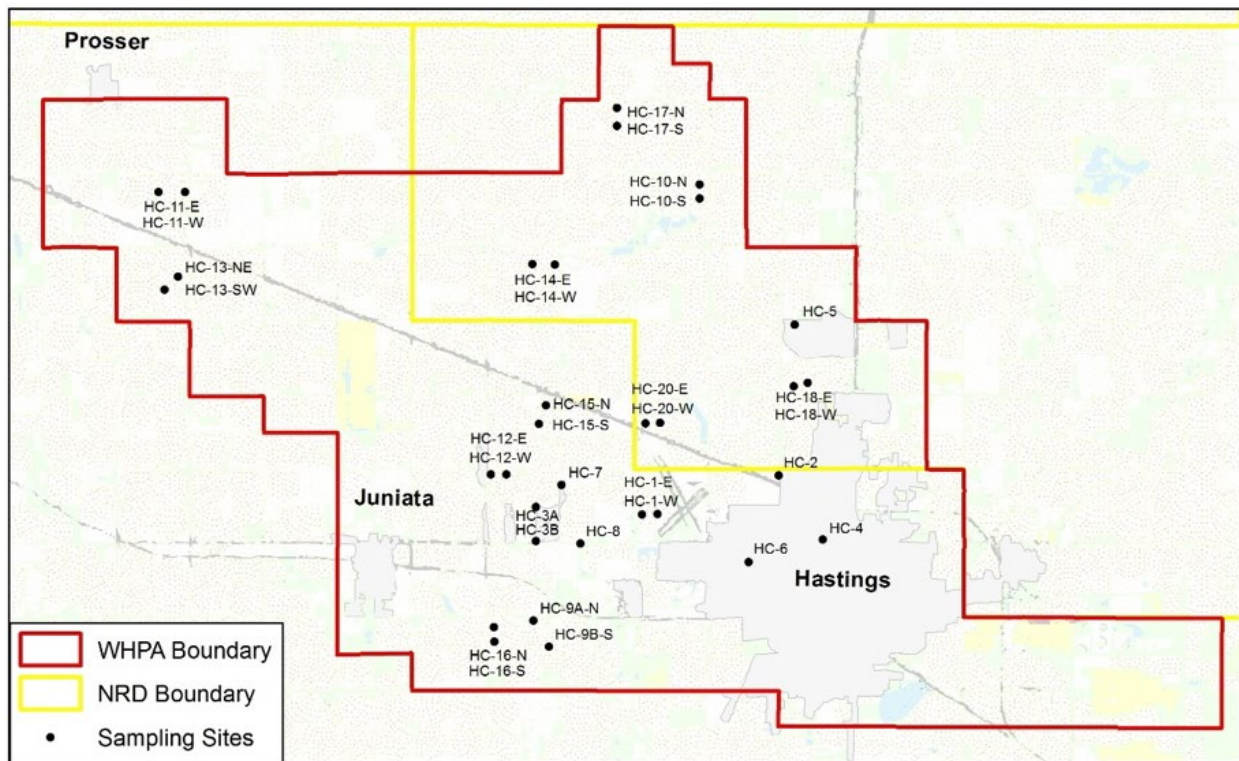


Figure 8: CME drill and Geoprobe vadoses zone core locations

Table 2: CME drill and Geoprobe vadoses zone cores and land use

<i>FID</i>	<i>Description</i>	<i>Land Use</i>
1	HC-1 Head (West)	Gravity irrigated
2	HC-1 Tail (East)	Gravity irrigated
3	HC-2	Non-irrigated
4	HC-3a (Marty)	Residential
5	HC-3b (Hurst)	Residential

<i>6</i>	HC-4	City Park
<i>7</i>	HC-5	Residential
<i>8</i>	HC-6	Residential
<i>9</i>	HC-7	Barnyard
<i>10</i>	HC-8	Barnyard
<i>11</i>	HC-9A (North)	Pivot irrigation
<i>12</i>	HC-9B (South)	Pivot irrigation
<i>13</i>	HC-10 Head (North)	Pivot irrigated
<i>14</i>	HC-10 Tail (South)	Pivot irrigated
<i>15</i>	HC-11 Head (West)	Pivot irrigated
<i>16</i>	HC-11 Tail (East)	Pivot irrigated
<i>17</i>	HC-12 Head (West)	Gravity irrigated
<i>18</i>	HC-12 Tail (East)	Gravity irrigated
<i>19</i>	HC-13 SW	Pivot irrigation
<i>20</i>	HC-13 NE	Pivot irrigation
<i>21</i>	HC-14 West	Pivot irrigation
<i>22</i>	HC-14 East	Pivot irrigation
<i>23</i>	HC-15 North	Pivot irrigation
<i>24</i>	HC-15 South	Pivot irrigation
<i>25</i>	HC-16 North	Pivot irrigation
<i>26</i>	HC-16 South	Pivot irrigation
<i>27</i>	HC-17 North	Pivot irrigation
<i>28</i>	HC-17 South	Pivot irrigation
<i>29</i>	HC-18 West	Pivot irrigation
<i>30</i>	HC-18 East	Pivot irrigation
<i>31</i>	HC-20 West	Pivot irrigation
<i>32</i>	HC-20 East	Pivot irrigation

Soil cores were divided into 2.5-foot intervals during drilling with either a CME hollow stem auger or Geoprobe Model 66DT direct push coring system. An ASTM standard guide for soil sampling from the vadose zone was utilized to ensure proper quality assurance practices (American Society for Testing and Materials, 1991). These drilling guidelines contributed to the proper capture of undisturbed cores and the avoidance of preventable sample loss. In 2016, coring at residential sites required a Geoprobe for sampling, which was unable to reach the groundwater table. The maximum coring depth at these sites was 60-70 ft. Fourteen agricultural sites experienced refusal during the coring process. Refusal occurs when the boring auger is unable to penetrate into deeper depths due to sediment compaction, typically in the form of cemented-sands. Any changes in observed lithology during core collection were documented in a field notebook.

Since initial coring in 2011, sites HC-10 and HC-11 have changed from gravity irrigation to pivot irrigation and these locations provide an ideal opportunity to evaluate the effect of pivot irrigation to nitrate-N leaching beneath these fields. Samples were collected throughout 2015 - 2017 before planting or after crop harvest. Vadose zone drilling operations were performed under the supervision of UNL's Field Service Coordinator Mathew Marxsen. All assisting staff followed an SOP (WSL SOP Field soil coring-001) for more detailed methodology (Appendix 1). Collected cores were used to help determine the impact of nitrate-N loading from potential nonpoint and point sources.

Nitrate, Ammonia and Pesticides

Core processing was completed at University of Nebraska Water Science Laboratory following standardized procedures (WSL SOP Processing Soil Core-001) described in Appendix 2. Lithologic descriptions were conducted during initial processing with profile descriptions summarized in the previous section. Soil moisture content and bulk density were determined by weighing a 2.5 cm aliquot of sample before and after drying at 105° C. Gravimetric water content was determined by taking the difference between the weights of the oven-dried soil from the initial soil and dividing by the weight of the oven-dried soil. A 5 g aliquot was mixed with 5 mL of DDI water. After 10 minutes the mixture was analyzed for pH using a pH electrode. Particle size analysis was completed in half of the cores collected to evaluate changes in hydraulic conductivity using an abbreviated method (Kettler et al., 2001). Determining soil particle size variation at different depths can contribute to the understanding of contaminant transport rates in the vadose zone.

Laboratory Methods

Nitrate-N and Ammonia-N

Nitrogen was determined using previously published methods for nitrate-N (Knepel, 2012) and ammonium-N (Hofer, 2003). Briefly, each 2.5 ft interval was described and subsampled for gravimetric moisture content, and divided lengthwise in half. One half was returned to the freezer for pesticide and pore water isotope measurement while the remaining half was air dried overnight. Dried intervals were homogenized in a Thomas-Wiley mill or mortar and pestle. A 10 g aliquot of homogenized sample was weighed into a flask, mixed with 100 mL of 1M potassium chloride (KCl), and shaken for 60 minutes. Extracts were then filtered, acidified with sulfuric acid, and frozen. Thawed extracts were subsequently analyzed on a Lachat 8500 flow injection autoanalyzer for nitrate-N using QuikChem Method 12-107-04-1-B (Knepel, 2012). Ammonium was analyzed using QuikChem Method 12-107-06-2-A (Hofer, 2003).

Concentrations of nitrate-N, pore water nitrate-N, ammonium-N, and moisture content were graphed versus depth for each of the 32 coring locations and compared to previous profiles. Expressing nitrate-N as pore water concentration reveals where in the profile plumes of nitrate-N exceed the MCL (Toavs & Spalding, 2011). Textural descriptions were used to generate unsaturated zone geologic profiles to identify areas of changing hydraulic conductivity and preferential flow. Comparison of zones of accumulated vadose zone nitrate-N may be tracked over time as they eventually move to and intercept the water table. Average nitrogen storage as nitrate-N was converted to lbs-N/Acre in the vadose zone to illustrate differences in accumulated nitrate-N between locations. Vadose zone profiles and accumulated nitrogen estimated in both the 2011 and 2016 study were compared and interpreted to evaluate impacts of nitrogen and water management at the surface. Land surface data was obtained and mapped for better prediction of changing land use effects, changing soil type/composition, and topography.

Pesticides

One hundred sixty-five samples evenly spaced from each core profile were analyzed for twenty-one residues of herbicides to provide a general screening across the Hastings WHPA. Sediments were processed using microwave assisted solvent extraction and pesticides were analyzed by gas chromatography-mass spectrometry (Cassada *et al.*, 1994). Two surrogates, terbuthylazine and butachlor, were added to check recovery on every sample. Stable isotope labelled atrazine, deethylatrazine (DEA), deisopropylatrazine (DIA) were added and used to quantify all residues.

Nitrate-N and Ammonia-N Concentrations in the Vadose Zone

Nitrate-N accumulations in the vadose zone beneath corn and soybean fields ranged from 230 to 1,400 lbs-N/Acre. These sites made up the largest majority of sampled sites; 23 of the 32 cores were collected beneath cropland, with cropland including both gravity and pivot irrigated fields, as well as one non-irrigated field (HC-2). Nitrate-N stored within the top 6 ft of soil has the potential to still be utilized by corn roots (R. Spalding & Toavs, 2011). Nitrate-N that has leached past 6 ft is not considered accessible to the crop and may travel further downward towards the water table.

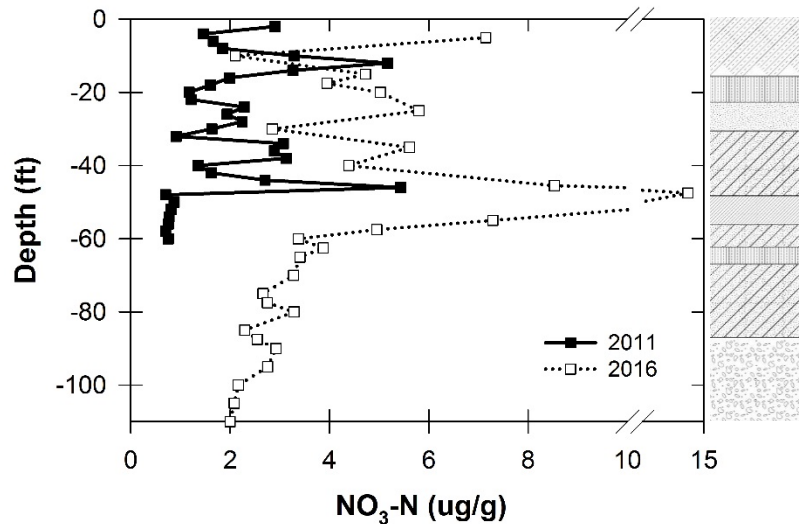


Figure 9: Nitrate-N in the vadose zone beneath gravity irrigated site HC-12-W.

Some agricultural sites showed increases in nitrate-N storage over the five-year sampling span, while others showed reductions. Overall, fluctuations of stored nitrate-N in producers' fields increased by 2,800 lbs-N/Acre. The average amount in 2011 and 2016 was 400 ± 140 and 520 ± 280 lbs-N/Acre, respectively, an increase of roughly 30%. Although totals increased, the stored amount in 2016 is similar to accumulations of nitrate-N at Clay Center, NE research plots taken in the mid-1990's underneath tilled cropland which totaled ~ 530 and ~ 620 lbs-N/Acre (Katupitiya, 1995). The largest difference was found beneath the gravity irrigated site HC-12-W seen in **Figure 9**, which went from 420 to 1,400 lbs-N/Acre in the top 60 ft. This site is located at the head of the field, while HC-12-E is located at the tail-end of the field. HC-12-W contained 590 lbs-N/Acre in 2016. Furrow irrigation systems present at sites like HC-12 typically have greater deep percolation of water loss at the upstream head of the field (Katupitiya, 1995). Water percolation at gravity irrigated locations like HC-12-W may be responsible for larger amounts of leached nitrate-N present in the underlying sediment. More sufficient

information on irrigation rates is needed to determine with more certainty the cause for changes in stored nitrate-N at the sampling locations.

Higher rates of nitrate-N leaching at gravity irrigated sites is common due to less uniformity in irrigation water applications. This lack of uniformity can lead to furrows being over-irrigated, causing ponding of water (Hergert & Shapiro, 2015). Rapid preferential flow of nitrate-N in low-lying regions can result in excess leaching along with overall reductions in crop yields. In contrast, pivot irrigated fields apply water more uniformly. Another potential cause of increases in leached nitrate-N may be from changes in N-fertilizer application. A 1988 study done near Clay Center found that vadose zone nitrate-N accumulations approximately doubled at plots with each 100 lbs-N/Acre/yr increase in N-fertilizer (R. F. Spalding & Kitchen, 1988).

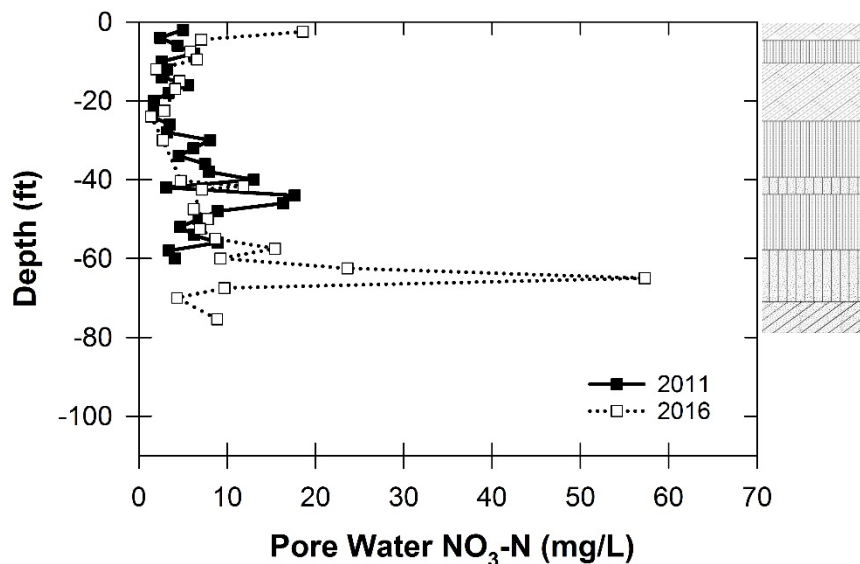


Figure 10: Pore water nitrate-N at dryland corn site HC-2.

Dryland site HC-2 showed a reduction in nitrate-N over the five-year span, although it was the smallest measured variation among all of the cored locations. The site contains an estimated 170 lbs-N/Acre in the top 60 ft, which was the lowest accumulation of comparable nitrate-N from the 2016 sampling. Maximum pore water nitrate-N was observed at 65 ft below the surface **Figure 10**, otherwise concentrations were below 10 mg/L. When summing the entire 75 ft profile from 2016, the total amount of nitrate-N is still relatively low at 250 total lbs-N/Acre. A zone of elevated nitrate-N was observed in a 15 ft deep layer of silty sand. In contrast to pivot and gravity irrigated locations, HC-2 would reflect nitrate occurrence and transport beneath dryland corn. A study done in Minnesota found groundwater nitrate-N concentrations in the Anoka Sand Plain Aquifer were significantly higher at irrigated sites than non-irrigated (Anderson Jr., 1993). Based on the low totals of nitrate-N stored in the vadose zone beneath site HC-2, one could expect lower nitrate-N leaching rates from this and other dryland fields than irrigated fields.

Significant leaching from irrigated fields may be avoided if irrigation water is properly scheduled and managed (Bobier et al., 1993). Inefficient irrigation or other management practices can be responsible for higher amounts of leached nitrate-N from certain irrigated cropland locations. In a 1993 study, transport rates of nitrate-N in similar fine-textured sediments were determined to be approximately 30

in./yr (Bobier et al., 1993). If this nitrate-N transport rate were applied to the vadose zone in Hastings' WHPA we should expect to find 12 - 14 ft of vertical movement over the 5-year period between 2011 and 2016.

Stored Nitrate-N beneath fields converted from gravity to pivot irrigation

Irrigated agricultural sites HC-10-N, HC-10-S, HC-11-E, and HC-11-W were gravity irrigated at the time of the 2011 sampling, as discussed in Section 1.1. Between the past and recent samplings, they have been converted to pivot irrigated cropland. Ariel imagery in Figure 1 shows the irrigation change occurring sometime between winter 2010 and fall 2011. Site HC-11 appears to have converted to pivot irrigation between spring 2014 and fall 2015. Before being converted to pivot irrigation, these fields may have experienced greater instances of mid-field ponding of irrigation water, which can result from furrows blocked by stalks and stover (R. Spalding & Toavs, 2011).

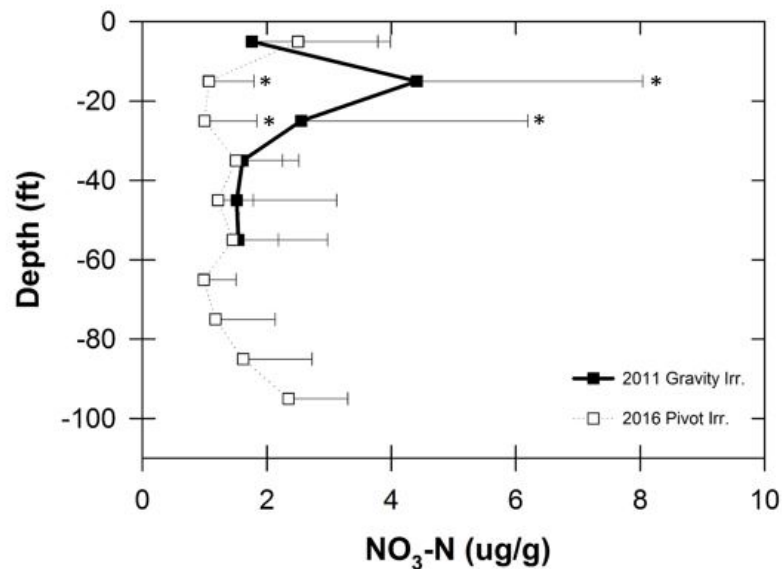


Figure 11: Average nitrate-N of gravity irrigated sites in 2011 that have since converted to pivot irrigation. Asterisks indicate a statistical significance (p-value ≤0.05) between the two groups at a particular depth.

In **Figure 11**, differences in average nitrate-N are evident. There is an average reduction of approximately 170 lbs-N/acre in the top 55 ft of the profile over a five-year time span. Ammonium-N findings weren't discussed in the 2011 Hastings vadose zone study report and methods of analysis were not reported, making comparisons of ammonium-N between the two sampling periods challenging. Differences in ammonium-N between the two sampling periods were not compared due to consistently lower 2011 concentrations, potentially due to improper sample storage. A statistically significant difference in nitrate-N was present at a depth of 15 and 25 ft. This reduction may be due to differences in how water applications were applied. Current pivot irrigation methods could apply water more uniformly and at times when crops can more readily absorb both the water and the nutrients. A 1990 study deemed effective irrigation management as a highly effective BMP to protect groundwater quality (Logan, 1990). If irrigation water wasn't properly scheduled or over-applied during gravity irrigated seasons, excessive leaching may have led to the higher amount of nitrate-N stored in the unsaturated

zones of these sites. Efforts to convert from gravity to pivot irrigation should be encouraged, especially in agricultural land within capture zones of municipal wells, such as those within the Hastings' WHPA.

Nitrate-N accumulations in sites beneath urban irrigated lawns

Unsaturated zones beneath residential homes also showed both positive and negative fluctuations of nitrate-N between the five-year sampling span. Urban sites HC-3A and HC-3B are located in a newly-developed suburb west of Hastings, three miles east of the village of Juniata. It is possible that nitrate-N stored at deeper depths under these sites was impacted by previous land use practices. Sites HC-3A and HC-3B showed increases of 280 and 200 lbs-N/Acre, respectively. The larger increase of nitrate-N at HC-3A is speculated to be from nutrient rich runoff coming from a chemigated agricultural field located a ½ mile east of HC-3A. Since 2010, the pivot irrigated NE ¼ and drip irrigated NW ¼ of this field has been permitted to chemigate, a process which utilizes fertilizer injected water to simultaneously irrigate and fertilize crops. Chemigation can improve yields but also lead to water quality issues (Hergert & Shapiro, 2015). Excess water coupled with applications of liquid nitrogen can lead to more leaching within crop rows of agricultural land. Additionally, surface runoff to down-gradient areas and windblown spray to up-wind areas have the ability to deposit unwanted nitrate-N at neighboring areas (Anderson Jr., 1993).

Overall, the estimated amount of nitrate-N stored in lawns decreased by 840 lbs-N/Acre. The average amount in 2011 and 2016 was 480 ± 440 and 270 ± 200 lbs-N/Acre, respectively. However, the overall decrease beneath urban locations can largely be attributed to a dramatic reduction in stored nitrate-N at site HC-6, an urban lawn located within the city of Hastings. This site contained the largest amount of stored nitrate-N (1,200 lbs-N/Acre) under all 32 sites in 2011. In 2016, this site was estimated to contain only 36 lbs-N/Acre, a decrease of 1,200 lbs over the five-year span. The 2011 plot in **Figure 12** shows a large peak extending from 6 - 20 ft beneath the lawns surface. This peak was expected to have been introduced five to ten years prior to the 2011 sampling from non-uniform fertilizer application, given the relatively low values of nitrate-N throughout the rest of the profile (R. Spalding & Toavs, 2011). The 2016 plot in Figure 12 shows both nitrate-N and pore water nitrate-N have decreased significantly throughout the profile and the large peak present in 2011 is no longer visible.

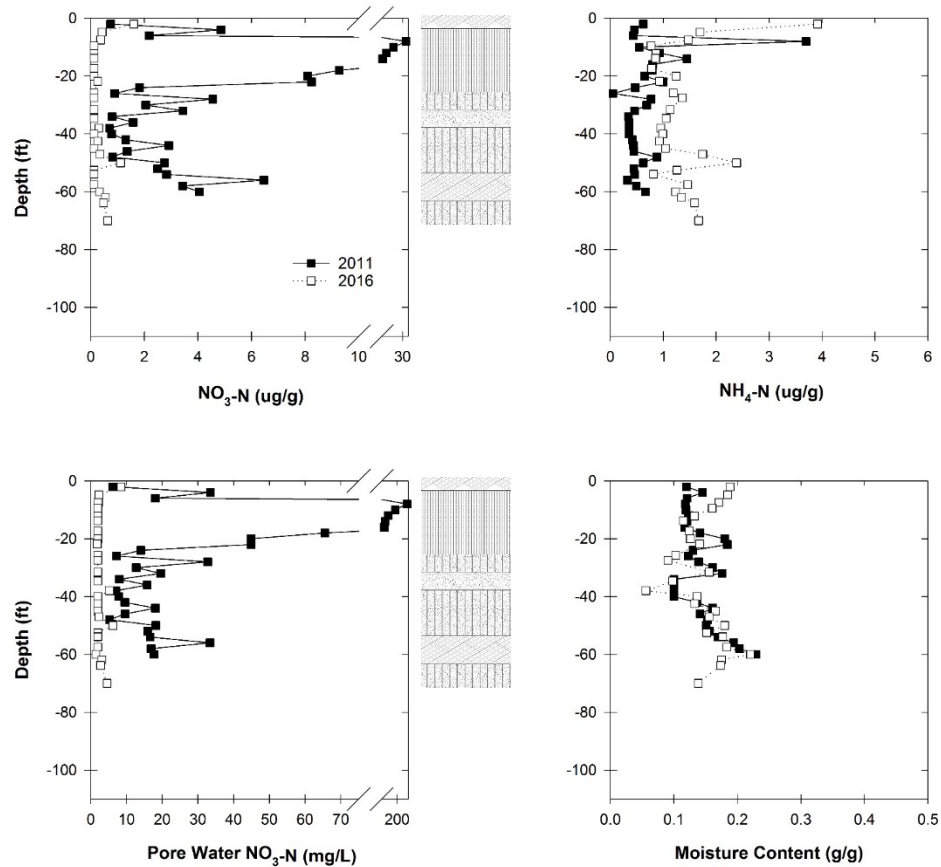


Figure 12: Profile characteristics beneath urban lawn site HC-6.

Although it is not certain what may have caused this drastic decrease, there are several possibilities that may have individually or in tandem contributed to the decrease in stored nitrate-N. For instance, fine-textured sediments underneath this site or others can prohibit the oxygen diffusion through the soil (Adelman et al., 1985). Anoxic conditions along with the presence of organic matter may have increased microbial denitrification, converting portions of the stored nitrate-N to nitrous oxide and nitrogen gas. Soil microbes could have also converted the tied-up nitrogen back into ammonium-N through mineralization, although 2016 concentrations of ammonium-N at HC-6 averaged only $1.3 \pm 0.63 \mu\text{g/g}$. Concentrations of ammonium-N in 2011 were lower ($0.67 \pm 0.62 \mu\text{g/g}$) but as mentioned previously, this increase in ammonium-N between sampling periods was common across nearly all of the sampling locations.

Historical application of fertilizer at site HC-6 was not made available, but given estimated transport rates of nitrate-N we would expect changes in landowner management practices to only be reflected within the top 12.5 ft. This may explain decreases in nitrate-N content in the upper 12.5 ft, but not below. Wetting fronts in the thick, lithologically varied WHPA unsaturated zone often travel from coarse sandy sediments into clay layers, such as those present 5 - 25 ft and 55 - 65 ft below the surface of HC-6. The small pores within the clay layers hold the water more tightly and can halt vertical movement (UNL Plant & Soil Sciences, 1999). The slowing of the wetting front causes water to move laterally in the overlying coarse sediment, which can lead to perched water tables. Drainage of water in coarse-grained sediments such as those present in HC-6 can be impeded by fine-grained sediment, increasing the chances of lateral movement between the two different layers (McMahon et al., 2003). Nitrate-N in the

pore water of the sandy loam may have been prevented from vertical movement when it reached a barrier of fine-textured sediment. Horizontal flow may have caused stored nitrate-N at HC-6 to travel away from the small cored area (0.034 ft²) into adjacent sediment. However, matric-potential measurements along these contacts would be needed to verify the occurrence of horizontal flow.

Unsaturated zones beneath barns and parks all showed increases in nitrate-N over the five-year span. Sites HC-7 and HC-8 are located in barnyards but are surrounded by irrigated agricultural land. In 2016 these sites contained 590 and 690 lbs-N/Acre in the top 60 ft, respectively. These totals are higher than 2016 accumulations at urban irrigated lawn sites. However, accumulations are lower than those at abandoned barnyard sites sampled in 2010 in Edgar, which contained 100 µg/g pulses of nitrate-N and exceeded 2,000 lbs-N/Acre in the top 45 ft (Olsson Associates, 2011). In contrast, spikes of nitrate-N under barnyard sites in Hastings didn't exceed 9 µg/g, with the largest spike located ~50 ft below the surface, as shown in **Figure 13**. Overall, the amount of nitrate-N stored under barnyard and residential park sites increased by 300 lbs-N/Acre. The average amount in 2011 and 2016 was 260±120 and 560±130 lbs-N/Acre, respectively. Portions of the nitrate-N in these regions may have accumulated from manure leachates, fertilizer applications at surrounding properties, and/or sub-surface horizontal flow of nitrate-N-rich water fronts from neighboring agricultural fields.

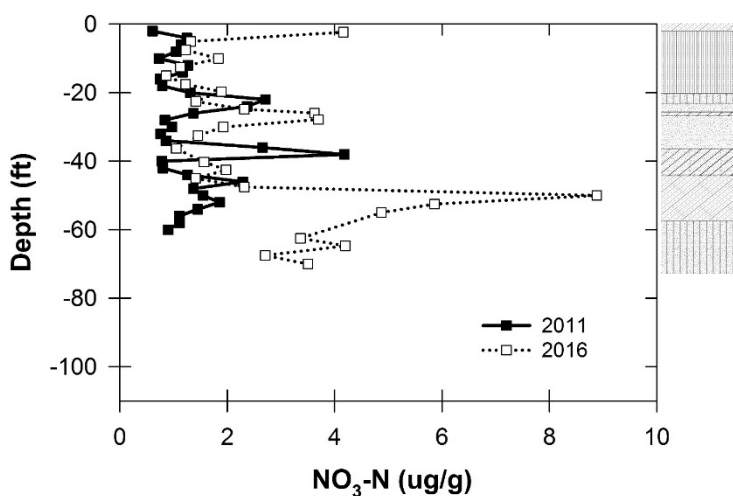


Figure 13: Nitrate-N in the vadose zone of barnyard site HC-7.

Differences between urban and rural groundwater nitrate-N concentrations can be both significant or negligible (Wakida & Lerner, 2005). Groundwater contamination by nitrate-N in urban areas typically comes from fertilizer application, as well as wastewater and solid waste disposal. A 2017 study found that rapid growth of residential land increased pools of reactive nitrogen in lawns (Raciti et al., 2017). Housing density and the availability of nitrate-N in residential soils were both determined to be useful indicators of groundwater quality on a landscape-scale. The amount of leaching in residential locations, such as site HC-6 depends on factors similar to agricultural regions. These include management practices such as water input, fertilizer usage, and land use within the urban environment.

Comparisons of stored nitrate-N and ammonium-N among different land uses

Unsaturated zones beneath urban irrigated lawns, gravity irrigated cropland, and pivot irrigated cropland collected in 2016 were grouped together and compared to show differences in average nitrate-N and ammonium-N among different types of land use. In Nebraska, most groundwater nitrate-N

comes from intensely irrigated cornfields (Hergert & Shapiro, 2015). The primary irrigation types within the Hastings' WHPA are made through gravity and pivot technologies. Pivot irrigation makes up 67% of the irrigation systems in South Central Nebraska (Hergert & Shapiro, 2015). There has been a movement to convert from primitive forms of irrigation (i.e., drip irrigation) to pivot irrigation. A 1998 study found that crop yields in large pivot irrigated fields (>160 acres) were typically higher than similar-sized drip irrigated fields (O'Brien et al., 1998). This is because pivots can make more uniform, properly timed applications. Even with increased yields, the amount of fertilizer applied to pivot irrigated fields typically remains the same due to improved timeliness of water applications.

In Hastings and the surrounding area an average annual water application of 7.38 ± 1.72 in./acre was applied to all irrigated land between 2012 and 2017 (Hastings Utilities, personal communication, March, 28, 2017). The largest annual amount (10.7 in./acre) was applied in 2012, which coincides with drought-like conditions and the lowest amount of annual rainfall during the five-year period. Although water applications of gravity and pivot irrigation were not reported separately, it is likely that the water efficiency of the pivot irrigated fields was greater than fields utilizing gravity/flood irrigation systems, especially if the pivots were low pressure (<30 psi) (Johnson et al., 2011). Irrigation rates for four urban irrigated lawns were reported between 2012 and 2016. Average urban application rates at these sites was lower and more variable than the irrigated cropland annual average, at 5.78 ± 5.07 in./acre. Similar to the total irrigated land, the largest annual average application at the urban sites was in 2012 at 9.53 in./acre. These homeowners apply their water using a mixture of manual sprinklers, underground sprinklers, and hoses. In the U.S., landscape irrigation makes up 40 - 70% of household water use and automated underground irrigation is the predominant method used to irrigate (Haley et al., 2007).

Soil in the WHPA is primarily a silt loam, which relative to other types of soil has a high available water capacity of 2.00 - 2.50 in./ft of depth (UNL Plant & Soil Sciences, 1999). Since the soil only has the ability to hold this much water, water applied in excess of this can leach past the crop's root zone into the unsaturated zone. Water use and management practices have large influences on the ability of nitrate-N to leach past the root zone (Anderson Jr., 1993). Differences in irrigation rate and type may impact the amount of water diffusing into the vadose zone. Unsaturated zones beneath the top 65 ft of urban irrigated lawns, pivot irrigated farmland, and gravity irrigated farmland had an average gravimetric water content of 0.14 ± 0.02 , 0.17 ± 0.04 , and 0.17 ± 0.04 g/g respectively.

Although urban lawns contained a lower amount of average water stored in the unsaturated zone than irrigated cropland, there was no difference between the water content of the pivot and gravity sites. The water content among both of these irrigation types generally decreased with depth, decreasing from $\sim 0.22 \pm 0.03$ g/g in the root zone to $\sim 0.05 \pm 0.05$ g/g at 105 ft deep. Depth to groundwater varied but averaged $\sim 100 \pm 8.50$ ft when sites were collected without experiencing refusal. It is possible that other sites have been converted from gravity to pivot irrigation in the last >five years. This may explain the similarities in average moisture content between the two irrigation types. Additionally, the proper timing and amount of water applied at gravity irrigated fields may have prevented runoff, ponding, or leaching from occurring during application periods.

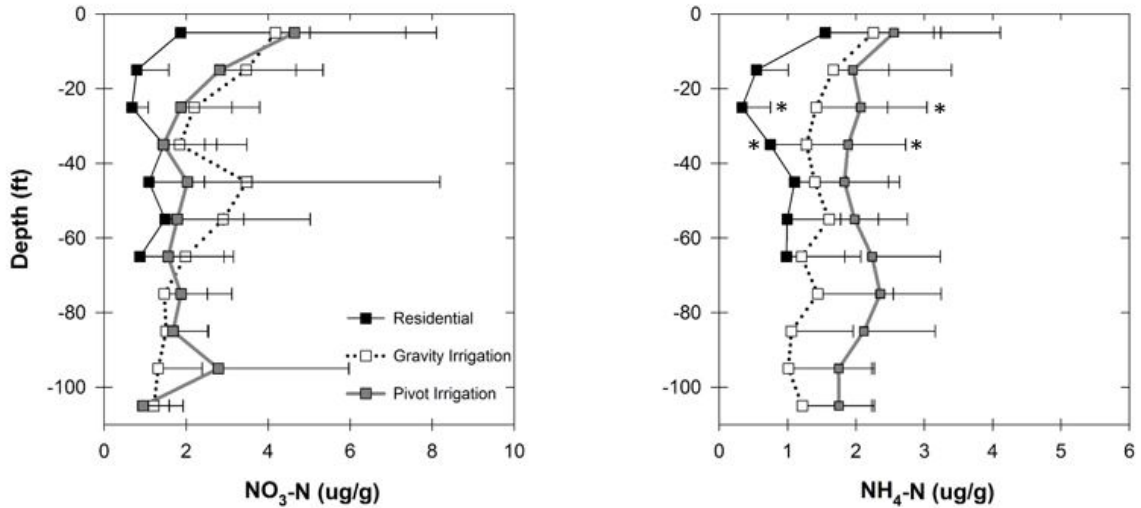


Figure 14: Average nitrate-N and ammonium-N of three different land use groups collected in 2016. Asterisks indicate a statistical significance (p -value ≤ 0.05) between different groups at a particular depth.

Land owner surveys indicated that on an average, 175 lbs-N/Acre is being applied to irrigated cropland fields within the WHPA. The recommended fertilizer application rate set by the UNL Irrigation and Nitrogen Management User Education/Certification Program for South Central Nebraska is 201 lbs-N/acre (Hergert & Shapiro, 2015). Recommended fertilizer rates with a corn and soybean rotation are lower, with no form of nitrogen fertilizer required during soybean season. Most of the farmers applied anhydrous ammonia for their source of nitrate-N in the spring. Some surveys indicated split applications were performed in more recent years. The WHPA is classified by the NRD as a GWMA, which regulates scheduling of fertilizer and irrigation applications (The Little Blue NRD, 2013). For instance, anhydrous ammonia may not be applied prior to November 1st and nitrification inhibitors must be used with fertilizers applied between November 1st and March 1st.

GWMA regulations are less strict for urban home owners. Most restrictions are directed towards lawn care services and those who fertilize >one acres of lawn. Survey responses from urban home owners indicated that most followed the recommendations set by their lawn fertilizers. A common brand of fertilizer (Scotts Lawn Food) recommends four split-applications of nitrogen fertilizer totaling 151 lbs-N/Acre. The typical application amount for urban lawns is lower than that of agricultural fields, but still plays a significant role in groundwater nitrate-N contamination due to large housing densities in Hastings and Juanita. The amount of leaching in these urban locations depends on factors similar to those of agricultural regions (Raciti et al., 2017). Management practices such as irrigation type and amount within an urban environment can impact leaching potential. Not enough land use data for urban and agricultural information was received to make site-specific statements about how fertilizer applications were impacting nitrate-N leaching. However, based on a previous study it is expected that vadose zone nitrate-N accumulations would approximately double at sites with each 100 lbs-N/Acre/Yr increase in N-fertilizer (R. F. Spalding & Kitchen, 1988).

Cumulative nitrate-N beneath the top 65 ft in 2016 for urban irrigated lawns, pivot irrigated farmland, and gravity irrigated farmland had an average of 320, 540, and 700 total lbs-N/acre respectively. Although no significant differences in nitrate-N were present at the different depths, trends of higher average nitrate-N under farmland vadose zones shown in **Figure 14** were present. On average, farmland

had nearly double the nitrate-N of urban irrigated lawns. Between irrigation methods, gravity sites had the largest amount of stored nitrate-N on average, 30% more than pivot irrigated sites. Nitrate-N is typically stored as pore water in sediments and can move with excess irrigation water.

The average pore water nitrate-N for urban irrigated lawns, pivot irrigated farmland, and gravity irrigated farmland was 10.66 ± 4.58 , 14.88 ± 2.75 , and 18.73 ± 4.71 mg/L respectively. Pore water nitrate-N was 25% higher in gravity irrigated profiles than pivot irrigated fields. Average pore water nitrate-N at each depth shown in **Figure 15** for urban irrigated lawns was lower except at 35 ft, which contained an average of 19.47 ± 27.51 for urban sites. The high variation at this depth can be attributed to site HC-3A, which contained >100 mg/L pore water nitrate-N 32 ft below the surface. Average pore water concentrations for both pivot and gravity irrigated farmland was at or above the MCL at each measured depth. Once a depth of 65 ft was reached, average concentrations showed steady increases with each 10 ft, increasing from 14.59 ± 6.29 to 39.48 ± 35.40 mg/L at gravity irrigated sites and 16.80 ± 17.42 to 45.09 ± 61.67 mg/L at pivot irrigated sites. As depth increases, sediments in the WHPA typically become sandier and hold less moisture. This is made apparent in **Figure 15**. Average moisture content from 65 to 105 ft decreased in gravity and pivot sites from 0.14 ± 0.07 to 0.06 ± 0.07 and 0.12 ± 0.05 to 0.04 ± 0.03 g/g, respectively. Even with low moisture content, there are still large amounts of nitrate-N presence at deeper depths. High average concentrations of pore water nitrate-N (>40 mg/L) at depths within 5 - 10 ft of the groundwater table will lead to further nitrate-N accumulation in the aquifer in the next few years.

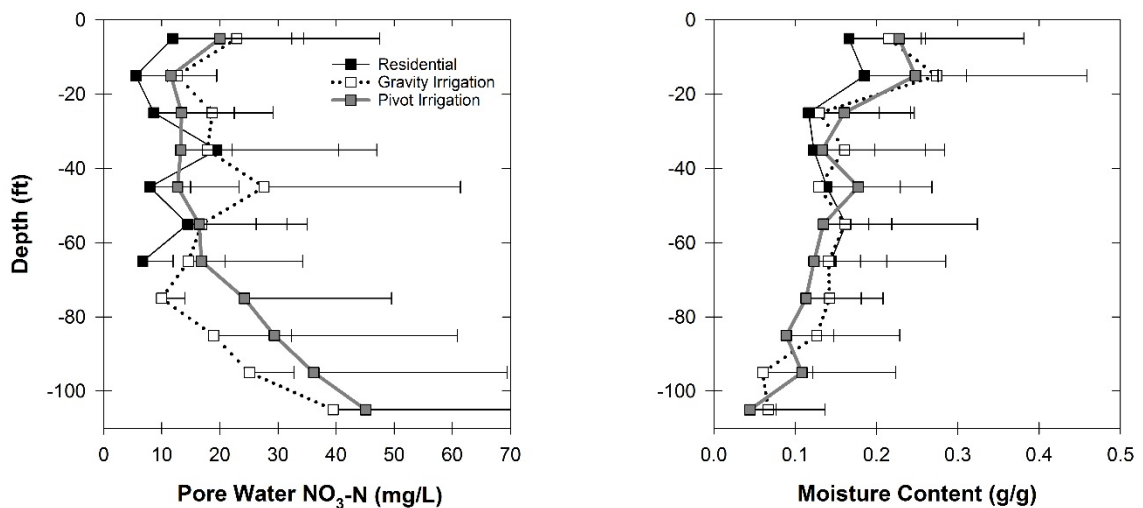


Figure 15: Average pore water nitrate-N and moisture content of three different land use groups collected in 2016.

Transport of ammonium-N diffuses through sediments more slowly and can be oxidized into nitrate-N through biological nitrification. Cumulative ammonium-N beneath the top 65 ft in 2016 for urban irrigated lawns, pivot irrigated farmland, and gravity irrigated farmland had an average of 200, 500, and 380 total lbs-NH₄-N/acre respectively. A statistically significant difference in ammonium-N was present between urban and pivot groups at depths of 25 and 35 ft. Ammonium-N can sorb to organic matter, preventing potential downward movement. In both 2011 and 2016 samplings, ammonium-N was present throughout the profile, indicating that given its chemical properties it is still leaching past the root zone into deep subsurface layers. It is also possible that nitrogen sorbed to organic matter

decayed, allowing microbes to convert the tied-up nitrogen into ammonium-N through mineralization (Adelman et al., 1985).

Similar to average nitrate-N accumulations, average ammonium-N in urban sites was lower at each depth than the irrigated farmland. Average ammonium-N beneath the top 65 ft for urban irrigated lawns was $0.89 \pm 0.36 \mu\text{g/g}$, compared to $2.07 \pm 0.23 \mu\text{g/g}$ for pivot and $1.54 \pm 0.32 \mu\text{g/g}$ for gravity irrigated sites. In contrast to total nitrogen loads from nitrate-N, the average loads from ammonium-N was greater under pivot irrigated fields than gravity. This may be due to the nitrification process being more inhibited at pivot irrigated sites than gravity. Both water and oxygen content within the pore space can influence nitrification by aerobic microbes (Linn & Doran, 1984). Further information on microbe population densities and historic management practices such as the utilization of nitrification inhibitors at these sites could assist in determining the cause of this trend. When combining average nitrate-N and ammonium-N accumulations in the top 65 ft, pivot and gravity irrigated sites had 1,040 and 1,080 total lbs-N/acre. Similarities in total stored nitrogen between the two irrigation practices may be due to shifting irrigation practices that impacted previous amounts of leached nitrate-N and ammonium-N. Previous research suggests that when irrigation water is applied at proper rates it does not increase leaching (Bobier et al., 1993). Proper water application timing and quantity at gravity irrigated fields may have prevented substantial leaching and significant differences in total nitrogen compared to pivot irrigated fields. Nearly two-thirds of the total stored nitrogen under pivot sites was in the form of ammonium-N, while only half of the stored nitrogen under gravity irrigated sites was in the form of ammonium-N.

Pesticide Results

Results are tabulated in the appendix. Most compounds were not detected or below detection. Compounds detected at or above the method detection limit (0.1 ng/g) includes atrazine, DEA, DIA, metolachlor and pendimethalin. **Table 3** provides summary statistics of the detections, including the average and standard deviation and number of detections at one-half the MDL or greater. Atrazine was the most commonly detected herbicide followed by metalochlor, DEA, DIA and pendimethalin. Nearly all samples with concentrations above the detection limits were located in the top 3' of the sediment profile. Repeated detections of atrazine occurred in cores HC10N and HC20-W suggesting that atrazine accumulation and transport may have occurred at these locations. Previous vadose zone monitoring at the Hastings WHPA also reported detections of atrazine and DEA ranging from 0.10 to 0.39 ng/g beneath pivot and gravity-irrigated crops (Spalding *et al.*, 2019).

Table 3: Summary statistics of detected Pesticide

	Atrazine	DEA	DIA	Metolachlor	Pendimethalin
Averages (ng/g)	0.13	0.03	0.01	0.24	0.06
Standard Dev (ng/g)	0.39	0.21	0.10	1.98	0.74
No. of Detections	32 (19%)	5(3%)	3(2%)	10 (6%)	1(0.6%)

Nitrate and Water Isotopes, Chloride and Groundwater Ages

Selected core samples from the Hastings Wellhead Protection area were processed for the stable isotope composition of extracted nitrate and water. Nitrate isotope analysis can help distinguish sources of nitrogen and evaluate the potential for nitrate attenuation in the vadose zone. The stable isotope composition of vadose zone pore water is determined in large part by the seasonal timing of recharge below the root zone, and this data can help evaluate when nitrate leaching is most prevalent. Finally, chloride was measured in two cores to look at the potential for use of a chloride mass balance method to estimate recharge in the area.

The isotope composition of nitrate can be used to distinguish nitrogen sources (e.g. - commercial fertilizer or livestock manure) and as an indicator of the effect of denitrification on nitrate. Samples were selected to provide a general cross section of the variability of the isotope composition of vadose zone nitrate under a variety of land uses. **Figure 16** indicates the expected general variation of the nitrogen and oxygen isotope composition in fertilizer sources, and that resulting from nitrification of ammonia or livestock (organic) nitrogen in soils. Once formed in soil and during transport, the nitrogen and oxygen isotope composition of nitrate affected by microbial denitrification can increase in a predictable way. The “1:1” and “2:1” arrows in **Figure 16** indicate the expected enrichment trends from denitrification (Kendall et al., 2008). Denitrification trends follow the same nitrate source composition through expected enrichments caused by microbial fractionation. In other words, the figure shows the predicted increase in both nitrogen and oxygen isotope composition due to denitrification of nitrate with an initial $\delta^{15}\text{N} = +6\text{‰}$ and $\delta^{18}\text{O}$ near -10‰ .

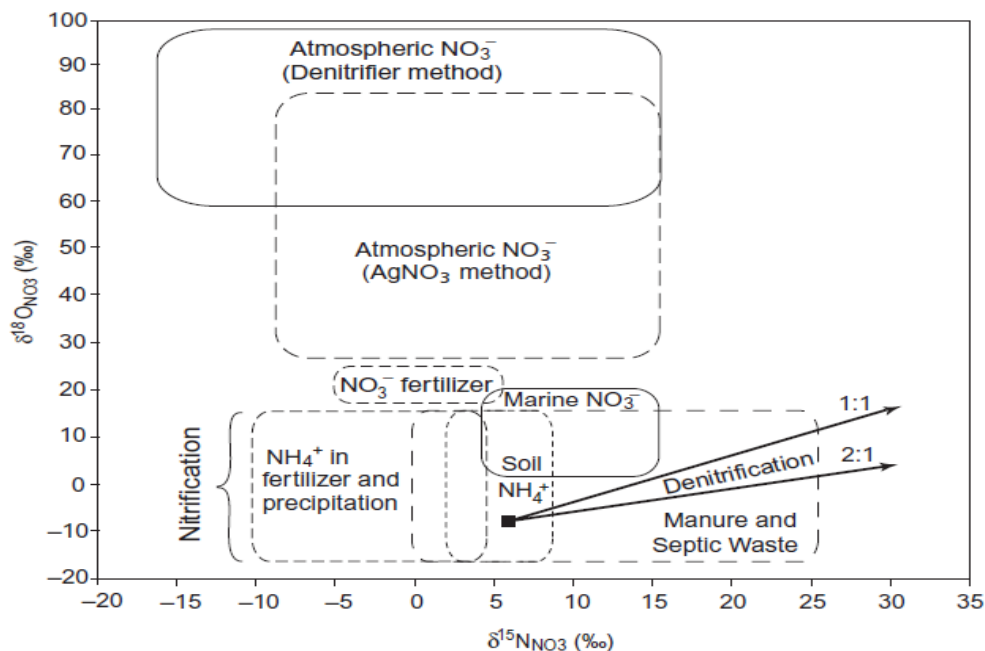


Figure 16. Expected variation of $\delta^{15}\text{N-NO}_3$ and $\delta^{18}\text{O-NO}_3$ from a variety of sources, along with the predicted trends due to denitrification (Kendall et al 2008).

Methods

Sixty-five core samples were selected from 12 of the 32 cores for measurement of nitrate and water isotopes. Core intervals were chosen to provide a representative cross section of vadose zone nitrate sources and depths. Core samples were extracted using 1 M KCl and analyzed for both $^{15}\text{N}\text{-NO}_3$ and $^{18}\text{O}\text{-NO}_3$ using an azide reduction method (McIlvin and Altabet, 2005). The azide reduction process uses a two-step chemical conversion involving alkaline Cd-reduction of dissolved nitrate to nitrite, followed by acidic reaction of nitrite with azide to produce nitrous oxide (N_2O) (McIlvin and Altabet, 2005). N_2O is purged and cryogenically trapped on an Isoprime Tracegas preconcentrator interfaced with a GVI Isoprime isotope ratio mass spectrometer. Trapped N_2O is chromatographically separated from nitrogen gas, and ions with $m/z = 44, 45,$ and 46 are simultaneously separate and monitored on a multi-collector magnetic sector mass spectrometer. Standard nitrate solutions of from known, isotopically-characterized nitrate are processed and analyzed in the same way as samples, and the results used for calibrating the mass spectrometer and determining. A working N_2O gas standard is measured between every sample and the ratios $44/45$ and $44/46$ converted to deltas (δ) using the instrument software and the following equation:

$$\delta(\text{‰}) = \frac{R_{\text{sample}} - R_{\text{standard}}}{R_{\text{standard}}} \times 1000 \quad [\text{Eq 1}]$$

where R_{sample} and R_{standard} are the measured ratios of the sample and standards respectively. In the case of nitrogen, “air” or atmospheric nitrogen gas is used as the reference standard with a very constant ^{15}N composition of 0.366% (Junk and Svec, 1958). The reference for oxygen isotopes is standard mean ocean water (SMOW) with a $^{18}\text{O}/^{16}\text{O} = 2005.2$ ppm. Reference materials (nitrate salts with known nitrogen and oxygen isotope composition) are used to calibrate the instrument and analyzed with samples. Expected precision is $\pm 0.2 \text{ ‰}$ for $\delta^{15}\text{N}\text{-NO}_3$ and $\pm 0.5 \text{ ‰}$ for $\delta^{18}\text{O}\text{-NO}_3$.

Vadose zone pore water was extracted using azeotropic distillation with toluene (Revesz and Woods, 1990) and analyzed for hydrogen and oxygen stable isotope composition by two different methods. Extracted pore water was analyzed for $\delta^2\text{H}\text{-H}_2\text{O}$ (deuterium) using an online chromium reduction technique (Morrison *et al.*, 2001) using a Eurovector EuroPyrOH-3110 pyrolysis furnace coupled to an GV Instruments Isoprime continuous flow isotope ratio mass spectrometer. The oxygen isotope composition $\delta^{18}\text{O}\text{-H}_2\text{O}$ was measured by the CO_2 equilibration technique using a GV Instruments Isoprep equilibration system interfaced with a GV2003 continuous flow isotope ratio mass spectrometer. Water isotope composition is expressed using the same delta convention [Eq 1] as nitrate isotopes with V-SMOW as the reference standard (Gat and Gonfiantini, 1981). Instruments were calibrated daily, with calibration checks interspersed throughout a run. Samples were analyzed in triplicate, averaged and reanalyzed if the standard deviation exceeded the measurement precision ($\pm 0.2 \text{ ‰}$ for $\delta^{18}\text{O}\text{-H}_2\text{O}$ and $\pm 2 \text{ ‰}$ for $\delta^2\text{H}\text{-H}_2\text{O}$). Six groundwater samples were analyzed by identical methods as the extracted pore water. Chloride was extracted from dried samples from two cores by mixing 40 milliliters of reagent water with 25 grams of dried sample, shaken for 4 hours, centrifuged and supernatant filtered for analysis by ion chromatography (Scanlon *et al.*, 2007).

concludes that nitrate originates primarily from nitrification of manure and commercial anhydrous ammonia. The isotope analysis in core samples from the Hastings WHPA vadose zone supports this conclusion. Moreover, there is no strong positive correlation between $\delta^{15}\text{N-NO}_3$ and $\delta^{18}\text{O-NO}_3$ in the vadose zone isotope results which would indicate enrichment due to denitrification. The absence of a strong positive correlation between nitrogen and oxygen isotope composition in groundwater suggestive of denitrification was also recently noted (Spalding *et al.*, 2019).

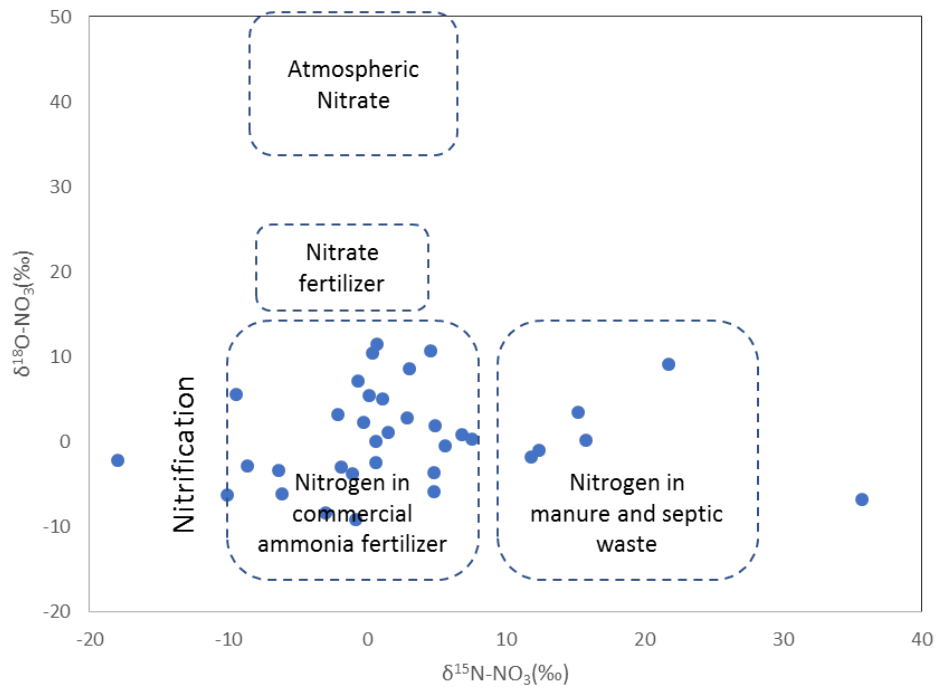


Figure 18. Plot of nitrogen versus oxygen isotope composition for nitrate in vadose zone core samples compared to expected ranges for nitrate (e.g. - KNO_3) fertilizer, nitrification of commercial ammonia and organic nitrogen sources.

Porewater Isotope Composition

The deuterium and oxygen isotope composition of precipitation varies spatially and seasonally as a function of the water sources. This predictable seasonal variation has been used to estimate the proportion and timing of recharge to groundwater and to the vadose zone. The spatial variability of precipitation generally follows a trend of fractionation that depletes both deuterium and oxygen-18 with distance from an oceanic source. Snowfall tends to be isotopically lighter and snowmelt carries this isotope signature. Temporal variations in precipitation are caused mainly by the temperature of water vapor, intensity of evaporation, and temperature during precipitation (Sprenger *et al.*, 2016). If measured in precipitation, this seasonal variation can be used as a signal in vadose zone pore water. The seasonal variation of water isotope composition of precipitation in Nebraska has been previously measured at several locations, including North Platte (Harvey and Welker, 2000). A synthesis of this seasonal trend is shown in **Figure 19**.

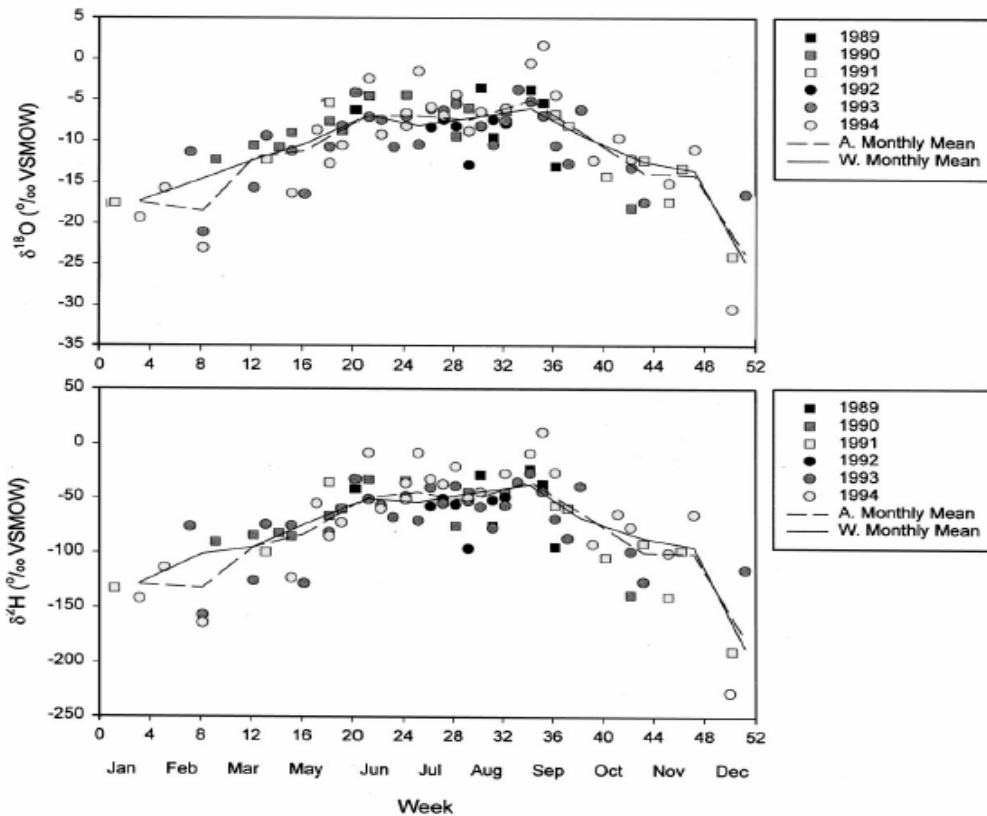


Figure 19. Weekly δD and $\delta^{18}O$ of water in precipitation between 1989 and 1994 from samples collected near North Platte, Nebraska together with the monthly averages for each isotope (Harvey and Welker, 2000).

The change in stable isotope composition of water flow below the root zone, and reflected in the vadose zone pore water, is complex but may provide clues on the major events leading to recharge. The overall variation of δD and $\delta^{18}O$ of extracted porewater is shown in **Figure 20** as compared to the local meteoric water line for the North Platte area reported for precipitation (Harvey and Welker, 2000). Roughly half of the samples fall within 10-15% of the predicted values for precipitation in this area, though a large proportion are enriched or depleted in deuterium relative to this curve. Excess deuterium values in precipitation are thought to be associated with precipitation from “recycled” moisture and low humidity precipitation sources, while those plotting below this line are generally thought to result from evaporation.

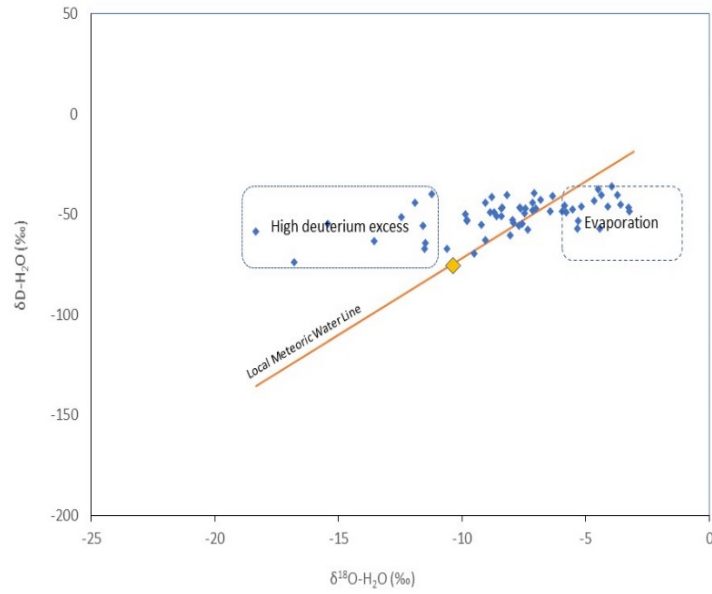


Figure 20. Dual isotope plot of δD and $\delta^{18}O$ of extracted pore water samples from cores HC3A and HC14.

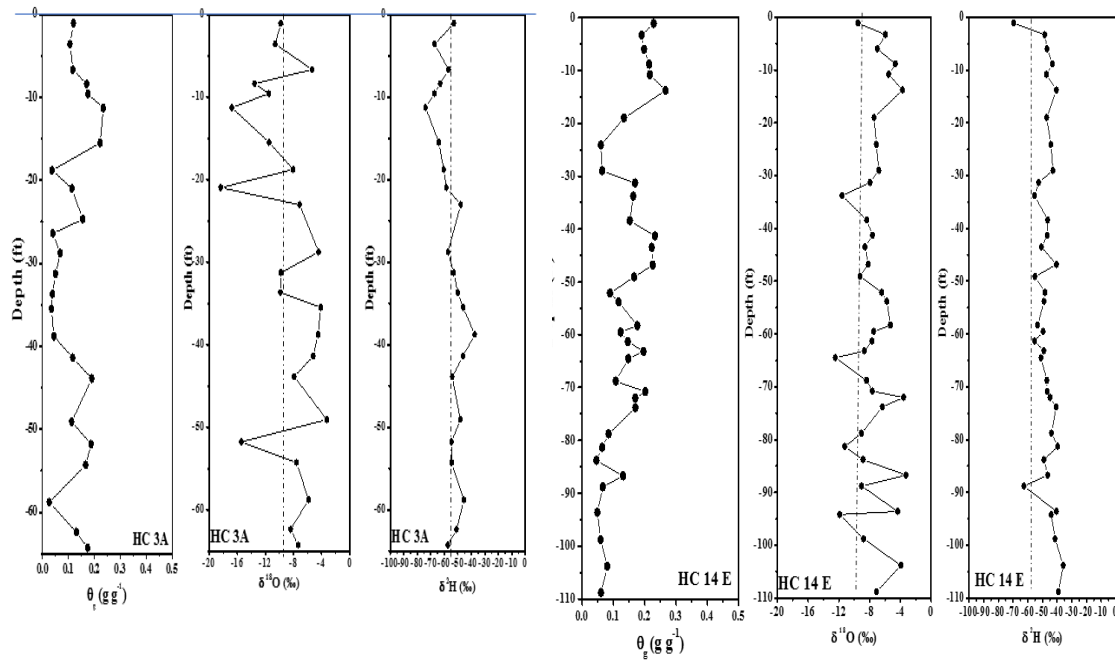


Figure 21. Variation of gravimetric moisture content θ for comparison to $\delta^{18}O$ and δD of extracted pore water from cores HC 3A and HC14. Vertical dashed lines correspond to average stable isotope composition of groundwater samples.

Using the monthly temperature correlations from δD and $\delta^{18}O$ for water reported by Harvey and Welker (2001), the average monthly mean temperature for both cores is $19\pm 2^\circ C$ and $17\pm 6^\circ C$, respectively. These temperatures are in the range of May-June and Sept-October between 1989 and 1994.

Figure 21 shows a comparison of gravimetric moisture content with δD and $\delta^{18}O$ composition versus depth for the two cores HC3A and HC14E. HC3A is a residential site while HC14E is pivot irrigated. The averages (-50.3 and -8.05‰) are similar and slightly enrich relative to the groundwater samples collected from the monitoring wells (-57.4 and -9.6‰) suggesting that irrigation inputs at the surface may likely affect the isotope composition of the vadose zone porewater. This observation is consistent with mixing of groundwater applied in summer as irrigation water with a relatively fixed isotope composition with seasonally variable component of precipitation.

Vadose Zone Chloride Composition

Chloride concentration profiles in the vadose zone can be used to show land use changes as well as determine relative differences in recharge rates and water movement (Scanlon *et al.*, 2007). In general, higher chloride concentrations in the vadose zone correspond to lower recharge rates under the same precipitation rates and vadose zone geology. Chloride is an inert tracer and readily moves with recharging pore water beneath the surface. Vadose zone chloride concentrations tend to increase with depth through the root zone as a result of evaporation. Under steady state conditions, vadose zone chloride concentrations are relatively uniform beneath the root zone and drainage (recharge) rates are inversely proportional to the uniform steady-state concentrations (Healy, 2010). Higher drainage rates flush chloride through the vadose zone profile more rapidly and result in lower steady state concentrations. The general equation used for estimating recharge is given by the equation:

$$D = \frac{(PC_p + QC_{on} - QC_{off} - M_{app})}{C_{uz}} \quad [Eq 2]$$

where “D” is the drainage (recharge) rate, “PC_p” is the rate of chloride deposition from precipitation, “QC_{on}” is the surface applied chloride deposition from irrigation and other sources, “QC_{off}” is the loss of chloride in surface runoff, “M_{app}” is the rate of chloride through dry deposition such as agricultural chemicals or road salt. “C_{uz}” is the unsaturated zone chloride concentration at steady state (Healy, 2010). The National Atmospheric Deposition Program provides maps showing estimated chloride concentrations in precipitation for the U.S. (roughly 0.1 mg/L). Road salt application in residential areas and potash fertilizer application in irrigated crops may confound the calculations by introducing a large uncertainty in the “M_{app}” term. The shape of the chloride profile provides a good indication of whether or not chloride in recharge water has reached a steady state. **Figure 22** shows the vadose zone chloride profiles for the cores HC3A and HC14 E. The spikes in chloride concentrations indicated in HC3A likely correspond to periods of road salt application or root zone conditions when chloride was concentrated due to evaporation. Thus, it is difficult to estimate a “steady state” concentration for the residential location. Interestingly, some of these intervals correspond to high deuterium excess measured in this core. High moisture content and low nitrate suggests that this may be a zone of preferential flow from the surface. High chloride surface seepage from snow melt could be accumulating in these zones. In

HC14 E, using the chloride concentration at 10 feet (126 mg/L) as the steady state concentration (C_{uz}), average annual precipitation of 28" (711 mm), 5.78" (147 mm) irrigation water with chloride at 13 mg/L, results in an estimated drainage rate of 15 mm/year. This value is comparable to other estimated recharge rates for this area (Szilagyi and Jozsa, 2013). Still, given the high uncertainty in the input terms this estimation should be viewed with skepticism.

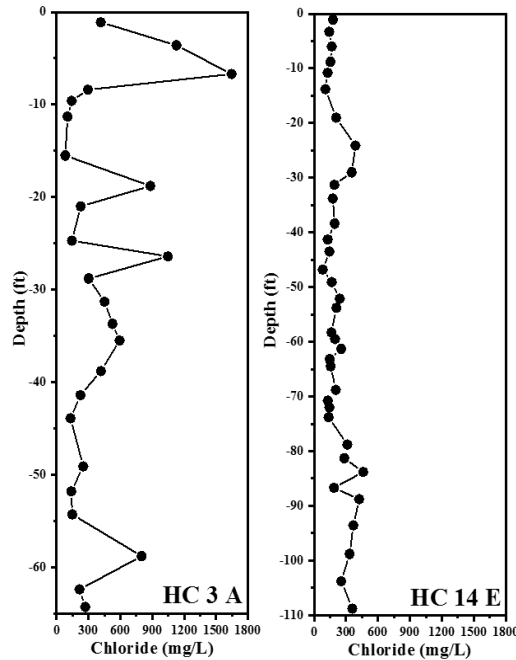


Figure 21. Vertical profiles of pore water chloride in Hastings cores HC3A and HC14 E.

Groundwater Gases, Chemistry and Model Age Measurements

Five groundwater samples were collected from monitoring wells in and upgradient of the Hastings WHPA in December 2017. HCGW1 (#G-173896) and HCGW2 (#G-173895) are from monitoring wells located east of Prosser, NE at the northwestern boundary of the Hastings WHPA. HCGW3 and HCGW 5 are from the Aquifer Storage and Recovery (ASR, #G-179001) monitoring well located just east of the Hastings Municipal Airport with the pump suspended at 120' and 160' below the surface. The sample from HCGW4 is from Hastings Industrial SW. All samples were analyzed for dissolved anions, organic carbon (DOC), stable isotopes of nitrate and water (reported earlier in this chapter), uranium, iron, arsenic. Samples from HCGW1, HCGW2, HCGW3 and HCGW 5 included those for dissolved gases and helium isotopes.

The results of the water chemistry measurements are summarized in **Table 4** together with screen depths and static water levels (SWL) from the Nebraska Department of Natural Resources well registration database. Most anion and DOC concentrations, with exception of nitrate-N and sulfate, are relatively uniform from upgradient to downgradient wells. Arsenic and uranium are highest in upgradient wells while iron is higher HCGW4 and the lower portion of the ASR monitoring well. Higher

sulfate in groundwater to the west of Hastings has been attributed to recharge from irrigation canals and Platte River system (McMahon *et al.*, 2006; McMahon *et al.*, 2010). For comparison, sulfate concentrations in samples from the shallow alluvial aquifer near Shelton, Nebraska were reported to average 211±51 mg/L, while chloride and DOC concentrations average 24±3 mg/L and 3.3 ±0.3 mg/L respectively (Spalding *et al.*, 2001).

Table 4. Results of groundwater chemistry for monitoring wells

Sample_ID	Screen		SWL	Sampling Depth	Chloride (mg/L)	Fluoride (mg/L)	Nitrate-N (mg/L)	Sulfate (mg/L)	DOC (mg/L)	Arsenic (µg/L)	Iron (µg/L)	Uranium (µg/L)
	Depth	Date										
HCGW1	180-190'	12/14/2017	102'	185'	9.9	0.35	19.51	50.2	0.92	3.3	2.9	27.9
HCGW2	135-145'	12/14/2017	102'	140'	13.8	0.31	11.59	145.7	0.63	1.3	11.1	15.4
HCGW3	105-170'	12/14/2017	108'	120'	13.0	0.25	3.88	69.7	0.72	0.8	2.8	14.5
HCGW4	--	12/14/2017	NM	--	16.6	0.18	1.64	45.0	0.71	0.6	280	9.8
HCGW5	105-170'	12/14/2017	108'	160'	12.1	0.25	3.78	69.7	0.72	0.8	125	13.7

Dissolved gases and estimated groundwater age

Samples for dissolved gases and tritium helium age-dating were collected and sealed in 3/8" copper tubes using custom fabricated tubing clamps in place of the commercial refrigeration clamps. Gas was extracted from these samples and measured using a custom-built high vacuum extraction system (Stanley *et al.*, 2009). Atmospheric sources of all gas species can affect the concentrations measured in groundwater samples, collection of sealed and intact samples is critical in providing useful results. Samples for this project were collected in sealed 3/8" O.D. copper tubes and sealed using clamps fabricated and specifically designed for this purpose. Each sample tube is mounted on an 8-port, custom-built high vacuum manifold using 3/8" Swagelok connections above a 200 mL stainless steel receiving vessel. After evacuation and ensuring that the connections are leak tight, a system blank is run for each port overnight. The next day each sample is sequentially de-crimped and opened to the receiving vessel for extraction of sample gases under vacuum.

Water and carbon dioxide are removed as gases pass first through isopropanol slurry and liquid nitrogen traps, and subsequently into an ultra-low temperature cryogenic water trap maintained at 180°K. Nitrogen, argon, oxygen, krypton, and xenon are trapped on a vacuum insulated, bare stainless steel trap maintained at 24°K by a CTI Cryogenics refrigeration and cold head unit. Helium and neon are trapped on a second carbon-coated trap cooled to 10°K. After trapping is complete, each gas is sequentially released and measured by slowly heating the trap into a selected detector. Oxygen is scrubbed from the sample gas using a heated SAES titanium getter to allow quantitative measurement of argon. Concentrations of nitrogen and argon are measured on capacitance manometers, while neon, krypton, and xenon are measured on a Hiden Instruments quadrupole mass spectrometer. Helium-4 and

helium-3 are measured separately on a Thermo Helix SFT high resolution noble gas mass spectrometer. All detectors are calibrated using standardized atmosphere with individual gases separated, purified, and measured under the same conditions as samples.

After the water sample has been degassed, it is resealed in the stainless-steel flask for tritium measurement using helium-3 ingrowth. The ingrowth period requires a minimum of 4-6 weeks, though a longer period (up to 4-6 months) can be required when tritium activity is low. Helium-3 is measured using the Thermo Helix SFT mass spectrometer calibrated with an ultra-low level air standard and corrected for background. Groundwater ages were estimated using tritium-helium age-dating with appropriate corrections for estimated recharge temperature (Solomon and Sudicky, 1991) and (Cey *et al.*, 2009). The models use the measured dissolved gas concentrations and helium isotope ratios to estimate recharge temperature, pressure, salinity, excess air, and the degree to which the gases have been fractionated, due to differences in gas solubilities (Kipfer *et al.*, 2002). Assumptions include that barometric pressure is determined by recharge elevation and salinity is negligible for fresh groundwater. Recharge temperatures are based on known solubilities and expected isotope fractionation. Measured gas concentrations, tritium activity, and model ages are summarized in **Table 5**.

Table 5. Dissolved gas concentrations, helium isotopes and tritium activity in four groundwater samples collected from the Hastings WHPA. Xenon and argon could not be measured because of a trap malfunction. Air-equilibrated water values at 25° are provided for comparison.

Sample ID	Date	N ₂ (cm ³ /gm)	Ar (cm ³ /gm)	Ne (cm ³ /gm)	Kr (cm ³ /gm)	⁴ He (cm ³ /gm)	³ He (cm ³ /gm)	Tritium (TU)	R/Rair	Model Age (yr)
HCGW1	12/14/2017	1.13E-02	2.90E-04	1.88E-07	1.23E-08	4.48E-08	8.80E-14	6.2	1.408	16.5
HCGW2	12/14/2017	1.08E-02	3.02E-04	1.99E-07	1.79E-08	8.03E-08	1.65E-13	3.2	1.466	44.6
HCGW3	12/14/2017	1.39E-02	NM	2.16E-07	3.38E-08	9.75E-08	1.17E-13	1.7	0.850	ND
HCGW5	12/14/2017	1.57E-02	NM	1.82E-07	1.88E-08	9.00E-08	1.07E-13	1.5	0.847	44.9
<i>Air-equilibrated Water</i>		<i>1.07E-02</i>	<i>3.00E-04</i>	<i>1.80E-07</i>	<i>1.54E-08</i>	<i>5.12E-08</i>			<i>1.02</i>	

Dissolved nitrogen, argon, neon, and krypton concentrations are consistent with reported groundwater values in other studies in western Nebraska (McMahon *et al.*, 2006) with N₂, Kr, and He concentrations 10-20% higher in the downgradient wells (Table 2). Tritium activity is highest in the deeper upgradient well near Prosser. For comparison tritium activity of shallow groundwater influenced by canal seepage near North Platte ranged from <0.5 to 20 TU (McMahon *et al.*, 2010). Estimated age of recharge, or the elapsed time after intercepting the water table, for three of the samples ranges from 16.5 to almost 45 years.

References

- Cey, B.D., Hudson, G.B., Moran, J.E., Scanlon, B.R., 2009. Evaluation of Noble Gas Recharge Temperatures in a Shallow Unconfined Aquifer. *Ground Water* 47, 646-659.
- Gat, J.R., Gonfiantini, R. (Eds.), 1981. *Stable isotope hydrology: Deuterium and oxygen-18 in the water cycle*. International Atomic Energy Agency, Vienna.
- Healy, R.W., 2010. *Estimating Groundwater Recharge*. Cambridge University Press, Cambridge.
- Kipfer, R., Aeschbach-Hertig, W., Peeters, F., Stute, M., 2002. Noble Gases in Lakes and Ground Waters. *Reviews in Mineralogy and Geochemistry* 47, 615-700.
- McIlvin, M.R., Altabet, M.A., 2005. Chemical Conversion of Nitrate and Nitrite to Nitrous Oxide for Nitrogen and Oxygen Isotopic Analysis in Freshwater and Seawater. *Anal. Chem.* 77, 5589-5595.
- McMahon, P., Dennehy, K., Bruce, B., Böhlke, J., Michel, R., Gurdak, J., Hurlbut, D., 2006. Storage and transit time of chemicals in thick unsaturated zones under rangeland and irrigated cropland, High Plains, United States. *Water Resour. Res.* 42.
- McMahon, P.B., Carney, C.P., Poeter, E.P., Peterson, S.M., 2010. Use of geochemical, isotopic, and age tracer data to develop models of groundwater flow for the purpose of water management, northern High Plains aquifer, USA. *Appl. Geochem.* 25, 910-922.
- Morrison, J., Brockwell, T., Merren, T., Fourel, F., Phillips, A.M., 2001. On-Line High-Precision Stable Hydrogen Isotopic Analyses on Nanoliter Water Samples. *Anal. Chem.* 73, 3570-3575.
- Revesz, K., Woods, P.H., 1990. A method to extract soil water for stable isotope analysis. *Journal of Hydrology* 115, 397-406.
- Scanlon, B.R., Reedy, R.C., Tachovsky, J.A., 2007. Semiarid unsaturated zone chloride profiles: Archives of past land use change impacts on water resources in the southern High Plains, United States. *Water Resour. Res.* 43.
- Solomon, D.K., Sudicky, E.A., 1991. Tritium and helium 3 isotope ratios for direct estimation of spatial variations in groundwater recharge. *Wat. Resour. Res.* 27, 2309-2319.
- Spalding, R.F., Hirsh, A.J., Exner, M.E., Stange, M., Aravena, R., 2019. Integrated Deep Soil N and Groundwater Isotope Investigation of N Sources Captured by Municipal Wells. *Groundwater Monitoring & Remediation* 39, 22-31.
- Spalding, R.F., Watts, D.G., Schepers, J.S., Burbach, M.E., Exner, M.E., Poreda, R.J., Martin, G.E., 2001. Controlling nitrate leaching in irrigated agriculture. *Journal of Environmental Quality* 30, 1184-1194.
- Stanley, R.H.R., Baschek, B., Lott, D.E., Jenkins, W.J., 2009. A new automated method for measuring noble gases and their isotopic ratios in water samples. *Geochem. Geophys. Geosyst.* 10, n/a-n/a.
- Szilagyi, J., Jozsa, J., 2013. MODIS-Aided Statewide Net Groundwater-Recharge Estimation in Nebraska. *Groundwater* 51, 735-744.

Nitrate Loading and Travel Time Estimates

Nebraska is an agriculturally intensive region and has a large number of wells with nitrate-N concentrations above the maximum contamination level (MCL) for drinking water (10 mg NO₃-N/L). Large amounts of nitrogen-based fertilizers are applied annually, and crops are heavily irrigated to maintain a high production output. Overuse of nitrogen-based fertilizers coupled with irrigation often leads to increased loading of nitrate-N to local groundwater. Nitrate-N, being a negatively charged anion, is known to leach rapidly through the vadose or unsaturated zone (Wang et al., 2015). Consumption of drinking water with elevated nitrate can cause health problems, primarily for infants “blue baby syndrome” and colon and rectal cancer in adults (Comly 1945; Schullehner et al., 2018). The occurrence of nitrate may also be linked with uranium and arsenic mobilization (Nolan and Weber, 2015, Smith et al., 2017), both of which can have adverse effects on human health. Understanding the occurrence of nitrate in the Nebraska’s groundwater system, and the protection of groundwater from further contamination, are among the major challenges that impose risks on Nebraska’s drinking water supplies. It is estimated that 85% of Nebraskans consume groundwater and many lack point of use filtering and knowledge about local groundwater quality (Reilly et al., 2008).

The goal of this chapter is to characterize nitrate-N loading and mobilization rates through the vadose zone in the Hastings, NE WHPA by coupling two types of unsaturated zone transport models. The coupled use of a “Root Zone Water Quality Model” (RZWQM2) and HYDRUS 1D unsaturated zone model will help estimate nitrate loading and transport time through the vadose zone. A coupled model takes advantage of the predictive strength of RZWQM2 in estimation of nitrate losses below the root zone together with the simple application of vertical transport rate with a one-dimensional unsaturated zone HYDRUS 1D model. This coupled model was run for expected nitrogen-intensive land use scenarios in the Hastings WHPA and included irrigation practices such as furrow and pivot, and land use such as urban, dryland, irrigated and crop rotation (see **Table 5**). The model estimated the nitrate transport under these different scenarios, this information can serve as a way to predict alternative management practices to reduce nitrate loading to the aquifer and will be elaborated in this chapter.

Objectives

The primary objective of this part of the study is to develop a coupled RZWQM2 and HYDRUS 1D model to better estimate the nitrate loading and transport in the Hastings WHPA. The coupled model takes advantage of the high density of geologic and nitrate data collected from the vadose zone for this and previous studies of the Hastings WHPA. Modeling of soil water movement and nitrate production and leaching in the crop root zone (soil surface to 180 cm, ~5.9 ft) utilizes RZWQM2. HYDRUS 1D used outputs from RZWQM2 to estimate soil pore water and nitrate travel time through the vadose zone. Scenarios simulated in the present study are listed in **Table 6**.

Table 6. List of all the scenarios for which coupled model was utilized to estimate nitrate transport

Scenario Number	Land Use	Irrigation Type	Crop Type
1	Urban/Barnyard	N.A.	Grass
2	Dryland	N.A.	Corn
3	Irrigated	Furrow or Gravity	Corn
4	Irrigated	Pivot or Sprinkler	Corn
5	Irrigated	Pivot or Sprinkler	Corn and Soybean rotation

N.A. = Not Applicable, where only precipitation was considered.

The coupled model was calibrated utilizing the soil water and nitrate-N data collected in year 2011 (Spalding and Toavs, 2011) and validated from data collected in 2016 by Adams (2018) at the University of Nebraska-Lincoln (UNL).

Methods

Site Description

The Hastings WHPA vadose zone monitoring sites are discussed in earlier chapters of this report. Vadose zone monitoring sites in the study area were carefully selected on the basis of site availability for sampling, land use, and cropping history. Sites were cored in 2011 and 2016, allowing a historical comparison of upper portions of the vadose zone profiles. Land use includes residential, barnyard, dryland, and irrigated crop land (Table S1 in Appendix C).

In the coupled model, 4 locations from the total of 32 vadose zone sites were selected to simulate soil water and nitrate-N production and movement. These 4 locations were selected based on land management practices such as barnyard, dryland and irrigated land, irrigation type such as gravity and pivot, and cropping

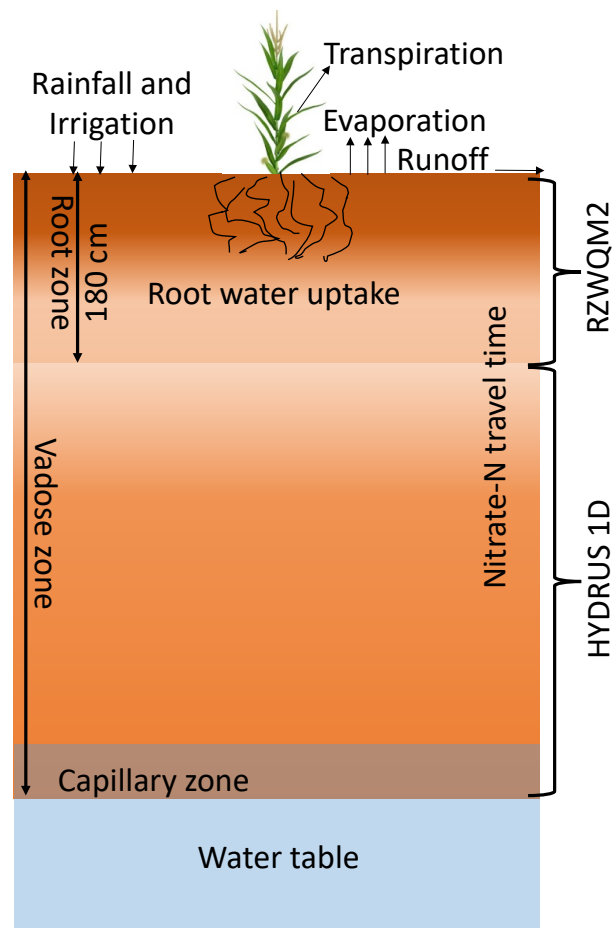


Figure 22. Compartments where RZWQM2 and HYDRUS 1D were used to estimate nitrate transport.

history such as corn, soybean and corn soybean rotation. The HC 1 East site (gravity irrigation), the HC 14 West site (pivot irrigation), the HC 2 site (dryland), and the HC 7 (barnyard) are summarized in **Table 7**.

Table 7. The description of site land use and soil samples from 32 sites at Hasting, NE.

Serial	Site	Land Use	Irrigation	Crop	Latitude (°)	Longitude (°)	Elevation (m)
1	HC-1-E	Agricultural Field	Gravity	Corn	40.60267	-98.43350	581.40
2	HC-2	Dryland	N.A.	Corn	40.61027	-98.40218	579.00
3	HC-7	Barnyard	N.A.	N.A.	40.60844	-98.45829	593.19
4	HC-14-W	Agricultural Field	Pivot	Corn	40.65158	-98.46003	593.45

N.A. = Not Applicable

Model Overview

The coupled model defines an active root zone from the surface to 180 cm where RZWQ2 is used to predict production and leaching loss of nitrate based on fertilizer and water application rates and timing. The model then simplifies water and nitrate movement in the intermediate vadose zone using a simplified HYDRUS 1D unsaturated zone transport model. A unique approach of utilizing two different models at different depth of the vadose zone is implemented in the current study. RZWQM2 model is effective for predicting nitrate leaching below the root zone, but estimation of transport rate and residence time for deep soil profile is limited, as a maximum 10 soil layers can be simulated. The data generated by RZWQM2 is utilized for rest of the vadose zone, which is simulated by HYDRUS 1D. The vertical and lateral transport of water and solute, infiltration, percolation and capillary rise process takes place in the intermediate vadose zone. In the current sequence based modeling approach both these zones have been dealt separately to replicate actual field conditions. However, the models may lack efficiency in appropriate prediction of different steps in the nitrogen cycle or any specific chemical transformation happening in the intermediate vadose zone.

RZWQM2: Biological, physical and chemical processes are combined together in RZWQM2 to simulate plant activity and water along with nutrient and pesticide movement in the root zone. The model can simulate multiple years processes in one-dimensional soil profile and various processes in RZWQM are calculated in two time scales (**Figure 24**). RZWQM was released and developed by the United States Department of Agriculture (USDA) under the agency of the Agricultural Research Service (ARS) (Ahuja et al., 1995, 2000; Ma et al., 2001, 2009). The latest version RZWQM2, has seven main modules such as soil water balance module, soil nutrient module, equilibrium soil chemistry module, potential evapotranspiration, surface energy balance, and heat transfer module (SHAW), pesticide processes module, plant growth modules and management practices module (Ma et al., 2011). In the present study, out of seven modules five modules are being utilized, SHAW and pesticide are not being used and will not be discussed further.

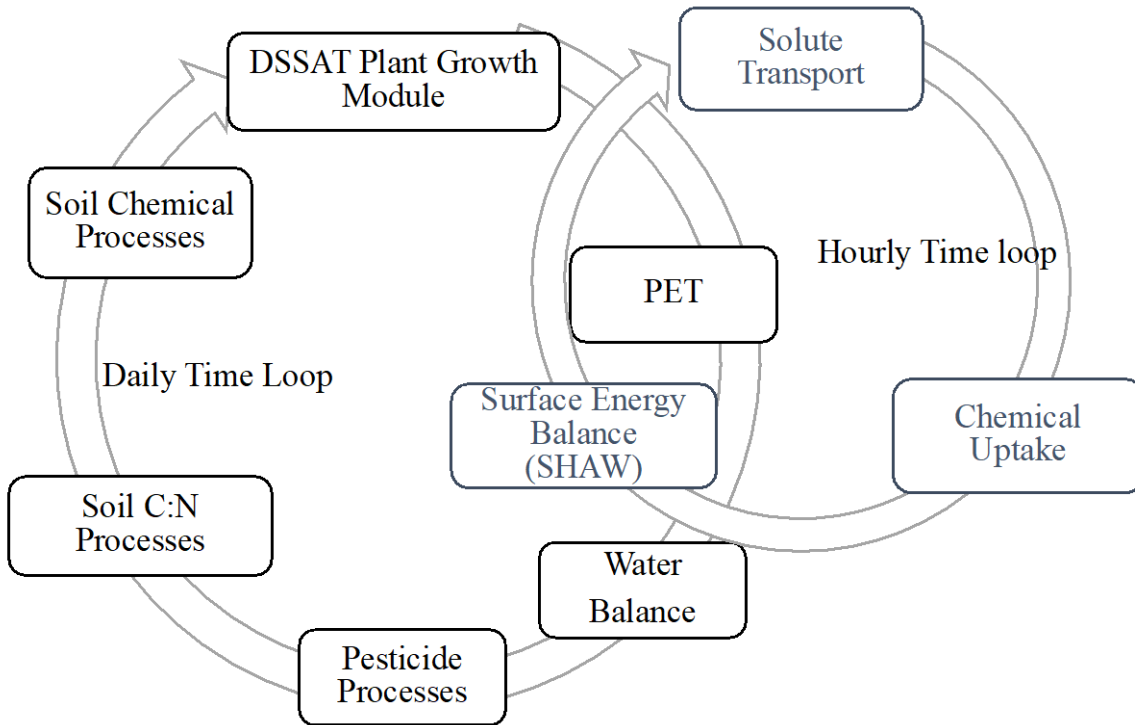


Figure 23. Main component of RZWQM2 model having daily loop and hourly time loop process. The all component are interlinked to each other in air soil water plant continuum (Ahuja et al., 2000).

In RZWQM2, the soil water and nitrate-N movement processes consist of two phases: infiltration and redistribution after infiltration (Ahuja et al., 1993, 1995). The relationship between soil moisture and soil hydraulic conductivity at a given pressure, described by the soil water retention curve (SWRC), is used to estimate soil water movement using the Green-Ampt equation for infiltration, and calculating the redistribution with the Richards equation (Ahuja et al., 2000). The Green-Ampt equation [1] for the infiltration phase in RZWQM2 (Green and Ampt, 1911; Hachum and Alfaro, 1980) is,

$$V = \frac{\bar{K}_s}{VRCF} \times \frac{H_c + H_o + Z_{wf}}{Z_{wf}} \quad [1]$$

Where, V is the infiltration rate at any given time (cmhr-1), $VRCF$ is the viscous resistance and entrapped air correction factor, \bar{K}_s is the effective average saturated hydraulic conductivity of the wetting zone (cmhr-1), H_c is the capillary pressure (cm), H_o is the depth of surface ponding (cm), and Z_{wf} is the depth of the wetting front (cm). The redistribution of soil water and nitrate-N is simulated after the infiltration. The redistribution of soil water between rainfall or irrigation events is calculated using the Richards equation (Richards, 1931):

$$\frac{\partial \theta}{\partial t} = \frac{\partial}{\partial z} \left[K(h, z) \frac{\partial h}{\partial z} - K(h, z) \right] - S(z, t) \quad [2]$$

where θ is the volumetric soil water content ($\text{cm}^3\text{cm}^{-3}$), t is time (hr), z is the soil depth (cm), h is the soil-water pressure head (cm), K is the hydraulic conductivity (cmhr^{-1}) with a function of h and z , and S is the sink term for root-water uptake and tile drainage rate (hr^{-1}).

The SWRC was measured from collected soil cores by the hanging water columns and the pressure plate apparatus, wherever SWRCs parameters were not available, soil hydraulic properties were assumed based on the modified Brooks-Corey equations in RZWQM2. The Brooks-Corey equation is described as equation 3 (Brooks and Corey, 1964; Ahuja et al., 2000):

$$\theta = \theta_s - \lambda_1|h| \text{ when } |h| < |h_b| \quad [3]$$

$$\theta = \theta_r - B|h|^{-\lambda_2} \quad \text{when } |h| \geq |h_b|$$

where θ_s and θ_r are saturated and residual soil water contents ($\text{cm}^3\text{cm}^{-3}$), λ_1 is a constant, h_b is the air-entry water suction for the θ - h curve (cm), and λ_2 is the slope of the $\log(\theta)$ - $\log(h)$ curve (dimensionless), and B is a constant by imposing continuity at h_b , obtained as $B = (\theta_s - \theta_r - \lambda_1 h_b) h_b^{\lambda_2}$.

In RZWQM2, the organic matter (OM) and nitrogen (N) cycling (OMNI) module is used to estimate soil organic carbon and nitrogen transformations. The OMNI is a state-of-the art model for carbon (C) and nitrogen (N) cycling in soil systems (Shaffer et al., 2000, 2001). OMNI can simulate several pathways including mineralization-immobilization of crop residues, manure and other organic wastes, mineralization of the soil humus fractions, inter-pool transfers of carbon and nitrogen, denitrification of N_2 and N_2O production, gaseous loss of ammonia (NH_3), nitrification of ammonium to produce nitrate-N, production and consumption of methane gas (CH_4) and carbon dioxide (CO_2), and microbial biomass growth and death (Shaffer et al., 2000, 2001).

The OM is distributed into five computational pools and is decomposed by three microbial biomass (MBM) populations. These five pools of the OM are further divided to slow and fast pools for soil residues; fast and intermediate pools for the potentially mineralizable N; and slow pools for soil humus. Each pool of the five OM pools is characterized by a specific carbon:nitrogen (C:N) ratio and a first-order decay constant. In this study, the slow and fast residue pools are initialized with C:N ratios of 8 and 80, respectively. The fast, intermediate, and slow organic matter pools have C:N ratios of 8, 10 and 12 (Appendix 1, Table S2), it is generally suggested not to modify the C:N ratios of the pools (Ma et al., 2011). The three MBM populations in the partitioning of OM in the model include two heterotrophic groups (soil fungi and facultative bacteria) and one autotrophic group (nitrifiers). All three microorganism pools are basically characterized with their specific C:N ratios of 8 (Shaffer et al., 2000, 2001), which responds dynamically to soil environmental factors such as soil oxygen content, water content, and temperature.

The model includes potential evapotranspiration, surface energy balance, and heat transfer modules. RZWQM2 uses the Penman type surface energy balance to calculate potential evaporation. RZWQM2 also have a plant growth modules (DSSAT), this module simulates above and below ground biomass, yield, phenology and water and nutrient uptake from soil by plants (Jones et al., 2003).

HYDRUS 1D: This model simulates one-dimensional water flow and solute transport in incompressible, porous, variably saturated media, in steady or transient regime, for a known metric system and various time steps. Richards equation is also utilized in HYDRUS 1D but here the root water uptake (S) is not considered (see equation 2). The model uses a van Genuchten – Mualem water retention model, and Genuchten equations (1980) are set using a water retention curve $\vartheta(h)$, which relates the volumetric water content in pressure potential to the hydraulic conductivity curve $K(h)$ as equation 4:

$$\theta(h) = \begin{cases} \theta_s & h \geq 0 \\ \theta_r + [\theta_s - \theta_r]/[1 + |\alpha h|^n]^m & h < 0 \end{cases} \quad [4]$$

where ϑ_r is the residual water content [$L^{-3}L^{-3}$], ϑ_s is the saturated water content [$L^{-3}L^{-3}$], h is the water pressure head [L], α [L^{-1}] and n [-] are shape parameters.

Equation 5 describes the hydraulic conductivity, given by Mualem (1976) as:

$$K(h) = \begin{cases} K_s & h \geq 0 \\ K_s r S_e^{1/2} [1 - (1 - S_e^{1/m})^m]^2 & h < 0 \end{cases} \quad [5]$$

Where $m=1-(1/n)$, $n>1$ and $S_e = (\vartheta - \vartheta_r) / (\vartheta_s - \vartheta_r)$, K_s is the saturated hydraulic conductivity [LT^{-1}], S_e is the effective saturation [-], and r is the pore connectivity parameter [-], equal to 0.5.

The equation that governs the nitrate-N transport in a variably saturated soil is the equation for advection–dispersion, defined as equation 6:

$$\frac{d\rho S}{dt} + \frac{d\theta C}{dt} = \frac{d}{dz} \left\{ \theta \cdot D \frac{dC}{dz} \right\} - q \frac{dC}{dz} \quad [6]$$

where z is the spatial coordinate, C and S are solute concentrations in the liquid [ML^{-3}] and solid [MM^{-1}] phases, respectively and $S = K_d C$ with K_d [$L^3 M^{-1}$] is the partition coefficient, q is the volumetric flux density [LT^{-1}], D is the dispersion coefficient [L^2T^{-1}] and ρ is the bulk soil density [ML^{-3}].

The input parameters of HYDRUS 1D (ϑ_r , ϑ_s , α , n and m) were measured and obtained from fitted retention curves for vadose zone samples collected from the Hastings WHPA. RETC software (Van Genuchten et al., 1991) was utilized to fit the experimentally generated data points from the hanging column and pressure plate experiments which are described below. The solute transport parameters such as dispersion coefficients were obtained from the literature for each type of texture (Hanson et al., 2006). **Table 8. Key parameters required for HYDRUS 1D model** shows minimum soil water parameter needed for HYDRUS 1D simulation.

Table 8. Key parameters required for HYDRUS 1D model

Soil parameters	Water flow parameters
Bulk Density	Residual Water Content
Dispersivity	Saturated Water Content
Soil Fractions	Curve fitting parameters ($\alpha, n, l, m,$)
	Saturated Hydraulic Conductivity

Calibration and Validation Procedures of RZWQM2 and HYDRUS 1D

The output of both models are dependent on input parameters, and these parameters were selected and optimized performance in simulating a real world phenomenon. Models are calibrated towards better optimization of site-specific condition (Šimunek et al., 2012). RZWQM2 model was calibrated for top 180 cm soil and HYDRUS 1D model (180 cm to water table depth) was using 2011 observed data. The process of determining the degree to which the model corresponds to the real system or at least specifically represent the model specification document is referred to as model validation. However, proving absolute validation is non-attainable (Refsgaard, 1997). In the present study both models were validated with 2016 observed data for soil water and nitrate-N profiles. Model calibration and validation used the root mean square error (RMSE) to assess the goodness-of-fit. The RMSE values closer to zero indicate better agreement between the simulated and observed data.

Key model components: A summary of variable input data is provided in **Table 9**. Meteorological data such as precipitation, solar radiation, temperature, evaporation, and transpiration is needed by both the models viz RZWQM2 and HYDRUS 1D. Soil properties such as bulk density, texture, saturated hydraulic conductivity (K_{sat}) of the vadose zone were obtained from core measurements and interpolated across sections where no samples were available. Nitrate-N solute specific properties like diffusion in water and adsorption coefficient values were taken from relevant literatures (Hanson et al., 2006; Li et al., 2015). Irrigation type of the particular site was obtained from the field survey. Site specific fertilizer type (urea, ammonium phosphate, anhydrous ammonia) were obtained from field survey wherever available and from relevant literature (Kranz 2008, Spalding et al., 1988, 2001). **Table 9** lists which inputs are measured and which are estimated with data sources.

Table 9. Summary of model components and input parameters needed.

Data Class	Data	Source (if estimated)	Range [Estimate/Measured [^]]
Meteorological	Rainfall	Climate data https://hprcc.unl.edu	350 – 750 mm [Estimated]
	Minimum temperature		-0.71 – 3.83 °C [Estimated]
	Maximum temperature		14.2 – 20.27 °C [Estimated]
	Wind speed		38.0 – 1011 Km/day [Estimated]
	Solar radiation		0.16 – 31.26 mj/m ² /d [Estimated]
	Relative humidity		21 – 99 % [Estimated]
	Evaporation		0 – 13.66 mm [Estimated]
Geographical	Latitude		40.57° – 40.67° [Measured]
	Longitude		-98.39° – -98.56° [Measured]
	Elevation		579 – 607 m [Measured]
	Water table depth		55—113ft [Measured]
Soil characteristics	Saturated hydraulic conductivity	NA	0.006 – 7.5 m/day [Measured]
	Bulk density		0.99 – 2.7 mg/L [Measured]
	Texture		6 class [Measured]
	% Sand, silt and clay		98-99% [Measured]
	Porosity		39-55 % [Measured]
	Soil moisture contents		$\theta_s = 0.21 – 0.57$ [Measured] $\theta_r = 0.001 – 0.07$ [Estimated]
	pH		5.2-9 [Measured]
	Nitrate-N		0-20 $\mu\text{g-N/g}$ [Measured]
Ammonia-N	0-15 $\mu\text{g-N/g}$ [Measured]		
Crop	Cultivar	Decision Support System for Agrotechnology Transfer (DSSAT)	IB0033PIO3780 [Estimated]
	Crop type		Maize , Soybean [Measured]
	Growing days		Plant height [Estimated] Plant biomass [Estimated]
Management	Seed density	Shapiro et al., 2006	Corn 36000/ac [Estimated]
	Row spacing	Ping et al., 2008	15-30 inches [Estimated]
	Fertilization		100-180 Kg/Ha [Estimated]

N.A. = Not Applicable, [^]Measured values were from the different experiments conducted at Water Sciences Laboratory

Climate and management practices: Hastings is semi-arid with an average annual rainfall of ~26 inches (~655 mm) between year 2010 to 2017 Most of the rain at Hastings occur between June and August. Summers are generally hot and dry, with average monthly temperature ~30 °C in July (NOAA, 2017; HPRCC, 2017). The surface soils in the study sites are mostly a series of silty clay loams with good drainage (USDA, 2016). The content of organic matter in the topsoil (0-150 cm) at the study area is less than 0.5%, as classified by the “Soil Taxonomy Classification” of USDA (USDA, 2016). The wells in the study area pump directly from the High Plains Aquifer. The thickness of the unconsolidated aquifer is roughly 100 ft (~30 m) at Hastings WHPA. The underlying geology varies with rocks exposed at the surface are older (Gutentag et al., 1984), which means the landscape is less flat, soil texture is coarser than in many of the easternmost parts of the state, and hydraulic conductivity is lower into the aquifer. The primary land use is for agriculture, consisting of irrigated corn with some soybean rotation. The agricultural fields are mostly irrigated with a pivot irrigation system (DNR, 2017; USDA-NASS, 2017).

Irrigation and fertilizer applications were estimated according to the farmer's normal practices, obtained from a field survey and peer reviewed literature (NRCS, 1997). Fertilizer, $\sim 170 \text{ Kg-N ha}^{-1}\text{yr}^{-1}$, were applied in early May and irrigation were carried out May through August to meet crop water demand. Fields are estimated to receive 20 cm of water under pivot irrigation and 35 cm under gravity irrigation (NRCS, 1997). The input of irrigation data in the model was assumed based on crop water demand. Table S3 present in appendix 1 shows general agricultural management practices, such as dates for farming operations and other activities at the study area based on field surveys.

Soil physical properties, moisture content and nitrate-N data: The model needs specific soil physical properties data as mentioned in **Table 9**. Soil physical properties, moisture content and nitrate-N content at different intervals in the vadose zone cores were measured in Water Sciences Laboratory and detailed earlier in this report. **Table 10** lists all the measured values for the 4 different sites used for model simulations. These measured data were fed to the model to predict biogeochemical cycle of the nitrate-N at the root zone and final nitrate-N flow through the vadose zone. Saturated hydraulic conductivity was also measured in selected samples based on the lithology, and texture using falling head test method (Head, 1982). SWRC was obtained from those results of which is elaborated in the appendix. Briefly hanging column method and pressure plate apparatus (Dane et al., 2002) were utilized to measure the hydraulic conductivity of the individual cores. The generated data was fitted in RETC software (Van Genuchten et al., 1991) using various curve fitting parameters discussed above to generate the SWRC for individual cores at a particular depth.

Table 10. Physical properties of soil horizon information from the laboratory.

Description	Depth (cm)	Sand (%)	Silt (%)	Clay (%)	Bulk density (g cm ⁻³)	Porosity (cm ³ cm ⁻³)	Soil Moisture Content (cm ³ cm ⁻³)	Nitrate-N content (µg-N/g)
HC 1 East – Gravity Irrigated Site								
Loam	60	40	40	20	1.40	0.47	0.132	10.91
Clay loam	120	28	37	35	1.13	0.57	0.132	10.91
Clay	680	22	8	70	1.27	0.52	0.079	0.85
Loamy sand	800	85	10	5	1.65	0.38	0.129	1.01
Loam	1000	40	40	20	1.59	0.40	0.369	1.16
Loamy sand	1100	85	10	5	1.47	0.45	0.081	1.48
Sand	1500	87	7	6	1.55	0.42	0.145	1.99
Sandy loam	1800	65	25	10	1.65	0.38	0.167	4.47
Sandy clay	2600	50	5	45	1.83	0.31	0.021	0.76
Sand	3000	91	6	3	1.70	0.36	0.011	0.60
HC 14 West – Pivot Irrigated Site								
Silty loam	60	20	65	15	1.17	0.56	0.271	6.72
Clay loam	180	28	37	35	1.21	0.54	0.240	1.59
Silty loam	540	20	65	15	1.32	0.50	0.246	1.78
Clay loam	780	28	37	35	1.42	0.46	0.238	1.32
Sandy clay loam	1100	60	13	27	1.59	0.40	0.043	0.90
Sandy loam	1494	65	25	10	1.34	0.49	0.154	0.38
Loam	1650	40	40	20	1.34	0.49	0.192	0.63
Sandy loam	1824	65	25	10	1.86	0.30	0.074	0.37
Loamy sand	2250	85	10	5	1.55	0.41	0.112	0.42
Sand	2400	91	6	3	1.54	0.42	0.054	0.46
HC 2 – Dryland (non-irrigated site)								
Clay loam	60	28	37	35	1.40	0.47	0.282	5.24
Silty clay loam	120	10	55	35	1.13	0.57	0.264	1.85
Silty loam	510	20	65	15	1.27	0.52	0.272	1.12
Loam	675	40	40	20	1.65	0.38	0.265	0.76
Silty loam	720	20	65	15	1.59	0.40	0.275	0.37
Sandy loam	900	65	25	10	1.47	0.45	0.140	0.38
Sandy clay loam	1250	60	13	27	1.55	0.42	0.115	1.36
Sandy loam	1500	65	25	10	1.65	0.38	0.110	0.86
Sand	1900	91	4	5	1.83	0.31	0.040	0.93
Loamy sand	2260	85	10	5	1.70	0.36	0.109	0.96
HC 7 – Urban/Barnyard								
Clay	60	10	55	35	1.38	0.47	0.104	4.16
Silty loam	180	20	65	15	1.09	0.58	0.155	1.23
Silty clay	510	40	40	20	1.30	0.50	0.175	1.22
Loam	675	20	65	15	1.28	0.51	0.193	1.41
Sand	780	65	25	10	1.47	0.44	0.045	3.70
Loamy sand	1100	60	13	27	2.22	0.16	0.076	1.05
Sandy clay	1250	65	25	10	1.83	0.30	0.092	1.98
Clay loam	1500	91	4	5	2.17	0.18	0.184	8.88
Sand	1900	85	10	5	1.91	0.27	0.099	3.36
Loamy sand	2050	10	55	35	2.02	0.23	0.090	2.71

N. A. = Not Available

Vadose Zone Travel Time Model Estimates

Saturated Hydraulic Conductivity and Soil Water Retention Curve

The measured saturated hydraulic conductivity of soil cores pertinent to the sites used in the model along with soil classification are presented in **Table 11**. Model input data is summarized in Table S4 in appendix 1, along with the soil texture, percentage of clay, silt and sand in the soil. The detailed method of saturated hydraulic conductivity and soil water retention parameters estimation of selected soil cores are presented in the appendix 2.

Table 11. Laboratory measured soil properties and saturated hydraulic conductivity of the soil cores.

Core ID	Depth (ft)	Soil Type	Class (UCSC)*	K _{sat} (m/day)	K _{sat} (µm/sec)	Range (µm/sec) (NRCS)**
HC 1E	32.5-35	Loamy sand	5	1.232	14.3	42.34 – 141.14
HC 1E	51.4-52.5	Clay	1	0.148	1.7	0.42 – 1.41
HC 2	5 - 7.5	Silt loam	3	4.392	50.8	4.23 – 14.11
HC 2	7.5 -9	Silt loam	3	0.010	0.1	4.23 – 14.11
HC 2	27.6 -30	Sandy loam	5	0.339	3.9	42.34 – 141.14
HC 7	19.7-22.5	Loam	3	0.615	7.1	4.23 – 14.11
HC 14W	4.5-6.7	Clay loam	1	1.23	14.2	0.42 – 1.41
HC 14 W	47.5-50	Loamy sand	5	0.494	5.7	42.34 – 141.14
HC 14 W	60.8	Loamy sand	5	0.059	0.7	42.34 – 141.14

*Universal Soil Classification Systems, ** Natural Resources Conservation Service

Laboratory measured saturated hydraulic conductivity is similar in some cases but also shows high variation with expected NRCS ranges. One main reason of this difference is compaction of soil cores. Hasting soil cores can be categorized into six different classes based on soil classification system (NRCS) and saturated hydraulic conductivity. The SWRC generated from RETC for the estimation of VG and BC pedotransfer of soil cores are shown in **Figure 25** for site HC 1E at two different depths, rest of the curves are represented in the appendix 1 (Figure S1-2).

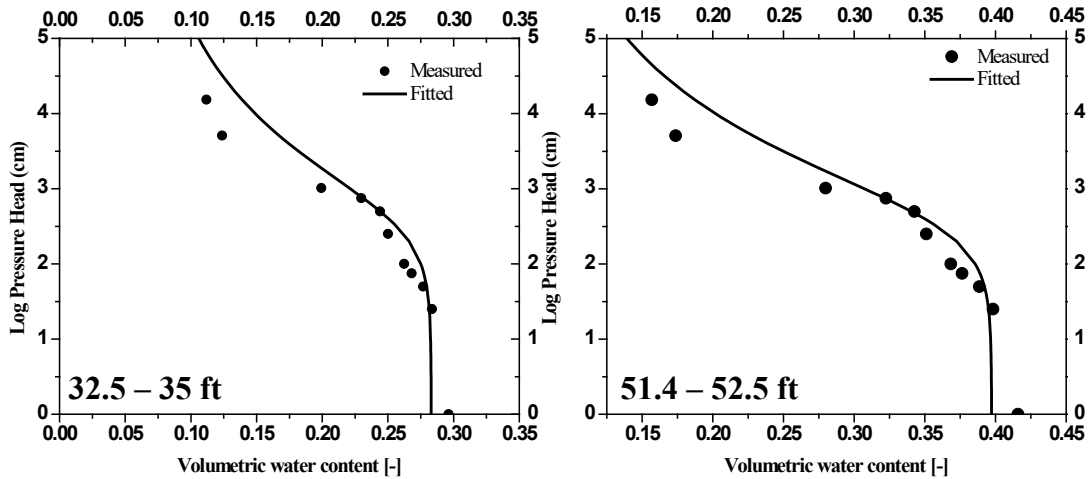


Figure 24. The SWRC for soil core HC1E generated after curve fitting by RETC. The black line represents fitted data and black circle shows observed values of the water content.

After curve fitting RETC generates the VG and BC parameters, which are shown in **Table 12** for different sites. Curve fitting parameters of others core are presented in appendix 1 (Table S5)

Table 12. Estimated pedotransfer function for the soil cores at different depth.

Core Id	θ_r	θ_s	α (1/cm)	N	m
HC1E (32.5-35)	0.057	0.282	0.0026	1.27	0.215
HC1E (51.4-52.4)	0.068	0.397	0.0026	1.27	0.215
HC14W (4.5-6.7)	0.045	0.550	0.0167	1.16	0.138
HC2 (5-7.5)	0.067	0.534	0.0231	1.14	0.123
HC 7 (19.7- 22.5)	0.078	0.492	0.0035	1.30	0.231

Calibration and validation of models

RZWQM2 Calibration and validation: RZWQM2 simulation was ran for 180 cm soil profile depth at site HC2 (dryland), HC1 E (gravity), and HC14 W (Pivot) for soil water and nitrate-N transport. The flow chart of calibration and validation of model are presented in appendix C (Figure S5). The climate data of selected sites are used for the atmospheric boundary condition inputs (Appendix C, Figure S3-4). In the simulation domain the root zone depth was distributed into 10 soil layers. 2011 observation data (Spalding and Toavs, 2011) were compared with the predicted output of the RZWQM2 model. The 2016 observed data were used for the validation of the model output. The RMSE of the model validation showed that predicted soil water contents in the RZWQM2 model were relatively close to the observed soil water contents, with the RMSE between 0.05 and 0.06 for the all sites (**Figure 26**). It should be

noted that soil physical properties play a significant role in moving soil water below the root zone. To see the impact of irrigation on dryland site the simulations run using 20 cm irrigation during the growing season of the corn at the selected site (HC2). Figure (S6-7) represent the moisture profile dynamics in the root zone under non irrigated and irrigated dryland. These represent the leaching seepage flux below the root zone and how is the moisture content varying during the year 2011 in the root zone systems. **Figure 26** shows the calibration and validation with observed and predicted soil water content in the upper 180 cm profile at the selected sites.

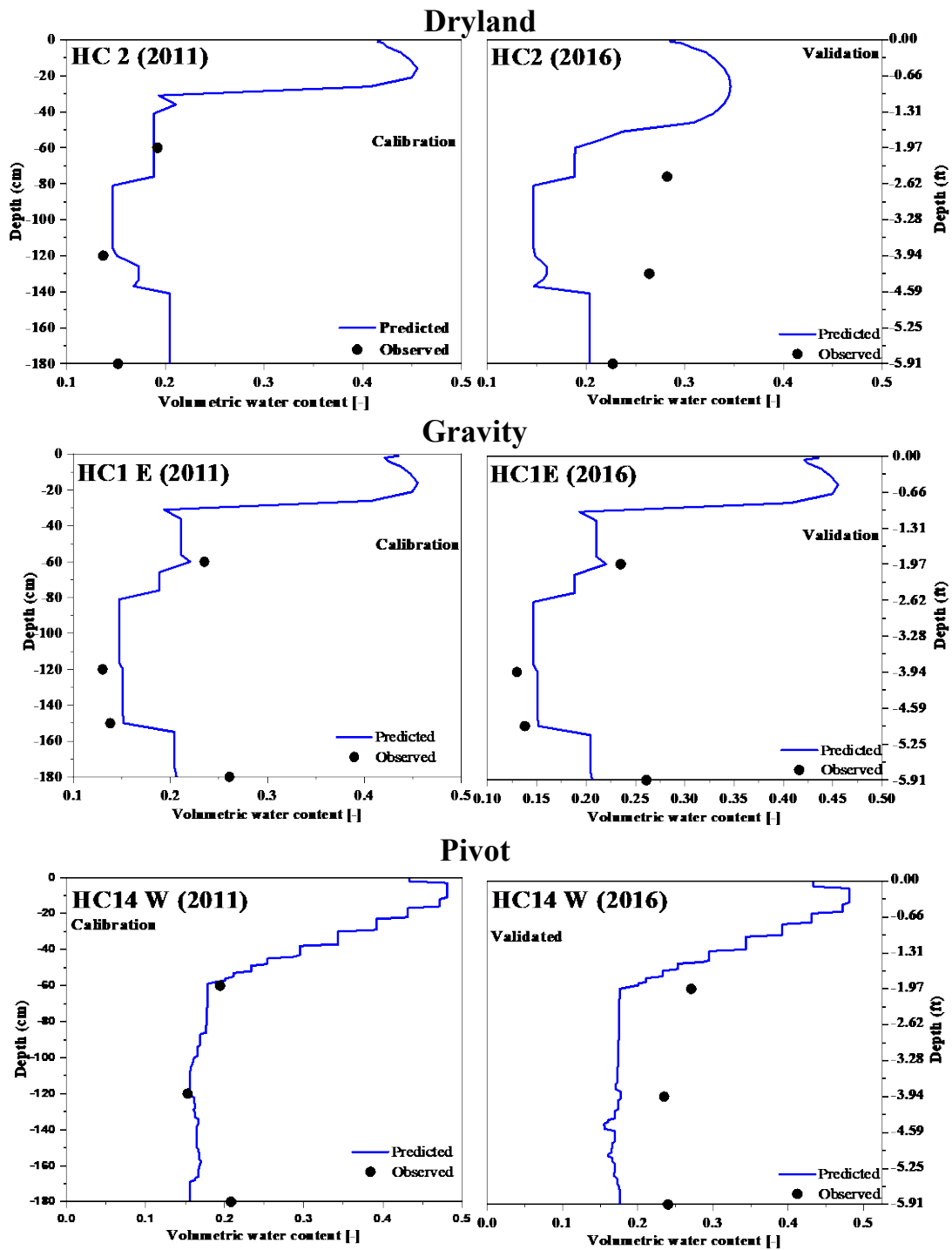


Figure 25. The calibration and validation with observed and predicted soil water content in the upper 180 cm profile at the selected sites

The soil moisture content decreasing with depth in irrigation and non-irrigation condition. In dryland condition maximum soil moisture content was predicted at 30 cm depth an obvious reason of this, the more evapotranspiration on the soil surface. When irrigation applied on the soil surface, the soil moisture content is more at 15 cm depth, so soil moisture content directly depends upon the amount of infiltrating water (Figure S7).

Figure 27 shows the calibration and validation with observed and predicted pore water nitrate-N concentrations in the upper 180 cm profile at the selected sites. The predicted values compared with the observed results at the laboratory during the November 2016. The RMSE for predicted pore water nitrate-N concentrations by the RZWQM2 model was between 3.87 and 5.48. Soil water contents likely influence the pore water nitrate-N concentrations in the root zone. Higher water content and infiltration rate can lower the pore water nitrate-N concentrations in the root, and result in more nitrate-N passage through the root zone systems.

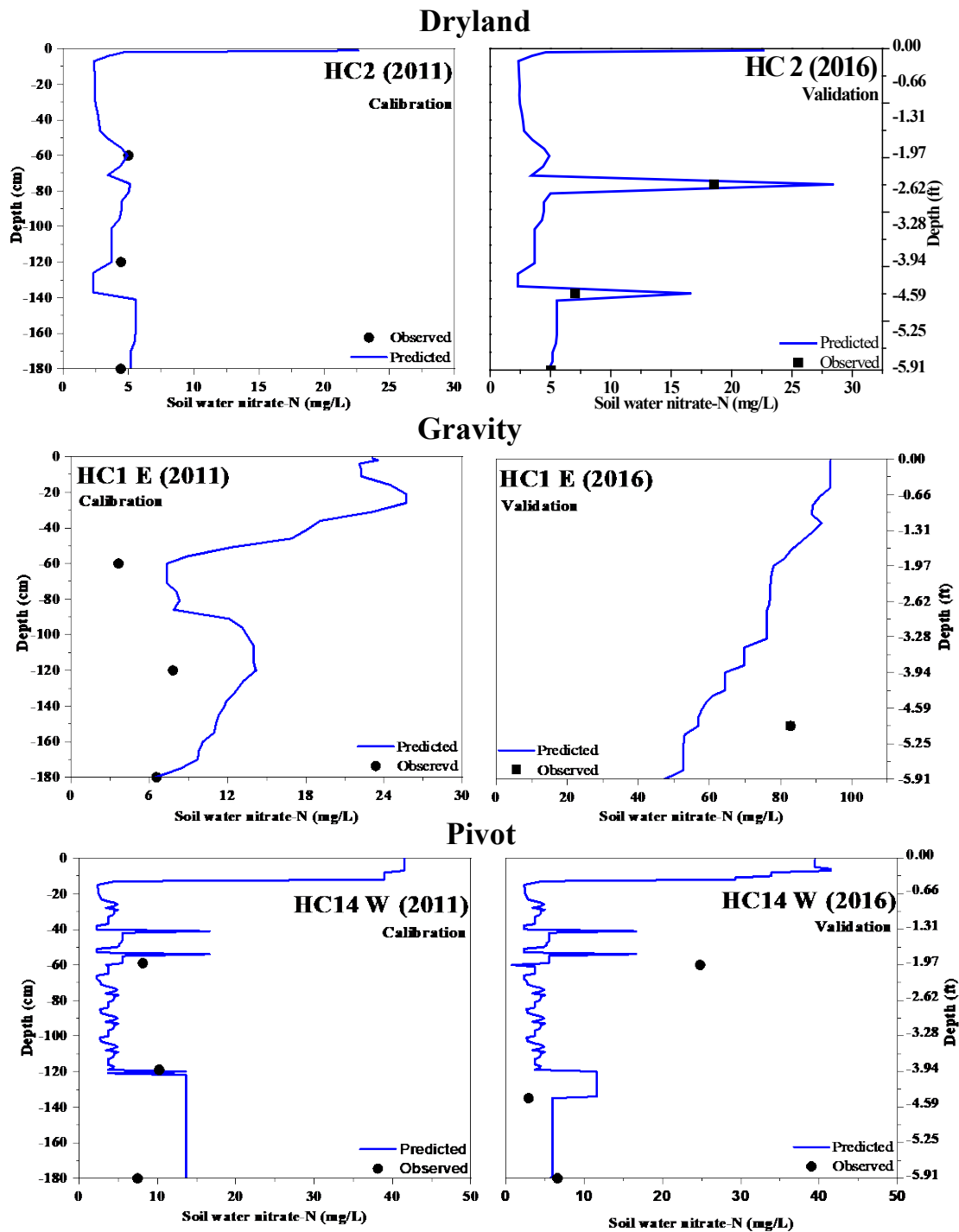


Figure 26. The calibration and validation with observed and predicted pore water nitrate-N concentrations in the upper 180 cm profile at the selected sites

HYDRUS 1D calibration and validation: HYDRUS 1D simulation was calibrated using the 2011 observation data compared with the predicted output of the HYDRUS model. The HYDRUS model was run from 2011 to 2016 for the model validation using the RZWQM2 output as a input. The results comparing model output to measured moisture content and nitrate concentrations are presented in **Figure 28** and **Figure 29**. The soil water flux in deep vadose zone significantly depend upon the soil properties. The deep vadose zone of all sites site, below 9-11 meter the mostly have sandy lithology, likely a factor in the smaller soil water content in the deep vadose zone.

The soil moisture flux and soil water nitrate –N was simulated for the selected soil cores for the year 2011 and 2016 (**Figure 28** and **Figure 29**). The simulated result was calibrated and validated for the year 2011 and 2016 respectively. The RMSE for predicted soil moisture flux and pore water nitrate-N concentrations by HYDRUS model was varying between 0.04 to 0.08 for moisture flux and 3.8 to 14.7 for the pore water nitrate-N for all the selected locations. The predicted soil water nitrate-N concentrations were same order of magnitude with observed nitrate-N concentrations with the small RMSE values during the prediction year. The model overestimated maximum nitrate-N concentrations in the vadose zone profile for HC2 dryland sites. Soil water contents likely influence the pore water nitrate-N concentrations in the vadose zone.

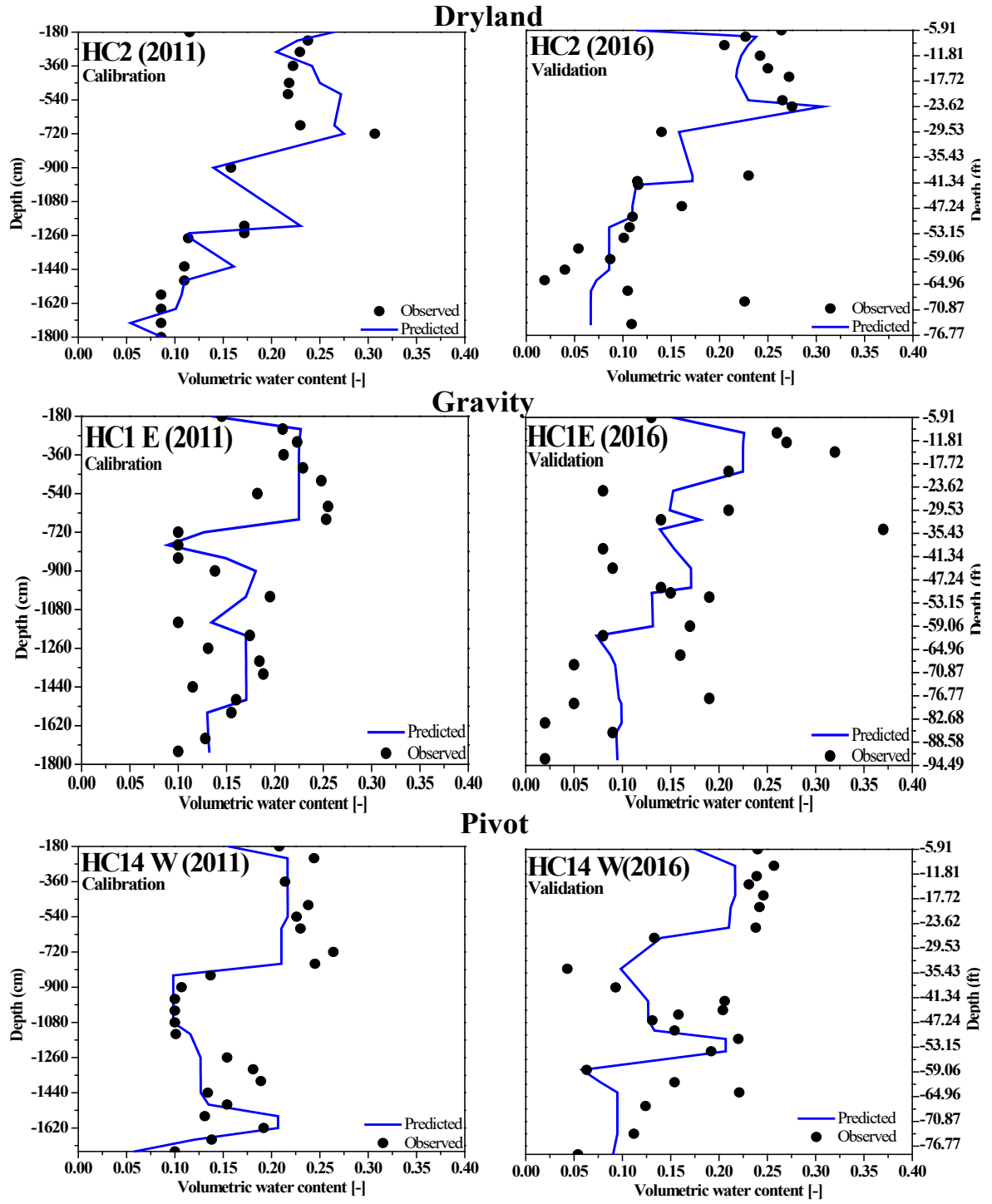


Figure 27. calibration and validation with observed and predicted soil moisture content from root zone to deep water table at the selected sites.

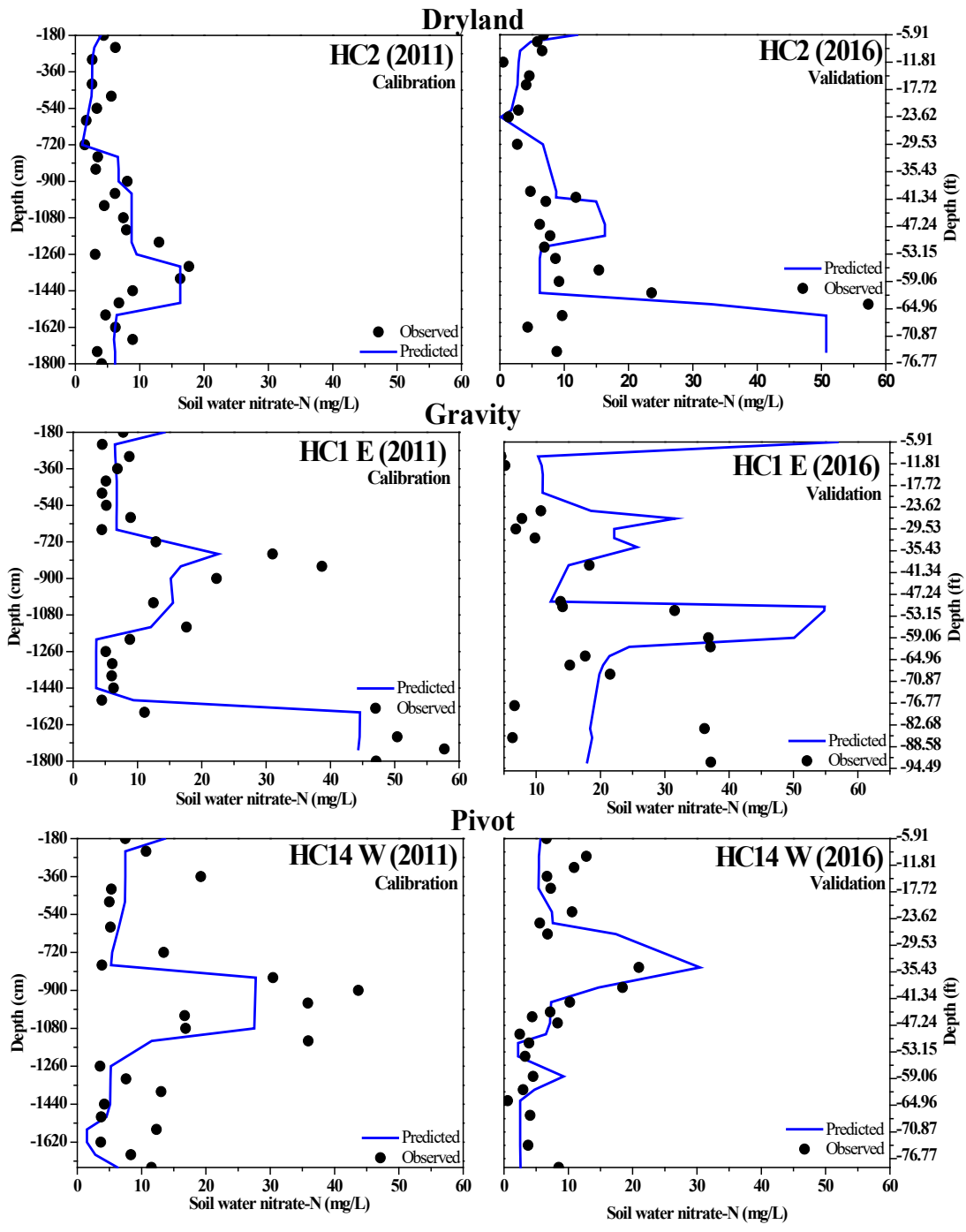


Figure 28. Calibration and validation with observed and predicted soil water nitrate-N concentrations from root zone to deep water table.

Figure 26 - 29 show the soil water contents and pore water nitrate-N concentrations in the vadose zone profile under the scenario of dryland, gravity and pivot irrigation. Based on the scenario results, pivot irrigation system can reduce nitrate-N concentrations in the unsaturated zone. The controlled irrigation system probably improves the plant uptake of nitrate-N, thus nitrate-N concentrations in the deep vadose zone are lower. The results also indicate that irrigation increases moisture content in the vadose zone. Both pivot and gravity irrigation likely increase nitrate-N loading to the deep vadose zone because of greater deep percolation as compared to dryland. Based on the scenario results, a change from continuous corn production to a corn-soybean rotation may reduce nitrate-N concentrations in the vadose zone. Result suggest that the corn-soybean rotation may result in lower nitrate-N concentrations in the vadose zone compared to continuous corn. Field investigations indicate however that a reduced nitrate leaching benefit is only realized when the full soil nitrogen credit from the legume crop is used to reduce total annual nitrogen application rate (Klocke at al 1999; Owens et al 2000).

Estimated Travel Time of Nitrate-N in Vadose Zone

Figure 30 shows the predicted nitrate-N concentrations in vadose zone with travel times using the coupled (RZWQM2 and HYDRUS) model. The simulation scenarios runs in the set of 20 years climate data (1997-2016) and after each run nitrate-N peak concentration estimated. The coupled model predicted soil nitrate-N concentration in the year 1997 used as soil initial conditions. Single fertilizer application (180 kg/Ha) in the growing season of 1997 was applied on the 10 cm depth of soil surface. The simulation run for 20 year in the cycle and every time highest peak concentration plotted with respect to depth. By using peak displacement method nitrate-N transport velocity was estimated. The predicted vertical transport rate at HC2 dryland site was between ~1.2 and 1.7 ft/year. The nitrate-N can be stored for many years in the vadose zone, especially in an agricultural area. Based on the model, nitrate-N is likely transported from land surface to depth of 80 ft over a period of ~47 years.

The estimated nitrate-N leaching rate under gravity irrigated crops was 2.6 ft/year. Sediments at the HC 2 site are primarily sandy soil below 50 ft depth. Sandy soil have high porosity due to which solute leach rapidly into the groundwater. A greater expected water flux under irrigation corresponds to a more rapid transport rate as compare to the dryland site. The effect of changing water availability on transport of nitrate-N in the vadose zone was evaluated under pivot irrigation. Under corn field condition and 20 cm water application during the growing season the estimated nitrate-N transport velocity was 1.9 ft/year. Nitrate-N leaching is faster as compare to the dryland is due to high moisture flux in the soil domain during the corn growing season. The effect of crop rotation on nitrate-N travel time a simulation performed considering pivot irrigation with crop rotation. Results suggest that crop rotation does not affect nitrate-N leaching velocity. Deep vadose zone nitrate-N concentration decrease under the crop rotation scenario as compared to pivot irrigation scenario. The estimated nitrate-N travel time at barnyard or urban site was 1.3 ft/year shows that planting of crop can reduced the nitrate-N pollution in the groundwater. The nitrate-N transport velocity varies from 1.2 to 2.6 ft/year under different irrigation conditions.

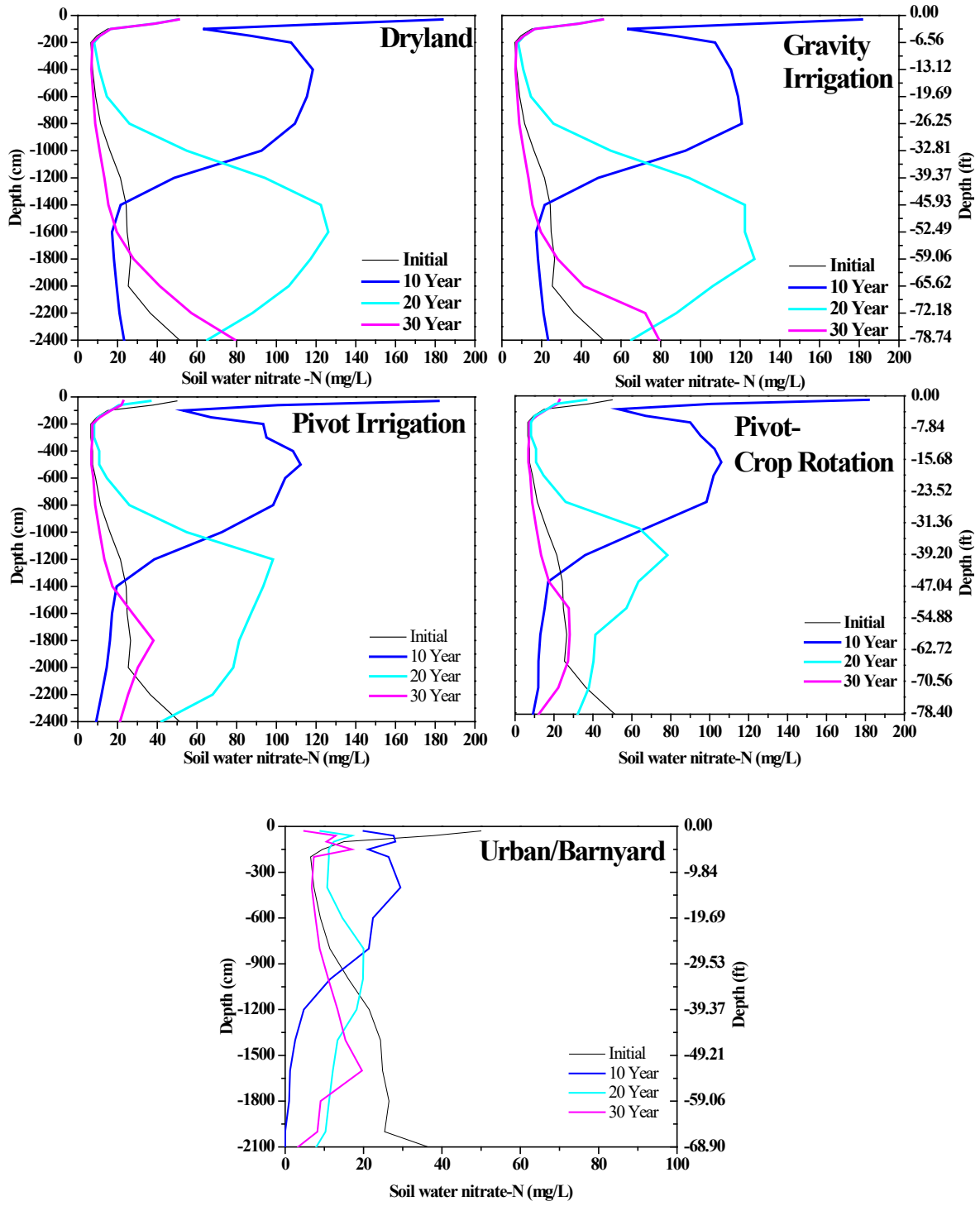


Figure 29. Pore water nitrate-N concentrations simulated using the coupled RZWQ2 and HYDRUS 1D model. Nitrate-N peak reach up to 1600 cm (52 ft) over a 20 year simulation

The estimated average vertical velocity is between 1.2 and 2.6 ft/year (**Figure 30**) under different irrigation and land use scenarios. The estimated velocity for non-irrigated continuous corn is between 1.2 and 1.7 ft/year (**Figure 30**) and similar to those previously reported under rain-fed agricultural fields, the average velocity is 1.77 ± 0.9 ft/year. (Baran et al., 2007; Huang, Pang, and Yuan, 2013). A reason for the lower velocity is that the saturated hydraulic conductivity of the sandy vadose zone is lower under the HC2 dryland corn. All locations below 45 feet have sandy layers in the deep vadose zone, and because of this Hasting WHPA groundwater is more vulnerable to the nitrate-N pollution. According to the model's estimated result, nitrate-N will contaminate the groundwater in around 30-45 years under different land use and management scenarios. At the HC14 W site, the shallow aquifer has a high vulnerability to nitrate-N contamination in spite of the low saturated hydraulic conductivity of the aquifer (Nolan et al., 1997). In this study, the estimated nitrate-N travel velocity under gravity-irrigated field conditions was 2.6 ft/year and somewhat lower than that reported for similar soil lithology (Min et al., 2017; Wang et al., 2019). In our study, laboratory-estimated soil parameters were used, so that may be one reason for the underestimation of travel time in the deep vadose zone. While the uncertainty of these transport velocities is acknowledged and the presence of several layers of soil, there is the possibility of more/less transport via preferential or matrix flow.

Conclusions

Vadose zone depth and soil parameters are important factors that need to be considered when designing sustainable land management. However, the root zone water solute balance has not been sufficiently examined, partly because numerical models have not fully considered all the interactions between the soil water balance and plant growth. In this study, simulations were performed by coupling RZWQM2 and HYDRUS-1D in a simplified manner. The coupled model was calibrated and evaluated for simulating soil water and nitrate-N movement through the deep vadose zone at a depth of 30 m under different scenarios. The model was calibrated using field data from the year 2011, then data from 2016 were used to evaluate model performance. The model performance was evaluated by a comparison of field-measured gravimetric water content and pore water nitrate-N concentrations with the values predicted by the RZWQM2 and HYDRUS 1D models. The resulting RMSE values were small. Thus, these models can be used as a predictive tool for agricultural management. Differences between observed and predicted values likely occurred because of the complexity of the deep vadose zone. The main objective of the coupled model was to estimate nitrate travel time through the deep vadose zone. Nitrate-N travels from the land surface to a depth of 80 ft with a vadose zone travel time of 30 years with a velocity of ~ 2.6 ft/year in Hastings, Nebraska. To reach the groundwater table for an 80 ft profile, it takes almost 30 years, so due to the storage of nitrate-N in the vadose zone at the study area, it is necessary to monitor and plan a suitable remediation strategy for groundwater management.

References

- Adams, C. (2018). The Impact of Land Use on Nitrate-N Movement and Storage in the Vadose Zone of the Hastings' WHPA.
- Ahuja, L. R., DeCoursey, D. G., Barnes, B. B., and Rojas, K. W. (1993). Characteristics of macropore transport studied with the ARS root zone water quality model. *Transactions of the ASAE*, 36(2), 369-380.
- Ahuja, L. R., Johnsen, K. E., and Heathman, G. C. (1995). Macropore transport of a surface-applied bromide tracer: Model evaluation and refinement. *Soil Science Society of America Journal*, 59(5), 1234-1241.
- Ahuja, L., Rojas, K. W., and Hanson, J. D. (2000). Root zone water quality model: modelling management effects on water quality and crop production. Water Resources Publication.
- Baran, N., Richert, J., and Mouvet, C. (2007). Field data and modelling of water and nitrate movement through deep unsaturated loess. *Journal of Hydrology*, 345(1-2), 27-37.
- Brooks, R., and Corey, T. (1964). Hydraulic properties of porous media. *Hydrology Papers*, Colorado State University, 24, 37.
- Comly, H. H. (1945). Cyanosis in infants caused by nitrates in well water. *Journal of the American Medical Association*, 129(2), 112-116.
- Dane, J. H., Hopmans, J. W., and Topp, G. C. (2002). Hanging water column. *Methods of soil analysis*. Part, 4, 680-683.
- Dane, J. H., Hopmans, J. W., and Topp, G. C. (2002). Pressure plate extractor. *Methods of soil analysis*. Part, 4, 688-690.
- DNR (Department of Natural Resources), (2017). The Nebraska Department of Natural Resources. <http://www.dnr.ne.gov/data>. (Accessed July 2019)
- Green, W. H., and Ampt, G. A. (1911). The flow of air and water through soils. *J. Agric. Sci*, 4, 1-24.
- Gutentag, E. D., Heimes, F. J., Krothe, N. C., Luckey, R. R., and Weeks, J. B. (1984). Geohydrology of the High Plains aquifer in parts of Colorado, Kansas, Nebraska, New Mexico, Oklahoma, South Dakota, Texas, and Wyoming (p. 63). Washington, DC: US Government Printing Office.
- Hachum, A. Y., and Alfaro, J. F. (1980). Rain infiltration into layered soils: Prediction. In *Journal of the Irrigation and Drainage Division*, American Society of Civil Engineers (Vol. 106, No. IR4, pp. 311-319).
- Hanson, B. R., Šimůnek, J., and Hopmans, J. W. (2006). Evaluation of urea–ammonium–nitrate fertigation with drip irrigation using numerical modeling. *Agricultural water management*, 86(1-2), 102-113.
- Hastings Utilities, (1997). Groundwater Modeling Study and Well Head Protection Area Delineation for Hastings Utilities Municipal Wellfield

- Head, K. H. (1980). *Manual of soil laboratory testing* (Vol. 1, No. 2). London: Pentech Press.
- HPRCC (High Plains Regional Climate Center), (2016). HPRCC Climate Summaries. <https://hprcc.unl.edu/climatesummaries.php>, last accessed on August, 2019.
- Huang, T., and Pang, Z. (2011). Estimating groundwater recharge following land-use change using chloride mass balance of soil profiles: a case study at Guyuan and Xifeng in the Loess Plateau of China. *Hydrogeology Journal*, 19(1), 177-186.
- Jones, J. W., Hoogenboom, G., Porter, C. H., Boote, K. J., Batchelor, W. D., Hunt, L. A., Wilkens, P.W., Singh, U., Gijsman, A.J. and Ritchie, J. T. (2003). The DSSAT cropping system model. *European journal of agronomy*, 18(3-4), 235-265.
- Kranz, W.L. (2008). Irrigation and nitrogen management. User education/certification program. Nebraska Extension, University of Nebraska–Lincoln. Report Ec-2008, 117 p
- Li, Y., Šimůnek, J., Zhang, Z., Jing, L., and Ni, L. (2015). Evaluation of nitrogen balance in a direct-seeded-rice field experiment using HYDRUS-1D. *Agricultural Water Management*, 148, 213-222.
- Ma, L., Ahuja, L. R., Ascough II, J. C., Shaffer, M. J., Rojas, K. W., Malone, R. W., and Cameira, M. R. (2001). Integrating system modeling with field research in agriculture: Applications of the Root Zone Water Quality Model (RZWQM).
- Ma, L., Ahuja, L. R., Saseendran, S. A., Malone, R. W., Green, T. R., Nolan, B. T., Bartling, P.N.S., Flerchinger, G.N., Boote, K.J. and Hoogenboom, G. (2011). A protocol for parameterization and calibration of RZWQM2 in field research. *Methods of introducing system models into agricultural research, (methodsofintrod)*, 1-64.
- Ma, L., Hoogenboom, G., Saseendran, S. A., Bartling, P. N. S., Ahuja, L. R., and Green, T. R. (2009). Effects of estimating soil hydraulic properties and root growth factor on soil water balance and crop production. *Agronomy journal*, 101(3), 572-583.
- Min, L., Shen, Y., Pei, H., and Jing, B. (2017). Characterising deep vadose zone water movement and solute transport under typical irrigated cropland in the North China Plain. *Hydrological Processes*, 31(7), 1498-1509.
- Mualem, Y. (1976). A new model for predicting the hydraulic conductivity of unsaturated porous media. *Water resources research*, 12(3), 513-522.
- Nakamura, K., Harter, T., Hirono, Y., Horino, H., and Mitsuno, T. (2004). Assessment of root zone nitrogen leaching as affected by irrigation and nutrient management practices. *Vadose Zone Journal*, 3(4), 1353-1366.
- NASS – USDA (2016) <https://nassgeodata.gmu.edu/CropScape/>.(Accessed July 2019)
- NOAA (National Oceanic and Atmospheric Administration), (2017). The National Oceanic and Atmospheric Administration, U.S. Department of Commerce, National Weather Service Forecast Office available at <http://w2.weather.gov/climate/xmacis.php?wfo=gid>. (Accessed July 2019)
- Nolan, B. T., Ruddy, B. C., Hitt, K. J., and Helsel, D. R. (1997). Risk of Nitrate in groundwater's of the United States a national perspective. *Environmental science & technology*, 31(8), 2229-2236.

- Nolan, J., and Weber, K. A. (2015). Natural uranium contamination in major US aquifers linked to nitrate. *Environmental Science & Technology Letters*, 2(8), 215-220.
- NRCS, U., (1997). Irrigation guide. *National Engineering Handbook*, 452.
- Ping, J. L., Ferguson, R. B., and Dobermann, A. (2008). Site-specific nitrogen and plant density management in irrigated maize. *Agronomy journal*, 100(4), 1193-1204.
- Refsgaard, J. C. (1997). Parameterisation, calibration and validation of distributed hydrological models. *Journal of hydrology*, 198(1-4), 69-97.
- Reilly, T. E., Dennehy, K. F., Alley, W. M., and Cunningham, W. L. (2008). Ground-water availability in the United States: US Geological Survey Circular 1323, 70 p. Reston, VA., also available on line at <http://pubs.usgs.gov/circ/1323>.
- Richards, L. A. (1931). Capillary conduction of liquids through porous mediums. *Physics*, 1(5), 318-333.
- Schullehner, J., Hansen, B., Thygesen, M., Pedersen, C. B., and Sigsgaard, T. (2018). Nitrate in drinking water and colorectal cancer risk: A nationwide population-based cohort study. *International journal of cancer*, 143(1), 73-79.
- Shaffer, M. J., Ma, L., and Hansen, S. (2001). Modeling carbon and nitrogen dynamics for soil management. CRC Press.
- Shaffer, M. J., Rojas, K. W., DeCoursey, D. G., Hebson, C. S., and Ahuja, L. R. (2000). Nutrient chemistry processes—OMNI. Root Zone Water Quality Model: Modeling management effects on water quality and crop production. *Water Resour. Publ.*, Highlands Ranch, CO, 119-144.
- Shapiro, C. A., and Wortmann, C. S. (2006). Corn response to nitrogen rate, row spacing, and plant density in eastern Nebraska. *Agronomy Journal*, 98(3), 529-535.
- Šimunek, J., Van Genuchten, M. T., and Šejna, M. (2012). HYDRUS: Model use, calibration, and validation. *Transactions of the ASABE*, 55(4), 1263-1274.
- Smith, R. L., Kent, D. B., Repert, D. A., and Böhlke, J. K. (2017). Anoxic nitrate reduction coupled with iron oxidation and attenuation of dissolved arsenic and phosphate in a sand and gravel aquifer. *Geochimica et Cosmochimica Acta*, 196, 102-120.
- Soil Data Viewer - USDA, 2017
https://www.nrcs.usda.gov/wps/portal/nrcs/detail/soils/survey/geo/?cid=nrcs142p2_053614
 (Access February 2019)
- Spalding, R. F., and Toavs, M. (2011). 2011 Vadose Zone Nitrate Study at Hastings, NE.
- Spalding, R. F., and Kitchen, L. A. (1988). Nitrate in the intermediate vadose zone beneath irrigated cropland. *Groundwater Monitoring & Remediation*, 8(2), 89-95.
- Spalding, R. F., Watts, D. G., Schepers, J. S., Burbach, M. E., Exner, M. E., Poreda, R. J., and Martin, G. E. (2001). Controlling nitrate leaching in irrigated agriculture. *Journal of Environmental Quality*, 30(4), 1184-1194.

- USDA, 2016. Web soil survey, Natural Resources Conservation Service Soils. United States Department of Agriculture (USDA). <https://websoilsurvey.sc.egov.usda.gov/App/WebSoilSurvey.aspx>. (Accessed July 2019)
- Van Genuchten, M. T. (1980). A closed-form equation for predicting the hydraulic conductivity of unsaturated soils 1. *Soil science society of America journal*, 44(5), 892-898.
- Van Genuchten, M. V., Leij, F. J., and Yates, S. R. (1991). The RETC code for quantifying the hydraulic functions of unsaturated soils.
- Wang, H., Gao, J. E., Li, X. H., Zhang, S. L., and Wang, H. J. (2015). Nitrate accumulation and leaching in surface and ground water based on simulated rainfall experiments. *PLoS One*, 10(8), e0136274.
- Wang, S., Wei, S., Liang, H., Zheng, W., Li, X., Hu, C., Currell, M.J., Zhou, F. and Min, L. (2019). Nitrogen stock and leaching rates in a thick vadose zone below areas of long-term nitrogen fertilizer application in the North China Plain: A future groundwater quality threat. *Journal of Hydrology*, 576, 28-40

Arsenic and Uranium in the Hastings WHPA Vadose Zone

The vadose, or unsaturated zone is termed as a natural filter for recharging groundwater below, and it is well-known to serve as a reservoir for nitrate and other contaminants before reaching the groundwater (Nimmo, 2009). However, some seemingly immobile trace elements in the unsaturated zone can be mobilized due to a number of factors including redox changes, fertilizer application and water loading (Cassiani et al., 2007). It is of utmost importance to understand the occurrence of potentially mobilized trace elements in the unsaturated zone that can later become contaminants in groundwater. Arsenic (As) and uranium (U) concentrations are known to be significantly high in the soils of Nebraska, mainly arising from different geogenic factors (Brown et al., 2007). As also has been used as a pesticide globally in agricultural areas and has been known to accumulate in the unsaturated zone due to the anthropogenic activity (Reedy et al., 2007). Around 36% wells in southern high plains region of Ogallala aquifer exceeds the Environmental Protection Agency (EPA) 10 µg/L standard for As (Reedy et al., 2007). The EPA risk-based soil screening levels (SSL) for protection of groundwater is considerably low for both As and U (see **Table 13**) (USEPA, 2019). Understanding the occurrence and forms of As and U in soil can serve as a proactive measure for groundwater protection. For the present study, easily mobilized As and U were quantified in soil cores collected at 32 different sites to evaluate the occurrence and potential for leaching to the local aquifer in the region.

Nitrate concentration natural or driven by fertilizers, is known to impact mobility of As and U under oxic and anoxic conditions (Herath et al., 2016; Neil et al., 2014; Nolan and Weber, 2015; Smith et al., 2017; Westrop et al., 2018). Therefore, the data of As and U were divided and analyzed as related to an increase or decrease in nitrate mass in the vadose zone under three different irrigation types - pivot or sprinkler irrigation, gravity or furrow irrigation, and residential area, barnyard or non-irrigated sites, as these irrigation types showed a varied quantity of nitrate in the unsaturated zone cores in Hastings (Adams, 2018). A decrease in nitrate concentration in the unsaturated zone was observed under pivot irrigation systems compared to gravity irrigation (Adams, 2018). Further, the application of water in pivot irrigation is much less as compared to gravity irrigation (United States Department of Agriculture, 2019), and the rate of water transport through unsaturated zone is higher in gravity irrigation (Bosch-rubia, 2015; Spalding et al., 2001), because water movement rates can also influence the transport of mobilized As and U. It was predicted that increase of nitrate in the unsaturated zone can enhance mobilization of As and U, thereby making them more vulnerable to be a possible contaminant in the groundwater. This chapter reports As and U distributions in the unsaturated zone of the Hastings WHPA area measured in selected samples. The profiles were compared with nitrate-N profiles and water soluble dissolved organic carbon (DOC) levels to help identify areas where leaching may be occurring and impacting groundwater quality.

Health Risks

As and U are known carcinogenic and are highly toxic to human health. Chronic exposure to high concentrations can cause cancer and for this reason the current EPA, maximum contaminant level (MCL) in drinking water are set at 10 µg/L and 30 µg/L for As and U respectively (**Table 13**). Low level chronic consumption such as ingestion from drinking water, of these naturally occurring trace elements can also have negative impacts on human health. As and U present in unsaturated zone soil can be a significant source from where the groundwater below can be contaminated by mobilization of these contaminants.

The concentration of As varies widely in soil, the mean value of As in Earth’s crust is considered to be 3.4 µg/g (Wedepohl, 1991). The USEPA Regional Screening Levels (RSLs) for soil is 0.39 µg/g, which is based on typical human exposure assessment assumptions (350 days/yr, 30 yr residence during a 70-yr lifetime, 100% relative bioavailability) and standard toxicological guidance values (Teaf et al., 2010). The USEPA risk assessment includes various exposure route such as dermal, inhalation, plant uptake however direct ingestion is the major exposure pathway for As (USEPA, 2019), which includes consumption of contaminated drinking water. The cancer target risk ranges from 1E-07 to 1E-04. At least 14 states employ the USEPA RSL methodology and a 1E-06 cancer risk level (USEPA, 2019), resulting in default guidelines that fall tightly between 0.38 µg/g and 0.41 µg/g but this level is less than commonly encountered background soil arsenic levels in much of the country (Teaf et al., 2010). However, values higher than the screening levels are routinely encountered and these concentrations serve more as a health guidelines from EPA (USEPA, 2019). The EPA MCL-based soil screening level for groundwater protection of As is set at 0.29 µg/g (Table 13).

Table 13: US-EPA Regional Screening Level (RSL) Resident Soil to GW Table (TR=1E-06, HQ=1) April 2019 (USEPA, 2019)

Contaminant	RfD _o (mg/kg-day)	Ingestion SL TR=1E-06 (µg/L)	Protection of Groundwater SSL		MCL (µg/L)
			Risk-based SSL (µg/g)	MCL-based SSL (µg/g)	
Arsenic (As) Inorganic	3.0E-04*	5.2E-02	1.5E-03	2.9E-01	10
Uranium (U) Soluble	2.0E-04		1.8E+00	1.4E+01	30

RfD_o= Reference Dose, TR= Cancer Target Risk, SL= Screening Level, SSL= Soil Screening Level, MCL= Maximum Contaminant Level, *Derived from drinking water studies

Irrigation can bring about a modification of As behavior in both unsaturated zone and aquifer below (Chi et al., 2018). Irrigation can cause changes in redox-sensitive processes, such as denitrification, and can mobilize naturally occurring As in soils (Chi et al., 2018). Dissolved As in groundwater used for irrigation can accumulate in the surface soil and can increase the concentration of As in the unsaturated zone (Farooq et al., 2019). The accumulated As in the surface soil can then be mobilized, leached and eventually released to groundwater (Chi et al., 2018). Recent studies have confirmed that irrigation can redistribute As in the unsaturated zone, and iron (Fe) is known to play a key role in these redistribution processes (Chi et al., 2018). High usage of groundwater for irrigation can impact As mobility in the unsaturated zone beneath crops and may be related to fluctuations of the water table and repeated changes in As levels in pore water, groundwater and surface soil (Xiao et al., 2018). Understanding occurrence and forms of As and mobilization mechanisms in soil and the unsaturated zone is critical for predicting how groundwater may be affected by increased As levels. As accumulation in soil can also be taken up by food crops (Malakar et al., 2019).

Inorganic As can exist as reduced arsenite oxyanion (As(III)) and oxidized arsenate oxyanion (As(V)). Arsenite is 25-60 times more toxic than arsenate and also more mobile (Malakar et al., 2016a). The occurrence and mobilization of As is redox and pH sensitive, As(III) is generally present in reducing

condition such as groundwater and As(V) in oxidizing condition such as surface water (Malakar et al., 2016a, 2016b). As(V) is charged species at the near-neutral to basic pH prevalent in natural systems. The charged species can chemisorb with iron oxides and iron oxy(hydroxides) making them immobile (Malakar et al., 2016b). However, As(III) is a neutral species at near-neutral pH and basic pH (till pH= 9), which gives it more mobility under natural pH conditions.

U exists in soils and groundwater primarily as redox determined complexes of U(IV) and U(VI), while the oxidized U(VI) is considered to be the most mobile and soluble form (Vodyanitskii, 2011). Redox conditions are affected by moisture content and microbial activity, it is likely that U mobilization is also affected by redox conditions in the unsaturated zone. Iron transformation is known to effect mobility of U (Roberts et al., 2017), and U is strongly bound to iron oxides (Lack et al., 2002). U content in the soils of the world can range between 0.7 to 10.7 $\mu\text{g/g}$. In US soils, U content ranged between 0.3 – 10.7 $\mu\text{g/g}$ and was found to be related to the soil texture rather than to the soil type, and coarse soils contained less U compared to fine soils (Vodyanitskii, 2011). The global average U content in soil is $\sim 3 \mu\text{g/g}$ (Keith et al., 2013). Few studies have examined U occurrence and mobilization in the unsaturated zone, though there is growing evidence that this reservoir may serve as a source to groundwater. For example, nitrate-N concentrations have been spatially correlated with dissolved U in U.S. groundwater (Nolan and Weber, 2015). Local mobilization of U in the unsaturated zone is likely related to various biogeochemical processes such as denitrification and iron reduction (Collins and Rosso, 2017).

Biogeochemical processes in the unsaturated zone are controlled to a large extent by moisture content and the presence of soluble DOC, which may also serve as a good predictor for microbial activity (Kaiser and Kalbitz, 2012). DOC leached from the surface or root zone soil can control microbial activity in the subsurface (Baker et al., 2017). DOC concentrations in soil have been related to mobilization of As and subsequent leaching to groundwater (Mladenov et al., 2010). The presence of organic carbon can stimulate denitrification processes in soil (Burford and Bremner, 1975), which may also provide the added benefit of nitrate attenuation prior to leaching.

Materials and Methods

Soil digestion and quantification of As and U

One hundred sixty-four (164) sediment samples were selected at 5 foot intervals from all the 32 coring locations for digestion and analysis of acid leachable As and U. Samples were air-dried for 24 hours and finely ground before digestion. Microwave digestion of soil samples was carried out following standard operating procedure (SOP) of Water Sciences Laboratory (WSL) based on EPA method 3051A. Briefly, 0.500 g portion of each sample was weighed out into a Teflon™ microwave digestion tubes and mixed with concentrated nitric acid, hydrochloric acid, and hydrogen peroxide. Samples were digested in MARS Xpress microwave digester to 175°C for 10 minutes. After digestion, the Teflon tubes were allowed to cool. Each digest was allowed to settle, filtered and diluted to a final volume of 50 mL with reagent water. Samples were analyzed using inductively coupled plasma mass spectroscopy (ICP-MS) using either a GVI Platform XS or Thermo ICAP RQ ICP-MS. Calibration standards were prepared and digested with samples. Certified reference materials were analyzed to verify the digestion and calibration methods.

DOC extraction method and analysis

Water soluble DOC was extracted utilizing hot water method following SOP of WSL. Soil samples were weighed, and 50 ml of reagent grade water was added to soil and mixed well. The mixture was heated for 90 min. on a heating block at 80 °C, then allowed to cool down, centrifuged and filtered. Samples were preserved by adding sulfuric acid before analysis using persulfate oxidation method on an OI Model 2020 TOC analyzer.

X-Ray Fluorescence

X-ray fluorescence (XRF) uses X-ray to generate fluorescence from samples. The generated fluorescence is specific to particular element present and the intensity of fluorescence can give quantitative information about that particular element under study. XRF is widely used method in mineralogy to measure the total elemental composition of minerals and soils. Approximately one quarter of the unsaturated zone samples used for ICP-MS analyses were analyzed under XRF to evaluate gross elemental composition of the soil minerals present. Variation of element concentrations were compared to As and U concentrations obtained from digestion and ICP-MS analysis for each core.

Statistical Treatment of Results

Normality tests were conducted (Ghasemi and Zahediasl, 2012), but the data obtained were not normally distributed in all the groups such as irrigation type and nitrate increase or decrease compared to 2011. The As data was normalized by using a cube root factor, which passed homogeneity of variance (*Levene's*) test and was analyzed for One-Way ANOVA for factors different irrigation type and nitrate increase and decrease compared to 2011 separately. As there was lack of normality among the data for U so, non-parametric statistical analysis was carried out. *Kruskal-Wallis* ANOVA with respect to irrigation type and nitrate-N increase or decrease compared to 2011 data in the unsaturated cores of different sites at Hastings WHPA was done. Statistical analysis and correlation coefficients were carried out in Origin Pro software.

Results and discussion

In total 164 soil cores were analyzed for acid digested As and U from all the 32 soil cores collected. Out of 164 soil cores, 107 cores were from pivot or sprinkler irrigated sites, 22 cores were from gravity irrigated sites and 35 cores were from non-irrigated sites. Unsaturated zone core samples were characterized based on land use and irrigation type (gravity or furrow, pivot) and non-irrigated/barnyard or residential area, and cores with nitrate decrease or increase compared to the previous 2011 Hastings study. Nitrate concentration was impacted by irrigation practices in the Hastings WHPA site and a decrease in nitrate concentration has been observed at pivot irrigation sites in comparison to 2011 study (Adams, 2018). This reduction in nitrate content can impact trace element chemistry by influencing redox and microbial processes, which can control mobilization of As and U in the unsaturated zone, impacting the contaminant levels in the groundwater below (Herath et al., 2016; Neil et al., 2014; Nolan and Weber, 2015; Smith et al., 2017; Westrop et al., 2018). The present study was carried out to understand the variation of As and U distribution in the unsaturated zone. This can serve as an indicator for future groundwater quality issues and groundwater is the major source of drinking water at Hastings. The arrows in **Figure 31** (a) indicates either higher than equal to (↑) or lower (↓) than average concentrations of As and U for all the cores (N=164) analyzed at Hastings WHPA site in that

particular location. Of the 32 coring locations analyzed, 21 sites showed presence of either As or U above the mean value and five sites showed presence of As and U above the mean value (**Figure 31** (b)). The mean value of As was found to be $3.66 \pm 1.06 \mu\text{g/g}$ and U was found to be $0.32 \pm 0.38 \mu\text{g/g}$.

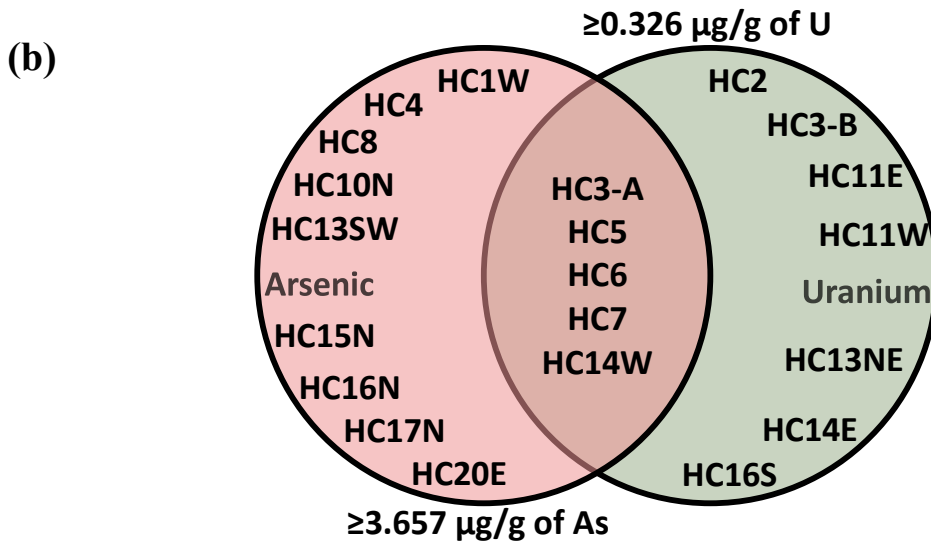
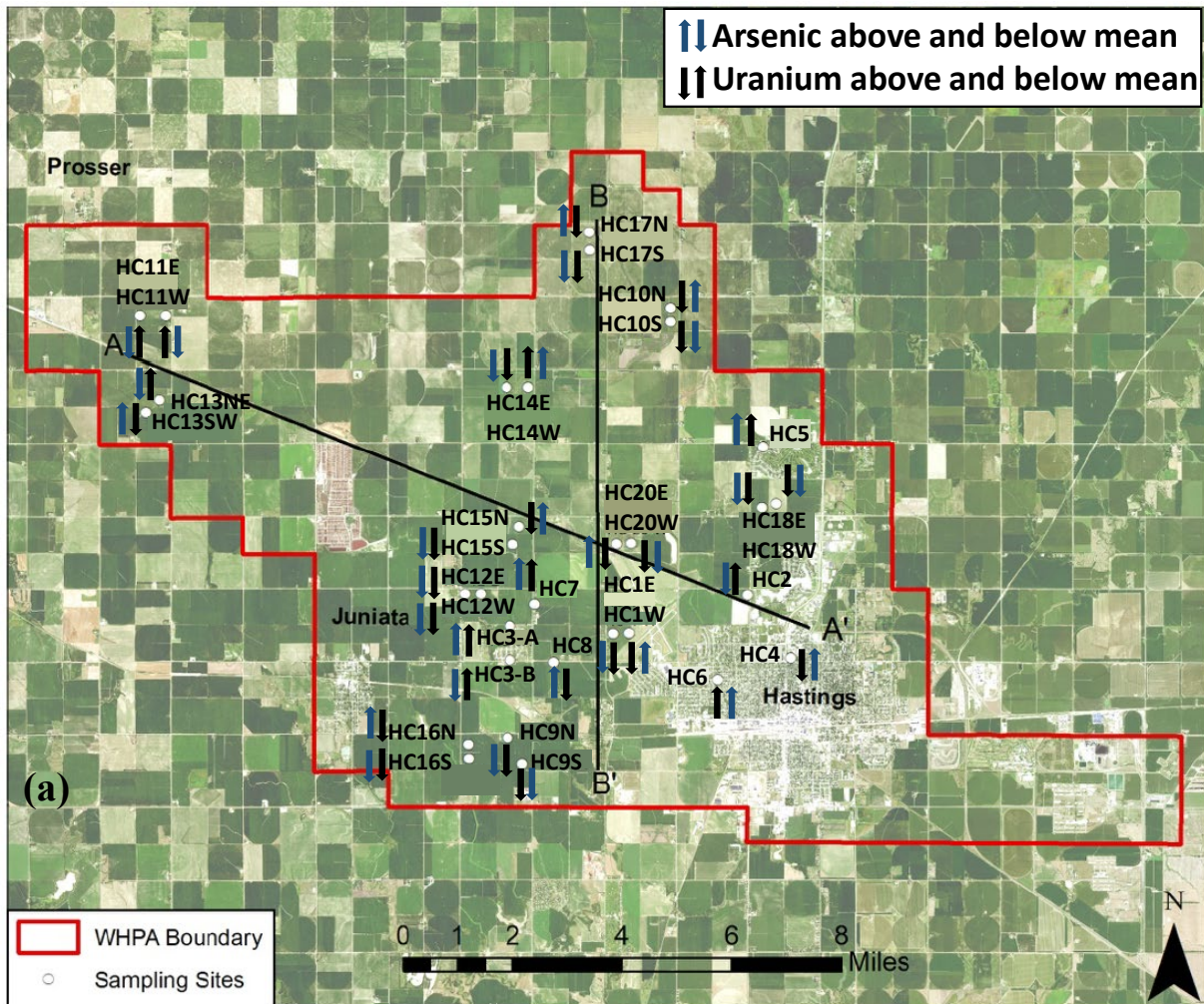


Figure 30: (a) Shows map of Hastings wellhead protection area (WHPA) where different locations were cored and arrows represent As and U values greater than equal to or less than the average concentrations observed in the present study, (b) shows a coring sites which have higher As and U than the average value of the study area.

Vadose Zone Arsenic

Core-averaged As concentrations at the Hastings WHPA site are shown in **Figure 31** (a), and the blue arrows show As amount more or less compared to average value at Hastings WHPA site. Fourteen core sites showed As concentrations above a total mean value of 3.66 $\mu\text{g/g}$, which is above the mean of As present in the Earth's crust (Wedepohl, 1991) but below the global average value reported for soils $\sim 5 \mu\text{g/g}$ (Chou et al., 2007). Core-averaged acid leachable As concentrations ranged between as low of 0.45 $\mu\text{g/g}$ to a maximum of 21.25 $\mu\text{g/g}$. The highest individual levels of As were found in the soil cores to the west of the Hastings city limits with site HC-20E, having samples with the highest As (21.25 $\mu\text{g/g}$) at 95 ft below. As in the soil cores of different sites were analyzed based on irrigation type and nitrogen content in the unsaturated zone. **Figure 32** shows the bar graph divided into three main irrigation types, gravity, pivot and non-irrigated and within the irrigation type further divided into two categories of increase and decrease in nitrate content in the unsaturated zone after 2011 study. These were further statistically analyzed utilizing Two-way ANOVA test to confirm the effects of irrigation type and nitrate content in the unsaturated zone.

Overall unsaturated zone As was found to be highest in the residential area, barnyard and non-irrigated regions, irrespective of decrease or increase in nitrate content in comparison to 2011 study in the unsaturated zone (Adams, 2018). Mean As concentrations were 4.51 and 3.93 $\mu\text{g/g}$ for cores showing a decrease and increase in nitrate content respectively in non-irrigated sites. The non-irrigated locations was followed by gravity irrigated sites and the mean As content was 4.32 and 2.97 $\mu\text{g/g}$ for decrease and increase in N content respectively (**Figure 32**). Pivot irrigated sites showed the lowest concentrations of As in the unsaturated zone, with values of 3.71 and 3.22 $\mu\text{g/g}$ for decrease and increase in N-content, respectively (**Figure 32**). The distribution of As seemed consistent throughout the Hastings WHPA area between irrigation types, with very few outliers.

Vadose Zone Uranium

Acid-leachable U was found throughout the Hastings WHPA site though its distribution was irregular and also varied by land use and irrigation type. Twelve sites had U concentrations above the total mean value of 0.32 $\mu\text{g/g}$, which is lower than average for US surface soils (Vodyanitskii, 2011). In **Figure 31**, black arrows show core-averaged U concentrations compared to the overall mean. Core averaged U concentration ranged between 0.009 to 1.68 $\mu\text{g/g}$. HC-14W contained the highest levels of unsaturated U at 4.5 ft below the surface. **Figure 32** shows that U distribution varied significantly among the irrigation type, and also between nitrate content in the unsaturated zone. Similar to As, the highest concentrations were found to be in the non-irrigated or residential area, with a mean value of 0.64 and 0.60 $\mu\text{g/g}$ for decrease and increase in N-content (**Figure 32**). However, pivot irrigated sites were found to contain 0.48 and 0.20 $\mu\text{g/g}$ for decrease and increase in N-content (**Figure 32**). Gravity irrigated region showed the lowest amount in the unsaturated zone, with mean value of 0.03 and 0.04 $\mu\text{g/g}$ for decrease and increase in N-content (**Figure 32**). The distribution of U throughout the Hastings WHPA was variable and showed dependence on irrigation type.

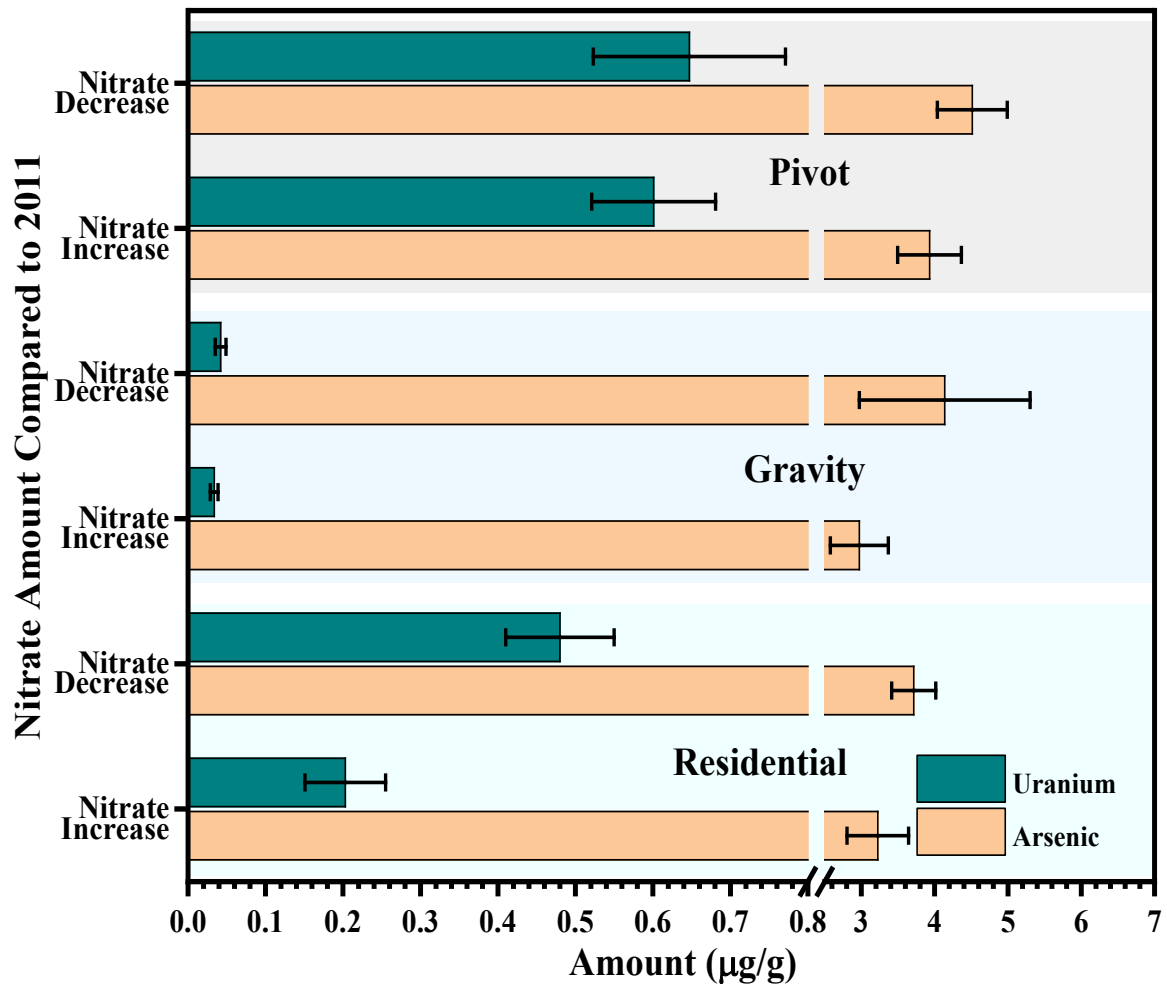


Figure 31: Shows mean concentration of arsenic and uranium for different irrigation type where there was increase or decrease of nitrate content in the unsaturated zone compared to 2011 Hastings study. The error bar represents standard error of mean.

Detailed As and U profiles Compared to Nitrate

Soil core samples from sites HC-3A and HC-14E were selected for DOC measurement and shown here together with As, U, water content, nitrate-N, ammonia-N, and particle size distribution. HC-3A is a residential site and HC-14E is a pivot irrigated site allowing comparison of the effect of irrigation and nitrate leaching. **Figure 33** and **34** show the concentration of nitrate, ammonia, gravimetric water content, pore water nitrate content, lithology and DOC content against depth. Core samples from HC-3A contained on an average $36.2 \pm 26.6 \mu\text{g-C/g}$ and ranged between 9.9 to 144.0 $\mu\text{g-C/g}$. HC-14E contained on an average $14.2 \pm 12.4 \mu\text{g-C/g}$ and range was between 1.2 to 48.2 $\mu\text{g-C/g}$. For both sites highest amount of DOC was found at the topsoil, but DOC was reasonably high in the deeper cores too. DOC for depth below 30 ft ranged between 9.93 to 55.27 $\mu\text{g-C/g}$ and 1.17 to 41.86 $\mu\text{g-C/g}$ for HC-3A and

HC-14E respectively.

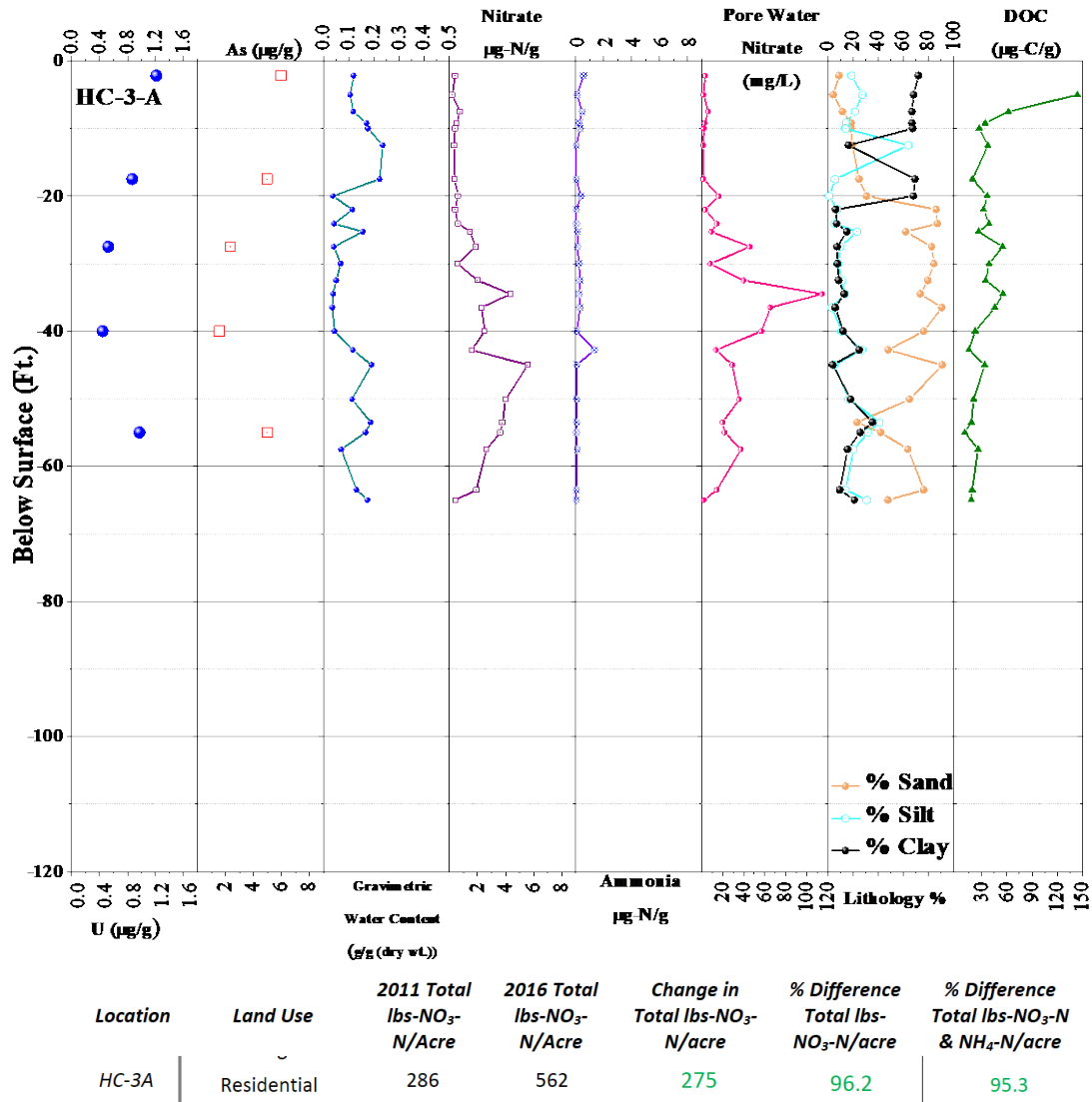


Figure 32: Shows arsenic, uranium, gravimetric water content, nitrate, ammonia, pore water nitrate, lithology and dissolved organic carbon (DOC) profile of site HC-3A against depth.

Elemental Composition of Vadose Zone Related to U and As

XRF analysis was carried out on 39 selected core samples to measure the overall elemental composition of the unsaturated zone soil cores, and to determine if there were any systematic variation compared to acid-leachable As and U concentrations. Sediment was found to be primarily aluminosilicate (silicon averaged 61.3±3.2%; aluminum averaged 13.6±0.8%) with high levels of iron (9.1±2.6%) and potassium (7.8±0.6%). Other elements which were present in lower amount in decreasing order are calcium (3.2±0.6%), magnesium (1.6±0.4%), sodium (1.3±0.3%), titanium (1.2±0.2%), phosphorus (0.15±0.04%), and manganese (0.14±0.07%). Detailed elemental composition obtained from XRF is shown in **Table 14**.

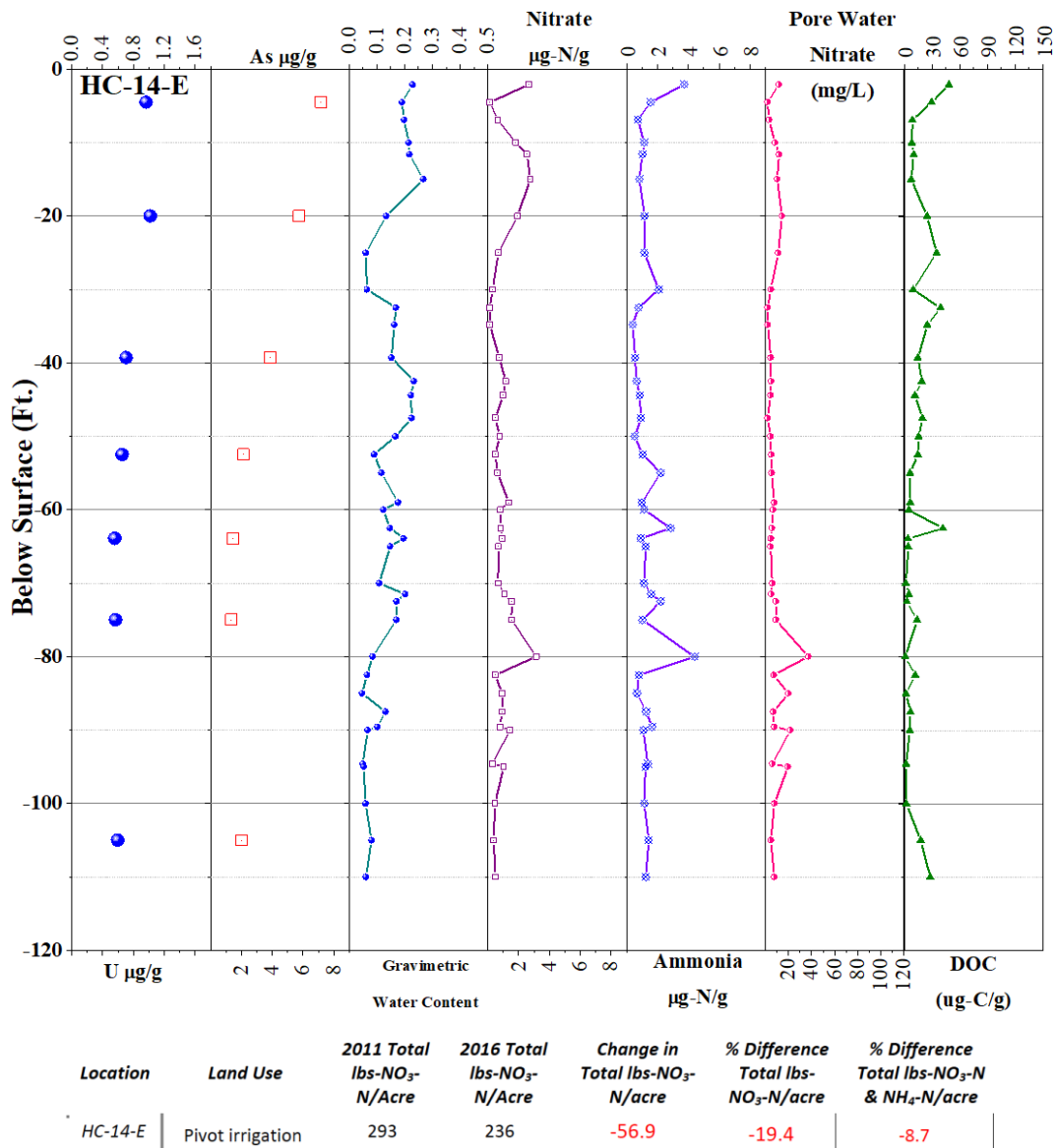


Figure 33: Arsenic, uranium, gravimetric water content, nitrate, ammonia, pore water nitrate and dissolved organic carbon (DOC) profile of site HC-14E against depth.

Fe is a very important component for redox processes, and XRF analyses confirmed presence of measurable quantity of Fe in the soil and the range varied between 3.6 to 14.8 % of Fe in the soil cores. Fe seems to preferentially bind with clay and also is more concentrated in the top 45 ft of the unsaturated zone. Phosphorus too seems to be more on the top layer of core and seems to be present with high Fe in soil (Table 14). Figure 35 shows scattered plot of U, As, Fe and % Clay among the samples analyzed in XRF. Distribution of U and As content is presented in Figure 35 (a, b). The distribution of U did not seem to be influenced by Fe content but As showed a very strong relationship with Fe % (Figure 35 (c, d)) Moreover, a higher percentage of clay particle size correlated with the percentage of Fe (Figure 35 (e)).

Table 14: Shows mass% of major elements in soil cores against depth and clay%.*

Core ID	Depth ft	%Clay	Na mass %	Mg	Al	Si	P	K	Ca	Ti	Mn	Fe
Pivot-Decrease												
13SW	-7.2		0.8	1.8	15.1	54.9	0.2	7.4	2.8	1.3	0.4	14.8
13SW	-20		1.1	1.9	13.7	59.0	0.2	7.9	3.3	1.4	0.1	10.8
13SW	-32.5		1.2	1.8	13.7	60.2	0.1	7.4	3.4	1.5	0.1	10.1
13SW	-47.5		1.3	1.5	12.9	67.1	0.1	8.1	3.4	0.8	--	4.5
13SW	-68.9		0.9	1.7	13.3	67.3	0.1	8.5	3.0	--	--	5.0
13SW	-80		1.2	1.7	13.6	64.2	0.2	8.0	3.2	1.0	0.1	6.6
17N	-7.5		1.0	2.3	13.0	56.8	0.2	7.4	6.3	1.5	0.1	10.9
17N	-22.5		2.1	1.8	14.2	61.0	0.2	7.2	3.1	1.2	0.1	8.6
17N	-45		1.2	1.6	14.3	58.7	0.1	7.5	2.9	1.4	0.1	11.6
17N	-82.5		1.5	1.6	13.5	62.4	0.2	7.3	3.8	1.3	0.1	7.8
HC14E	-20		1.4	2.0	13.3	59.4	0.2	7.8	3.5	1.3	0.1	10.5
HC14E	-39.3		1.3	1.9	14.1	59.3	0.2	7.7	3.9	1.3	--	9.8
HC14E	-52.5		1.3	1.6	14.5	62.0	0.1	7.8	3.4	1.1	0.2	7.7
HC14E	-63.9		1.4	1.9	13.9	60.2	0.2	7.4	3.3	1.3	0.1	9.9
HC14E	-105		1.3	1.5	12.0	64.3	0.1	8.3	3.6	1.3	0.1	7.0
Pivot-Increase												
13NE	-11.2	30.6	1.5	1.7	14.1	61.0	0.1	7.6	2.7	1.5	0.1	9.3
13NE	-22.6	20.8	1.1	1.7	13.8	60.4	0.1	8.0	2.9	1.5	0.1	10.0
13NE	-43.6	19.1	1.5	2.1	15.1	59.9	0.1	7.1	2.6	1.4	0.1	9.7
13NE	-61.9	12.8	1.5	1.6	13.3	61.1	0.1	8.2	3.4	1.5	0.1	8.7
13NE	-74.4	9.4	1.2	1.4	13.3	66.0	0.1	7.8	3.5	0.8	--	5.1
13NE	-101.7	32.8	1.5	1.5	12.6	63.3	0.1	7.8	4.1	1.0	0.1	7.4
Gravity -Decrease												
HC1W	-17.5		1.1	2.0	13.2	59.1	0.2	7.7	3.2	1.5	0.1	11.5
HC1W	-32.5		1.2	1.7	13.9	60.4	0.2	7.6	2.7	1.5	0.1	10.3
HC1W	-49.3		1.2	1.8	14.0	59.1	0.2	8.0	3.0	1.4	0.1	10.7
HC1W	-70		1.6	1.2	12.0	68.3	0.1	8.0	3.5	0.9	0.1	4.1
HC1W	-110		1.1	2.0	13.4	58.2	0.2	8.0	3.5	1.2	0.1	11.8
Gravity -Increase												
HC1E	-12.5	37.5	1.0	2.1	13.4	58.2	0.2	7.6	3.6	1.6	0.1	11.6
HC1E	-32.5	68.2	1.1	1.9	14.9	60.2	0.2	7.6	3.0	1.1	0.1	9.7
HC1E	-50	8.3	1.4	1.4	14.1	63.7	0.2	7.5	3.4	1.2	0.1	6.7
HC1E	-67.5	12.0	1.3	1.5	13.0	63.1	0.1	8.0	2.8	1.2	0.2	8.4
HC1E	-80	1.5	2.2	0.8	10.8	68.4	0.1	9.5	3.2	0.8	0.1	3.8
HC1E	-105	3.1	2.6	0.5	10.7	66.0	0.2	10.8	3.1	0.5	0.4	5.0
Non-irrigated-Decrease												

HC2	-7.5	13.5	1.0	1.8	13.6	57.2	0.3	7.9	3.4	1.3	0.3	12.8
HC2	-17	22.6	1.0	1.8	13.4	59.0	0.2	7.9	3.5	1.5	0.1	11.1
HC2	-40.3	23.9	1.0	1.5	14.3	59.2	0.1	7.6	2.8	1.5	0.1	10.9
HC2	-52.5	13.0	1.0	1.6	13.9	61.3	0.1	7.8	3.2	1.2	0.1	9.1
HC2	-65	5.4	1.3	1.5	12.4	65.8	0.1	7.7	3.7	0.9	0.1	6.2
HC6	-2	56.2	1.1	1.5	13.5	59.8	0.2	7.3	3.1	1.2	0.2	11.6
HC6	-13.8	65.4	1.2	2.0	13.5	57.9	0.2	7.4	3.3	1.5	0.2	11.4
HC6	-27.5	29.4	1.2	1.3	14.0	62.0	0.1	7.3	2.5	1.2	0.2	9.4
HC6	-31.6	24.2	1.2	1.6	14.2	60.3	0.1	7.4	2.5	1.4	0.1	10.8
HC6	-45	37.7	1.2	1.9	14.3	58.4	0.2	7.8	2.9	1.5	0.2	10.8
HC6	-57.5	--	1.0	2.2	13.8	58.6	0.2	7.8	3.2	1.6	0.2	11.0
Non-irrigated-Increase												
HC3A	-2.2	71.9	1.4	1.5	13.0	60.9	0.2	7.2	2.8	1.4	0.2	10.9
HC3A	-17.5	69.3	1.3	1.8	13.4	60.2	0.2	8.0	3.2	1.3	0.2	10.0
HC3A	-27.5	7.4	2.2	1.0	13.8	64.9	0.1	8.5	3.2	0.9	0.1	4.9
HC3A	-40	12.4	1.5	0.8	13.4	69.0	0.2	7.4	3.2	0.6	0.1	3.6
HC3A	-55	26.0	1.0	1.8	14.7	57.9	0.1	7.7	3.1	1.4	0.2	11.8
HC4	-10	17.0	1.3	2.1	13.7	58.5	0.2	7.3	3.0	1.6	0.2	11.7
HC4	-32.9	19.4	1.4	1.9	14.2	60.2	0.2	7.4	2.9	1.4	0.1	10.0
HC4	-45	9.9	1.2	1.6	13.9	64.4	0.1	7.6	3.0	0.9	0.2	6.4
HC4	-57.9	21.9	1.4	2.2	13.7	59.8	0.2	7.5	3.6	1.4	0.2	9.6

*Blank if not detected or data not available

Relationship of Irrigation to Vadose Zone As and U

As and U concentrations in the unsaturated zone are likely affected by recharge, nitrate leaching and potentially from recurrent microbial activity driven by changing moisture content and readily available organic carbon in pore water. As concentrations did show a relationship between changes in nitrate concentration in the unsaturated zone but was evenly distributed throughout Hastings WHPA, and subsequent less concentration in groundwater predicts immobilized As in unsaturated zone. U concentration was found to be negatively correlated with nitrate content in the unsaturated zone and was significantly different ($p=0.0002$) between sites where there was increase in nitrate compared to reduction in nitrate quantity in the unsaturated zone from 2011 study. This difference in U concentration at two sites can indicate mobilization of U. The U concentration were also found to be elevated compared to As in the groundwater. Water soluble DOC were measured in the unsaturated zone suggests that microbial activity may be possible and influence As and U mobilization. While the initial occurrence of As and U in the unsaturated zone is likely geogenic trace element deposited with alluvial sediment, subsequent agricultural land use and irrigation using groundwater may encourage mobilization (Xiao et al., 2018). Anthropogenic activities such as irrigation, fertilization and nitrate leaching can influence the transportation of As and U to the groundwater below (Chi et al., 2018).

Figure 32 shows the distribution of As grouped based on irrigation practices and further sub-divided to decrease and increase in nitrate content in the unsaturated zone. In the sites, where there has been

reduction of nitrate content in the unsaturated zone has shown better retention of As in the soil cores, irrespective of irrigation type. One-way ANOVA shows a significant difference for increase or decrease in nitrate content for overall data but no such difference was found for different irrigation practices. Depth of the unsaturated zone showed a weak correlation with As concentration which was found to be significant ($r = 0.351$ $p = 0.00003$), indicating an increase in As in deeper cores (Figure 33, 34 and Appendix A).

As concentrations show a weak positive correlation with U concentrations, which was statistically significant ($r = 0.178$ $p = 0.02$). However, As did show very weak negative correlation with nitrate or ammonia content in the unsaturated zone, but was not significant. As showed a positive correlation with % of Fe in the soil ($r = 0.326$ $p = 0.0018$), indicating that As is more bound to Fe in the soil cores, which also explains the positive correlation between As and clay content ($r = 0.577$ $p = 0.00053$) as most of iron was clay bound (**Figure 35**). As is known to strongly bound to different iron oxide minerals (Wang et al., 2018). Further, the unsaturated zone has high content of Fe. This low value of As in the groundwater and high values in the unsaturated zone suggests that the unsaturated zone can attenuate As efficiently by immobilizing As. Further, the pH observed at Hastings soil core were mostly near-neutral, more on the basic side and almost all pH values were below 9. So, if As(V) is the dominant species it is expected the charged system would make it less mobile and prevent any further transportation from the unsaturated zone. This attenuation process is very important in protecting the groundwater below with As contamination and can be related to lower As concentration found in the groundwater, at just 1.54 $\mu\text{g/L}$. However the reductive dissolution of this iron oxides can release As and mobilize them impacting groundwater quality and iron oxides seems to play a key role in the attenuation process. The reductive dissolution of iron oxides is fairly possible due to the high levels of DOC in the unsaturated zone (Oppong-Anane et al., 2018), which can initiate mobilization of As.

Figure 32 shows the distribution of U in the unsaturated zone based on irrigation practices and further divided to decrease and increase in total N content in the unsaturated zone compared to 2011. In here also amount of U is less compared to the mean values of the Hastings, in sites where there is increase in nitrate content in the unsaturated zone in pivot and residential sites, but in gravity sites these two values are comparable. U data could not be normalized so *Kruskal-Wallis* ANOVA was done and irrigation type and nitrate increase or decrease as factor showed significant difference among the concentration of U. These suggest U concentration in the unsaturated zone has been influenced by land use, which is clear from the mean values and bar graph in **Figure 32** showing a tenfold increase from gravity to pivot and further 1.3 fold increase from pivot to non-irrigated sites, signifying that the unsaturated zone can immobilize U better in pivot or non-irrigated sites than gravity irrigation, where the water infiltration rates are the highest. In *Kruskal-Wallis* ANOVA there was significant difference between increase and decrease in nitrate content and among different irrigation practices for U data. This may be due to limited data in gravity irrigation sites and a small rise in U concentration in gravity field where decrease in N-content was observed. To confirm that N-content in unsaturated zone can influence U immobilization, one way ANOVA analysis of the pivot irrigation was carried out which found that U concentration in the unsaturated zone is significantly different between sites with increase in nitrate content compared to decrease in nitrate content (Figure 3) ($p = 0.001$).

Similar to As, U did show a significantly weak correlation with depth ($r = 0.215$ $p = 0.005$). U did not show any significant correlation with percentage of Fe and clay in soil cores, which can indicate that iron oxide may not bind U species, and U immobilization in unsaturated zone may happen due to the

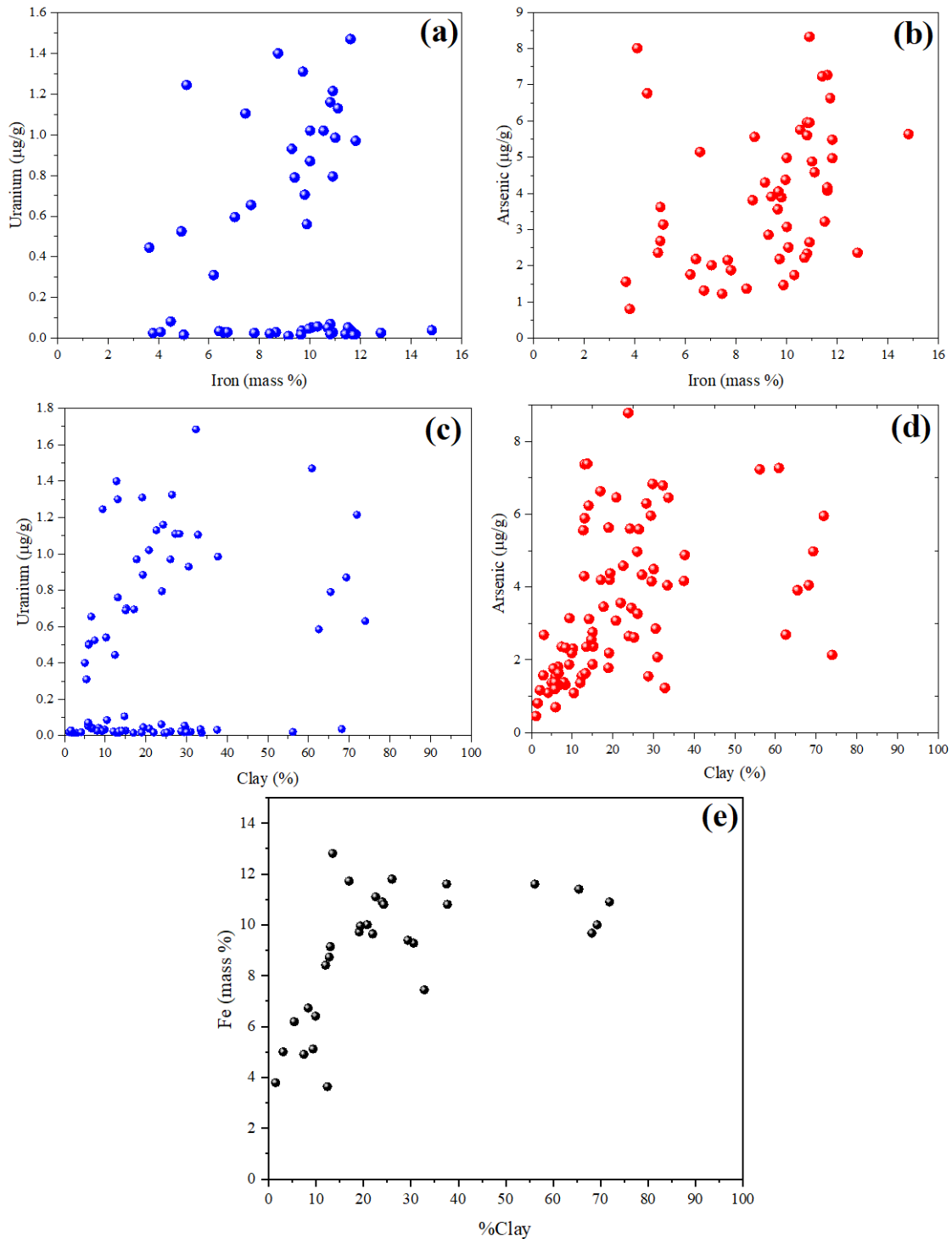


Figure 34: Shows scatter plot of (a) U vs Fe, (b) As vs Fe, (c) U vs Clay, (d) As vs Clay, and (e) Fe vs Clay

reduction to U(IV), in the presence of DOC. U showed weak negative correlation with nitrate concentration ($r = -0.234$ $p = 0.002$), and ammonia concentration ($r = -0.194$ $p = 0.01$) in the unsaturated zone, which were significant, which confirms the data shown in **Figure 32** that increase in nitrate can

reduce U concentration in the unsaturated zone. This explains the reason for the high concentration of U in the groundwater samples, as excess nitrate in the unsaturated zone can impact U immobilization, releasing U to the groundwater below. It is predicted that U concentration would increase in the groundwater below, due to the mobilization of U from the unsaturated zone which is related to high nitrate load in the soil adding to groundwater quality issues.

Pore water DOC in the deep unsaturated zone soil core samples suggests leaching of DOC from the surface. In both the sites highest DOC was at the surface, which is expected due to the influence of the root zone. Mobility and availability of nutrients and contaminants in soil are largely determined by DOC (Sopliniak et al., 2017). The presence of pore water DOC can influence microbial respiration and redox processes, as a consequence can control various biogeochemical processes such as denitrification, ammonification, metal ion reduction, and mobilization/immobilization in the unsaturated zone (Oppong-Anane et al., 2018; Sopliniak et al., 2017). The elevated levels of DOC and presence of high Fe in the soil cores, coupled with reduction of As and U in the unsaturated zone based on nitrate content in the soil indicates that Fe chemistry in the unsaturated zone can play a key role in mobilization of these

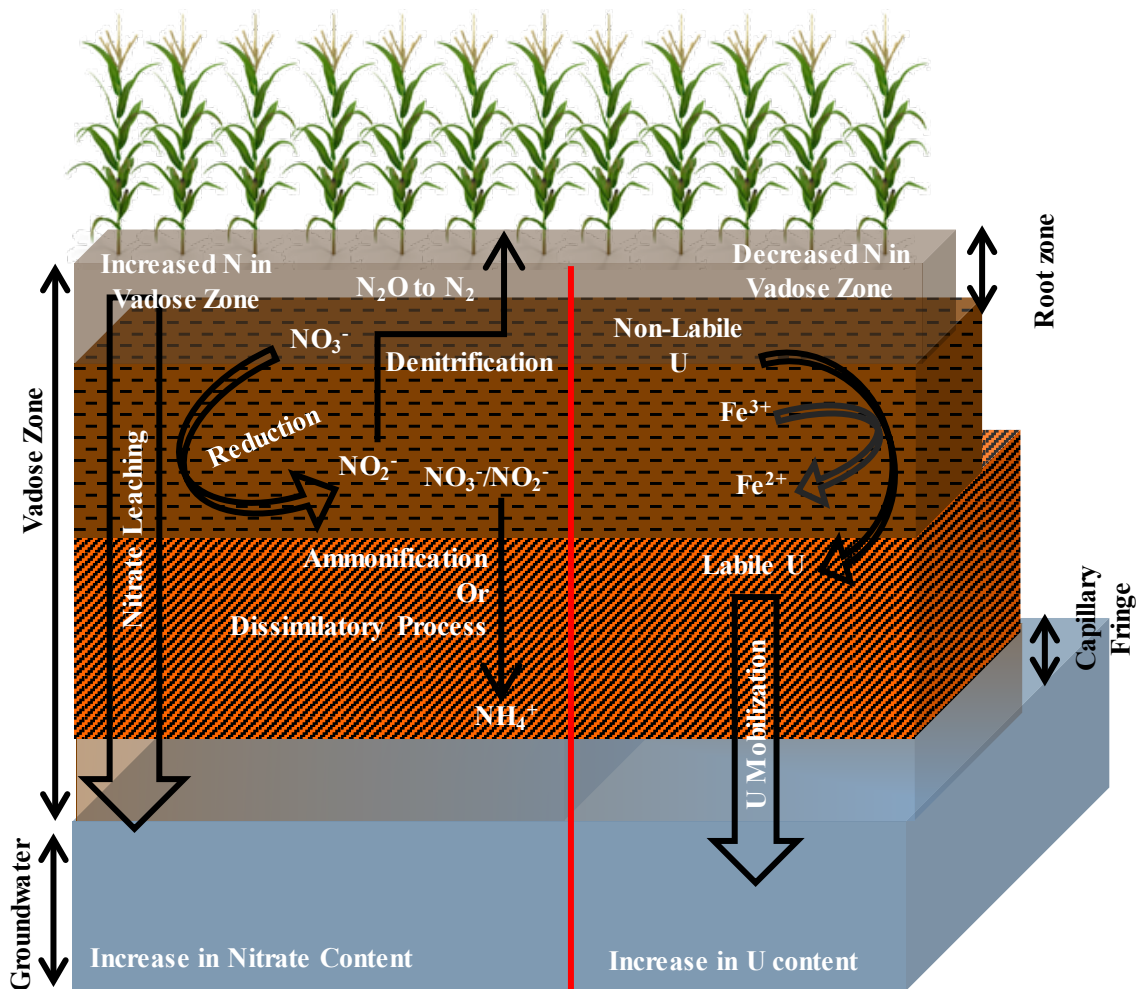
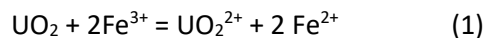


Figure 35: Conceptual hypothesis about U mobilization and ammonia formation in the unsaturated zone

trace elements (**Figure 36**). The redox process of Fe reduction and oxidation can initiate U oxidation, making them mobile (Reaction 1).



Further reduced Fe can mineralize such as, green rust, which can influence abiotic nitrate reduction (Hansen et al., 1996). Iron reduction and denitrification may also occur intermittently through changes in moisture content and DOC which can drive pore water microbial respiration in the unsaturated zone (Oppong-Anane et al., 2018; Rivett et al., 2008).

Comparison to Groundwater As and U

Four groundwater samples were analyzed from monitoring wells of Hastings WHPA to the west of the city limits. As was found to be 1.54 ± 1.18 $\mu\text{g/L}$ in the groundwater samples. U was found to be 17.82 ± 6.74 $\mu\text{g/L}$ in the groundwater samples, and highest value was observed to be 27.9 $\mu\text{g/L}$ near-site HC-20, where U concentration is less than the average value observed for Hastings site in the present study. Moreover, the groundwater showed elevated levels of U compared to As though the former is almost ten times less in concentration in the unsaturated zone compared to As. This enhanced concentration may indicate processes leading to mobilization of elements to groundwater below which may impact water quality in the near future (**Figure 36**).

Conclusions

The occurrence and distribution of elevated levels of As and U in the unsaturated zone of the Hastings WHPA suggest that mobilization and leaching may lead to increasing levels in the local groundwater. In Hastings WHPA, elevated levels of U are already being observed in the groundwater below and increase in nitrate content in the unsaturated zone seems to influence the mobilization of U, which is finally ending in the groundwater. Currently, As concentrations are high but do not seem to be affected by the same processes controlling U. Continued monitoring of groundwater is necessary to ensure that these trends are significant. The presence of high iron in the soil coupled with elevated levels of DOC can influence various microbial processes and can control mobilization or immobilization process as iron oxides are known to bind both As and U strongly. An iron-rich vadose zone coupled with water-soluble carbon may influence subsurface microbial redox processes controlling forms of iron and mobilization of both As and U and subsequent leaching to the water table. Future in-depth analysis of iron chemistry, in addition to continued monitoring of nitrate transformation and movement, is suggested to provide more information about specific biogeochemical processes controlling As and U mobilization in the unsaturated zone.

References

- Adams, C.J., 2018. The Impact of Land Use on Nitrate-N Movement and Storage in the Vadose Zone of the Hastings ' WHPA by Presented to the Faculty of The Graduate College at the University of Nebraska In Partial Fulfillment of Requirements For the Degree of Master of Science. University of Nebraska Lincoln.
- Baker, A., Duan, W., Rutledge, H., McDonough, L., Oudone, P., Meredith, K., Andersen, M.S., O'Carroll, D.M., Coleborn, K., Treble, P.C., 2017. Dissolved organic matter in the unsaturated zone: the view from the cave. Am. Geophys. Union, Fall Meet. 2017, Abstr. #B43F-2186.
- Bosch-rubia, G., 2015. Land Use and Water and Soil Management Practices Impacts on Potential Groundwater Recharge in Loess Regions of South Central Nebraska. University of Nebraska - Lincoln.
- Brown, C.J., Jurgens, B.C., Katz, B.G., Landon, M.K., Eberts, S.M., 2007. Arsenic and Uranium in Four Aquifer Settings : Occurrence , Distribution , and Mechanisms for Transport to Supply Wells. In: 2007 NGWA Naturally Occurring Contaminants COnference: Arsenic, Radium, Radon, Uranium. Charleston, SC.
- Burford, J.R., Bremner, J.M., 1975. Relationships between the denitrification capacities of soils and total, water-soluble and readily decomposable soil organic matter. *Soil Biol. Biochem.* 7, 389–394.
- Cassiani, G., Binley, A., Ferré, T.P.A., 2007. UNSATURATED ZONE PROCESSES. In: Applied Hydrogeophysics. Springer Netherlands, Dordrecht, pp. 75–116.
- Chi, Z., Xie, X., Pi, K., Wang, Y., Li, J., Qian, K., 2018. The influence of irrigation-induced water table fluctuation on iron redistribution and arsenic immobilization within the unsaturation zone. *Sci. Total Environ.* 637–638, 191–199.
- Chou, S., Harper, C., Ingerman, L., Lladós, F., Colman, J., Chappell, L., Osier, M., Odin, M., Sage, G., 2007. Toxicological Profile for Arsenic. Atlanta.
- Collins, R.N., Rosso, K.M., 2017. Mechanisms and Rates of U(VI) Reduction by Fe(II) in Homogeneous Aqueous Solution and the Role of U(V) Disproportionation. *J. Phys. Chem. A* 121, 6603–6613.
- Farooq, S.H., Chandrasekharan, D., Dhanachandra, W., Ram, K., 2019. Relationship of arsenic accumulation with irrigation practices and crop type in agriculture soils of Bengal Delta, India. *Appl. Water Sci.* 9, 1–11.
- Ghasemi, A., Zahediasl, S., 2012. Normality tests for statistical analysis: A guide for non-statisticians. *Int. J. Endocrinol. Metab.* 10, 486–489.
- Hansen, H.C.B., Koch, C.B., Nancke-Krogh, H., Borggaard, O.K., Sørensen, J., 1996. Abiotic nitrate reduction to ammonium: Key role of green rust. *Environ. Sci. Technol.* 30, 2053–2056.
- Herath, I., Vithanage, M., Bundschuh, J., Maity, J.P., Bhattacharya, P., 2016. Natural Arsenic in Global Groundwaters: Distribution and Geochemical Triggers for Mobilization. *Curr. Pollut. Reports.*
- Kaiser, K., Kalbitz, K., 2012. Cycling downwards – dissolved organic matter in soils. *Soil Biol. Biochem.* 52, 29–32.

Keith, S.K., Faroon, O., Roney, N.R., Scinicariello, F., Wilbur, S., Ingerman, L., Lladós, F., Plewak, D., Wohlers, D., Diamond, G., 2013. Toxicological Profile for Uranium. ATSDR Toxicol. profiles.

Lack, J.G., Chaudhuri, S.K., Kelly, S.D., Kemner, K.M., O'Connor, S.M., Coates, J.D., 2002. Immobilization of radionuclides and heavy metals through anaerobic bio-oxidation of Fe(II). *Appl. Environ. Microbiol.*

Malakar, A., Das, B., Islam, S., Meneghini, C., De Giudici, G., Merlini, M., Kolen'ko, Y. V., Iadecola, A., Aquilanti, G., Acharya, S., Ray, S., 2016a. Efficient artificial mineralization route to decontaminate Arsenic(III) polluted water - the Tooeleite Way. *Sci. Rep.* 6, 26031.

Malakar, A., Islam, S., Ali, M.A., Ray, S., 2016b. Rapid decadal evolution in the groundwater arsenic content of Kolkata, India and its correlation with the practices of her dwellers. *Environ. Monit. Assess.* 188, 1–22.

Malakar, A., Snow, D.D., Ray, C., 2019. Irrigation Water Quality—A Contemporary Perspective. *Water* 11, 1482.

Mladenov, N., Zheng, Y., Miller, M.P., Nemergut, D.R., Legg, T., Simone, B., Hageman, C., Rahman, M.M., Ahmed, K.M., McKnight, D.M., 2010. Dissolved Organic Matter Sources and Consequences for Iron and Arsenic Mobilization in Bangladesh Aquifers. *Environ. Sci. Technol.* 44, 123–128.

Neil, C.W., Yang, Y.J., Schupp, D., Jun, Y.S., 2014. Water chemistry impacts on arsenic mobilization from arsenopyrite dissolution and secondary mineral precipitation: Implications for managed aquifer recharge. *Environ. Sci. Technol.* 48, 4395–4405.

Nimmo, J.R., 2009. Vadose Water. In: *Encyclopedia of Inland Waters*. Elsevier, pp. 766–777.

Nolan, J., Weber, K.A., 2015. Natural Uranium Contamination in Major U.S. Aquifers Linked to Nitrate. *Environ. Sci. Technol. Lett.* 2, 215–220.

Oppong-Anane, A.B., Deliz Quiñones, K.Y., Harris, W., Townsend, T., Bonzongo, J.C.J., 2018. Iron reductive dissolution in vadose zone soils: Implication for groundwater pollution in landfill impacted sites. *Appl. Geochemistry* 94, 21–27.

Reedy, R.C., Scanlon, B.R., Nicot, J.-P., Tachovsky, J.A., 2007. Unsaturated zone arsenic distribution and implications for groundwater contamination. *Environ. Sci. Technol.* 41, 6914–6919.

Rivett, M.O., Buss, S.R., Morgan, P., Smith, J.W.N., Bemment, C.D., 2008. Nitrate attenuation in groundwater: A review of biogeochemical controlling processes. *Water Res.*

Roberts, H.E., Morris, K., Law, G.T.W., Mosselmans, J.F.W., Bots, P., Kvashnina, K., Shaw, S., 2017. Uranium(V) Incorporation Mechanisms and Stability in Fe(II)/Fe(III) (oxyhydr)Oxides. *Environ. Sci. Technol. Lett.* 4, 421–426.

Smith, R.L., Kent, D.B., Repert, D.A., Böhlke, J.K., 2017. Anoxic nitrate reduction coupled with iron oxidation and attenuation of dissolved arsenic and phosphate in a sand and gravel aquifer. *Geochim. Cosmochim. Acta.*

Soplinski, A., Elkayam, R., Lev, O., 2017. Quantification of dissolved organic matter in pore water of the vadose zone using a new ex-situ positive displacement extraction. *Chem. Geol.*

- Spalding, R.F., Watts, D.G., Schepers, J.S., Burbach, M.E., Exner, M.E., Poreda, R.J., Martin, G.E., 2001. Controlling Nitrate Leaching in Irrigated Agriculture. *J. Environ. Qual.* 30, 1184.
- Teaf, C.M., Covert, D.J., Teaf, P.A., Page, E., Starks, M.J., 2010. Arsenic cleanup criteria for soils in the US and abroad: comparing guidelines and understanding inconsistencies. In: *Proceedings of the Annual International Conference on Soils, Sediments, Water and Energy*. pp. 94–102.
- United States Department of Agriculture, 2019. USDA ERS - Irrigation & Water Use [WWW Document]. URL <https://www.ers.usda.gov/topics/farm-practices-management/irrigation-water-use/> (accessed 10.7.19).
- USEPA, 2019. Regional Screening Levels (RSLs) - Generic Tables [WWW Document]. URL <https://www.epa.gov/risk/regional-screening-levels-rsls-generic-tables> (accessed 10.8.19).
- Vodyanitskii, Y.N., 2011. Chemical aspects of uranium behavior in soils: A review. *Eurasian Soil Sci.*
- Wang, Y., Le Pape, P., Morin, G., Asta, M.P., King, G., Bártová, B., Suvorova, E., Frutschi, M., Ikogou, M., Pham, V.H.C., Vo, P. Le, Herman, F., Charlet, L., Bernier-Latmani, R., 2018. Arsenic Speciation in Mekong Delta Sediments Depends on Their Depositional Environment. *Environ. Sci. Technol.* 52, 3431–3439.
- Wedepohl, K.H., 1991. Chemical composition and fractionation of the continental crust. *Geol. Rundschau*.
- Westrop, J.P., Nolan, P.J., Healy, O.M., Bone, S., Bargar, J.R., Snow, D., Weber, K.A., 2018. MOBILIZATION OF NATURALLY OCCURRING URANIUM FOLLOWING THE INFLUX OF NITRATE INTO AQUIFER SEDIMENTS.
- Xiao, Z., Xie, X., Pi, K., Yan, Y., Li, J., Chi, Z., Qian, K., Wang, Y., 2018. Effects of irrigation-induced water table fluctuation on arsenic mobilization in the unsaturated zone of the Datong Basin, northern China. *J. Hydrol. (Amsterdam, Netherlands)* 564, 256–265.

Summary & Conclusions

An improved understanding of the occurrence, rate of transport, and breakdown of agrichemicals in the vadose zone allows municipalities to better anticipate and predict groundwater contamination. By sampling previously collected sites, it is possible to determine if changing practices and the use of BMPs such as improvements in water and fertilizer application input have a measurable effect on nitrate-N loading to the vadose zone and the underlying groundwater. Quantifying the contaminant mass in the entire vadose zone allows for a more complete representation of stored agrichemicals. It also more effectively reveals nitrate-N concentrations in recharge water close to the groundwater table. Recharge water that is approaching or exceeding the 10 mg/L MCL for nitrate-N has implications towards water quality within the capture zones of municipal wells. Concentrations of ammonium-N should also be taken into consideration, as it also has been observed accumulating in the vadose zone and can be biologically converted to nitrate-N under certain conditions.

This investigation quantified the mass of agrichemicals in Hastings' WHPA and compared them to estimations made five years previously in a 2011 study (R. Spalding & Toavs, 2011). Land use among the sampled locations varied from urban land, pivot/gravity irrigated cropland, and non-irrigated cropland. Certain lithologic properties seemed to correlate with concentrations of agrichemicals. High nitrate-N concentrations were commonly found in sediments consisting of clay and silt loams. Overall, fluctuations of stored nitrate-N varied site by site over the five-year span. Potential nitrogen sources at these sites varied from nonpoint sources in row-cropped farmland to suspected point source releases (R. Spalding & Toavs, 2011).

Producer fields increased by 2,800 lbs-N/Acre of stored nitrate-N in the top 60 ft. Sites that were converted from gravity to pivot irrigation showed a reduction of approximately 170 lbs-N/acre in the top 55 ft of the profile over a five-year time span. This reinforces the idea that irrigation management can be an effective BMP to protect groundwater quality. Overall, amount of nitrate-N stored under urban lawns decreased by 840 lbs-N/Acre. The amount of vadose zone contamination from urban locations depends on factors similar to agricultural regions, such as water input, fertilizer usage, and land use within the urban environment. Cumulative nitrate-N beneath the top 65 ft for urban irrigated lawns, pivot irrigated farmland, and gravity irrigated farmland had an average of 320, 540, and 700 total lbs-N/acre respectively. Although no significant differences between their nitrate-N were present at the different depths, trends of higher nitrate-N under cropland vadose zones were present.

A better understanding of urban and rural BMPs would allow for more definitive statements to be made about how the adoption of new practices are influencing agrichemical leaching. Additionally, understanding irrigation management can help provide insights as to why high concentrations of nitrate-N in groundwater are common in certain agricultural and residential regions. It is likely that improved management practices have positively reduced the amount of nitrate-N being leached in certain locations. Continuing the transition from gravity to pivot irrigation can allow for more uniform water applications, eliminating potential leaching at the head and tail rows of gravity irrigated fields. The importance of vadose zone monitoring in evaluating and protecting groundwater is beneficial in determining connections between surface activities and the underlying groundwater.

The occurrence and distribution of elevated levels of As and U in the unsaturated zone of the Hastings WHPA suggest that mobilization and leaching may lead to increasing levels in the local groundwater. In

Hastings WHPA, elevated levels of U are already being observed in the groundwater below and increase in nitrate content in the unsaturated zone seems to influence the mobilization of U, which is finally ending in the groundwater. Currently, As concentrations are high but do not seem to be affected by the same processes controlling U. Continued monitoring of groundwater is necessary to ensure that these trends are significant. The presence of high iron in the soil coupled with elevated levels of DOC can influence various microbial processes and can control mobilization or immobilization process as iron oxides are known to bind both As and U strongly. Further in-depth analysis of iron chemistry will provide more information about the biogeochemical processes controlling As and U mobilization in the unsaturated zone.

References

- Adelman, D.D. (1985). Overview of nitrate in Nebraska's ground water. *Nebraska Academy of Sciences*, (220), 75.
- American Society for Testing and Materials. (1991). Standard guide for soil sampling from the vadose zone. *ASTM*.
- American Society for Testing and Materials. (2004). Standard test methods for particle-size distribution (gradation) of soils using sieve analysis. *ASTM*.
- Anderson Jr., H.W. (1993). Effects of agricultural and residential land use on ground-water quality, Anoka Sand Plain aquifer, east-central Minnesota. *U.S. Geological Survey Water-Resources Investigations Report 93-4074*.
- Bobier, M.W., Frank, K.D., & Spalding, R.F. (1993). Nitrate-N movement in a fine textured vadose zone. *Journal of Soil and Water Conservation*, 48(4), 350-354.
- Cassada, D.A., Spalding, R.F., Cai, Z., & Gross, M.L. (1994). Determination of atrazine, deethylatrazine and deisopropylatrazine in water and sediment by isotope dilution gas chromatography—mass spectrometry. *Analytica chimica acta*, 287(1), 7-15.
- Chang, C.C.Y., Langston, J., Riggs, M., Campbell, D.H., Silva, S.R., & Kendall, C. (1999). A method for nitrate collection for $\delta^{15}\text{N}$ and $\delta^{18}\text{O}$ -analysis from waters with low nitrate concentrations. *Can. J. Fish. Aquat. Sci.*, 56, 1856-1864.
- Haley, M., Dukes, M., & Miller, G. (2007). Residential irrigation water use in Central Florida. *Journal of Irrigation and Drainage Engineering*, 133(5), 427-434.
- Hastings Utilities. (1997). Groundwater modeling study and well head protection area delineation for Hastings Utilities municipal wellfield.
- Herbel, M.J., & Spalding, R.F. (1993). Vadose zone fertilizer-derived nitrate and $\delta^{15}\text{N}$ extracts. *Ground Water*, 31(3), 376-382.
- Hergert, G.W., & Shapiro, C.A. (2015). Irrigation and nitrogen management. *University of Nebraska—Lincoln Extension*.
- Johnson, B., Thompson, C., Giri, A., & NewKirk, S.V. (2011). Nebraska irrigation fact sheet. *Department of Agricultural Economics*.
- Katupitiya, A. (1995). Long-term tillage effects on nitrate movement and accumulation and denitrification in the root and intermediate vadose zones. *ETD collection for University of Nebraska - Lincoln*. Retrieved from <http://digitalcommons.unl.edu/dissertations/AAI9614988>.
- Keech, C.F., & Dreeszen, V.H. (1968). Availability of ground water in Adams County, Nebraska (HA-287). Denver, CO.
- Kettler, T.A., Doran, J.W., & Gilbert, T.L. (2001). Simplified method for soil particle-size determination to

- accompany soil-quality analyses. *Soil Science Society of America Journal*, 65(3), 849.
<https://doi.org/10.2136/sssaj2001.653849x>.
- Little Blue NRD. (2011). Little Blue NRD geologic & hydro-geologic information. Davenport. Retrieved from http://www.littlebluenrd.org/hydrogeologic_study.html.
- Logan, T.J. (1990). Agricultural best management practices and groundwater protection. *Journal of Soil & Water Conservation*, 45(2), 201.
- McMahon, P.B., Dennehy, K.F., Michel, R.L., Sophocleous, M., Ellett, K.M., & Hurlbut, D.B. (2003). Water movement through thick unsaturated zones overlying the Central High Plains Aquifer, southwestern Kansas, 2000-2001. *Water-Resources Investigations Report 03-4171*.
- Morrison, J., Brockwell, T., Merren, T., Fourel, F. & Phillips, A.M. (2001) On-line high-precision stable Hydrogen isotopic analyses on nanoliter water samples. *Anal. Chem.*, 73(15), 3570-3575.
- O'Brien, D.M., Rogers, D.H., Lamm, F.R., & Clark, G.A. (1998). An economic comparison of subsurface drip and center pivot sprinkler irrigation systems. *Applied Engineering in Agriculture*, 14, 391–398.
- Ollevent, N.A. (1995). Tukey multiple comparison test. *Journal of Clinical Nursing*, 310(8), 299–304. Retrieved from http://www.blackwellpublishing.com/specialarticles/jcn_8_304.pdf
- Olsson Associates. (2011). *Final Nitrate Alternatives Analysis Report City of Edgar, NE*.
- Raciti, S.M., Groffman, P.M., Jenkins, J.C., Pouyat, R.V, Fahey, T.J., Pickett, S.T.A., ... Cadenasso, M.L. (2017). Nitrate production and availability in residential soils. *Ecological Applications*, 21(7), 2357–2366.
- Revesz, K. & Woods, P.H. (1990). A method to extract soil water for stable isotope analysis. *J. Hydrol.*, 115 (1-4), 397-406.
- Spalding, R.F., & Kitchen, L. A. (1988). Nitrate in the intermediate vadose zone beneath irrigated cropland. *Groundwater Monitoring & Remediation*, 8(2), 89–95.
- Spalding, R., & Toavs, M. (2011). 2011 Vadose zone nitrate study at Hastings, NE.
- Solomon, D.K. & Sudicky, E.A. (1991) Tritium and Helium 3 isotope ratios for direct estimation of spatial variations in groundwater recharge. *Wat. Resour. Res.*, 27(9), 2309-2319.
- Stanley, R.H., Baschek, B., Lott, D.E., & Jenkins, W.J. (2009). A new automated method for measuring noble gases and their isotopic ratios in water samples. *Geochemistry, Geophysics, Geosystems*, 10(5).
- The Little Blue NRD. (2013). NRD GWMA. Retrieved from http://www.littlebluenrd.org/pdf%27s/groundwater/hastings_rules_map.pdf.
- UNL Plant & Soil Sciences. (1999). Irrigation mManagement. Retrieved March 1, 2018, from <https://passel.unl.edu>.

USDA. (2014). Soil survey field and laboratory methods manual.

Wakida, F.T., & Lerner, D.N. (2005). Non-agricultural sources of groundwater nitrate: A review and case study. *Water Research*, 39(1), 3–16.

Appendix A: Nitrate, Ammonia and Pesticides

Vadose Zone Profile Data by Site

Site ID: HC-1-E, Gravity Irrigated Corn - Cored November '16

Depth	Gravimetric Water Content	Bulk Density	pH	NO3-N (ug/g)	NH4-N (ug/g)	Pore Water NO3-N (mg/L)	lbs-N/Acre-ft	lbs-N/Acre-ft in Cored Interval	Lithologic Description
2.5-5	0.132	1.13	5.83	10.91	2.27	82.79	33.62	84.06	clay loam - black
7.5-10	0.260	1.55	6.86	1.19	1.37	4.57	5.01	12.52	silty clay - Fe C - light brown
10-12.5	0.269	1.06	7.16	1.39	1.32	5.17	4.03	10.07	silty clay - Fe C - light brown
12.5-15	0.324	1.27	7.14	1.15	0.88	3.55	3.98	9.95	clay - Fe C - OM - light brown
18.1-20	0.208	1.57	7.16	0.88	0.79	4.24	3.77	7.17	sandy clay loam - Fe C - tan
22.5-25	0.079	1.74	6.99	0.85	0.70	10.74	4.02	10.06	sand - light tan
25.9-27.1	0.129	1.65	7.16	1.01	1.32	7.80	4.53	5.44	loamy sand - Fe C - tan
27.1-30	0.205	1.57	7.16	1.40	1.04	6.84	6.01	17.42	clay loam - brown
31.7-32.5	0.135	1.30	7.17	1.33	1.19	9.82	4.69	3.75	loam - Fe C - OM - light brown
32.5-35	0.369	1.15	7.05	1.16	1.00	3.16	3.64	9.11	loamy sand - tan
37.5-40	0.081	1.47	7.02	1.48	1.07	18.26	5.91	14.77	loamy sand - tan
42.5-45	0.092	1.84	7.05	1.42	1.26	15.48	7.13	17.82	sand - Fe C - Fe P - tan
47.5-50	0.145	1.58	7.14	1.99	0.78	13.79	8.56	21.39	sand - Fe C - Fe P - light tan
50.6-51.4	0.153	1.41	7.03	2.16	0.77	14.12	8.31	6.65	sand - Fe C - Fe P - light tan
51.4-52.5	0.193	1.79	6.55	4.16	1.99	21.53	20.29	22.32	clay - Fe P - light brown
57.8-60	0.167	1.81	6.70	4.47	1.69	26.80	21.98	48.35	sandy clay - Fe P - OM - light brown
61.4-62.5	0.077	1.50	6.73	2.09	0.76	27.10	8.54	9.40	sandy clay - Fe C - light brown
62.5-65	0.127	1.81	5.97	2.24	0.05	17.64	11.05	27.61	sandy clay - Fe P - OM - brown
65-67.5	0.155	1.61	6.76	2.37	1.03	15.25	10.36	25.89	sandy clay - Fe C - light brown
67.5-70	0.055	1.30	6.64	1.18	0.05	21.49	4.18	10.44	loamy sand - light brown
77.5-78.7	0.185	1.89	6.62	1.23	0.05	6.64	6.32	7.58	sandy clay - Fe C - OM - light brown
78.7-80	0.046	2.24	6.86	0.50	0.05	10.87	3.06	3.98	sand - tan
82.5-85	0.021	1.83	6.92	0.76	0.05	36.17	3.75	9.39	rocky sand - Fe C - tan
85-87.5	0.090	1.44	6.87	0.57	0.05	6.33	2.22	5.54	rocky sand - Fe C - tan
92.5-94.3	0.021	1.51	6.77	0.77	0.05	37.17	3.18	5.72	rocky sand - tan
101-102.5	0.011	1.53	6.72	0.60	0.21	55.67	2.51	3.76	rocky sand - tan
102.9-105	0.068	2.06	6.86	1.05	0.05	15.41	5.87	12.33	rocky sand - Fe C - dark tan

Total lbs-N/Acre = 722.46

Site ID: HC-1-W, Gravity Irrigated Corn - Cored November '16

Depth	Gravimetric Water Content	Bulk Density	pH	NO3-N (ug/g)	NH4-N (ug/g)	Pore Water NO3-N (mg/L)	lbs-N/Acre-ft	lbs-N/Acre-ft in Cored Interval	Lithologic Description
3.7-5	0.167	1.18	5.93	3.93	2.26	23.52	12.64	16.43	clay loam - OM - black
7.8-10	0.214	1.54	7.35	0.73	0.51	3.40	3.04	6.69	silty clay loam - light brown
12.5-15	0.248	1.50	7.58	1.03	0.52	4.16	4.20	10.51	clay - light brown
15-17.5	0.282	1.05	7.46	2.45	0.86	8.67	7.02	17.54	clay - Fe P - OM - light brown
17.5-20	0.270	1.30	7.57	3.59	1.04	13.31	12.72	31.80	clay - Fe P - OM - light brown
22.9-25	0.061	1.40	7.72	1.37	0.29	22.42	5.24	11.00	loamy sand - dark tan
25-27.5	0.069	1.63	7.77	1.01	0.24	14.58	4.45	11.12	sand - tan
27.5-30	0.058	1.46	7.68	1.22	0.34	20.99	4.85	12.12	clay - Fe P - OM - brown
30-32.5	0.079	1.55	7.64	1.99	0.57	25.27	8.43	21.08	clay loam - Fe P - OM - brown
32.5-34.7	0.314	1.39	7.59	1.39	0.83	4.42	5.23	11.50	clay loam - Fe P - OM - brown
37.5-38.9	0.084	1.85	6.89	0.48	0.14	5.69	2.39	3.35	loamy sand - light brown
38.9-40.1	0.176	1.88	7.16	0.88	0.80	5.00	4.50	5.40	sandy clay loam - Fe C - brown
40.1-42.5	0.106	1.65	7.29	0.91	0.42	8.59	4.07	9.76	sandy loam - Fe C - light brown
45.9-49.3	0.169	1.64	7.25	1.05	0.35	6.18	4.67	15.87	clay loam - Fe C - light brown
49.4-51.9	0.157	1.34	7.22	0.95	0.95	6.02	3.44	8.60	loam - Fe C - OM - brown
51.9-55	0.144	1.30	7.31	0.93	0.80	6.42	3.29	10.19	sandy clay loam - grey
57.5-60	0.073	1.98	7.39	0.71	0.91	9.75	3.83	9.58	sand - tan
62.5-65	0.068	1.52	7.37	0.72	0.86	10.66	2.99	7.48	loamy sand - tan
67.5-70	0.049	2.01	7.50	0.44	0.65	8.95	2.41	6.03	sand - tan
71.4-72.5	0.195	1.72	6.89	1.35	2.89	6.91	6.32	6.96	clay loam - grey
72.5-74.1	0.043	1.66	7.54	0.29	0.32	6.74	1.32	2.11	sand - tan
77.7-80	0.059	1.70	6.81	0.63	0.68	10.65	2.93	6.73	sand - Fe C - tan
82.5-85	0.183	1.81	7.40	0.99	1.23	5.39	4.85	12.13	clay loam - dark brown
87.5-90	0.016	1.64	7.15	0.51	0.35	31.08	2.27	5.67	rocky sand - Fe C - dark tan
92.5-95	0.018	2.25	7.33	0.43	0.19	24.50	2.66	6.64	rocky sand - dark tan
95-97.5	0.023	1.54	7.38	0.45	0.20	19.91	1.89	4.73	rocky sand - dark tan
103.3-105	0.067	1.76	7.17	0.34	0.70	5.09	1.63	2.78	sand - tan
107.5-110	0.202	1.84	6.79	1.20	2.09	5.93	6.00	14.99	sandy clay - grey

Total lbs-N/Acre = 442.80

Site ID: HC-2, Dryland Corn - Cored November '16

Depth	Gravimetric Water Content	Bulk Density	pH	NO3-N (ug/g)	NH4-N (ug/g)	Pore Water NO3-N (mg/L)	lbs-N/Acre-ft	lbs-N/Acre-ft in Cored Interval	Lithologic Description
0-2.5	0.282	0.57	5.80	5.24	12.90	18.56	8.08	20.20	clay loam - dark black
2.5-4.5	0.264	0.64	6.33	1.85	2.40	7.04	3.25	6.49	silty clay loam - Fe P - dark brown
5-7.5	0.227	0.54	6.95	1.32	3.26	5.82	1.95	4.88	silt loam - Fe P - brown
7.5-9.5	0.205	0.59	7.46	1.34	1.28	6.57	2.16	4.31	silt loam - light brown
10.0-12.0	0.242	0.69	7.64	0.13	0.71	2.00	0.23	0.47	clay - Fe P - brown
12.5-15	0.250	0.69	7.62	1.15	1.33	4.58	2.15	5.37	clay - Fe P - brown
15.0-17.0	0.272	0.69	7.78	1.12	1.64	4.10	2.10	4.21	clay - Fe P - brown
20.6-22.5	0.265	0.72	7.69	0.76	1.37	2.88	1.50	2.84	clay - brown
22.5-24	0.275	0.85	7.81	0.37	1.40	1.36	0.86	1.30	clay - OM - Fe P - brown
27.6-30	0.140	0.88	7.73	0.38	1.30	2.71	0.91	2.18	sandy loam - dark brown
37.5-40.3	0.230	1.80	6.78	1.10	0.43	4.76	5.36	15.01	clay - Fe C - Fe P - brown
40.3-41.6	0.115	2.26	7.17	1.36	1.09	11.82	8.34	10.85	loam - Fe P - grey
41.6-42.5	0.116	2.01	7.32	0.83	1.19	7.14	4.51	4.06	sandy loam - grey
45-47.5	0.161	1.66	7.29	1.00	0.10	6.20	4.51	11.28	loam - Fe C - Fe P - grey
47.5-50	0.110	1.48	7.28	0.86	0.05	7.81	3.44	8.59	sandy loam - Fe P - OM - light brown
51.5-52.5	0.107	1.78	7.30	0.74	0.05	6.92	3.57	3.57	loamy sand - Fe P - light brown
52.5-55	0.101	1.87	7.36	0.87	0.18	8.66	4.45	11.12	loamy sand - Fe P - light brown
55-57.5	0.054	2.18	7.32	0.83	0.19	15.41	4.91	12.28	sand - Fe C - Fe P - brown
57.5-60	0.087	1.89	7.17	0.80	0.05	9.21	4.13	10.31	sand - Fe P - tan
60-62.5	0.040	1.92	7.20	0.93	0.05	23.61	4.89	12.23	sand - Fe P - tan
62.5-65	0.019	1.56	6.09	1.07	0.05	57.30	4.53	11.32	sand - Fe C - tan
65-67.5	0.105	1.69	6.43	1.02	0.18	9.68	4.68	11.71	sand - light tan
67.5-70	0.226	1.88	6.62	0.98	0.05	4.32	4.99	12.48	loam - light brown
72.5-75.4	0.109	2.05	6.81	0.96	0.05	8.86	5.37	15.59	loam - light brown

Total lbs-N/Acre = 246.94

Site ID: HC-3A, Residential - Cored August '16

Depth	Gravimetric Water Content	Bulk Density	pH	NO3-N (ug/g)	NH4-N (ug/g)	Pore Water NO3-N (mg/L)	lbs-N/Acre-ft	lbs-N/Acre-ft in Cored Interval	Lithologic Description
0-2.2	0.120	0.70	6.71	0.40	0.57	3.34	0.76	1.67	clay - black
2.2-5	0.106	0.57	7.53	0.19	0.10	1.77	0.29	0.82	silty clay - light tan
5.8-7.5	0.118	0.59	7.74	0.73	0.46	6.19	1.17	1.98	silt loam - light tan
7.5-9.2	0.171	0.60	7.88	0.49	0.27	2.90	0.81	1.37	loam - tan
9.2-10	0.176	0.65	7.95	0.39	0.31	2.22	0.69	0.55	sandy clay loam - dark tan
10-12.5	0.235	1.35	7.67	0.33	0.05	1.41	1.21	3.02	silty clay - light brown
13.5-17.5	0.222	0.68	8.03	0.36	0.05	1.61	0.66	2.63	loamy sand - tan
17.5-20	0.037	0.86	8.03	0.60	0.38	16.41	1.41	3.52	sand - OM - tan
20-22	0.114	1.96	7.96	0.40	0.05	3.50	2.13	4.26	sand - light brown
22-24.1	0.041	1.97	8.08	0.60	0.05	14.50	3.21	6.75	sand - OM - brown
24.1-25.3	0.155	1.87	7.68	1.46	0.13	9.42	7.43	8.92	sandy clay loam - dark brown
25.3-27.5	0.040	1.98	8.02	1.85	0.14	45.82	9.96	21.91	sand - brown
27.5-30	0.069	1.97	7.87	0.57	0.24	8.29	3.04	7.61	loamy sand - brown
30-32.5	0.050	2.01	7.77	2.00	0.31	40.01	10.92	27.31	loamy sand - brown
32.8-34.5	0.038	1.74	8.02	4.35	0.25	114.68	20.54	34.92	sandy loam - dark brown
34.5-36.5	0.035	2.07	8.11	2.29	0.32	65.51	12.88	25.77	sand - brown
37.5-40	0.044	1.97	7.83	2.50	0.09	57.01	13.42	33.54	sand - brown
40-42.8	0.117	1.74	8.18	1.59	1.35	13.59	7.53	21.08	loamy sand - dark brown
42.8-45	0.191	1.77	7.46	5.59	0.09	29.31	26.97	59.33	sand - brown
48.1-50.1	0.112	2.15	7.52	4.01	0.06	35.68	23.44	46.87	sand - brown
50.1-53.5	0.188	1.83	7.47	3.77	0.07	20.08	18.76	63.78	sandy loam - brown
53.5-55	0.166	1.93	7.55	3.64	0.05	21.84	19.06	28.59	clay - brown
55-57.5	0.070	2.09	7.76	2.62	0.12	37.52	14.89	37.22	clay loam - brown
57.5-60	0.026	2.08	7.73	1.43	0.05	54.72	8.07	20.18	clay - OM - brown
61.2-63.5	0.131	1.75	6.35	1.91	0.05	14.61	9.06	20.83	sand - Fe P - light brown
63.5-65.0	0.174	1.92	6.59	0.40	0.05	2.30	2.10	3.14	sandy clay loam - OM - brown

Total lbs-N/Acre = 599.87

Site ID: HC-3B, Residential - Cored August '16

Depth	Gravimetric Water Content	Bulk Density	pH	NO3-N (ug/g)	NH4-N (ug/g)	Pore Water NO3-N (mg/L)	lbs-N/Acre-ft	lbs-N/Acre-ft in Cored Interval	Lithologic Description
0-1.9	0.146	1.17	6.60	2.71	5.35	18.48	8.63	16.40	clay - black
1.9-5	0.146	1.16	6.80	0.48	1.07	3.25	1.50	4.64	silt - light brown
6.7-8.7	0.183	1.24	7.67	0.78	1.07	4.25	2.62	5.25	silt loam - Fe C - light brown
8.7-10	0.230	1.32	7.74	0.54	0.50	2.35	1.94	2.52	silty clay loam - Fe C - light brown
10-12.5	0.257	1.53	7.65	0.94	1.41	3.65	3.91	9.77	clay loam - dark brown
12.5-14.1	0.295	1.42	7.82	0.86	0.63	2.92	3.32	5.31	clay - dark brown
14.1-15	0.050	1.85	7.84	0.99	0.05	19.86	5.01	4.50	sand - tan
15-16.4	0.232	1.86	7.69	1.09	1.23	4.70	5.50	7.70	clay - dark brown
16.4-19.7	0.062	2.08	7.94	0.57	0.05	9.19	3.24	10.68	sand - tan
20-22.5	0.052	1.97	7.40	0.65	0.21	12.52	3.49	8.74	sandy clay - dark tan
22.5-25	0.073	1.99	7.75	0.61	0.05	8.35	3.32	8.30	sand - dark tan
28.9-31.7	0.116	2.27	7.55	0.40	0.86	3.41	2.44	6.83	loamy sand - dark tan
31.7-34.8	0.199	1.88	7.50	3.08	0.48	15.46	15.76	48.86	clay loam - Fe P - OM - dark tan
34.8-35.3	0.152	1.93	7.62	1.09	1.06	7.13	5.70	2.85	sandy clay - dark tan
35.3-36.4	0.163	2.13	7.54	3.26	0.77	19.96	18.86	20.74	clay - OM - brown
37.3-40	0.221	2.20	7.20	4.07	0.36	18.47	24.42	65.93	clay - OM - dark grey
45-46	0.181	1.59	7.28	0.59	2.20	3.26	2.56	2.56	clay - brown
46-49.7	0.197	1.76	6.90	1.11	0.16	5.65	5.32	19.69	sandy clay loam - OM - dark tan

Total lbs-N/Acre = 322.61

Site ID: HC-4, City Park - Cored August '16

Depth	Gravimetric Water Content	Bulk Density	pH	NO3-N (ug/g)	NH4-N (ug/g)	Pore Water NO3-N (mg/L)	lbs-N/Acre-ft	lbs-N/Acre-ft in Cored Interval	Lithologic Description
0-1.7	0.162	1.37	7.03	11.72	2.51	72.52	43.68	74.26	clay - black
2.5-5	0.145	1.44	6.46	9.91	5.18	68.41	38.80	97.01	clay loam - brown
5-7.5	0.169	1.30	7.00	2.48	0.13	14.63	8.76	21.91	silty clay - Fe C - tan
7.5-10	0.166	1.15	7.14	0.78	0.05	4.68	2.44	6.10	silty clay - Fe C - tan
10-12.5	0.158	1.06	7.16	2.15	0.23	13.59	6.18	15.46	silty clay - Fe C - OM - tan
12.5-15	0.168	1.10	7.45	1.08	0.27	6.41	3.22	8.05	silt - Fe C - tan
15-17.5	0.181	1.16	7.59	0.56	0.05	3.07	1.75	4.38	silt - tan
17.5-20	0.185	1.27	7.43	0.62	0.05	3.36	2.14	5.34	silt - tan
20-22.2	0.226	1.27	7.36	0.51	0.05	2.25	1.76	3.87	silty clay - light brown
22.5-25	0.194	1.33	7.35	0.59	0.05	3.03	2.13	5.33	clay loam - black
25-27.5	0.119	1.41	7.30	0.66	0.05	5.59	2.54	6.35	loam - light brown
27.5-28.7	0.111	1.57	7.31	0.67	0.05	6.10	2.89	3.46	loam - brown
28.7-30	0.092	1.56	7.27	0.93	0.05	10.03	3.95	5.13	sandy loam - dark tan
30-32.9	0.161	1.34	6.56	0.96	1.37	5.99	3.51	10.18	clay loam - brown
32.9-35.9	0.191	1.81	6.70	0.72	1.33	3.77	3.54	10.63	clay - brown
35.9-37.5	0.119	1.53	6.63	0.77	1.21	6.43	3.18	5.09	loamy sand - light brown
37.5-40	0.031	2.08	6.76	0.58	0.85	18.40	3.26	8.16	sand - tan
40-42.5	0.146	2.00	6.76	1.00	1.56	6.88	5.45	13.62	sandy clay - OM - brown
42.5-45	0.050	2.05	6.76	0.48	1.03	9.47	2.65	6.63	sand - tan
45-47.5	0.088	1.79	6.72	0.87	1.56	9.89	4.23	10.58	sandy clay - brown
47.5-49	0.085	1.94	6.62	0.69	1.09	8.15	3.66	5.48	loamy sand - OM - tan
49-52.1	0.175	2.03	6.59	1.18	1.63	6.76	6.54	20.26	sandy clay - OM - brown
52.1-55.3	0.149	2.15	6.76	0.97	2.14	6.53	5.68	18.19	clay loam OM - brown
55.3-57.9	0.353	1.60	6.83	1.21	1.82	3.43	5.28	13.74	loam - dark tan
57.8-60.6	0.129	2.28	6.29	0.72	1.87	5.57	4.44	12.44	clay loam - OM - brown
60.6-64.3	0.103	2.17	6.53	0.97	1.56	9.39	5.69	21.06	loam - brown

Total lbs-N/Acre = 418.29

Site ID: HC-5, Residential - Cored August '16

Depth	Gravimetric Water Content	Bulk Density	pH	NO3-N (ug/g)	NH4-N (ug/g)	Pore Water NO3-N (mg/L)	lbs-N/Acre-ft	lbs-N/Acre-ft in Cored Interval	Lithologic Description
0-2.3	0.164	1.24	6.66	1.40	2.16	8.50	4.70	10.82	clay loam - OM - black
2.5-5	0.212	1.31	6.42	0.83	1.85	3.93	2.95	7.38	clay loam - OM - dark brown
5-7.5	0.217	1.53	6.28	0.84	1.03	3.89	3.51	8.76	clay - brown
7.5-10	0.218	1.19	6.17	0.69	1.08	3.14	2.22	5.55	loam - OM - brown
10-12.5	0.237	1.58	6.10	0.67	0.49	2.83	2.88	7.21	clay loam - OM - brown
12.5-15	0.258	1.29	6.10	0.76	0.46	2.95	2.67	6.68	clay - OM - light brown
15-17.5	0.293	0.80	6.48	0.54	1.37	1.86	1.19	2.97	clay - OM - brown
17.5-20	0.294	1.37	6.26	3.55	0.45	12.07	13.21	33.02	clay - brown
20-22.9	0.267	1.32	6.30	0.74	0.79	2.79	2.67	7.74	clay - light brown
22.5-23.2	0.227	1.65	6.72	0.79	0.22	3.46	3.52	2.47	clay loam - brown
23.2-25	0.117	1.79	6.30	0.66	0.65	5.63	3.22	5.79	sandy clay - brown
25.8-27.5	0.054	2.19	6.30	0.63	0.35	11.63	3.75	6.37	sand - dark brown
27.5-30	0.049	2.01	6.26	0.68	0.05	14.04	3.75	9.37	sand - tan
30-32.5	0.103	2.17	6.25	0.90	0.31	8.71	5.28	13.20	sand - tan
32.5-35	0.164	2.12	7.56	0.83	0.18	5.06	4.76	11.90	loam - Fe P - light brown
35-36.2	0.116	1.95	6.48	1.87	1.63	16.07	9.88	11.86	sand - light brown
36.2-37.5	0.123	2.43	7.52	0.95	0.85	7.68	6.27	8.15	sandy clay - Fe P - light brown
37.5-40	0.235	1.94	6.53	0.83	0.05	3.53	4.39	10.97	clay loam - light brown
45-46.7	0.118	1.67	6.79	0.85	0.17	7.20	3.85	6.55	sandy loam - light brown
46.7-50	0.141	1.99	6.70	0.74	0.14	5.26	4.03	13.29	sandy clay loam - light brown

Total lbs-N/Acre = 144.90

Site ID: HC-6, Residential - Cored August '16

Depth	Gravimetric Water Content	Bulk Density	pH	NO3-N (ug/g)	NH4-N (ug/g)	Pore Water NO3-N (mg/L)	lbs-N/Acre-ft	lbs-N/Acre-ft in Cored Interval	Lithologic Description
0-2	0.189	0.92	7.31	1.60	3.91	8.50	4.00	8.00	clay - black
2.7-4.8	0.185	0.73	6.60	0.42	1.69	2.28	0.72	1.15	clay loam - light brown
5.9-7.5	0.171	0.58	7.25	0.36	1.47	2.13	0.66	1.40	silt loam - light tan
7.5-9.5	0.160	0.65	6.97	0.13	0.77	2.00	0.22	0.44	silt loam - light brown
10-12.2	0.132	0.67	7.18	0.13	0.86	2.00	0.23	0.50	silt - Fe C - light brown
12.2-13.8	0.115	0.62	7.22	0.13	0.86	2.00	0.21	0.34	silt - light brown
15-17.3	0.125	0.55	7.26	0.13	0.78	2.00	0.19	0.43	silt loam - light brown
17.3-20	0.126	0.62	7.22	0.13	1.24	2.00	0.21	0.57	silt - light brown
20-21.8	0.141	0.64	7.33	0.26	0.93	1.81	0.45	0.80	silty clay - brown
21.8-25.8	0.103	0.71	7.30	0.13	1.19	2.00	0.24	0.96	loam - dark brown
26.2-27.5	0.091	0.74	7.26	0.13	1.36	2.00	0.25	0.33	sandy loam - brown
30.3-31.6	0.156	0.94	7.34	0.13	1.13	2.00	0.32	0.42	sandy loam - light brown
32.2-34.6	0.098	1.20	7.47	0.13	1.06	2.00	0.41	0.98	sand - light tan
35-37.5	0.056	0.86	7.59	0.29	0.95	5.25	0.69	2.07	sand - tan
37.5-40	0.136	0.75	6.71	0.13	0.99	2.00	0.25	0.63	sandy loam - tan
40.6-42.5	0.133	0.89	7.56	0.26	0.93	1.98	0.64	1.21	loamy sand - brown
42.9-45	0.166	1.07	7.55	0.13	1.04	2.00	0.36	0.76	loam - brown
45-47	0.155	1.09	7.57	0.35	1.74	2.24	1.04	2.07	loamy sand - brown
47.9-50	0.180	0.99	7.23	1.11	2.38	6.18	2.99	6.28	loam - OM - brown
50.6-52.5	0.152	0.89	7.50	0.13	1.26	2.00	0.30	0.58	loamy sand - brown
52.5-53.9	0.177	1.01	7.31	0.13	0.81	2.00	0.34	0.48	clay - brown
55.5-57.5	0.183	1.02	7.45	0.13	1.46	2.00	0.35	0.69	clay loam - brown
57.5-60	0.221	0.93	7.48	0.32	1.23	1.44	0.81	2.02	clay loam - brown
60-61.9	0.175	0.93	7.64	0.54	1.35	3.11	1.37	2.61	clay loam - brown
62.5-63.8	0.174	1.24	7.72	0.47	1.59	2.73	1.60	2.08	sandy clay loam - brown
67.5-70	0.139	1.04	7.69	0.63	1.67	4.54	1.77	4.43	sandy loam - brown

Total lbs-N/Acre = 51.36

Site ID: HC-7, Barnyard - Cored August '16

Depth	Gravimetric Water Content	Bulk Density	pH	NO3-N (ug/g)	NH4-N (ug/g)	Pore Water NO3-N (mg/L)	lbs-N/Acre-ft	lbs-N/Acre-ft in Cored Interval	Lithologic Description
0-2.3	0.104	1.38	7.00	4.16	5.33	40.01	15.67	36.03	clay - black
2.3-5	0.131	1.18	7.36	1.32	0.14	10.06	4.21	11.38	silty clay - light brown
5.-7.5	0.155	1.09	7.42	1.23	0.05	7.90	3.64	9.09	silt loam - Fe C - light brown
7.5-10	0.154	1.15	7.32	1.83	0.29	11.93	5.74	14.35	silt - Fe C - light tan
10-12.5	0.169	1.07	7.27	1.12	0.26	6.64	3.28	8.19	silty clay - Fe C - light tan
12.5-15	0.164	1.29	7.31	0.86	0.05	5.26	3.03	7.58	silty clay - light tan
15-17.5	0.175	1.30	7.35	1.22	0.05	6.98	4.33	10.83	silty clay - light tan
17.5-19.7	0.178	1.35	7.32	1.89	0.19	10.61	6.93	15.25	silty clay - light tan
19.7-22.5	0.193	1.28	7.27	1.41	0.05	7.32	4.93	13.81	loam - light brown
22.5-24.8	0.051	1.68	7.24	2.32	0.05	45.11	10.58	24.32	sand - light brown
24.8-25.9	0.184	1.42	7.17	3.63	0.39	19.71	13.98	15.38	sandy clay - brown
25.9-27.8	0.045	1.47	7.14	3.70	0.05	82.01	14.76	28.05	sand - light brown
27.8-30	0.097	1.61	7.46	1.92	0.05	19.77	8.42	18.52	sand - Fe C - light tan
30-32.5	0.077	1.99	7.53	1.45	0.07	18.84	7.86	19.65	sand Fe C - light tan
35-36.3	0.076	2.22	6.79	1.05	1.81	13.85	6.32	8.22	loamy sand - tan
36.3-40.2	0.177	2.00	7.02	1.57	1.60	8.86	8.51	33.17	loam - Fe C - OM - brown
40.2-42.5	0.092	1.83	7.00	1.98	0.63	21.56	9.86	22.68	sandy clay - brown
42.5-45	0.198	1.80	6.98	1.41	2.58	7.13	6.90	17.24	clay - OM - brown
45-47.5	0.234	2.01	7.06	2.32	1.17	9.92	12.69	31.72	clay - OM - brown
47.5-50	0.184	2.17	7.11	8.88	1.22	48.28	52.44	131.10	clay loam - brown
50-52.5	0.215	2.02	7.12	5.86	1.50	27.26	32.27	80.67	clay - OM - brown
52.5-55	0.217	1.70	7.11	4.87	1.58	22.42	22.54	56.34	clay - brown
60-62.5	0.099	1.91	7.86	3.36	0.16	33.94	17.46	43.65	sand - tan
62.5-64.7	0.077	2.11	7.58	4.20	0.05	54.89	24.05	52.91	loamy sand - dark tan
64.7-67.5	0.090	2.02	7.64	2.71	1.38	29.96	14.86	41.62	loamy sand - dark tan
67.5-70	0.047	2.36	7.50	3.50	0.05	75.21	22.52	56.29	sand - tan

Total lbs-N/Acre = 885.30

Site ID: HC-8, Barnyard - Cored August '16

Depth	Gravimetric Water Content	Bulk Density	pH	NO3-N (ug/g)	NH4-N (ug/g)	Pore Water NO3-N (mg/L)	lbs-N/Acre-ft	lbs-N/Acre-ft in Cored Interval	Lithologic Description
0-1.9	0.146	1.48	5.86	2.12	1.86	14.54	8.56	16.27	clay loam - OM - black
1.9-5	0.116	1.25	7.06	0.86	0.70	7.42	2.94	9.10	silty clay loam - tan
5-7.5	0.134	1.15	7.40	0.90	0.44	6.74	2.84	7.09	silty clay loam - Fe C - tan
7.5-10	0.120	1.27	7.77	1.34	0.37	11.18	4.62	11.56	silty clay loam - Fe C - tan
10-12.5	0.188	1.20	7.80	0.81	0.37	4.33	2.66	6.66	silty clay - Fe C - OM - tan
12.5-15	0.195	1.23	7.86	1.10	0.16	5.66	3.69	9.23	silty clay - Fe C - tan
15-17.5	0.198	1.20	7.80	1.42	0.38	7.21	4.63	11.58	silty clay - OM - tan
17.5-20	0.224	1.35	7.88	2.09	0.28	9.35	7.66	19.16	silty clay - OM - tan
20-22.5	0.235	1.47	7.74	4.44	0.41	18.93	17.70	44.25	clay - Fe - brown
22.5-25	0.193	1.83	7.56	7.04	0.05	36.53	34.99	87.48	clay loam - dark brown
25-26.1	0.221	1.78	7.68	2.44	3.13	11.05	11.80	12.98	clay - OM - brown
26.1-27.5	0.119	1.81	7.73	3.15	0.54	26.54	15.52	21.73	sandy clay loam - dark brown
27.5-30	0.085	1.79	7.43	2.85	0.91	33.65	13.92	34.79	sandy clay loam - dark brown
30-32.5	0.186	1.93	7.53	2.76	0.81	14.78	14.43	36.08	sandy clay - OM - dark brown
32.5-35	0.150	2.04	7.61	3.41	0.51	22.69	18.95	47.37	sandy clay - OM - dark brown
35-36.8	0.171	1.92	7.73	1.72	2.20	10.04	8.99	16.18	clay loam - dark brown
36.8-40	0.142	1.76	7.78	2.89	1.11	20.37	13.81	44.19	sandy clay - OM - dark brown
45-47.5	0.124	1.69	7.77	2.69	1.21	21.72	12.34	30.85	sandy clay - OM - dark brown
47.5-50	0.152	1.99	7.73	3.41	0.43	22.45	18.47	46.18	sandy loam - OM - dark tan
50-52.5	0.142	2.09	7.77	2.40	0.99	16.91	13.63	34.07	loamy sand - OM - dark tan
52.5-55	0.057	0.98	7.73	2.65	1.25	46.58	7.11	17.77	sand - OM - tan
55-56.5	0.191	1.68	7.48	4.70	0.52	24.58	21.52	32.27	loamy sand - OM - brown
57.5-60	0.145	1.90	7.44	3.91	0.85	27.03	20.20	50.49	sandy clay loam - OM - light brown
60-62.4	0.065	0.96	7.45	0.92	0.05	14.22	2.39	5.75	sandy loam - OM - brown
62.5-64.5	0.140	2.21	7.24	3.12	0.14	22.24	18.75	37.50	sandy clay - Fe P - OM - brown
64.5-67.5	0.148	2.00	7.30	2.65	1.66	17.89	14.41	43.22	sandy clay - Fe P - OM - brown
67.5-70	0.044	0.99	7.36	2.34	9.57	53.74	6.32	15.80	sand - tan
70-72.5	0.120	2.36	7.25	1.57	0.81	13.15	10.09	25.22	loamy sand - light brown
72.5-75	0.033	2.29	7.13	1.46	0.49	44.77	9.12	22.80	sand - Fe C - OM - tan

Total lbs-N/Acre = 861.77

Site ID: HC-9A, Pivot Irrigated Soybeans - Cored March '17

Depth	Gravimetric Water Content	Bulk Density	pH	NO3-N (ug/g)	NH4-N (ug/g)	Pore Water NO3-N (mg/L)	lbs-N/Acre-ft	lbs-N/Acre-ft in Cored Interval	Lithologic Description
0-0.8	0.207	1.26	5.70	9.14	3.94	44.27	31.36	25.09	clay loam - OM - black
0.8-3.3	0.180	1.84	6.04	2.50	4.55	13.94	12.50	31.25	clay loam - OM - black
5-6.5	0.218	1.77	6.54	1.59	3.22	7.29	7.67	11.50	silty clay - OM - dark brown
10-11.5	0.176	1.80	7.28	1.97	2.39	11.21	9.64	14.45	clay loam- Fe C - light brown
15-17.5	0.263	1.27	7.58	3.15	2.10	11.99	10.92	27.29	silt loam - OM - brown
20-22	0.097	2.10	7.57	2.48	2.42	25.51	14.17	28.33	sandy loam - brown
25-27	0.057	1.76	7.63	3.61	2.18	63.57	17.28	34.56	sand - dark tan
30-31.2	0.136	1.22	7.85	2.39	2.04	17.62	7.94	9.53	sandy clay loam - dark brown
31.2-32.9	0.054	1.95	7.88	2.18	2.06	40.29	11.59	19.70	loamy sand - dark brown
35-36.8	0.099	2.08	7.90	1.94	1.96	19.63	10.97	19.74	sandy loam - dark tan
40.2-42.7	0.164	1.66	7.56	4.11	2.19	25.13	18.61	46.52	loam - OM - Fe P - light brown
45.4-47.5	0.174	1.83	7.32	1.82	2.35	10.45	9.06	19.03	silty clay - OM - Fe P - light brown
50-52.5	0.176	1.44	6.96	0.87	1.51	4.91	3.39	8.49	sandy clay - OM - Fe C - dark brown
52.5-55	0.172	1.41	6.90	1.10	2.81	6.39	4.22	10.54	silt loam - OM - light brown
55-56	0.116	1.76	6.78	1.14	1.43	9.85	5.47	5.47	sandy clay loam - dark brown
56-58.2	0.105	1.35	6.78	1.08	1.18	10.27	3.96	8.72	sandy loam - light brown
60-62.3	0.052	1.90	6.80	0.95	0.88	18.29	4.87	11.21	loamy sand - light brown
65-67.5	0.049	2.05	7.07	0.93	1.95	19.02	5.19	12.96	loamy sand - tan
70-72.5	0.045	2.03	7.14	1.42	1.13	31.63	7.86	19.65	sandy loam - tan

Total lbs-N/Acre = 727.00

Site ID: HC-9B, Pivot Irrigated Soybeans - Cored March '17

Depth	Gravimetric Water Content	Bulk Density	pH	NO3-N (ug/g)	NH4-N (ug/g)	Pore Water NO3-N (mg/L)	lbs-N/Acre-ft	lbs-N/Acre-ft in Cored Interval	Lithologic Description
0-2.5	0.138	1.18	5.74	10.60	3.53	76.76	34.08	85.21	clay loam - OM - black
0.5-2.7	0.151	1.42	7.44	0.95	3.32	6.28	3.66	8.05	silt loam - OM - brown
5.0-7	0.176	1.57	6.94	1.81	2.93	10.28	7.74	15.47	silty clay - Fe C - light brown
10.0-12	0.155	1.49	7.60	1.12	2.27	7.27	4.55	9.11	clay loam - OM - Fe C - brown
15-16.7	0.189	1.71	7.58	1.76	2.29	9.31	8.19	13.92	silty clay - OM - brown
17.5-20	0.172	1.59	7.64	4.28	1.72	24.91	18.56	46.40	loam - OM - brown
20-22	0.164	1.51	7.45	3.17	2.26	19.33	12.96	25.92	sandy clay loam - dark brown
25-27	0.066	1.93	7.37	1.88	2.35	28.41	9.88	19.76	sandy loam - brown
30-30.5	0.106	1.44	7.24	1.38	2.61	12.93	5.39	2.70	loamy sand - dark tan
30.5-33	0.101	1.72	7.13	1.37	2.27	13.62	6.42	16.04	loamy sand - dark tan
35-37	0.157	1.93	6.95	1.48	1.83	9.40	7.74	15.48	sandy clay - brown
40.3-42.8	0.102	1.86	7.00	1.66	2.03	16.20	8.39	20.97	sandy loam - brown
45-47	0.049	1.46	7.10	1.39	2.10	28.50	5.54	11.08	loamy sand - OM - dark tan
50-51	0.120	1.58	6.96	1.84	2.21	15.40	7.91	7.91	sandy clay loam - dark tan
51-53.5	0.058	1.26	6.90	1.50	1.99	25.88	5.15	12.87	sandy loam - OM - dark tan
55-57	0.145	1.74	6.83	1.72	2.37	11.82	8.11	16.22	sandy clay - OM - brown
60-62	0.112	1.93	6.98	1.30	2.11	11.65	6.84	13.68	sandy clay loam - brown
65-67.5	0.077	1.82	7.02	1.12	2.11	14.51	5.54	13.85	sandy clay loam - brown
70-72	0.088	1.82	7.09	1.28	3.26	14.65	6.36	12.71	loamy sand - light tan

Total lbs-N/Acre = 532.09

Site ID: HC-10-N, Pivot Irrigated Soybeans - Cored March '16

Depth	Gravimetric Water Content	Bulk Density	pH	NO3-N (ug/g)	NH4-N (ug/g)	Pore Water NO3-N (mg/L)	lbs-N/Acre-ft	lbs-N/Acre-ft in Cored Interval	Lithologic Description
0-0.8	0.219	1.33	6.19	5.56	4.78	25.36	20.06	16.05	clay loam - OM - black
10-12.5	0.234	0.92	7.13	0.70	0.77	2.98	1.74	4.35	silty clay - grey
13.6-15	0.262	0.99	7.17	0.34	1.06	1.29	0.91	1.28	clay loam - grey
15.3-17.1	0.156	1.40	7.12	0.48	0.80	3.05	1.81	3.26	sandy clay - dark brown
17.1-20	0.075	1.54	7.21	0.31	0.64	4.20	1.31	3.81	loamy sand - dark brown
20.7-23.2	0.089	1.55	7.28	0.42	0.88	4.76	1.78	4.44	loamy sand - brown
23.5-25.9	0.117	1.92	7.27	1.65	0.75	14.10	8.64	20.73	sandy clay loam - light brown
32.4-36.2	0.227	1.72	7.05	0.53	0.96	2.34	2.49	9.45	clay loam - Fe C - OM - light brown
35-36.2	0.176	1.17	7.27	0.56	1.19	3.19	1.79	2.15	clay loam - Fe C - light brown
40-42.5	0.084	1.85	7.43	0.52	0.46	6.26	2.64	6.61	sandy loam - light brown
45-47.5	0.142	1.44	7.28	1.03	0.97	7.26	4.02	10.06	sandy clay - OM - dark tan
47.5-50	0.084	1.41	7.18	0.74	0.85	8.84	2.86	7.14	sandy clay - Fe P - OM - brown
50-52.5	0.097	1.46	7.35	0.61	0.81	6.27	2.41	6.03	sand - brown
57.5-59.7	0.092	1.35	7.21	0.80	1.07	8.70	2.93	6.44	sandy clay - Fe P - OM - brown
62.1-63.3	0.173	1.50	7.13	0.58	1.30	3.38	2.39	2.86	clay loam - Fe C - OM - light brown
63.3-64.6	0.079	1.35	7.10	0.57	0.87	7.19	2.10	2.72	loamy sand - light brown
65-67.5	0.468	1.19	7.00	0.47	0.97	1.00	1.52	3.79	clay loam - Fe P - brown
67.5-70	0.199	1.65	7.05	0.52	0.87	2.62	2.33	5.82	clay loam - OM - Fe C - light brown
72.5-75	0.168	1.66	7.04	0.33	1.44	1.99	1.51	3.77	clay loam - OM - Fe C - light brown
75-77.3	0.042	1.67	7.22	0.23	0.58	5.36	1.04	2.38	sand - Fe C - light tan
80-82.3	0.042	1.48	7.19	0.44	0.66	10.48	1.77	4.08	sand - Fe C - tan
85-87.5	0.154	1.73	7.19	0.69	1.54	4.48	3.25	8.13	sandy clay loam - Fe P - tan
85.8-88.8	0.282	1.21	7.02	4.00	0.50	14.22	13.21	39.64	sandy clay - grey

Total lbs-N/Acre = 325.14

Site ID: HC-10-S, Pivot Irrigated Soybeans - Cored March '16

Depth	Gravimetric Water Content	Bulk Density	pH	NO3-N (ug/g)	NH4-N (ug/g)	Pore Water NO3-N (mg/L)	lbs-N/Acre-ft	lbs-N/Acre-ft in Cored Interval	Lithologic Description
0-1.7	0.211	1.28	5.64	2.66	2.73	12.64	9.27	15.76	clay loam - OM - black
1.7-5	0.245	1.17	6.02	0.62	0.49	2.53	1.97	6.51	loam - Fe C - OM - black
5-7.5	0.202	0.98	6.89	0.60	0.14	2.96	1.59	3.99	silt loam - Fe C - OM - brown
7.5-10	0.216	0.98	7.30	1.59	0.68	7.33	4.21	10.52	silt loam - Fe C - OM - brown
10-12.5	0.215	1.01	7.33	0.58	0.19	2.71	1.60	4.01	silty clay loam - Fe C - OM - brown
12.5-15	0.219	1.04	7.23	1.79	1.21	8.16	5.04	12.61	silty clay loam - Fe C - OM - brown
15-17.5	0.251	1.53	7.22	1.83	0.88	7.30	7.61	19.04	silty clay loam - Fe C - OM - brown
20-23.1	0.261	1.42	7.21	2.87	1.27	11.01	11.07	34.32	clay - Fe C - brown
25.7-28.2	0.163	1.77	7.18	1.94	0.56	11.92	9.33	23.34	sandy loam - light brown
30-32.5	0.050	1.56	7.31	2.09	0.51	42.08	8.86	22.15	sand - tan
32.5-35	0.065	1.74	7.24	1.32	0.05	20.32	6.27	15.67	sand - light tan
40-42.2	0.135	1.64	6.74	1.57	0.20	11.65	6.99	15.37	loamy sand - light brown
45-47.4	0.124	1.71	7.13	1.08	0.05	8.70	5.02	12.05	loamy sand - dark tan
50-51	0.053	2.17	7.02	0.81	0.05	15.40	4.82	4.82	loamy sand - dark tan
51-53.3	0.226	1.87	7.03	2.22	0.53	9.82	11.28	25.95	sandy clay - Fe P - light brown
53.3-56.7	0.177	1.57	6.95	2.02	0.81	11.40	8.67	29.47	sandy clay - Fe P - light brown
56.7-59.2	0.181	1.78	7.03	2.03	0.66	11.20	9.82	24.56	sandy clay - Fe C - light brown
60-62.3	0.175	1.34	6.87	1.78	0.28	10.16	6.49	14.93	sandy clay - Fe C - dark brown
62.3-64.6	0.136	1.66	6.93	1.47	0.42	10.75	6.63	15.25	sandy clay - dark brown
64.6-67.2	0.060	1.70	7.09	0.85	0.05	14.19	3.93	10.23	sand - light tan
75-77	0.141	1.90	7.14	0.66	0.05	4.71	3.43	6.87	sand - light tan
80-82.5	0.196	1.72	7.20	2.42	0.89	12.35	11.30	28.25	clay - Fe C - light brown
82.5-85.2	0.188	1.63	7.34	2.34	0.34	12.44	10.39	28.04	sandy clay - grey

Total lbs-N/Acre = 556.24

Site ID: HC-11-E, Pivot Irrigated Corn - Cored December '15

Depth	Gravimetric Water Content	Bulk Density	pH	NO3-N (ug/g)	NH4-N (ug/g)	Pore Water NO3-N (mg/L)	lbs-N/Acre-ft	lbs-N/Acre-ft in Cored Interval	Lithologic Description
1.5-4	0.188	1.08	6.86	4.25	1.03	22.63	12.47	31.19	clay loam - dark brown
4.0-5.0	0.148	1.19	7.33	2.29	1.91	15.53	7.40	7.40	sandy clay loam - brown
7.5-9.5	0.228	1.47	7.61	0.56	0.65	2.44	2.22	4.44	clay loam - OM - brown
11.5-13.5	0.197	1.01	7.58	0.78	0.52	3.95	2.13	4.27	clay loam - OM - brown
13.5-15	0.267	1.15	7.60	0.35	0.55	1.33	1.11	1.67	clay loam - dark brown
15-17	0.273	0.96	6.39	0.73	0.85	2.66	1.90	3.79	silty clay - brownish grey
17-19	0.278	1.14	6.57	0.87	0.71	3.14	2.72	5.43	loam - dark brown
20.5-22.5	0.192	1.17	6.99	1.08	0.75	5.62	3.44	6.88	loam - dark brown
22.5-24	0.290	1.13	7.15	0.84	0.61	2.89	2.58	3.87	clay loam - brown
24-25	0.083	1.21	7.16	0.50	1.19	6.10	1.65	1.65	silt loam -OM - light brown
27.5-30	0.101	1.29	7.24	0.33	0.77	3.30	1.16	2.91	loamy sand - light brown
30-32.5	0.175	1.17	7.39	1.71	0.85	9.76	5.41	13.54	loam - Fe chemical - brown
32.5-35	0.223	1.24	7.36	0.91	0.57	4.07	3.07	7.67	clay - OM - brown
37.5-38.5	0.174	1.44	5.72	1.76	2.60	10.10	6.87	6.87	silty clay - OM - brown
38.5-40	0.188	1.54	5.94	2.88	2.24	15.33	12.07	18.10	clay loam - dark brown
45-47.5	0.212	1.16	7.26	1.27	0.68	6.01	3.29	8.22	clay loam - OM - Fe chemical - brown
50-51.5	0.086	1.72	6.03	0.73	5.45	8.42	3.40	5.10	sand - dark tan
54-55	0.063	1.65	6.07	0.92	2.04	14.57	4.12	4.12	loamy sand - OM - dark tan
57.5-59	0.146	1.51	6.40	0.92	1.37	6.29	3.77	5.65	loam - OM - brown
59-60	0.072	1.34	6.46	0.91	1.88	12.63	3.31	3.31	sandy loam - light brown
62.5-63.5	0.062	1.40	6.31	0.92	2.64	14.97	3.51	3.51	loamy sand - dark brown
63.5-65	0.071	1.37	6.40	0.94	1.34	13.16	3.50	5.24	sand - dark brown
67.5-70	0.039	1.21	6.41	0.67	1.59	17.09	2.21	5.52	loamy sand - dark brown
70-72.5	0.082	1.29	6.44	1.06	1.17	12.90	3.74	9.34	loamy sand - OM - dark tan
75-77	0.038	1.90	7.38	1.57	1.54	41.30	8.15	16.29	sandy clay - OM - dark brown
78-80	0.046	2.01	7.48	0.47	7.37	10.17	2.57	5.13	sand - dark tan
82.5-83.5	0.096	1.87	6.79	0.61	0.96	6.31	3.09	3.09	sand - tan
88-89	0.155	2.08	6.99	0.72	1.19	4.66	4.10	4.10	sand - OM - dark tan
90-92	0.096	1.59	7.24	1.25	0.95	13.03	5.40	10.80	sand - Fe chemical - dark tan
93.5-95	0.320	0.94	7.51	1.64	0.61	5.12	4.17	6.26	sandy loam - Fe chemical - dark tan
101-102.5	0.343	0.99	7.65	1.75	0.90	5.11	4.72	7.09	sand - dark tan

Total lbs-N/Acre = 410.34

Site ID: HC-11-W, Pivot Irrigated Corn - Cored December '15

Depth	Gravimetric Water Content	Bulk Density	pH	NO3-N (ug/g)	NH4-N (ug/g)	Pore Water NO3-N (mg/L)	lbs-N/Acre-ft	lbs-N/Acre-ft in Cored Interval	Lithologic Description
1.2-2.5	0.239	1.01	7.00	1.99	1.06	8.34	5.47	7.10	clay loam - dark brown
2.5-3.5	0.433	1.09	7.09	2.70	3.30	6.23	8.01	8.01	clay - OM - brown
4.5-6.8	0.333	1.01	7.44	3.59	0.91	10.79	9.88	22.72	silty clay - Fe chemical - light brown
6.8-8	0.351	1.31	7.25	3.34	1.21	9.53	11.91	14.30	clay - Fe chemical - tan
8.0-10	0.545	1.09	7.30	2.73	0.68	5.00	8.10	16.21	clay - OM - brown
10.0-12.0	0.292	1.35	6.89	2.47	7.92	8.45	9.08	18.16	clay - Fe physical - OM - light brown
12.0-14.0	0.282	1.20	6.99	1.78	2.41	6.31	5.83	11.65	clay - Fe physical - light brown
15.5-17.5	0.320	1.03	7.13	1.20	0.93	3.74	3.34	6.69	clay loam - light brown
18.7-20	0.227	1.20	7.21	0.47	0.67	2.09	1.54	2.00	silty clay - dark brown
22-23.1	0.117	1.16	7.34	0.88	0.82	7.50	2.75	3.03	silty clay loam - dark brown
23.1-25	0.074	1.79	7.31	0.32	0.41	4.33	1.56	2.96	loamy sand - light brown
27.5-29.5	0.087	1.95	7.46	0.13	0.53	2.00	0.66	1.32	sand - OM - light brown
32-33.3	0.223	1.65	7.13	1.98	1.27	8.89	8.90	11.57	silt loam - light brown
33.3-35	0.489	1.30	6.91	0.76	0.41	1.54	2.67	4.55	sandy loam - light brown
37.5-40	0.064	1.30	6.91	2.00	0.52	31.17	7.08	17.71	loamy sand - light brown
42.5-44.5	0.039	1.51	6.27	1.34	1.19	34.05	5.50	10.99	sand - tan
45-47.5	0.058	1.36	6.04	0.89	2.03	15.31	3.29	8.22	loamy sand - tan
47.5-50	0.069	1.11	6.29	2.47	1.14	35.93	7.48	18.69	loamy sand - Fe chemical - tan
52.5-55	0.070	1.25	6.41	1.85	0.96	26.33	6.28	15.70	loamy sand - light tan
55-57.5	0.082	1.26	6.42	1.44	1.42	17.62	4.97	12.42	sandy loam - OM - brown
58.5-60	0.093	1.38	6.56	2.91	1.39	31.22	10.89	16.34	sandy clay loam - OM - brown
67.5-69.5	0.042	1.47	6.39	2.08	1.13	49.80	8.33	16.65	sand - tan
73-75	0.070	1.55	6.64	2.86	1.35	40.72	12.07	24.14	sand - brown
77.5-80	0.045	1.27	5.87	2.19	2.32	48.18	7.57	18.93	sand - tan
82.5-84.5	0.037	1.35	6.27	1.39	1.67	37.31	5.10	10.21	sand - Fe chemical - tan
86.5-88	0.066	1.70	6.47	1.60	1.88	24.28	7.39	11.08	loamy sand - dark brown
88-90	0.063	1.52	6.74	1.95	1.31	31.21	8.08	16.16	sand - dark tan
92.5-94	0.061	1.66	7.04	3.66	2.11	59.55	16.54	24.80	sand - dark tan
95-97	0.060	1.26	7.19	3.33	2.80	55.73	11.45	22.91	silt loam - Fe chemical - brown
97-99	0.047	1.79	7.26	2.16	1.29	45.49	10.53	21.05	silty clay loam - Fe chemical - dark brown
99-101	0.045	1.90	7.31	2.04	1.18	45.79	10.52	21.04	clay loam - OM - dark brown

Total lbs-N/Acre = 720.58

Site ID: HC-12-E, Gravity Irrigated Soybeans - Cored April '17

Depth	Gravimetric Water Content	Bulk Density	pH	NO3-N (ug/g)	NH4-N (ug/g)	Pore Water NO3-N (mg/L)	lbs-N/Acre-ft	lbs-N/Acre-ft in Cored Interval	Lithologic Description
3.4-5	0.266	1.54	6.84	4.59	3.07	17.26	19.20	30.72	clay loam - OM - black
5-7.5	0.218	1.62	7.54	3.02	2.12	13.86	13.35	33.36	silty clay - OM - Fe P - brown
8.0-10	0.263	1.34	7.58	3.98	1.87	15.13	14.44	28.88	silty clay - Fe C - brown
10-12.5	0.306	1.02	7.31	4.83	2.45	15.80	13.41	33.53	silty clay - Fe C - OM - brown
12.5-15	0.254	1.54	7.33	6.20	2.41	24.42	26.00	65.00	clay - Fe C - brown
15.8-17.5	0.342	1.34	5.37	5.61	2.31	16.40	20.52	34.88	clay - light brown
17.5-18.9	0.234	1.57	5.60	4.21	2.91	18.02	17.92	25.09	sandy clay loam - Fe C - light brown
22.5-25	0.110	1.69	5.96	3.10	2.39	28.23	14.20	35.49	sandy loam - OM - dark gray
25-27.5	0.214	1.49	6.00	1.48	2.17	6.92	6.02	15.04	sandy clay - Fe C - OM - light brown
29-30	0.157	1.86	6.09	4.11	3.22	26.19	20.79	20.79	sandy clay loam - Fe C - OM - light brown
32.5-35	0.185	1.68	6.23	0.71	2.08	3.84	3.25	8.12	sandy clay - OM - light brown
35-37.5	0.177	1.29	6.52	1.01	2.33	5.69	3.55	8.87	sandy clay - OM - brown
38-40	0.140	1.35	6.64	0.74	1.85	5.31	2.72	5.43	sandy loam - Fe C - brown
45.6-47.5	0.149	1.86	6.64	1.19	3.80	8.01	6.03	11.46	loamy sand - brown
47.9-50	0.059	1.88	6.48	1.06	2.21	17.93	5.42	11.38	sand - Fe C - tan
53.7-55	0.073	1.71	6.32	1.19	2.40	16.35	5.54	7.20	sand - Fe C - tan
57.5-60	0.154	1.71	6.50	1.72	2.63	11.16	8.03	20.07	sandy clay - Fe C - tan
63.0-65.0	0.150	1.42	6.11	1.01	2.58	6.70	3.89	7.79	loamy sand - tan
68.2-70	0.185	1.66	6.20	1.21	2.57	6.54	5.45	9.81	sandy clay loam - OM - Fe c - light brown
72.5-75	0.171	1.76	6.46	0.86	2.45	5.00	4.09	10.22	sandy clay loam - OM - Fe C - light brown
78.1-80	0.151	1.40	6.46	1.12	2.82	7.44	4.25	8.08	loamy sand - tan

Total lbs-N/Acre = 684.04

Site ID: HC-12-W, Gravity Irrigated Soybeans - Cored March '17

Depth	Gravimetric Water Content	Bulk Density	pH	NO3-N (ug/g)	NH4-N (ug/g)	Pore Water NO3-N (mg/L)	lbs-N/Acre-ft	lbs-N/Acre-ft in Cored Interval	Lithologic Description
3.3-5	0.198	1.82	6.35	7.15	3.92	36.11	35.32	60.05	clay loam - OM - black
7.9-10	0.219	1.10	6.92	2.10	2.90	9.61	6.28	13.19	silty clay - Fe C - brown
13.5-15	0.252	1.55	7.14	4.72	2.14	18.74	19.95	29.92	clay - Fe C - light brown
15.9-17.5	0.272	1.25	7.25	3.95	1.54	14.53	13.41	21.46	clay - Fe C - light brown
17.5-20	0.298	1.22	7.29	5.02	2.53	16.87	16.63	41.56	clay - Fe C - Fe P - light brown
22.5-25	0.275	1.63	7.37	5.80	2.70	21.12	25.68	64.19	loam - Fe C - Fe P - light brown
27.7-30	0.072	1.24	7.51	2.85	1.20	39.83	9.57	22.00	sand - dark tan
33.5-35	0.150	1.95	7.35	5.61	1.34	37.34	29.70	44.56	sandy clay loam - Fe C - brown
37.5-40	0.057	1.72	7.55	4.39	1.65	77.50	20.55	51.38	sand - Fe C - tan
44.2-45.5	0.095	1.84	7.48	8.53	1.41	90.17	42.71	55.52	loamy sand - Fe C - tan
46-47.5	0.171	1.58	7.47	14.23	1.55	83.19	60.94	91.42	sandy loam - light brown
52.5-55	0.192	1.59	7.11	7.29	1.15	37.88	31.50	78.74	clay - Fe P - dark brown
56.3-57.5	0.279	0.96	6.81	4.95	2.46	17.75	12.88	15.46	clay loam - Fe C - brown
57.5-60	0.191	1.42	6.92	3.37	1.95	17.61	13.07	32.66	clay - Fe C - OM - light brown
60.9-62.5	0.224	1.78	7.00	3.88	1.51	17.31	18.75	30.00	clay loam - brown
63.2-65	0.237	1.75	6.80	3.41	1.69	14.39	16.21	29.17	sandy clay - Fe C - light brown
67.5-70	0.226	1.48	6.88	3.28	1.49	14.51	13.15	32.88	clay - OM - Fe C - light brown
72.5-75	0.186	1.45	6.89	2.66	1.75	14.29	10.48	26.19	clay loam - OM - Fe C - light brown
75-77.5	0.186	1.84	6.92	2.75	1.62	14.80	13.71	34.28	sandy clay - Fe C - light brown
77.5-80	0.203	1.68	6.99	3.29	1.81	16.23	15.06	37.65	clay loam - Fe C - light brown
83.7-85	0.073	1.63	6.94	2.29	2.18	31.61	10.16	13.21	sandy clay - light brown
85-87.5	0.258	1.31	6.99	2.55	1.54	9.85	9.05	22.62	sandy clay - light brown
87.5-90	0.246	1.51	7.11	2.92	1.98	11.87	11.96	29.89	sandy clay loam - Fe C - light brown
94-95	0.159	1.56	7.03	2.75	2.66	17.32	11.69	11.69	sandy clay loam - light brown
98.5-100	0.082	1.62	7.02	2.16	1.96	26.41	9.50	14.25	sand - tan
103.5-105	0.031	1.93	7.62	2.08	1.92	66.40	10.91	16.36	gravely sand - tan
108.7-110	0.023	1.50	7.60	2.00	2.32	88.40	8.15	10.59	gravely loamy sand - tan
114-115	0.031	1.76	7.50	1.77	2.03	56.38	8.49	8.49	gravely sand - tan
118.9-120	0.024	1.53	7.48	1.42	1.27	59.84	5.91	6.50	gravely sand - tan

Total lbs-N/Acre = 2,062.50

Site ID: HC-13-N, Pivot Irrigated Corn - Cored March '16

Depth	Gravimetric Water Content	Bulk Density	pH	NO3-N (ug/g)	NH4-N (ug/g)	Pore Water NO3-N (mg/L)	lbs-N/Acre-ft	lbs-N/Acre-ft in Cored Interval	Lithologic Description
0-0.9	0.323	0.89	7.19	19.22	4.08	59.43	46.73	42.06	clay loam - dark brown
0.9-1.2	0.212	1.24	6.45	5.97	1.73	28.24	20.21	6.06	clay loam - dark brown
1.2-3.4	0.229	1.58	6.08	5.59	1.86	24.45	23.98	52.75	clay loam - dark brown
5-6.3	0.330	1.33	6.15	6.95	2.26	21.03	25.22	32.78	clay loam - brown
6.3-7.5	0.267	1.46	5.83	5.19	1.96	19.42	20.60	24.72	clay loam - brown
7.5-8.4	0.242	1.69	5.83	6.05	1.78	25.03	27.87	25.08	silt loam - brown
10-11.2	0.257	1.17	5.95	4.02	2.39	15.65	12.75	15.30	silt loam - brown
12.5-14.5	0.317	0.95	6.10	7.66	1.90	24.15	19.86	39.73	silt loam - brown
17.5-20	0.302	0.99	6.14	5.84	1.33	19.35	15.69	39.22	silt loam - brown
20-22.6	0.277	1.48	5.47	3.26	1.51	11.75	13.10	34.07	sandy clay loam - light brown
25.8-26.3	0.318	1.09	5.76	1.67	1.50	5.24	4.91	2.46	sandy loam - dark brown
26.3-28.3	0.299	1.26	5.90	1.14	0.84	3.81	3.91	7.82	loamy sand - tan
30-31.8	0.145	1.48	6.06	1.03	0.90	7.07	4.13	7.43	loamy sand - tan
35-36.5	0.177	1.50	5.91	1.08	1.39	6.10	4.41	6.62	sand - light tan
40-41.6	0.323	1.21	6.36	2.33	1.27	7.22	7.63	12.21	clay loam - light brown
41.6-43.6	0.154	1.82	6.63	2.14	1.62	13.91	10.64	21.28	sandy clay loam - lighter brown
45-47.2	0.215	1.75	6.46	1.41	1.50	6.55	6.72	14.79	sand - light tan
50-51.7	0.173	1.29	6.25	0.84	1.11	4.84	2.94	5.00	sand - light tan
57.5-60.9	0.119	1.46	5.81	0.68	1.67	5.75	2.72	9.26	sandy clay loam - Fe - dark tan
60.9-61.9	0.147	1.04	6.09	0.83	1.00	5.63	2.34	2.34	sandy clay loam - Fe - light brown
61.9-63.4	0.120	1.57	5.85	0.39	0.98	3.24	1.66	2.49	sand - Fe - light brown
65-66.7	0.071	1.61	5.80	0.45	0.99	6.26	1.95	3.32	sand - Fe - dark tan
66.7-67.5	0.067	1.70	5.96	0.44	0.96	6.54	2.04	1.63	loamy sand - tan
70-71.9	0.238	1.28	5.99	0.84	0.99	3.55	2.94	5.58	silty clay - Fe - OM - brown
71.9-73.1	0.137	1.43	6.00	1.12	0.93	8.14	4.36	5.23	clay loam - brown
75-77.5	0.043	1.81	5.47	1.02	1.05	23.63	5.02	12.54	sandy loam - Fe - light brown
80.5-82.5	0.044	1.66	5.41	0.54	0.64	12.15	2.44	4.88	sand - light tan
90-92	0.034	1.54	5.94	1.01	0.45	30.03	4.22	8.44	sand - light tan
95-97	0.101	1.34	5.97	0.79	0.48	7.87	2.89	5.78	sand - tan
100-101.7	0.188	1.25	6.39	2.42	0.81	12.88	8.25	14.03	sandy clay loam - brown
103.2-104.2	0.211	1.48	7.11	1.28	0.68	6.07	5.15	5.15	sandy clay loam - brown

Total lbs-N/Acre = 831.93

Site ID: HC-13-S, Pivot Irrigated Soybeans - Cored March '16

Depth	Gravimetric Water Content	Bulk Density	pH	NO3-N (ug/g)	NH4-N (ug/g)	Pore Water NO3-N (mg/L)	lbs-N/Acre-ft	lbs-N/Acre-ft in Cored Interval	Lithologic Description
0-2.7	0.194	1.27	6.47	8.26	2.87	42.63	28.53	77.03	clay loam - OM - black
2.7-4.7	0.184	1.41	6.21	9.07	2.04	49.29	34.69	69.38	loam - OM - dark brown
5-7.2	0.206	1.06	6.10	6.27	1.94	30.45	18.09	39.80	clay loam - OM - black
7.2-9.7	0.177	1.17	6.18	8.49	1.48	47.94	26.92	67.31	loam - OM - dark brown
10-12.5	0.209	1.18	6.38	3.08	2.17	14.78	9.87	24.67	silt loam - OM - brown
12.8-15	0.216	1.13	6.52	4.46	1.44	20.70	13.71	30.16	silt loam - Fe P - OM - light brown
15-17.5	0.217	1.12	6.87	4.55	1.94	20.98	13.80	34.50	silt loam - Fe C - OM - light brown
17.5-20	0.300	1.41	6.70	5.67	1.24	18.91	21.82	54.54	clay - Fe P - OM - light brown
20-22.5	0.322	1.05	7.01	5.58	2.17	17.32	16.01	40.03	clay - Fe P - OM - light brown
22.5-25	0.363	1.22	7.16	7.98	2.39	21.98	26.50	66.26	clay - Fe P - OM - light brown
25-27.5	0.360	1.25	7.15	7.14	2.06	19.86	24.27	60.66	clay - Fe P - brown
30-32.5	0.334	1.00	7.05	6.25	4.05	18.73	16.93	42.32	clay - Fe C - brown
32.5-35	0.195	1.61	6.94	5.20	2.17	26.66	22.75	56.87	sandy clay - dark brown
35-37.6	0.184	1.28	7.02	4.47	1.30	24.23	15.54	40.39	sandy clay - dark brown
37.6-40	0.157	1.59	7.13	2.83	1.11	17.98	12.20	29.28	sandy loam - tan
42-43.2	0.161	1.60	7.25	4.04	0.59	25.02	17.60	21.12	sand - tan
45-47.5	0.154	1.32	6.52	1.37	0.35	8.90	4.90	12.25	clay loam - Fe C - dark brown
47.5-50	0.151	1.60	6.70	1.96	0.91	12.95	8.54	21.35	sandy clay loam - dark brown
50-52.5	0.066	1.38	6.76	3.16	1.07	47.73	11.86	29.65	loamy sand - tan
55-57.2	0.053	1.59	6.87	3.52	1.20	66.43	15.26	33.58	sand - light tan
60-62.5	0.056	1.62	6.90	3.09	1.39	55.08	13.66	34.16	sand - light tan
65-66.4	0.083	1.98	6.58	2.17	0.45	26.10	11.71	16.40	loamy sand - tan
66.4-68.9	0.080	1.70	6.98	1.47	0.69	18.43	6.78	16.96	sandy clay loam - brown
70-72.5	0.126	1.64	6.83	3.90	0.90	30.98	17.36	43.41	sandy clay - brown
72.5-74	0.180	1.69	6.90	3.46	0.75	19.16	15.84	23.76	sandy clay - brown
75-77.5	0.221	1.30	6.81	5.34	1.22	24.22	18.94	47.36	clay - dark brown
77.5-80	0.208	1.72	6.92	5.05	1.05	24.27	23.60	59.01	clay loam - Fe C - Fe P - dark brown
80-82.2	0.167	1.43	7.00	4.19	0.73	25.14	16.29	35.83	sandy clay - Fe C - OM - brown
82.2-83.7	0.109	1.86	7.03	3.50	0.51	31.99	17.65	26.47	loamy sand - Fe C - light brown
85-88.7	0.160	1.87	7.09	5.93	0.79	37.05	30.17	111.64	clay loam - Fe C - brown
90-93.1	0.084	1.63	7.06	3.45	0.25	41.23	15.23	47.21	loamy sand - brown

Total lbs-N/Acre = 1,572.73

Site ID: HC-14-E, Pivot Irrigated Soybeans - Cored April '16

Depth	Gravimetric Water Content	Bulk Density	pH	NO3-N (ug/g)	NH4-N (ug/g)	Pore Water NO3-N (mg/L)	lbs-N/Acre-ft	lbs-N/Acre-ft in Cored Interval	Lithologic Description
0-2.1	0.229	0.99	6.32	2.66	3.72	11.64	7.17	15.05	clay loam - dark brown
2.1-4.5	0.191	1.21	6.51	0.05	1.54	2.00	0.41	0.99	silt loam - brown
5-6.9	0.198	0.91	7.00	0.64	0.73	3.25	1.59	3.02	silty clay loam - Fe C - brown
7.5-10	0.214	0.95	7.00	1.81	1.14	8.43	4.69	11.72	silty clay - brown
10-11.6	0.216	1.20	7.46	2.54	1.02	11.72	8.28	13.25	clay loam - brown
12.5-15	0.267	1.12	7.71	2.75	0.84	10.32	8.36	20.90	clay - brown
17.9-20	0.134	1.93	7.61	1.92	1.16	14.40	10.09	21.18	clay loam - dark brown
23.1-25	0.060	1.71	7.73	0.67	1.14	11.23	3.14	5.96	sand - light brown
27.9-30	0.064	1.47	8.06	0.30	2.09	4.74	1.21	2.55	sand - light brown
30-32.5	0.169	1.18	7.61	0.05	0.79	2.00	0.40	1.00	sandy loam - Fe C - dark brown
32.7-34.8	0.163	1.25	7.69	0.05	0.40	2.00	0.42	0.89	sandy loam - Fe P - OM - brown
37.5-39.3	0.152	1.59	7.78	0.73	0.55	4.79	3.15	5.68	clay loam - light brown
40-42.5	0.233	1.21	7.72	1.16	0.64	4.99	3.82	9.54	clay - OM - light brown
42.5-44.4	0.223	1.66	7.13	0.99	0.84	4.45	4.48	8.52	clay - OM - light brown
46.1-47.5	0.226	1.91	7.26	0.47	0.94	2.10	2.47	3.45	clay loam - dark brown
48.1-50	0.166	1.62	7.30	0.77	0.53	4.65	3.39	6.45	loam - OM
51.7-52.5	0.090	0.97	6.90	0.48	1.04	5.31	1.26	1.01	sandy loam - light brown
52.5-55	0.117	1.98	7.10	0.63	2.21	5.43	3.41	8.54	loamy sand - OM - light brown
57.5-59	0.177	1.92	7.14	1.35	1.00	7.64	7.03	10.54	loam - OM - brown
60-62.5	0.147	1.30	7.44	0.83	2.84	5.65	2.94	7.35	sandy clay loam - OM - light brown
62.5-63.9	0.196	1.42	7.02	0.93	0.92	4.75	3.61	5.05	sandy clay loam - Fe C - light brown
63.9-65	0.147	1.73	7.24	0.68	1.24	4.64	3.22	3.54	loamy sand - Fe C - OM - light brown
67.5-70	0.107	1.46	6.57	0.67	1.13	6.24	2.67	6.67	loamy sand - OM - brown
70-71.5	0.202	1.10	7.17	1.07	1.58	5.28	3.18	4.77	clay loam - Fe C - OM - dark tan
71.5-72.5	0.170	1.38	7.98	1.55	2.21	9.08	5.82	5.82	sandy clay loam - Fe P - OM - dark tan
72.5-75	0.170	1.50	6.97	1.54	1.03	9.04	6.26	15.66	sandy loam - Fe P - OM - dark tan
77.5-80	0.085	2.09	7.36	3.14	4.41	37.17	17.82	44.55	loamy sand - Fe P - Fe C - tan
82.5-85	0.046	1.76	7.01	0.93	0.68	20.11	4.43	11.09	loamy sand - Fe P - OM - tan
85.9-87.5	0.131	1.57	7.05	0.92	1.25	7.07	3.94	6.30	sandy loam - OM - light brown
87.5-90	0.066	1.53	6.81	1.44	1.09	21.67	5.98	14.95	sand - Fe C - Fe P - dark tan
92.5-94.6	0.049	1.72	6.38	0.30	1.37	6.04	1.39	2.92	sand - tan
97.5-100	0.059	1.38	6.64	0.46	1.15	7.88	1.74	4.34	sand - tan
102.5-105	0.080	1.54	6.71	0.38	1.44	4.75	1.60	4.00	sand - tan
107.5-110	0.061	1.50	6.88	0.47	1.25	7.76	1.92	4.79	sand - light tan

Total lbs-N/Acre = 432.55

Site ID: HC-14-W, Pivot Irrigated Corn - Cored April '16

Depth	Gravimetric Water Content	Bulk Density	pH	NO3-N (ug/g)	NH4-N (ug/g)	Pore Water NO3-N (mg/L)	lbs-N/Acre-ft	lbs-N/Acre-ft in Cored Interval	Lithologic Description
0-2	0.271	1.17	6.13	6.72	3.18	24.81	21.34	42.68	loam - dark brown
2.5-4.5	0.235	1.50	6.40	0.69	2.61	2.92	2.80	5.59	clay loam - dark brown
4.5-6.7	0.240	1.21	6.47	1.59	1.04	6.61	5.22	11.48	clay - OM - brown
7.5-10	0.257	1.47	6.62	3.28	1.03	12.80	13.09	32.72	clay OM - Fe P - Fe C - brown
10-12.5	0.239	1.15	6.91	2.60	2.08	10.89	8.12	20.29	clay OM - Fe P - Fe C - brown
12.5-14.5	0.231	1.15	6.98	1.55	1.00	6.69	4.82	9.64	clay OM - Fe P - brown
15-17.2	0.246	1.13	7.01	1.78	1.07	7.26	5.50	12.11	clay OM - Fe P - brown
18.1-20	0.242	1.12	7.19	2.02	2.68	8.38	6.18	11.75	clay - OM - Fe P - brown
20-22.5	0.267	1.14	7.34	2.83	1.47	10.58	8.79	21.97	silty clay - OM - Fe P - brown
22.5-24.5	0.238	1.36	7.69	1.32	1.69	5.56	4.87	15.10	silty clay - brown
26.1-28	0.133	1.29	7.60	0.90	1.36	6.77	3.17	11.74	loam - dark brown
30.5-32.5	0.056	2.12	7.30	0.60	2.04	10.74	3.43	6.87	loamy sand - tan
33-35	0.043	1.67	7.89	0.90	2.09	20.96	4.12	8.23	sand - light tan
37.5-39.5	0.093	1.79	7.72	1.70	3.33	18.42	8.31	16.62	sand - Fe C - tan
40-40.8	0.149	1.60	7.89	2.47	2.64	16.57	10.73	8.59	sandy loam - Fe P - OM - tan
40.8-42.8	0.206	1.11	7.90	2.11	1.47	10.23	6.38	12.77	clay loam - brown
42.8-45	0.204	1.38	7.78	1.46	1.75	7.17	5.48	12.05	clay - brown
45-46.1	0.158	1.03	7.87	0.69	0.78	4.38	1.93	2.12	sandy clay - OM - light brown
46.1-47.5	0.131	1.31	7.80	1.09	0.95	8.34	3.88	5.44	sandy loam - OM - light brown
47.5-50	0.154	1.95	9.96	0.38	0.80	2.45	2.01	5.03	loamy sand - OM - light brown
50-52	0.220	1.34	9.92	0.86	1.76	3.89	3.12	6.25	loamy sand - Fe P - brown
52.5-55	0.192	1.26	9.98	0.63	2.70	3.28	2.16	5.41	clay loam- Fe P - Fe C - brown
57.5-59.5	0.063	1.30	10.02	0.29	0.77	4.54	1.01	2.02	sand - Fe P - dark tan
59.5-60.8	0.074	1.73	9.99	0.37	1.03	4.96	1.73	2.25	loamy sand - dark tan
60.8-62.5	0.154	1.51	9.96	0.46	1.90	2.97	1.89	3.21	sandy loam - dark tan
62.3-65	0.221	1.37	9.91	0.13	1.01	2.00	0.47	1.26	loamy sand - OM - dark tan
66.8-68.3	0.120	1.51	10.01	0.50	0.99	4.06	2.07	3.10	loamy sand - dark tan
72.5-75	0.112	1.55	10.05	0.42	1.44	3.76	1.78	4.45	loamy sand - OM - dark tan
78.2-80	0.054	1.54	10.04	0.46	2.04	8.52	1.93	3.47	sand - dark tan

Total lbs-N/Acre = 351.05

Site ID: HC-15-N, Pivot Irrigated Soybeans - Cored March '17

Depth	Gravimetric Water Content	Bulk Density	pH	NO3-N (ug/g)	NH4-N (ug/g)	Pore Water NO3-N (mg/L)	lbs-N/Acre-ft	lbs-N/Acre-ft in Cored Interval	Lithologic Description
4.0-5.0	0.244	1.42	7.66	7.02	240.09	28.81	27.03	27.03	clay loam - OM - black
7.5-10	0.227	1.62	6.73	5.55	3.41	24.45	24.51	61.27	clay loam - OM - dark brown
12.9-15	0.228	1.71	6.67	5.83	9.18	25.56	27.17	57.06	clay loam - OM - dark brown
18.3-20	0.229	1.46	6.71	8.29	1.66	36.13	32.98	56.06	silty clay - brown
23.7-25	0.243	1.39	6.84	4.57	1.85	18.81	17.27	22.46	silty clay - Fe C - light brown
27.5-30	0.267	1.14	6.95	2.28	4.25	8.54	7.06	17.66	silty clay - Fe C - light brown
33.4-35	0.179	1.70	6.89	1.76	3.12	9.82	8.14	13.02	sandy clay loam - brown
38.3-40	0.049	1.68	7.62	1.40	1.73	28.57	6.39	10.86	loamy sand - dark tan
43.1-45	0.081	1.64	7.22	1.34	1.94	16.58	6.00	11.40	sandy clay loam - tan
45-47.5	0.213	1.76	7.10	2.20	2.97	10.34	10.55	26.39	clay loam - brown
47.5-50	0.206	1.77	7.06	1.85	3.60	8.97	8.88	22.20	clay loam - OM - brown
51-52.5	0.135	1.31	6.76	1.51	2.85	11.22	5.40	8.10	sandy clay loam - OM - dark brown
52.5-55	0.143	1.79	7.18	1.64	3.17	11.43	8.00	20.01	sandy clay - OM - light brown
57.5-60	0.190	1.64	7.24	1.81	3.69	0.11	0.53	1.32	sandy clay - dark brown
63-65	0.095	1.61	7.03	3.47	2.58	36.53	15.20	30.40	sand - tan
68.1-70	0.048	1.60	6.71	3.67	3.60	76.24	15.93	30.26	sand - light tan
72.5-75	0.072	1.49	7.05	3.12	4.05	43.19	12.66	31.65	sand - Fe C - light tan
75.5-77.5	0.186	1.29	6.93	2.00	2.56	10.74	7.02	14.04	sandy loam - Fe C - light brown
77.5-80	0.175	1.14	7.13	3.33	2.98	19.02	10.30	25.76	silty clay - Fe C - light brown
82.5-85	0.172	1.97	6.85	3.05	2.99	17.74	16.36	40.89	silt loam - light brown
87.5-90	0.065	1.59	7.22	2.24	3.73	34.19	9.68	24.20	sandy loam - Fe C - tan

Total lbs-N/Acre = 1,167.69

Site ID: HC-15-S, Pivot Irrigated Corn - Cored April '17

Depth	Gravimetric Water Content	Bulk Density	pH	NO3-N (ug/g)	NH4-N (ug/g)	Pore Water NO3-N (mg/L)	lbs-N/Acre-ft	lbs-N/Acre-ft in Cored Interval	Lithologic Description
3.3-5	0.264	1.33	6.11	11.30	4.21	42.86	40.75	69.27	clay loam - OM - black
5-7.5	0.253	1.18	6.30	7.33	2.43	28.93	23.58	58.96	silty clay - OM - light brown
8.0-10	0.272	1.31	6.84	7.16	2.28	26.36	25.43	50.87	silty clay - OM - light brown
12.9-15	0.287	1.12	7.00	2.65	2.56	9.23	8.08	16.97	silty clay - OM - light brown
15-17.5	0.268	1.17	7.08	1.79	2.28	6.69	5.69	14.23	clay loam - OM - light brown
17.5-20	0.282	1.15	7.10	2.23	2.34	7.90	6.96	17.41	clay loam - OM - Fe C - light brown
22.7-25	0.237	1.20	6.65	2.13	2.54	8.96	6.96	16.00	clay - Fe C - dark brown
28.1-30	0.140	1.70	7.30	1.79	2.36	12.79	8.28	15.73	sandy loam - Fe C - dark brown
32.9-35	0.146	1.43	7.19	1.21	2.13	8.27	4.69	9.85	loamy sand - tan
38-40.0	0.102	1.78	7.17	1.34	3.16	13.15	6.49	12.98	sandy loam - light brown
42.5-45	0.175	1.75	7.16	1.89	2.34	10.81	8.98	22.46	sandy clay loam - Fe C - light brown
45.7-47.5	0.279	1.38	7.15	2.27	2.88	8.16	8.51	15.32	loam - Fe C - OM - brown
47.9-50	0.283	1.38	6.85	2.19	3.09	7.74	8.21	17.23	loam - Fe C - OM - brown
53.1-55	0.212	1.22	6.98	1.83	3.27	8.62	6.08	11.55	sandy clay - OM - dark brown
57.5-60	0.186	1.40	7.28	1.58	2.76	8.47	6.01	15.03	sandy clay loam - dark brown
63.1-65	0.237	1.17	7.32	1.25	3.02	5.29	3.98	7.55	sandy clay - light brown
65.9-67.5	0.166	1.21	7.22	1.56	3.50	9.37	5.12	8.19	sandy clay - light brown
67.5-70	0.237	1.19	7.09	1.77	3.51	7.47	5.73	14.33	sandy clay - light brown
77.7-80	0.264	1.18	6.80	1.63	3.05	6.18	5.22	12.00	sandy clay - Fe C - light brown
84-85	0.104	1.84	6.87	1.84	2.83	17.73	9.19	9.19	loamy sand - Fe C - tan
87.5-90	0.168	1.92	6.87	2.74	2.67	16.30	14.31	35.78	clay loam - Fe C - brown
91-93.5	0.043	1.75	7.30	1.98	2.06	46.11	9.42	23.55	loamy sand - Fe C - tan
98-100	0.033	2.50	7.19	1.58	2.04	47.83	10.77	21.54	sand - Fe C - light tan
103.6-105	0.010	2.44	7.26	1.82	2.58	179.60	12.06	16.88	sand - light tan

Total lbs-N/Acre = 902.84

Site ID: HC-16-N, Pivot Irrigated Soybeans - Cored March '17

Depth	Gravimetric Water Content	Bulk Density	pH	NO3-N (ug/g)	NH4-N (ug/g)	Pore Water NO3-N (mg/L)	lbs-N/Acre-ft	lbs-N/Acre-ft in Cored Interval	Lithologic Description
1.4-2.5	0.232	1.84	5.99	9.92	3.76	42.77	49.72	54.69	clay loam - OM - black
5.4-7.5	0.228	1.60	6.79	2.52	2.23	11.05	10.95	23.00	silty clay - OM - dark brown
11.1-12.5	0.249	1.75	7.00	1.77	1.93	7.10	8.42	11.78	silty clay - OM - dark brown
15.5-17.5	0.264	1.46	7.07	2.17	1.94	8.22	8.64	17.27	clay loam - OM - dark brown
21-22.5	0.272	1.31	7.22	3.35	1.86	12.33	11.95	17.93	clay - OM - dark brown
25.5-27.5	0.091	1.46	7.32	2.11	2.08	23.19	8.37	16.74	loamy sand - brown
28.6-30	0.107	1.93	7.31	3.06	1.92	28.47	16.05	22.47	sandy clay loam - brown
38.9-40	0.068	1.64	7.52	2.24	1.95	32.84	9.98	10.98	sand - brown
43.6-45	0.056	1.93	7.48	2.24	2.16	39.86	11.78	16.50	sand - light brown
47.5-50	0.169	1.98	7.31	2.78	2.34	16.49	14.96	37.39	sandy clay - brown
53-55	0.090	1.74	6.75	2.22	2.10	24.68	10.52	21.04	sandy loam - tan
57.8-60	0.189	1.73	6.74	2.22	2.33	11.74	10.45	23.00	sandy clay loam - dark tan
63.1-65	0.170	1.97	6.55	2.89	2.55	17.00	15.45	29.36	sandy loam - OM - light brown
67.5-70	0.116	1.92	6.50	2.64	1.93	22.74	13.75	34.37	sandy clay - light brown
72.5-75	0.132	1.61	6.76	1.40	2.92	10.65	6.17	15.41	sandy clay - light brown
77.8-80	0.098	2.19	6.64	1.25	1.91	12.76	7.42	16.33	loamy sand - tan
82.5-85	0.087	1.95	6.86	0.98	2.42	11.30	5.19	12.96	sandy loam - light brown

Total lbs-N/Acre = 996.13

Site ID: HC-16-S, Pivot Irrigated Soybeans - Cored March '17

Depth	Gravimetric Water Content	Bulk Density	pH	NO3-N (ug/g)	NH4-N (ug/g)	Pore Water NO3-N (mg/L)	lbs-N/Acre-ft	lbs-N/Acre-ft in Cored Interval	Lithologic Description
10.5-12	0.215	1.72	7.19	0.96	1.76	4.47	4.52	6.77	silty clay loam - OM - Fe P - light brown
15-17.2	0.226	1.58	7.31	0.89	1.95	3.94	3.82	8.40	silty clay loam - OM - Fe P - light brown
20-22.5	0.205	2.05	7.26	1.62	1.31	7.94	9.07	22.68	clay - light brown
25-26.8	0.150	1.87	7.31	1.73	1.29	11.52	8.77	15.78	sandy clay - black
26.8-29.3	0.097	1.70	7.41	6.03	4.71	61.84	27.80	69.49	sandy loam - black
30-32.5	0.153	2.07	7.40	1.53	1.15	10.03	8.63	21.59	sandy clay - dark brown
35.5-37.5	0.180	1.13	7.22	2.54	1.66	14.08	7.79	15.57	loam - Fe C - light brown
37.5-40	0.212	1.35	7.31	2.83	1.48	13.32	10.37	25.93	sandy clay loam - Fe C - brown
40.9-43.2	0.188	1.64	7.41	2.97	1.53	15.79	13.31	30.60	silty clay loam - Fe C - brown
43.2-45	0.186	1.87	7.24	2.17	1.99	11.68	11.07	19.93	sandy clay - Fe C - OM - brown
45-47	0.183	1.50	7.26	1.88	2.35	10.27	7.64	15.29	silty clay - OM - brown
47-49.5	0.188	1.79	7.17	1.77	1.99	9.40	8.59	21.48	silty clay - OM - brown
51-53.5	0.161	1.79	6.85	1.50	2.14	9.31	7.30	18.25	clay loam - OM - brown
55-57.5	0.168	1.27	6.88	1.67	1.75	9.95	5.74	14.36	silt loam - light brown
57.5-60	0.163	1.89	6.83	1.74	1.59	10.68	8.93	22.33	sandy loam - light brown
60-61.5	0.169	1.32	6.84	1.87	2.02	11.05	6.70	10.05	sandy clay loam - brown
61.5-63.6	0.165	1.45	6.76	1.58	2.27	9.63	6.24	13.11	loamy sand - OM - light brown
63-65	0.157	1.80	6.74	1.89	2.53	12.05	9.27	18.55	loamy sand - OM - light brown
65.5-67.5	0.087	2.10	7.13	1.18	1.17	13.55	6.70	13.40	sandy loam - dark tan
67.5-69.4	0.181	1.93	7.14	1.63	1.55	8.97	8.55	16.24	sandy clay - light brown
70.9-72.5	0.172	1.17	7.17	1.61	1.12	9.35	5.13	8.21	sandy clay loam - light brown
72.5-75	0.119	1.48	7.16	1.83	1.72	15.45	7.36	18.39	loamy sand - light brown
80-81.2	0.136	1.98	7.21	1.37	1.59	10.14	7.39	8.86	sand - light brown
85.4-87.5	0.118	1.50	7.48	1.29	1.70	10.94	5.25	11.03	loamy sand - Fe P - light brown

Total lbs-N/Acre = 629.93

Site ID: HC-17-N, Pivot Irrigated Corn - Cored November '16

Depth	Gravimetric Water Content	Bulk Density	pH	NO3-N (ug/g)	NH4-N (ug/g)	Pore Water NO3-N (mg/L)	lbs-N/Acre-ft	lbs-N/Acre-ft in Cored Interval	Lithologic Description
0-1.8	0.187	1.59	6.09	3.77	4.08	20.19	16.33	29.40	clay loam - OM - black
5-7.5	0.193	1.10	7.09	1.83	0.46	9.49	5.48	13.69	silt loam - Fe P - brown
10-12.5	0.239	1.26	7.58	0.27	0.92	1.12	0.92	2.29	silt loam - Fe P - brown
12.5-15	0.247	1.33	7.65	0.51	0.33	2.09	1.86	4.66	silt loam - Fe P - brown
15-17.1	0.249	1.23	6.95	5.12	0.81	20.57	17.15	36.02	silty clay - Fe C - light brown
17.1-19.6	0.259	1.14	7.34	1.00	3.33	3.86	3.11	7.77	silty clay - Fe P - light brown
19.6-22.5	0.137	1.81	7.53	1.15	5.50	8.35	5.64	16.35	sandy clay loam - OM - black
25-27.1	0.050	1.53	7.76	0.85	2.44	16.98	3.55	7.45	sandy loam - dark tan
31.6-32.5	0.110	1.77	7.83	1.19	1.42	10.77	5.70	5.13	sand - Fe C - tan
37.8-40	0.111	1.49	7.96	0.64	0.94	5.73	2.59	5.70	sand - light tan
41.3-43.2	0.228	1.42	7.43	0.14	1.57	0.63	0.55	1.04	clay - Fe C - tan
43.2-45	0.198	1.77	7.42	1.24	2.23	6.27	5.98	10.76	clay - brown
48.4-50	0.189	1.83	7.34	0.58	0.68	3.07	2.90	4.63	clay loam - Fe C - OM - dark brown
50.5-52.5	0.114	2.05	7.56	0.42	0.39	3.70	2.35	4.70	sandy clay loam - dark brown
57.5-60	0.094	1.78	7.53	1.10	1.62	11.61	5.32	13.29	sand - tan
62.5-65	0.083	1.45	7.31	2.05	2.00	24.68	8.06	20.14	sand - Fe C - light tan
65-67.5	0.121	1.29	6.54	0.77	3.79	6.37	2.70	6.75	sandy loam - Fe C - brown
67.5-70	0.101	1.68	6.82	0.84	3.15	8.33	3.84	9.59	sandy loam - Fe C - brown
72.5-74.4	0.182	1.69	6.94	2.34	2.09	12.89	10.75	20.42	clay loam - Fe C - dark tan
74.4-75	0.063	1.26	7.00	0.76	2.17	12.12	2.62	1.57	loamy sand - Fe C - dark tan
75-77.5	0.053	1.61	7.05	0.70	2.24	13.36	3.08	7.70	sand - Fe C - dark tan
80.5-82.5	0.052	1.64	7.05	0.85	2.14	16.57	3.82	7.64	loamy sand - dark tan
85-87.5	0.042	2.18	7.07	0.85	1.64	20.49	5.06	12.64	sand - light tan
93-95	0.179	1.59	7.27	0.74	1.46	4.15	3.21	6.41	sand - light tan

Total lbs-N/Acre = 453.87

Site ID: HC-17-S, Pivot Irrigated Soybeans - Cored November '16

Depth	Gravimetric Water Content	Bulk Density	pH	NO3-N (ug/g)	NH4-N (ug/g)	Pore Water NO3-N (mg/L)	lbs-N/Acre-ft	lbs-N/Acre-ft in Cored Interval	Lithologic Description
0-1.5	0.235	1.31	5.70	4.52	2.40	19.25	16.07	24.11	clay loam - OM - black
5.9-7.5	0.187	1.57	7.11	2.64	1.48	14.13	11.27	18.04	silty clay - Fe C - OM - light brown
11.4-12.5	0.235	1.68	7.30	1.87	1.17	7.96	8.52	9.37	silty clay - light brown
16.1-18.6	0.261	1.03	7.36	2.04	1.27	7.79	5.69	14.22	silty clay - light brown
18.6-20	0.291	1.53	7.39	1.06	1.31	3.65	4.43	6.20	clay - Fe C - light brown
20-22.5	0.256	1.47	7.37	1.26	1.14	4.92	5.05	12.63	clay - Fe C - OM - brown
26.4-27.5	0.126	1.66	7.41	1.02	0.86	8.06	4.59	5.05	sandy clay loam - black
30-32.5	0.139	1.57	7.49	1.12	0.33	8.04	4.78	11.95	sand - Fe C - dark tan
35.6-37.5	0.130	1.53	7.64	1.63	0.57	12.58	6.80	12.92	sand - dark tan
40-42.5	0.184	1.66	7.48	3.89	1.96	21.10	17.61	44.02	sandy clay loam - dark brown
47.5-50	0.203	1.70	7.42	7.56	2.15	37.25	35.02	87.56	clay loam - dark brown
50-52.5	0.078	1.60	7.58	4.46	2.13	57.04	19.48	48.70	sandy clay loam - dark tan
56.1-57.5	0.041	1.72	7.70	3.02	1.86	74.33	14.10	19.74	sand - tan
62.9-65	0.049	1.67	7.70	2.42	1.86	49.72	10.99	23.07	sand - tan
67.5-70	0.180	1.47	7.54	7.28	1.82	40.39	29.08	72.71	sandy clay loam - Fe C - brown
72.7-75	0.054	2.00	7.25	2.32	1.46	42.56	12.58	28.93	loamy sand - light brown
77.5-80	0.054	1.57	7.40	1.76	2.36	32.34	7.48	18.71	loamy sand - light brown
80-82.5	0.174	1.45	7.06	2.78	3.93	15.98	10.94	27.35	loam - Fe C - dark grey
82.5-85	0.180	1.74	6.97	2.17	4.64	12.06	10.23	25.58	loam - Fe C - dark grey
87.5-89.4	0.190	1.85	6.94	2.24	3.11	11.83	11.29	21.46	clay - Fe C - grey
89.4-90	0.089	2.15	7.03	1.74	2.30	19.62	10.17	6.10	sandy loam- tan
93.7-95	0.030	1.92	7.23	0.91	1.11	30.26	4.73	6.15	sand - Fe C - tan
97.5-100	0.169	1.74	7.11	2.71	2.15	16.01	12.80	32.01	sandy clay - Fe C - dark grey

Total lbs-N/Acre = 1,213.68

Site ID: HC-18-E, Pivot Irrigated Soybeans - Cored March '17

Depth	Gravimetric Water Content	Bulk Density	pH	NO3-N (ug/g)	NH4-N (ug/g)	Pore Water NO3-N (mg/L)	lbs-N/Acre-ft	lbs-N/Acre-ft in Cored Interval	Lithologic Description
3.0-5.0	0.184	1.46	5.83	6.35	2.77	34.52	25.22	50.43	clay loam - OM - black
9.0-10	0.201	1.78	7.20	1.89	2.31	9.39	9.16	9.16	loam - light brown
12.9-15	0.238	1.38	7.32	3.12	2.41	13.08	11.68	24.52	silty clay - light brown
18.4-20	0.260	1.45	7.42	2.66	2.45	10.26	10.53	16.84	clay - Fe C - light brown
22.9-25	0.283	1.53	7.48	2.20	2.18	7.77	9.14	19.19	silty clay - Fe C - brown
28.5-30	0.059	1.67	7.37	1.81	1.71	30.78	8.23	12.34	sandy loam - dark brown
32.5-35	0.223	1.69	7.49	4.12	2.05	18.43	18.93	47.32	silty clay - Fe C - brown
38.4-40	0.215	1.54	7.50	4.20	2.19	19.50	17.54	28.06	silty clay - Fe C - brown
42.8-45	0.170	1.68	7.46	5.18	1.95	30.45	23.63	51.98	silty clay loam - Fe C - brown
48.1-50	0.119	1.76	6.97	3.44	2.21	28.80	16.40	31.17	sandy clay - Fe C - brown
53.5-55	0.081	1.83	7.24	2.14	2.28	26.56	10.66	16.00	loamy sand - Fe C - light brown
58.3-60	0.066	1.65	7.67	1.59	3.41	24.19	7.15	12.16	sand - Fe C - tan
63.5-65	0.045	2.45	7.81	1.59	2.55	35.35	10.58	15.88	sandy loam - Fe C - tan
67.5-70	0.053	1.44	7.98	1.82	3.47	34.53	7.11	17.78	loamy sand - tan
72.5-73.9	0.047	1.68	7.94	1.48	5.02	31.14	6.76	9.47	loamy sand - tan
73.9-75	0.130	1.41	7.74	5.43	2.29	41.79	20.82	22.90	loamy sand - brown
77.5-80	0.040	2.47	7.87	2.34	1.85	58.85	15.70	39.26	gravely sand - tan
82.5-85	0.019	2.46	7.80	1.84	1.96	98.64	12.30	30.74	gravely sand - tan
88.1-90	0.027	2.57	7.92	2.01	1.71	73.15	14.03	26.66	gravely sand - tan
92.5-95	0.107	1.84	7.59	3.57	2.96	33.46	17.93	44.82	sandy loam - brown
96.2-97.5	0.322	1.44	6.58	7.81	1.81	24.30	30.65	39.84	silty clay - light brown
98.3-100	0.298	1.43	6.74	10.59	2.49	35.51	41.25	70.13	sandy clay - light brown
102.5-105	0.087	2.26	7.10	1.83	2.36	21.18	11.28	28.19	loamy sand - dark tan

Total lbs-N/Acre = 1,480.12

Site ID: HC-18-W, Pivot Irrigated Corn - Cored March '17

Depth	Gravimetric Water Content	Bulk Density	pH	NO3-N (ug/g)	NH4-N (ug/g)	Pore Water NO3-N (mg/L)	lbs-N/Acre-ft	lbs-N/Acre-ft in Cored Interval	Lithologic Description
0-2.5	0.232	1.31	6.32	9.73	3.64	41.94	34.73	86.83	clay loam - black
10-12.5	0.256	1.06	7.11	4.02	2.82	15.75	11.57	28.92	silty clay - Fe C - dark brown
15-17	0.304	1.51	7.19	2.71	2.65	8.92	11.18	22.36	clay - OM - Fe C - dark brown
20-22	0.045	2.35	6.66	1.35	1.70	30.05	8.66	17.32	sand - dark tan
25-27	0.146	2.03	6.95	2.43	2.03	16.61	13.39	26.79	loamy sand - dark tan
30-32.5	0.119	1.76	7.21	2.76	2.16	23.19	13.20	32.99	loamy sand - tan
35-37	0.092	1.91	7.21	2.90	2.02	31.49	15.07	30.14	loamy sand - tan
40-42.5	0.194	1.70	7.39	3.24	2.49	16.72	14.97	37.43	silty clay loam - Fe C - OM - light brown
42.5-45	0.126	1.88	7.23	3.76	2.59	29.79	19.23	48.07	silty clay - Fe C - OM
45.8-47.5	0.109	1.72	7.30	3.78	2.35	34.85	17.71	30.11	sandy loam - Fe C - OM - light brown
47.5-50	0.279	1.80	7.18	5.06	2.74	18.17	24.73	61.82	clay - Fe C - OM - light brown
50-52.5	0.190	1.20	7.22	5.21	2.58	27.46	17.06	42.64	silty clay - Fe C - OM - light brown
52.5-54.2	0.187	1.75	7.11	5.89	2.47	31.41	28.08	47.73	silty clay - Fe C - OM - light brown
55-57	0.111	2.17	7.27	3.78	2.21	33.90	22.28	44.56	sandy clay loam - Fe C - OM - dark tan
60.5-62	0.058	1.88	7.32	3.23	1.99	56.14	16.53	24.79	sand - Fe C - dark tan
65-67.5	0.092	1.87	6.83	3.89	1.88	42.29	19.78	49.46	loamy sand - Fe C - dark tan
70-72.5	0.032	2.40	7.13	3.17	2.05	98.01	20.72	51.80	loamy sand - Fe C - dark tan
75-77.5	0.029	2.86	7.37	2.81	1.75	96.63	21.88	54.69	sand - Fe C - dark tan
81-82.5	0.023	3.28	7.42	2.48	1.79	107.55	22.15	33.23	gravely sand - Fe C - tan
85-87	0.024	3.46	7.58	2.30	1.87	96.60	21.63	43.26	gravely sand - tan
90.8-92	0.028	3.43	7.62	2.37	1.85	84.37	22.09	26.51	sandy clay - Fe C - brown
97.5-100	0.333	1.25	7.27	8.04	1.94	24.17	27.33	68.33	sandy clay loam - OM - brown

Total lbs-N/Acre = 1,830.04

Site ID: HC-20-E, Pivot Irrigated Soybeans - Cored November '16

Depth	Gravimetric Water Content	Bulk Density	pH	NO3-N (ug/g)	NH4-N (ug/g)	Pore Water NO3-N (mg/L)	lbs-N/Acre-ft	lbs-N/Acre-ft in Cored Interval	Lithologic Description
3.4-5	0.241	1.44	6.50	6.30	3.68	26.15	24.67	39.47	clay loam - OM - black
7.1-9.1	0.176	1.43	7.26	1.48	2.11	8.38	5.77	11.54	silty clay loam - OM - dark brown
9.1-10	0.223	1.41	7.34	3.10	1.68	13.91	11.88	10.69	clay loam - Fe C - OM - dark brown
12.9-15	0.249	1.55	7.31	6.65	1.89	26.73	28.02	58.84	clay loam - Fe C - dark brown
17.5-20	0.247	1.63	7.36	7.94	2.02	32.08	35.09	87.72	silty clay - Fe C - OM - dark brown
23.7-25	0.153	1.92	7.04	5.62	1.65	36.76	29.38	38.19	sandy clay loam - dark brown
31.5-33.4	0.269	1.44	7.33	1.22	1.95	4.55	4.81	9.13	sandy loam - light brown
33.4-35	0.255	1.45	7.34	1.06	1.79	4.14	4.16	6.66	sandy clay - Fe C - OM - light brown
35-37.5	0.089	2.15	7.43	1.35	1.92	15.29	7.92	19.81	clay loam - Fe C - OM - light brown
37.5-40	0.184	1.66	7.53	1.27	1.80	6.87	5.74	14.34	clay - Fe C - OM - light brown
42.5-45	0.089	2.15	7.73	1.28	1.88	14.44	7.49	18.71	sandy loam - Fe C - tan
47.8-50	0.184	1.66	7.81	0.72	1.74	3.89	3.24	7.14	loamy sand - light brown
53-55	0.153	1.92	7.62	1.07	1.77	6.99	5.59	11.18	sandy clay loam - OM - brown
57.5-58.4	0.078	1.78	7.71	1.12	1.73	14.26	5.41	4.87	loamy sand - tan
58.4-60	0.084	2.15	7.60	1.62	2.33	19.22	9.49	15.18	loam - dark tan
62.5-65	0.061	2.18	7.60	1.80	4.40	29.50	10.69	26.72	silty clay loam - Fe C - grey
66.5-67.5	0.089	2.15	7.18	1.75	4.09	19.73	10.22	10.22	silty clay loam - Fe C - OM - grey
67.5-70	0.089	2.15	7.34	1.40	1.99	15.82	8.20	20.50	sandy loam - Fe C - grey
72.5-74.4	0.193	1.10	7.16	1.56	2.43	8.06	4.65	8.84	silt loam - Fe C - OM - light brown
74.4-77.5	0.261	1.03	7.12	3.29	2.80	12.60	9.20	28.51	silty clay - Fe C - OM - light brown
77.5-79.6	0.089	2.15	7.19	3.72	2.35	42.04	21.79	45.76	sandy loam - Fe P - OM - light brown
82.5-85	0.078	1.78	7.42	1.90	1.36	24.24	9.20	22.99	loamy sand - Fe C - tan
88.1-90	0.161	1.45	7.47	2.43	1.40	15.06	9.60	18.25	sand - Fe C - tan
92.5-95	0.014	2.23	7.28	1.73	1.21	127.61	10.48	26.20	gravely sand - Fe C - Fe P - tan
97.5-100	0.015	2.26	7.63	1.00	1.42	67.14	6.16	15.40	gravely sand - light tan
103.7-105	0.045	2.18	7.63	0.99	1.75	22.07	5.85	7.61	gravely sand - Fe C - light tan

Total lbs-N/Acre = 1,218.90

Site ID: HC-20-W, Pivot Irrigated Soybeans - Cored November '16

Depth	Gravimetric Water Content	Bulk Density	pH	NO3-N (ug/g)	NH4-N (ug/g)	Pore Water NO3-N (mg/L)	lbs-N/Acre-ft	lbs-N/Acre-ft in Cored Interval	Lithologic Description
1-2.5	0.224	1.23	6.03	12.95	8.56	57.86	43.37	65.06	clay loam- OM - dark brown
2.5-5	0.223	1.22	6.73	8.83	2.28	39.63	29.33	73.33	clay loam - Fe C - dark brown
8.6-10.7	0.269	1.44	7.03	2.94	1.49	10.93	11.55	24.26	silty clay loam - OM - Fe C - dark brown
10.7-13.1	0.231	1.69	7.20	3.15	1.77	13.59	14.46	34.70	clay loam - Fe C - dark brown
13.1-15	0.240	1.16	7.25	3.30	1.57	13.72	10.43	19.82	clay loam - Fe C - dark brown
18.1-20	0.264	1.49	7.13	2.46	1.69	9.31	9.99	18.99	clay - OM - light brown
20.9-22.5	0.132	1.31	7.26	0.75	2.03	5.65	2.65	4.24	sandy clay - dark brown
22.5-25	0.078	1.78	7.23	1.24	3.33	15.82	6.00	15.01	loamy sand - brown
27.9-30	0.107	1.74	7.15	0.51	2.21	4.77	2.41	5.06	sand - Fe P - tan
32.5-35	0.177	1.59	7.15	0.77	2.05	4.35	3.33	8.32	clay loam - light brown
38.4-40	0.208	1.66	7.14	1.04	2.86	5.02	4.71	7.54	clay loam - OM - light brown
43.6-45	0.169	1.89	7.24	0.70	2.00	4.14	3.60	5.03	sandy clay - light brown
52.8-55	0.153	1.92	7.68	0.76	2.03	4.99	3.99	8.77	sandy clay loam - light brown
58.2-60	0.041	1.58	7.73	0.73	1.48	17.76	3.13	5.64	sand - dark tan
63.9-65	0.161	1.45	7.72	0.23	1.82	1.43	0.91	1.00	sand - dark tan
67.9-70	0.099	1.79	7.66	0.13	1.49	1.26	0.61	1.28	sandy clay - tan
72.5-75	0.118	1.87	7.60	0.45	1.86	3.80	2.27	5.68	sandy clay loam - tan
77.5-80	0.061	1.30	7.59	0.50	1.95	8.15	1.75	4.38	sand - light tan
83.6-85	0.057	1.80	7.25	0.13	1.01	2.18	0.61	0.86	sand - dark tan
87.5-90	0.032	1.49	7.53	0.26	1.37	8.02	1.05	2.62	sand - dark tan
92.5-95	0.019	1.57	7.56	0.13	1.70	6.58	0.53	1.34	sand - Fe C - tan
97.5-100	0.038	1.54	7.74	0.64	1.26	16.95	2.70	6.75	gravely loamy sand - Fe C - tan
102.5-105	0.016	1.69	7.73	0.37	1.43	23.54	1.69	4.22	gravely sand - tan
107.5-110	0.014	2.23	7.87	0.77	1.47	56.77	4.66	11.66	gravely sand - tan
112.9-115	0.030	2.06	7.51	0.52	1.69	17.27	2.92	6.14	gravely sand -Fe C - tan

Total lbs-N/Acre = 570.94

Pesticide residues occurring at or above the detection limits. Compounds not detected include *acetochlor, alachlor, butylate, chlorthalonil, cyanazine, dimethenamid, EPTC, metribuzin, norflurazon, prometon, propachlor, propazine, simazine, telfluthrin, and trifluralin.*

Sample_ID	Atrazine	DEA	DIA	Metolachlor	Pendamethalin	Batch	%Butachlor	%Terbutylazine	Analysis Date
Detection Limits (ng/g)	0.1	0.1	0.1	0.1	0.1				
HC1E 10-12.5	0.33					W17018	136	125	4/10/2017
HC1E 31.7-32.5	0.28					W17018	144	132	4/10/2017
HC1E 47.5-50						W17018	145	131	4/10/2017
HC1E 65-67.5						W17018	143	132	4/10/2017
HC1E 78.7-80						W17018	144	134	4/10/2017
HC1E 102.9-105						W17018	147	134	4/10/2017
HC1W 15-17.5	0.26					W17067	134	123	4/10/2017
HC1W 30-32.5						W17067	128	120	4/10/2017
HC1W 45.9-49.3						W17067	127	116	4/10/2017
HC1W 67.5-70						W17067	131	126	4/10/2017
HC1W 107.5-110						W17067	123	118	4/10/2017
HC2 5-7.5	0.29					W16177	81	114	4/4/2017
HC2 37.5-40.3						W16538	113	112	4/7/2017
HC2 51.5-52.5						W16538	115	114	4/7/2017
HC2 62.5-65						W16538	117	117	4/7/2017
HC3A 0-2.2	2.41					W16465	80	107	4/4/2017
HC3A 13.5-17.5	0.28					W16465	86	118	4/4/2017
HC3A 25.3-27.5						W16538	111	112	4/7/2017
HC3A 37.5-40						W16538	117	115	4/7/2017
HC3A 53.5-55						W16538	110	110	4/7/2017
HC3B 1.9-5						W16538	115	111	4/7/2017
HC3B 14.1-15						W16538	113	114	4/7/2017
HC3B 28.9-31.7						W16538	118	114	4/7/2017
HC3B 45-46						W16538	118	115	4/7/2017
HC4 7.5-10						W17018	135	123	4/10/2017
HC4 20-22.2						W17018	130	116	4/10/2017

Pesticide residues occurring at or above the detection limits. Compounds not detected include *acetochlor, alachlor, butylate, chlorthalonil, cyanazine, dimethenamid, EPTC, metribuzin, norflurazon, prometon, propachlor, propazine, simazine, telfluthrin, and trifluralin.*

Sample_ID	Atrazine	DEA	DIA	Metolachlor	Pendamethalin	Batch	%Butachlor	%Terbutylazine	Analysis Date
Detection Limits (ng/g)	0.1	0.1	0.1	0.1	0.1				
HC4 30-32.9						W17018	145	128	4/10/2017
HC4 42.5-45						W17018	140	129	4/10/2017
HC4 55.3-57.9						W17018	145	131	4/10/2017
HC5 5-7.5						W16538	105	103	4/7/2017
HC5 17.5-20						W16538	104	102	4/7/2017
HC5 25.8-27.5						W16538	117	118	4/7/2017
HC5 45-46.7						W16538	115	114	4/7/2017
HC6 0-2						W16465	78	108	4/4/2017
HC6 12.2-13.8						W16465	82	110	4/4/2017
HC6 26.2-27.5						W16465	85	116	4/4/2017
HC6 30.3-31.6	0.29					W16465	79	109	4/4/2017
HC6 42.9-45						W16465	83	111	4/4/2017
HC6 55.5-57.5						W16465	79	111	4/4/2017
HC7 7.5-10						W16538	112	111	4/7/2017
HC7 19.7-22.5						W16538	133	130	4/7/2017
HC7 30-32.5						W16538	114	114	4/7/2017
HC7 45-47.5						W16538	104	105	4/7/2017
HC7 62.5-64.7						W16538	114	114	4/7/2017
HC8 1.9-5						W16538	110	110	4/7/2017
HC8 15-17.5						W17018	129	119	4/10/2017
HC8 26.1-27.5						W17018	139	128	4/10/2017
HC8 36.8-40						W17018	133	125	4/10/2017
HC8 70-72.5						W16465	88	118	4/4/2017
HC8 72.5-75						W17018	142	132	4/10/2017
HC9A 0.8-3.3	2.00	2.36		0.24		W17353	126	127	4/9/2018
HC9A 30-31.2						W17353	69	130	4/9/2018

Pesticide residues occurring at or above the detection limits. Compounds not detected include *acetochlor, alachlor, butylate, chlorthalonil, cyanazine, dimethenamid, EPTC, metribuzin, norflurazon, prometon, propachlor, propazine, simazine, telfluthrin, and trifluralin.*

Sample_ID	Atrazine	DEA	DIA	Metolachlor	Pendamethalin	Batch	%Butachlor	%Terbutylazine	Analysis Date
Detection Limits (ng/g)	0.1	0.1	0.1	0.1	0.1				
HC9A 52.5-55						W17353	99	121	4/9/2018
HC9A 65-67.5						W17353	104	132	4/9/2018
HC9B 5.0-7						W17353	113	125	4/9/2018
HC9B 15-16.7						W17353	110	124	4/9/2018
HC9B 35-37						W17353	113	131	4/9/2018
HC9B 55-57						W17353	112	130	4/9/2018
HC10-N 0-0.8	2.27	0.50	1.05	20.19		W17067	139	122	4/10/2017
HC10-N 17.1-20	0.30					W17067	143	126	4/10/2017
HC10-N 45-47.5	0.40					W17067	140	123	4/10/2017
HC10-N 65-67.5	0.56					W17067	134	124	4/10/2017
HC10-N 67-5-70	0.52					W17067	136	123	4/10/2017
HC10-S 1.7-5	0.34					W17018	142	127	4/10/2017
HC10-S 15-17.5	0.29					W17018	141	126	4/10/2017
HC10-S 40-42.2						W17018	137	125	4/10/2017
HC10-S 56.7-59.2						W17018	142	129	4/10/2017
HC10-S 80-82.5						W17018	140	127	4/10/2017
HC11-1 20.5-22.5	0.30					W16177	79	114	4/4/2017
HC11-1 32.5-35						W16177	76	111	4/4/2017
HC11-1 50-51.5						W16177	78	111	4/4/2017
HC11-1 67.5-70						W16177	75	110	4/4/2017
HC11-1 7.5-9.5	0.46					W16177	73	106	4/4/2017
HC11-1 78-80						W16177	75	110	4/4/2017
HC11-1 101-102.5						W16177	77	113	4/4/2017
HC11-2 8.0-10	0.32					W16177	77	108	4/4/2017
HC11-2 15.0-17.0	0.32					W16177	83	112	4/4/2017
HC11-2 17.5-18.7						W16177	78	110	4/4/2017

Pesticide residues occurring at or above the detection limits. Compounds not detected include *acetochlor, alachlor, butylate, chlorthalonil, cyanazine, dimethenamid, EPTC, metribuzin, norflurazon, prometon, propachlor, propazine, simazine, telfluthrin, and trifluralin.*

Sample_ID	Atrazine	DEA	DIA	Metolachlor	Pendamehalin	Batch	%Butachlor	%Terbutylazine	Analysis Date
Detection Limits (ng/g)	0.1	0.1	0.1	0.1	0.1				
HC11-2 32-33.3						W16177	82	115	4/4/2017
HC11-2 47.5-50						W16177	77	110	4/4/2017
HC11-2 67.5-69.5						W16177	78	113	4/4/2017
HC11-2 92.5-94						W16177	77	115	4/4/2017
HC12-E 3.4-5	1.01	0.57				W17256	129	128	4/9/2018
HC12-E 15.8-17.5						W17256	126	127	4/9/2018
HC12-E 32.5-35						W17256	106	131	4/9/2018
HC12-E 53.7-55						W17256	108	134	4/9/2018
HC12-E 72.5-75						W17256	112	133	4/9/2018
HC12-W 13.5-15	0.47		0.41			W17149	146	112	5/12/2017
HC12-W 33.5-35						W17149	160	126	5/12/2017
HC12-W 56.3-57.5						W17149	161	117	5/12/2017
HC12-W 67.5-70						W17149	160	130	5/12/2017
HC12-W 85-87.5						W17256	106	134	4/9/2018
HC12-W 108.7-110						W17256	109	135	4/9/2018
HC13-NE 10-11.2						W16177	82	112	4/4/2017
HC13-NE 41.6-43.6						W16177	64	105	4/4/2017
HC13-NE 20-22.6						W16177	80	110	4/4/2017
HC13-NE 60.9-61.9						W16177	73	113	4/4/2017
HC13-NE 73.1-74.4						W16177	72	110	4/4/2017
HC13-NE 100-101.7						W16177	73	107	4/4/2017
HC13-SW 5-7.2						W17067	124	113	4/10/2017
HC13-SW 17.5-20						W17067	113	118	4/10/2017
HC13-SW 30-32.5						W17067	117	116	4/10/2017
HC13-SW 45-47.5						W17067	135	129	4/10/2017
HC13-SW 66.4-68.9						W17067	130	123	4/10/2017
HC13-SW 77.5-80						W17067	125	124	4/10/2017

Pesticide residues occurring at or above the detection limits. Compounds not detected include *acetochlor, alachlor, butylate, chlorthalonil, cyanazine, dimethenamid, EPTC, metribuzin, norflurazon, prometon, propachlor, propazine, simazine, telfluthrin, and trifluralin.*

Sample_ID	Atrazine	DEA	DIA	Metolachlor	Pendamethalin	Batch	%Butachlor	%Terbutylazine	Analysis Date
Detection Limits (ng/g)	0.1	0.1	0.1	0.1	0.1				
HC14-E 2.1-4.5	0.28					W16465	73	96	4/4/2017
HC14-E 17.9-20	0.31					W16465	84	113	4/4/2017
HC14-E 37.5-39.3						W16465	83	113	4/4/2017
HC14-E 51.7-52.5						W16465	82	114	4/4/2017
HC14-E 62.5-63.9						W16465	85	115	4/4/2017
HC14-E 72.5-75						W16465	86	117	4/4/2017
HC14-E 102.5-105						W16465	85	117	4/4/2017
HC14-W 2.5-4.5	0.40					W16177	84	115	4/4/2017
HC14-W 15-17.2						W16177	81	110	4/4/2017
HC14-W 22.5-24.5						W16465	81	109	4/4/2017
HC14-W 40-40.8						W16465	83	116	4/4/2017
HC14-W 47.5-50						W16465	80	113	4/4/2017
HC14-W 60.8-62.5						W16465	83	116	4/4/2017
HC15-N 12.9-15	0.47			0.37		W17256	123	127	4/9/2018
HC15-N 38.3-40						W17256	109	134	4/9/2018
HC15-N 72.5-75						W17353	120	133	4/9/2018
HC15-S 12.9-15						W17256	109	132	4/9/2018
HC15-S 32.9-35	0.36					W17256	131	133	4/9/2018
HC15-S 53.1-55						W17256	106	130	4/9/2018
HC15-S 77.7-80						W17353	112	134	4/9/2018
HC15-S 91-93.5						W17353	102	133	4/9/2018
HC16-N 11.1-12.5						W17256	111	124	4/9/2018
HC16-N 38.9-40						W17256	124	134	4/9/2018
HC16-N 63.1-65						W17256	112	132	4/9/2018
HC16-S 25-26.8						W17353	111	135	4/9/2018
HC-16-S 40.9-43.2						W17478	99	130	4/9/2018

Pesticide residues occurring at or above the detection limits. Compounds not detected include *acetochlor, alachlor, butylate, chlorthalonil, cyanazine, dimethenamid, EPTC, metribuzin, norflurazon, prometon, propachlor, propazine, simazine, telfluthrin, and trifluralin.*

Sample_ID	Atrazine	DEA	DIA	Metolachlor	Pendamethalin	Batch	%Butachlor	%Terbutylazine	Analysis Date
Detection Limits (ng/g)	0.1	0.1	0.1	0.1	0.1				
HC16-S 55-57.5						W17478	100	131	4/9/2018
HC16-S 65.5-67.5						W17478	108	132	4/9/2018
HC16-S 85.4-87.5						W17478	100	131	4/9/2018
HC17-N 5-7.5						W17067	139	125	4/10/2017
HC17-N 19.6-22.5						W17067	136	121	4/10/2017
HC17-N 43.2-45						W17149	146	130	5/12/2017
HC17-N 65-67.5						W17149	159	136	5/12/2017
HC17-N 80.5-82.5						W17149	160	133	5/12/2017
HC17-S 0-1.5	2.67	1.01	0.65	15.36	9.49	W17067	141	122	4/10/2017
HC17-S 20-22.5						W17067	134	120	4/10/2017
HC17-S 50-52.5						W17149	163	134	5/12/2017
HC17-S 77.5-80				0.30		W17149	166	134	5/12/2017
HC18-E 18.4-20						W17256	102	127	4/9/2018
HC18-E 42.8-45						W17256	113	127	4/9/2018
HC18-E 58.3-60						W17256	120	134	4/9/2018
HC18-E 77.5-80						W17256	114	136	4/9/2018
HC18-E 98.3-100						W17256	108	124	4/9/2018
HC18-W 0-2.5	0.68	0.49		1.34		W17353	122	127	4/9/2018
HC18-W 30-32.5						W17353	113	132	4/9/2018
HC18-W 47.5-50						W17353	122	131	4/9/2018
HC18-W 65-67.5						W17353	115	129	4/9/2018
HC18-W 85-87						W17353	104	132	4/9/2018
HC20-E 35-37.5						W17149	179	143	5/12/2017
HC20-E 57.5-58.4						W17149	166	130	5/12/2017
HC20-E 72.5-74.4						W17149	164	130	5/12/2017
HC20-E 92.5-95						W17149	165	132	5/12/2017

Pesticide residues occurring at or above the detection limits. Compounds not detected include *acetochlor, alachlor, butylate, chlorthalonil, cyanazine, dimethenamid, EPTC, metribuzin, norflurazon, prometon, propachlor, propazine, simazine, telfluthrin, and trifluralin.*

Sample_ID	Atrazine	DEA	DIA	Metolachlor	Pendamethalin	Batch	%Butachlor	%Terbutylazine	Analysis Date
Detection Limits (ng/g)	0.1	0.1	0.1	0.1	0.1				
HC20-W 10.7-12.9	1.02			0.38		W17149	162	130	5/12/2017
HC20-W 12.9-15	0.38					W17149	117	93	5/12/2017
HC20-W 27.9-30	0.33			0.27		W17149	166	134	5/12/2017
HC20-W 58.2-60				0.19		W17149	171	136	5/12/2017
HC20-W 83.6-85				0.39		W17149	165	134	5/12/2017
HC20-W 107.5-110	0.39					W17149	169	137	5/12/2017

Appendix B: Nitrate and Water Isotopes, Chloride and Groundwater Ages

Nitrate and Water Isotope Results

Sample_ID	Collection Date	NO3-N (ug/g)	$\delta^{15}\text{N-NO}_3$ (‰)	$\delta^{18}\text{O-NO}_3$ (‰)	Analysis Date	Batch
HC-1-W 15-17.5	9/5/2018	2.45	2.95	2.72	9/14/2018	W18645
HC-1-W 30-32.5	9/5/2018	1.99	6.93	0.73	9/14/2018	W18645
HC-1-W 45.9-49.3	9/5/2018	1.05	-2.07	3.17	9/14/2018	W18645
HC-1-W 67.5-70	9/5/2018	0.44	NM	NM	9/14/2018	W18645
HC-1-W 107.5-110	9/5/2018	1.2	4.93	1.82	9/14/2018	W18645
HC-2 37.5-40.3	9/5/2018	1.1	0.68	0.07	9/14/2018	W18645
HC-2 51.5-52.5	9/5/2018	0.74	0.78	11.42	9/14/2018	W18645
HC-2 62.5-65	9/5/2018	1.07	4.65	10.60	9/14/2018	W18645
HC-3A 53.5-55	9/5/2018	3.64	5.64	-0.56	9/14/2018	W18645
HC-3B 1.9-5	9/5/2018	0.48	NM	NM	9/14/2018	W18645
HC-3B 45-46	9/5/2018	0.59	-0.57	7.14	9/14/2018	W18645
HC-4 7.5-10	9/5/2018	0.78	0.23	5.44	9/14/2018	W18645
HC-4 20-22.2	9/5/2018	0.51	0.46	10.37	9/14/2018	W18645
HC-4 42.5-45	9/5/2018	0.48	NM	NM	9/14/2018	W18645
HC-5 5-7.5	9/5/2018	0.84	1.57	1.00	9/14/2018	W18645
HC-5 17.5-20	9/5/2018	3.55	21.81	9.08	9/14/2018	W18645
HC-5 25.8-27.5	9/5/2018	0.63	1.18	5.02	9/14/2018	W18645
HC-5 45-46.7	9/5/2018	0.85	0.68	-2.48	9/14/2018	W18645
HC-7 7.5-10	9/5/2018	1.83	15.80	0.15	9/14/2018	W18645
HC-7 19.7-22.5	9/5/2018	1.41	4.90	-3.68	9/15/2018	W18646
HC-7 30-32.5	9/5/2018	1.45	15.27	3.46	9/15/2018	W18646
HC-8 1.9-5	9/5/2018	0.86	12.47	-1.02	9/15/2018	W18646
HC-8 26.1-27.5	9/5/2018	3.15	-0.79	-9.12	9/15/2018	W18646
HC-8 36.8-40	9/5/2018	2.89	4.91	-5.89	9/15/2018	W18646
HC-8 72.5-75	9/5/2018	1.46	-1.84	-2.96	9/15/2018	W18646
HC-10-N 0-0.8	9/5/2018	5.56	-1.04	-3.74	9/15/2018	W18646
HC-10-N 45-47.5	9/5/2018	1.03	35.73	-6.86	9/15/2018	W18646
HC-10-N 65-67.5	9/5/2018	0.47	NM	NM	9/15/2018	W18646
HC-10-N 67.5-70	9/5/2018	0.52	-9.35	5.50	9/15/2018	W18646
HC-10-S 1.7-5	9/5/2018	0.62	-17.92	-2.22	9/15/2018	W18646
HC-10-S 40-42.2	9/5/2018	1.57	-0.20	2.31	9/15/2018	W18646
HC-13-S 5-7.2	9/5/2018	6.27	11.86	-1.84	9/15/2018	W18646
HC-14-E 37.5-39.3	9/5/2018	0.73	3.14	8.51	9/15/2018	W18646

HC-14-W 40-40.8	9/5/2018	2.47	7.65	0.26	9/15/2018	W18646
HC-16-S 40.9-43.2	9/5/2018	2.97	-6.06	-6.22	9/15/2018	W18646
HC-16-S 55-57.2	9/5/2018	1.67	-6.32	-3.36	9/15/2018	W18646
HC-16-S 85.4-87.5	9/5/2018	1.29	-8.59	-2.88	9/15/2018	W18646
HC-17-S 0-1.5	9/5/2018	4.52	-2.94	-8.36	9/15/2018	W18646
HC-17-S 20-22.5	9/5/2018	1.26	-10.01	-6.25	9/15/2018	W18646

Appendix C: Travel Time Estimates for Nitrate

Table S1: The description of site land use and soil samples from 32 sites at Hasting, NE.

No.	Site	Land-use (9 different)	Latitude	Longitude	Elevation (m)
1	HC-1-E	Gravity-Irrigated Corn	40.60267	-98.4335	581.409
2	HC-1-W	Gravity-Irrigated Corn	40.60261	-98.43758	581.847
3	HC-2	Dryland Corn	40.61027	-98.40218	579.003
4	HC-3-A	Residential	40.60411	-98.46496	593.151
5	HC-3-B	Residential	40.59739	-98.46495	590.085
6	HC-4	City Park	40.59774	-98.39085	579.765
7	HC-5	Residential	40.63978	-98.39809	585.708
8	HC-6	Residential	40.59329	-98.41002	580.251
9	HC-7	Barnyard	40.60844	-98.45829	593.196
10	HC-8	Barnyard	40.59695	-98.4534	587.901
11	HC-9-A	Pivot-Irrigated Soybeans	40.58182	-98.46554	586.797
12	HC-9-B	Pivot-Irrigated Soybeans	40.57668	-98.46159	588.567
13	HC-10-N	Pivot-Irrigated Soybeans	40.66732	-98.4226	588.423
14	HC-10-S	Pivot-Irrigated Soybeans	40.66454	-98.42262	587.016
15	HC-11-E	Pivot-Irrigated Corn	40.66577	-98.5556	605.328
16	HC-11-W	Pivot-Irrigated Corn	40.66579	-98.5624	607.956
17	HC-12-E	Drip/Gravity-Irrigated Corn	40.61046	-98.47262	589.074
18	HC-12-W	Drip/Gravity-Irrigated Corn	40.61049	-98.47663	592.653
19	HC-13-NE	Pivot-Irrigated Corn	40.64919	-98.55736	605.418
20	HC-13-SW	Pivot-Irrigated Soybeans	40.64668	-98.56088	606.888
21	HC-14-E	Pivot-Irrigated Soybeans	40.65165	-98.46582	596.985
22	HC-14-W	Pivot-Irrigated Corn	40.65158	-98.46003	593.451
23	HC-15-N	Pivot-Irrigated Soybeans	40.62398	-98.46234	593.202
24	HC-15-S	Pivot-Irrigated Corn	40.6204	-98.46415	588.867
25	HC-16-N	Pivot-Irrigated Soybeans	40.5805	-98.47578	590.94
26	HC-16-S	Pivot-Irrigated Corn	40.57771	-98.47573	585.423
27	HC-17-N	Pivot-Irrigated Corn	40.68229	-98.44398	594
28	HC-17-S	Pivot-Irrigated Soybeans	40.67871	-98.44393	594.261
29	HC-18-E	Pivot-Irrigated Soybeans	40.62844	-98.39469	576.834
30	HC-18-W	Pivot-Irrigated Corn	40.62771	-98.39833	576.102
31	HC-20-E	Pivot-Irrigated Soybeans	40.62063	-98.43282	585.666
32	HC-20-W	Pivot-Irrigated Soybeans	40.62053	-98.43664	587.646

Table S2: The default nitrogen cycle parameters for the RZWQM2 model (Shaffer et al., 2000)

		Parameter	Unit	Default Baseline
1		Slow residue pool	-	8
2		Fast residue pool	-	80
3		Fast humus pool	-	8
4	C:N Ratio	Intermediate humus pool	-	10
5		Slow humus pool	-	12
6		Aerobic heterotrophs (decomposers)	-	8
7		Autotrophs (nitrifiers)	-	8
8		Anaerobic heterotrophs (denitrifiers)	-	8
9	Transformation coefficient	Slow residue pool to Intermediate humus pool	-	0.3
10		Fast residue pool to Fast humus pool	-	0.6
11		Fast humus pool to Intermediate humus pool	-	0.6
12		Intermediate humus pool to Slow humus pool	-	0.7
13	Organic matter decay coefficient	Slow residue pool	s day ⁻¹	1.67E-07
14		Fast residue pool	s day ⁻¹	8.14E-06
15		Fast humus pool	s day ⁻¹	2.50E-07
16		Intermediate humus pool	s day ⁻¹	5.00E-08
17		Slow humus pool	s day ⁻¹	4.50E-10
18	Reaction rate coefficient	NH ₃ Volatilization	s day ⁻¹	1000
19		Nitrification	s day ⁻¹	1.00E-09
20		Denitrification	s day ⁻¹	1.00E-13
21		Hydrolysis of urea	s day ⁻¹	2.50E-4
22	Activation energy coefficient	Aerobic heterotrophs (decomposers)	-	88.6
23		Autotrophs (nitrifiers)	-	61
24		Anaerobic heterotrophs (denitrifiers)	-	63.1
25		Oxygen limitation	-	0.05
26	Assimilation factor	Converting decayed OM to assimilated biomass	-	0.267
27		Converting nitrified NH ₄ ⁺ to Autotroph biomass	-	0.010
28		Efficiency factor for denitrifiers nitrogen uptake	-	0.133
29		Denitrification rate converting to anaerobic OM decay rate	-	0.10
30	Population conversion factor	Aerobic heterotrophs (decomposers)	#orgs g ⁻¹ soil	950
31		Autotrophs (nitrifiers)	#orgs g ⁻¹ soil	9500
32		Anaerobic heterotrophs (denitrifiers)	#orgs g ⁻¹ soil	9500
33	Death rate coefficient	Aerobic heterotrophs (decomposers)	s day ⁻¹	5.00E-035
34		Autotrophs (nitrifiers)	s day ⁻¹	4.77E-40
35		Anaerobic heterotrophs (denitrifiers)	s day ⁻¹	3.40E-33

Table S3: Site specific agricultural practices and land use information

Year	Land Use	Date	Planting			Harvesting Date	N Fertilizer Application (kg ha ⁻¹) [†]
			Density (seeds/acre)	Row Spacing (cm)	Depth (cm)		
HC 1 East – Gravity Irrigated Site							
2011	Soybean	13 May	160,000	38	4	13 Oct	100
2012	Corn	25 Apr	36,000	75	5	5 Oct	170
2013	Corn	25 Apr	36,000	75	5	5 Oct	170
2014	Soybean	13 May	160,000	38	4	13 Oct	100
2015	Corn	25 Apr	36,000	75	5	5 Oct	170
2016	Corn	25 Apr	36,000	75	5	5 Oct	170
HC 14 West – Pivot Irrigated Site							
2011	Corn	25 Apr	36,000	75	5	5 Oct	170
2012	Corn	25 Apr	36,000	75	5	5 Oct	170
2013	Corn	25 Apr	36,000	75	5	5 Oct	170
2014	Corn	25 Apr	36,000	75	5	5 Oct	170
2015	Corn	25 Apr	36,000	75	5	5 Oct	170
2016	Corn	25 Apr	36,000	75	5	5 Oct	170
HC 2 – Dryland (non-irrigated site)							
2011	Soybean	13 Apr	160,000	38	4	13 Oct	90
2012	Corn	25 Apr	36,000	75	5	5 Oct	90
2013	Corn	25 Apr	36,000	75	5	5 Oct	90
2014	Corn	25 Apr	36,000	75	5	5 Oct	90
2015	Soybean	13 Apr	160,000	38	4	13 Oct	90
2016	Corn	25 Apr	36,000	75	5	5 Oct	90

[†]Shapiro et al., 2006 , Ping et al., 2008

Table S4: Laboratory measured soil properties and saturated hydraulic conductivity of the soil cores.

Core ID	Depth (ft)	Soil Texture	Soil Type	Class (UCSC)*	Sand %	Silt %	Clay %	Bulk density (gm//L)	K _{sat} (m/day)	K _{sat} (µm/sec)	Range (µm/sec) (NRCS)**
HC1 W	12.5-15	clay - light brown	clay	1				1.50	0.048	0.6	0.42-1.41
HC 1 E	32.5-35	loamy sand – tan	loamy sand	5	81.6	14.9	3.5	1.15	1.232	14.3	42.34-141.14
HC 1 E	51.4-52.5	clay - Fe P - light brown	clay	1	45.09	32.59	22.31	1.79	0.148	1.7	0.42-1.41
HC2	5 - 7.5	silt loam - Fe P - brown	silt loam	3	26.0	60.5	13.5	0.97	4.392	50.8	4.23-14.11
HC 2	7.5 -9	silt loam - light brown	silt loam	3	22.8	56.8	20.4	1.06	0.010	0.1	4.23-14.11
HC 2	27.6 -30	sandy loam - dark brown	sandy loam	5	58.8	24.1	17.1	1.54	0.339	3.9	42.34-141.14
HC 3 A	7.5-9.2	loam – tan	loam	3	18.7	14.4	67.0	1.08	0.150	1.7	4.23-14.11
HC 3 B	1.9-5	silt - light brown	silt	3				0.99	0.270	3.1	4.23-14.11
HC 3 B	12.5-14.1	clay - dark brown	clay	1				1.21	1.074	12.4	0.42-1.41
HC 4	2.5-5	clay loam – brown	clay loam	1	25.6	45.3	29.1	1.23	0.499	5.8	0.42-1.41
HC 5	20- 22.5	clay loam – brown	clay loam	1	48.0	38.9	13.1	1.41	0.094	1.1	0.42-1.41
HC 5	32.5-35	loam - Fe P - light brown	loam	3	58.2	21.4	20.4	1.80	0.360	4.2	4.23-14.11
HC 6	5.9 - 7.5	silt loam - light tan	silt loam	3	11.2	39.7	49.1	1.54	0.253	2.9	4.23-14.11
HC 6	37.5-40	sand – tan	sand	6	74.6	13.4	12.0	1.34	2.048	23.7	42.34-141.14
HC 7	19.7-22.5	loam - light brown	loam	3				1.09	0.615	7.1	4.23-14.11
HC 9 B	20-22	sandy clay loam - dark brown	sandy clay loam	4				1.51	1.149	13.3	1.41-4.23
HC 9 B	70 -72	loamy sand - light tan	loamy sand	5				1.82	4.637	53.7	42.34-141.14
HC 10 N	10-12.5	silty clay – grey	silty clay	2	30.8	52.5	16.7	0.92	0.239	2.8	1.41-4.23
HC 10 N	57.5 - 59.7	sandy clay - Fe P - OM – brown	sandy clay	4	49.1	37.2	13.7	1.35	0.035	0.4	1.41-4.23
HC 10 S	10 -12.5	silty clay loam - Fe C - OM – brown	silty clay loam	2				1.01	0.416	4.8	1.41-4.23
HC 10 S	25.7-28.2	sandy loam - light brown	sandy loam	5				1.77	0.939	10.9	42.34-141.14
HC 11 E	27.5 - 30	loamy sand - light brown	loamy sand	5	85.5	6.9	7.7	1.29	3.724	43.1	42.34-141.14
HC 11 E	75 - 77	sandy clay - OM - dark brown	sandy clay	4	69.4	18.0	12.6	1.90	1.645	19.0	1.41-4.23
HC 12 E	12.5-15	clay - Fe C – brown	clay	1	20.0	57.9	22.1	1.54	0.006	0.1	0.42-1.41

HC 12 E	22.5- 25	sandy loam - OM - dark gray	sandy loam	5	72.9	17.2	9.9	1.69	0.780	9.0	42.34-141.14
Core ID	Depth (ft)	Soil Texture	Soil Type	Class (UCSC)*	Sand %	Silt %	Clay %	Bulk density (gm//L)	K_{sat}(m/day)	K_{sat} (µm/sec)	Range (µm/sec) (NRCS)**
HC 12 W	56.3 - 57.5	clay loam - Fe C - brown	clay loam	1				0.96	0.125	1.4	0.42-1.41
HC12 W	63.2-65	sandy clay - Fe C - light brown	sandy clay	4				1.75	0.089	1.0	1.41-4.23
HC 12 W	98.5 -100	sand – tan	sand	6				1.62	6.284	72.7	42.34-141.14
HC 13 NE	66.7 - 67.5	loamy sand – tan	loamy sand	5	85.9	6.6	7.5	1.70	1.813	21.0	42.34-141.14
HC 13 NE	70- 71.9	silty clay - Fe - OM – brown	silty clay	2	47.5	34.8	17.6	1.28	0.100	1.2	1.41-4.23
HC 13 NE	100	sandy clay loam - brown	sandy clay loam	4	58.3	8.9	32.8	1.25	0.302	3.5	1.41-4.23
HC 14 E	59	loam - OM – brown	loam	3				1.83	0.650	7.5	4.23-14.11
HC 14 E	80	loamy sand - Fe P - Fe C – tan	loamy sand	5				2.09	1.119	12.9	42.34-141.14
HC 14 W	4.5-6.7	clay loam - dark brown	clay loam	1	13.8	53.8	32.3	1.21	1.230	14.2	0.42-1.41
HC 14 W	47.5-50	loamy sand - OM - light brown	loamy sand	5	73.7	11.3	15.0	1.95	0.494	5.7	42.34-141.14
HC 14 W	60.8	loamy sand - dark tan	loamy sand	5	77.0	11.5	11.5	1.73	0.059	0.7	42.34-141.14
HC 15 N	18.3 - 20	silty clay – brown	silty clay	2	33.4	48.0	18.6	1.46	0.036	0.4	1.41-4.23
HC 15 N	77.5 -80	silty clay - Fe C - light brown	silty clay	2	59.7	21.5	18.9	1.14	0.061	0.7	1.41-4.23
HC 15 S	28.1 - 30	sandy loam - Fe C - dark brown	sandy loam	5				1.70	0.111	1.3	42.34-141.14
HC 15 S	45.5-47.5	loam - Fe C - OM – brown	loam	3				1.38	0.079	0.9	4.23-14.11
HC 16 S	25-26.8	sandy clay – black	sandy clay	4				1.87	3.807	44.1	1.41-4.23
HC 16 S	51 - 53.5	clay loam - OM - brown	clay loam	1				1.79	0.076	0.9	0.42-1.41
HC 16 N	47.5-50	sandy clay – brown	sandy clay	4				1.98	0.237	2.7	1.41-4.23
HC 16 N	77.8 - 80	loamy sand – tan	loamy sand	5				2.19	1.848	21.4	42.34-141.14
HC 17 N	5-7.5	silt loam - Fe P - brown	silt loam	3				1.10	0.970	11.2	4.23-14.11

HC 17 N	19.6-22	sandy clay loam - OM – black	sandy clay loam	4				1.81	0.174	2.0	1.41-4.23
---------	---------	------------------------------	-----------------	---	--	--	--	------	-------	-----	-----------

Core ID	Depth (ft)	Soil Texture	Soil Type	Class (UCSC)*	Sand %	Silt %	Clay %	Bulk density (gm//L)	K _{sat} (m/day)	K _{sat} (µm/sec)	Range (µm/sec) (NRCS)**
HC 17 N	50.5 - 52.5	sandy clay loam - dark tan	sandy clay loam	4				2.05	0.319	3.7	1.41-4.23
HC 17 S	26.4 - 27.5	sandy clay loam - black	sandy clay loam	4	56.2	25.7	18.0	1.66	0.124	1.4	1.41-4.23
HC 17 S	67.5-70	sandy clay loam - Fe C – brown	sandy clay loam	4	62.1	24.8	13.1	1.47	0.648	7.5	1.41-4.23
HC 17 S	80-82.5	loam - Fe C - dark grey	loam	3	36.2	38.9	24.8	1.45	0.016	0.2	4.23-14.11
HC 18 E	12.9-15	silty clay - light brown	silty clay	2				1.38	5.530	64.0	1.41-4.23
HC 18 E	48.1 - 50	sandy clay - Fe C – brown	sandy clay	4				1.76	0.872	10.1	1.41-4.23
HC 18 W	15-17	clay - OM - Fe C - dark brown	clay	1	35.8	49.5	14.7	1.51	0.084	1.0	0.42-1.41
HC18 W	47.5-50	clay - Fe C - OM - light brown	clay	1	32.0	39.2	28.7	1.80	0.010	0.1	0.42-1.41
HC 20 W	2.5 - 5	clay loam - Fe C - dark brown	clay loam	1	30.0	48.1	21.9	1.22	0.149	1.7	0.42-1.41
HC 20 W	27.9 - 30	sand - Fe P – tan	sand	6	89.6	3.7	6.7	1.74	7.503	86.8	42.34-141.14
HC 20 W	43.6-45	sandy clay - light brown	sandy clay	4	61.1	20.8	18.1	1.89	0.121	1.4	1.41-4.23
HC 20 E	37.5-40	clay - Fe C - OM - light brown	clay	1				1.66	0.010	0.1	0.42-1.41
HC 20 E	58.4 - 60	loam - dark tan	loam	3				21.50	0.015	0.2	4.23-14.11

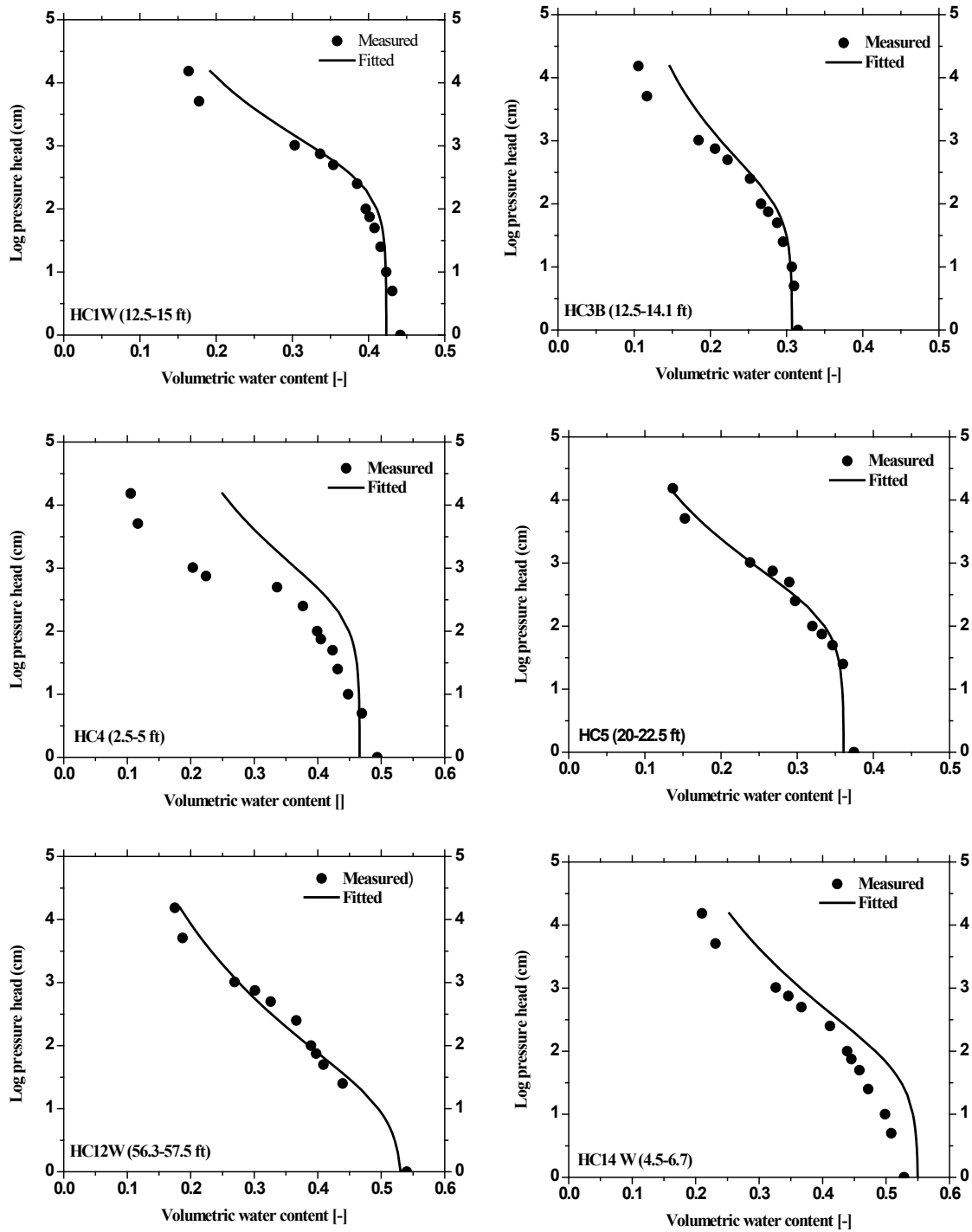


Figure S1: Soil water retention curves of some selected cores

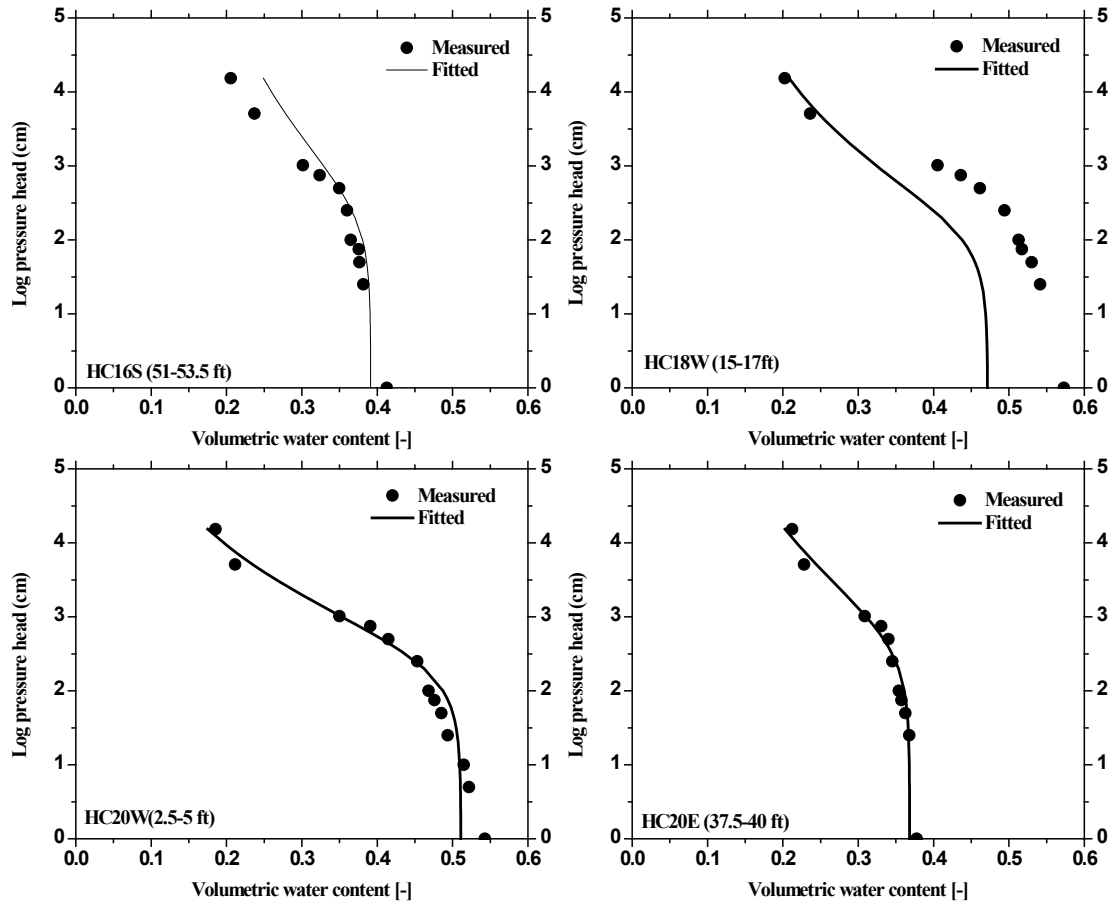


Figure S2: Soil water retention curves of some selected cores

Table S5: Estimated pedotransfer function for the soil cores at different depth.

Core Id	θ_r	θ_s	α (1/cm)	n	m
HC1E (32.5-35)	0.057	0.282	0.0026	1.27	0.215
HC1E (51.4-52.4)	0.068	0.397	0.0026	1.27	0.215
HC14W (4.5-6.7)	0.045	0.550	0.0167	1.16	0.138
HC2 (5-7.5)	0.067	0.534	0.0231	1.14	0.123
HC7(19.7-22.5)	0.078	0.49162	0.00305	1.30109	0.231414
HC1W (12.5-15)	0.068	0.423	0.0025	1.29	0.222
HC3A(7.5-9.2)	0.078	0.60169	0.00116	1.39507	0.28319
HC3B(1.9-5)	0.034	0.47556	0.02363	1.15056	0.130858
HC3B(12.5-14.1)	0.068	0.3073	0.008	1.2317	0.188114
HC4(2.5-5)	0.095	0.46606	0.0037	1.21612	0.177713
HC5(20-22.5)	0.001	0.36105	0.00551	1.22654	0.184698
HC5(32.5-35)	0.001	0.47103	0.02183	1.17344	0.147805
HC6(5.9-7.5)	0.067	0.60108	0.00271	1.31219	0.237915
HC6(37.5-40)	0.065	0.36192	0.00671	1.33994	0.253698
HC9B(20-22)	0.01	0.3948	0.02744	1.23908	0.19295
HC10N (10-12.5)	0.07	0.4841	0.00293	1.32625	0.245994
HC10N (57.5-59.7)	0.1	0.3501	0.00281	1.19359	0.162191
HC10S (10-12.5)	0.001	0.51549	0.00546	1.2438	0.196012
HC11E (27.5-30)	0.001	0.2756	0.4145	1.23711	0.191664
HC11E (75-77)	0.1	0.37307	0.07392	1.15883	0.137061
HC12W (56.3-57.5)	0.001	0.53425	0.08058	1.15092	0.13113
HC12W (63.2-65)	0	0.41891	0.00697	1.21461	0.17669
HC12W (98.5-100)	0.045	0.3855	0.0326	1.17956	0.152226
HC13NE(67.5)	0.05667	0.37122	0.0344	1.36456	0.267163
HC13NE(70-71.9)	0.07	0.36131	0.00292	1.24762	0.198474
HC14W (4.5-6.7)	0.045	0.55048	0.01671	1.16022	0.138094
HC15 N (18.3-20)	0.14165	0.41088	0.00217	1.40664	0.289086
HC15N(77.5-80)	0.07	0.41174	0.00174	1.135682	0.119472
HC16S(51-53.5)	0.095	0.39132	0.00359	1.16334	0.140406
HC16N(47.5-50)	0.1	0.40581	0.00403	1.23633	0.191154

Core Id	θ_r	θ_s	α (1/cm)	n	m
HC17S(67.5-70)	0.089	0.41539	0.00422	1.16856	0.144246
HC17S(80-82.5)	0.078	0.33588	0.00475	1.14544	0.126973
HC18E(12.9-15)	0.01189	0.3649	0.04335	1.47829	0.323543
HC18W(15-17)	0.078	0.47158	0.00654	1.23976	0.193392
HC20W (2.5-5.0)	0.001	0.51091	0.00335	1.27269	0.214263
HC20W (27.9-30)	0.045	0.40067	0.01678	1.33012	0.248188
HC20W(43.6-45)	0.1	0.40043	0.00197	1.25068	0.200435
HC20E (37.5-40)	0.001	0.3682	0.00188	1.17737	0.150649
HC20E (58.4-60)	0.001	0.53745	0.00747	1.08233	0.076067

Meteorology of the selected sites.

The RZWQM2 model requires daily climate input data for precipitation, maximum and minimum air temperature, wind speed, short wave radiation, and relative humidity. Weather data (2011-2016) for the RZWQM2 model were presented in Figure S3-4.

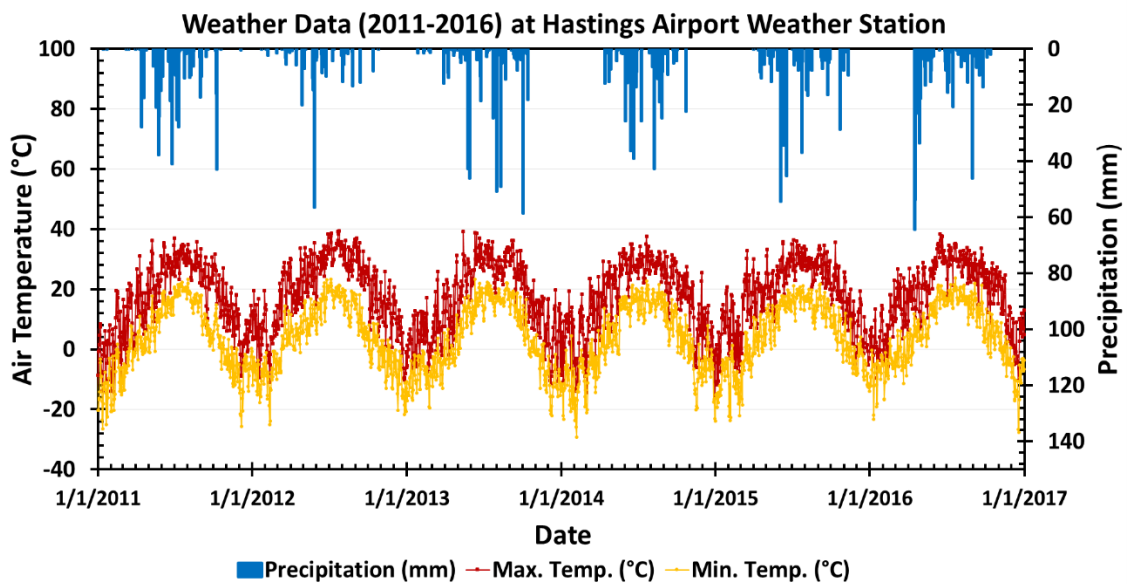
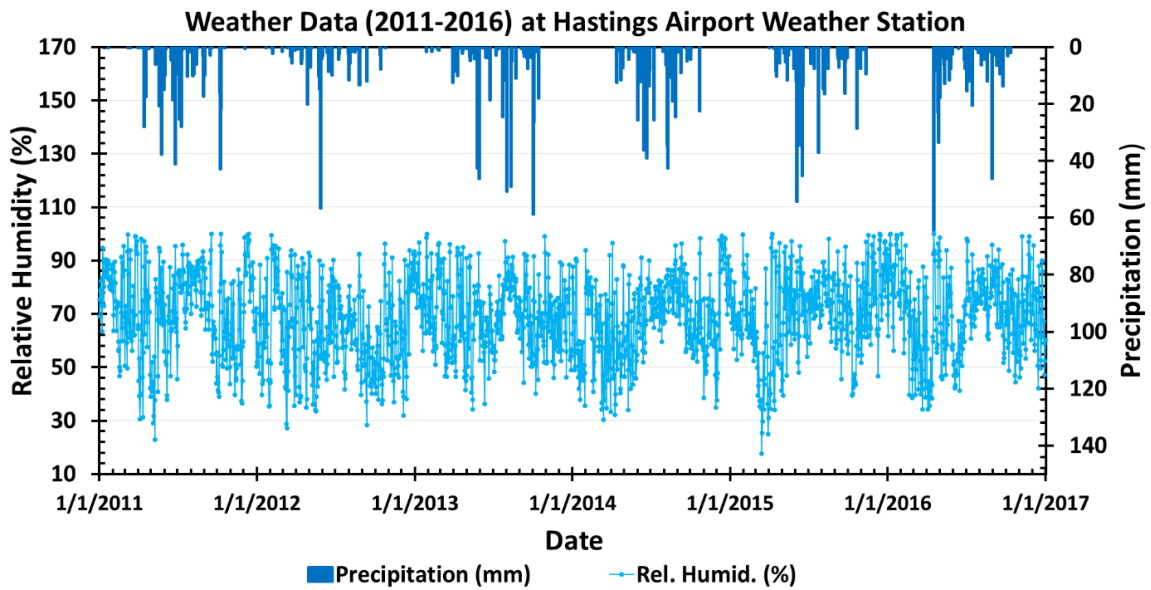


Figure S3: Weather data (2011-2016) at the Hastings Airport Weather Station, Nebraska in the U.S., presenting max/min air temperature (above) and relative humidity (bottom).

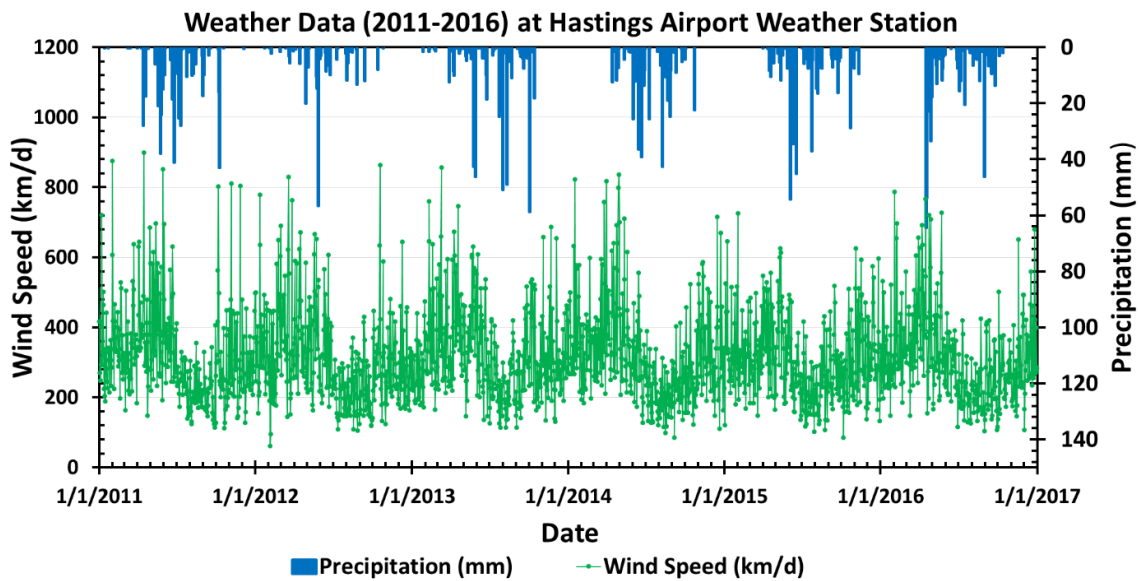
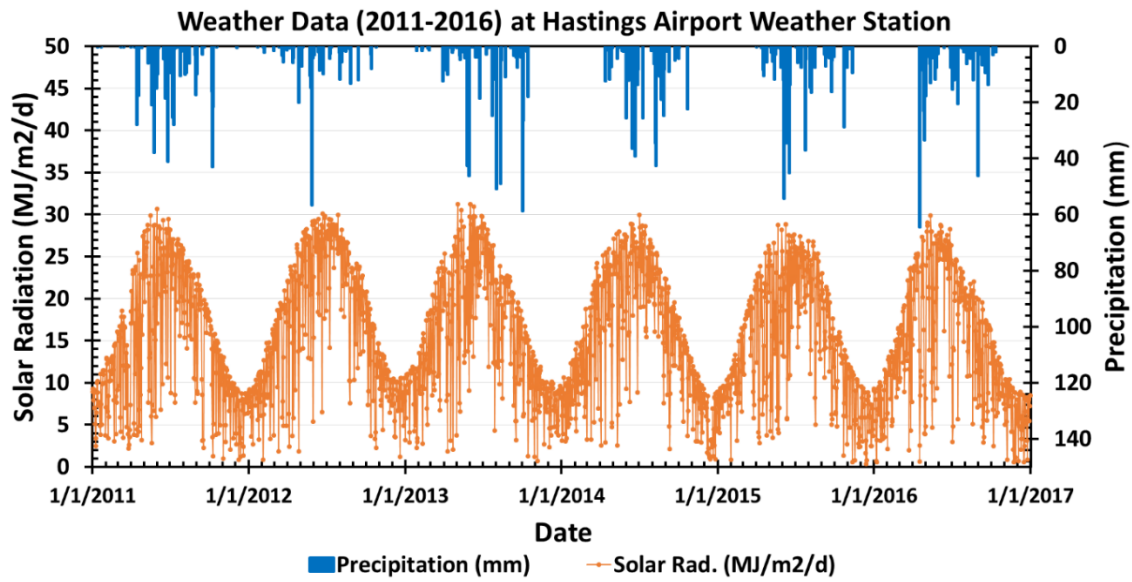


Figure S4: Weather data (2011-2016) at the Hastings Airport Weather Station, Nebraska in the U.S., presenting solar radiation (above) and wind speed (bottom).

Calibration and Validation Procedures of RZWQM2 and HYDRUS -1D:

Before designated scenarios of agricultural management practices were tested and evaluated in RZWQM2 in order to optimize the BMPs, the RZWQM2 model was initially calibrated with 2011 observed data for 180 cm soil depth and validated with 2016 observed data for soil water and nitrate-N profiles. The 2011 and 2016 observed data were obtained from the Department of Agronomy and Horticulture (Spalding and Toavs, 2011) and the Nebraska Water Science Laboratory (Adams, 2018) at the University of Nebraska-Lincoln. For RZWQM2 calibration and validation, the root mean square error (RMSE) was used to assess the goodness-of-fit. The RMSE values closer to zero indicate better agreement between the simulated and observed data. The RMSE is described as the equation 1:

$$RMSE = \sqrt{\frac{\sum_{i=1}^n (S_i - O_i)^2}{n}} \quad [1]$$

where S_i is the simulated value, O_i is the observed value, and n is the number of measurements.

HYDRUS1D model (180 cm to water table depth) was calibrated and validated as using same procedure like RZWQM2. The flow chart of the calibration and validation procedures for RZWQM2 is presented in Figure S5.

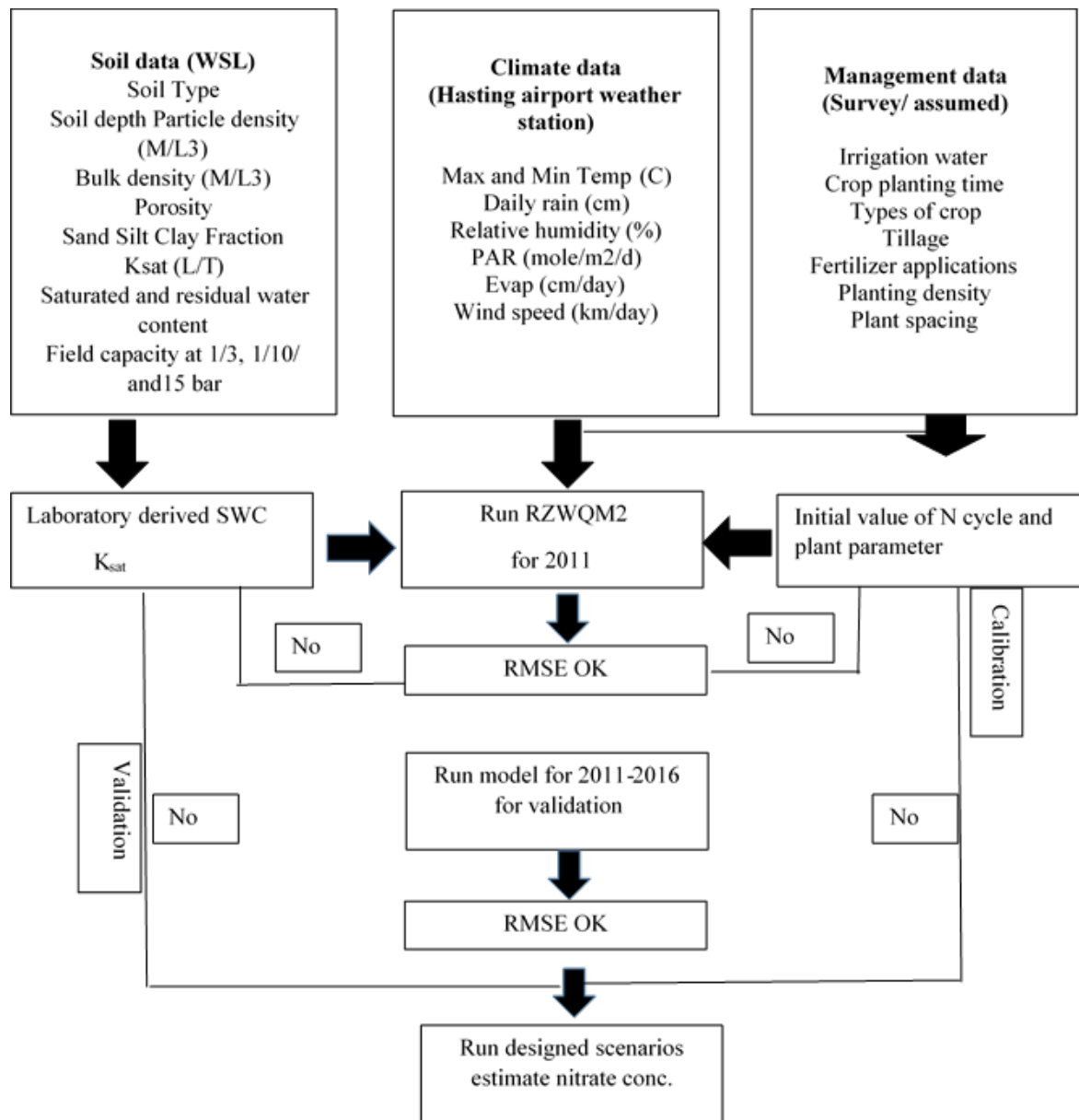


Figure S5: The flow chart of the calibration and validation procedures in the study by using RZWQM2 up to 180 cm soil depth.

Figure (S6-7) shows the climatic variables impact on the moisture dynamics within the root zone. The moisture profile at 15, 30 and 60 cm variation depends upon the climatic variables at the soil surface. The soil moisture content decreasing with depth in irrigation and non-irrigation condition. In dryland condition maximum soil moisture content was predicted at 30 cm depth an obvious

reason of this, the more evapotranspiration on the soil surface. When irrigation applied on the soil surface, the soil moisture content is more at 15 cm depth, so soil moisture content directly depends upon the amount of infiltrating water.

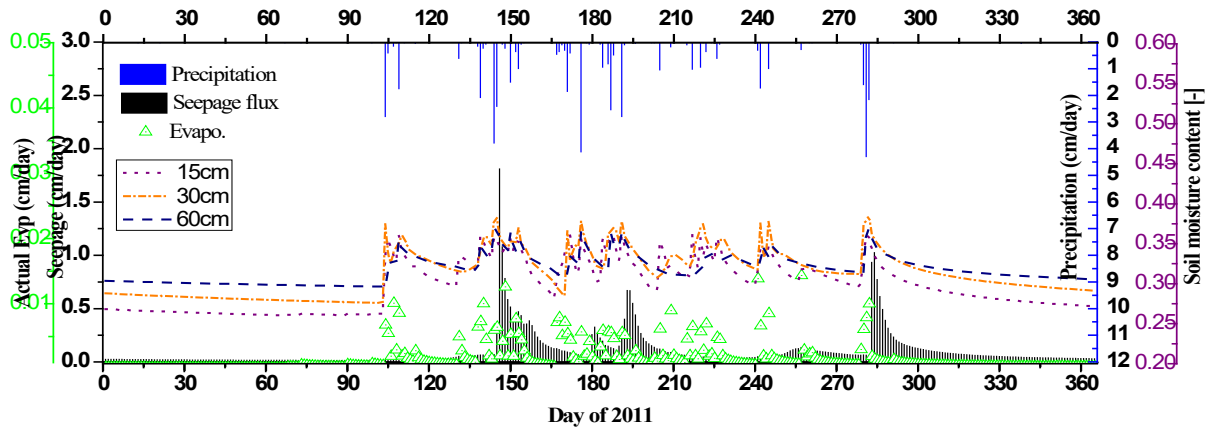


Figure S6: Moisture content variation at different depth of root zone and leaching of seepage flux under non irrigation condition during the year 2011 at the HC2 dryland site.

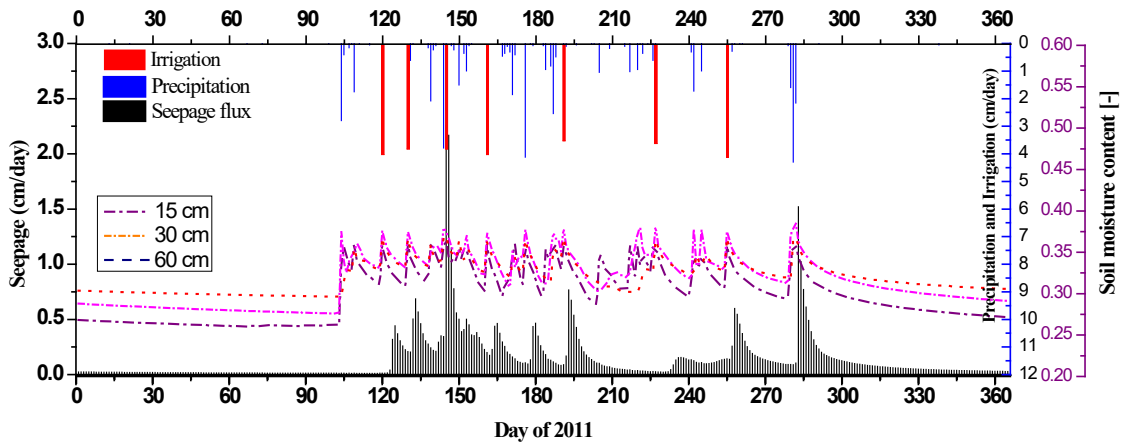


Figure S7: Moisture content variation at different depth of root zone and leaching of seepage flux under irrigation condition during the year 2011 at the HC2 dryland site.

Appendix 2

Laboratory method for saturated hydraulic conductivity and Soil water retention parameter of soil cores.

The K_{sat} values are measured by Falling Head test method (Figure 1s and 2s) and estimated using equation 1:

$$K_s = \frac{\ln\left(\frac{H_0}{H_t}\right)}{\frac{At}{aL}} \quad [1]$$

where, H_0 (cm) and H_t (cm) water level in cylinder at 0 and time t (sec/min), A (cm^2) area of the soil core, a (cm^2) area of the funnel, and L (cm) soil core length. Table S1 shows the laboratory generated data of falling head test experiments, which were used for estimation of K_{sat} value of different soil cores.

Table S1: Shows data required for the estimation of K_{sat} generated from the falling head test method.

TIME (min)	H (cm)	$\ln(H_0/H_t)$	At/aL
0	3.4	0.159	0
2.90	2.9	0.348	0.457
4.25	2.4	0.582	0.669
9.45	1.9	0.887	1.488
12.29	1.4	1.329	1.935
15.18	0.9	2.140	2.391
18.41	0.4	0.000	2.899
	K_s	0.454199	m/hr
	K_S	10.90077	m/day

Saturated Hydraulic Conductivity Measurement in Laboratory:

Figure S1-2 represent the apparatus used for the measurement of K_{sat} in the laboratory by the falling head method (Head 1982)



Figure S1: Falling head setup with soil core

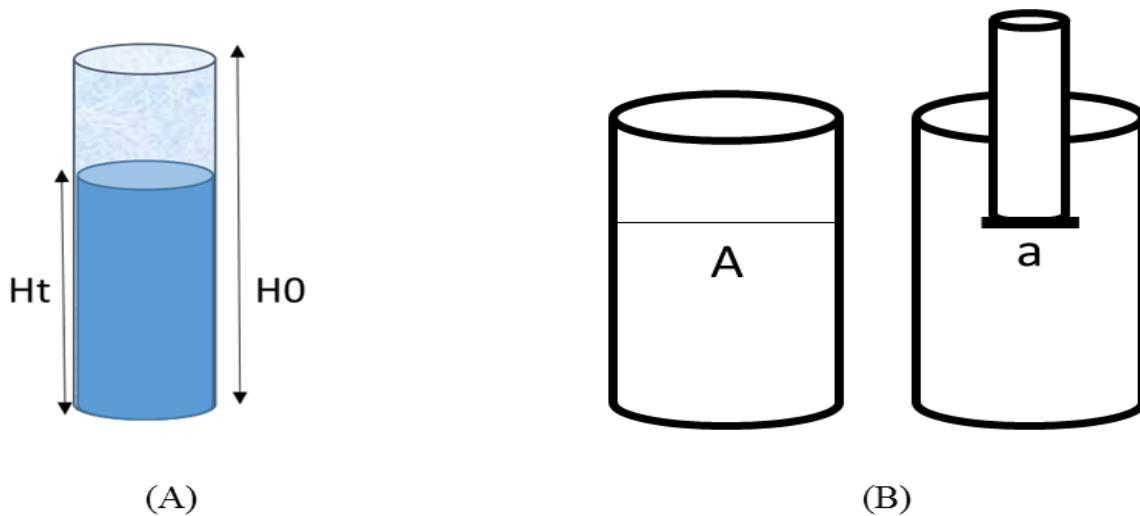


Figure S2: (A) Schematic representation of water level in acrylic cylinder at different time, (B) Area of soil core and funnel of the setup

Soil Water Retention Curve

Gradients in soil water potential (SWP) are the primarily driving forces of water movement, affecting water infiltration, redistribution, percolation, and evapotranspiration (Radcliffe and Šimůnek, 2010). Knowledge of the SWP is therefore useful to optimize effective water for plants, as well as to be able to estimate percolation of solutes from the vadose zone into

the groundwater. Basically, the SWP is defined as the potential energy of water in soil and determined by a variety of forces including gravitational, matric (capillary and adsorptive), osmotic, and hydrostatic (Radcliffe and Šimůnek, 2010). The gravitational potential is usually determined by the elevation of the soil water and the chosen reference elevation, which is commonly the soil surface. The matric potential is determined by the forces exerted by the soil matrix (soil pores and particles) on water under unsaturated conditions. These forces basically include the capillarity and adsorption. The osmotic potential is given by the presence of solutes in the soil solution, which decrease the potential energy of water. The hydrostatic potential is determined by a pressure exerted by overlaying water over a point of interest in the soil.

The SWRC presents the relationship between the water potential and the corresponding values of soil water content. Naturally, the greater the clay content (small soil pores) in a soil layer, the greater the water holding capacity, while the greater the sand content (large soil pores), the smaller the water holding capacity. The depth of the soil profile also has a significant role in determining the soil water holding capacity due to compaction or age of the soil. The SWRC and the hydraulic conductivity (K) make up the soil hydraulic properties, which significantly affect soil water balance, plant available water, and the amount of water and solute percolating into groundwater. Thus, soil samples in the study area were collected and tested in the laboratory in order to determine the SWRC and K in different depths of soil profiles for use in modeling. The laboratory methods of this study include the use of hanging water columns (lower water potential) and pressure plate apparatus (higher water potential). The measured saturated hydraulic conductivity (K_{sat}) and estimated SWRC for the RZWQM2 and HYDRUS model for soil samples are presented in result section.

The hanging water column is a technique to determine a SWRC in the wet range. The soil sample is saturated for at least 24 hr and placed onto a porous cup that is in direct contact with water (Dane et al., 2002). At the beginning of the experiment, the gas pressure in the soil sample is at atmospheric pressure. A reference bottle or burette, which is connected with the water under the porous plate, is lowered by lowering the water level in the burette. The lower water potential induces a drainage of water from the soil sample. The soil sample is then removed from the sample holder and weighed for the gravimetric determination of soil water content. The procedure is repeated at further values (i.e., 10 cm, 50 cm, and 100 cm) of water potential. Figure S3 shows a schematic representation of the hanging water column for experimental procedure.

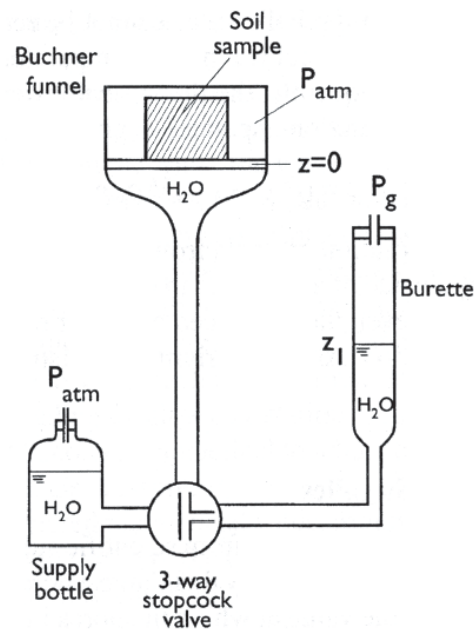


Figure S3: The diagram of the hanging water column (from Dane and Hopmans, 2002)

The pressure plate apparatus is a sealed metal chamber. A ceramic porous plate is used for placing soil samples in the chamber. The ceramic plates are soaked in water overnight (~24 hr) before loading soil samples in the chamber. The soil samples should have enough moisture on the ceramic plates to have a good contact between the soil and plate (Dane et al., 2002). The pressure

chambers are closed with a specified pressure applied by a gas tank or by an air compressor. Then, the sample starts losing water that moves through the ceramic porous plate and draining water outside the pressure chamber. After the water ceases to drain, the soil samples are collected and weighted for gravimetric determination of soil water content. The method is repeated at increasing pressures (i.e., 1 bar, 3 bar, 5 and 15 bar) of water potential. Figure S4 shows a picture of the pressure plate apparatus used in the experiment.

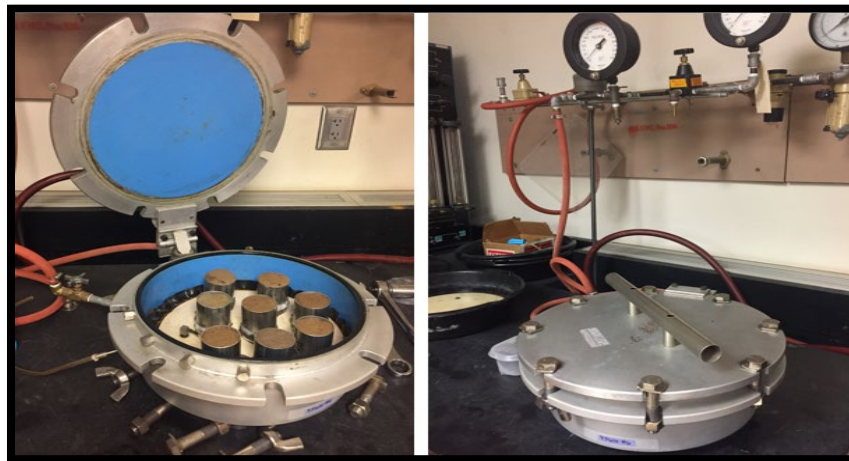


Figure S4: Picture of the pressure plate apparatus experiment.

Reference

Dane, J. H., Hopmans, J. W., and Topp, G. C. (2002). Hanging water column. *Methods of soil analysis. Part, 4*, 680-683.

Dane, J. H., Hopmans, J. W., and Topp, G. C. (2002). Pressure plate extractor. *Methods of soil analysis. Part, 4*, 688-690.

Head, K. H. (1980). *Manual of soil laboratory testing (Vol. 1, No. 2)*. London: Pentech Press.

Radcliffe, D. E., and Simunek, J. (2010). *Soil physics with HYDRUS: Modeling and applications*. CRC press.

